ICHNOLOGY, DEPOSITIONAL DYNAMICS AND SEQUENCE STRATIGRAPHY OF THE PLIO-PLEISTOCENE ORINOCO DELTA: MAYARO AND MORNE L'ENFER FORMATIONS, SOUTHERN TRINIDAD

A Thesis Submitted to the

College of Graduate Studies and Research

In Partial Fulfillment of the Requirements

For the Degree of Doctor of Philosophy (Ph.D.)

In the Department of Geological Sciences,

University of Saskatchewan,

Saskatoon, Saskatchewan, Canada

By

SUDIPTA DASGUPTA

PERMISSION TO USE

In presenting this thesis as the partial fulfillment of requirements for a Ph.D. degree from the University of Saskatchewan, I understand and confirm that the Libraries of this University may make it freely available for inspection. I agree that permission for copying of this thesis in any manner, in whole or in part, for scholarly purposes may be allowed by the Dr. Luis A. Buatois who supervised my thesis work or, in his absence, by the Head, Department of Geological Sciences, or the Dean of the Colleges of Graduate Studies and Research (CGSR), in which my thesis work was done. It is understood that any copying or publication or use of this thesis or parts thereof for any direct or indirect financial gain shall not be allowed without my written permission or, in my absence, without written permission from my immediate heir. It is also implicit that appropriate recognition shall be given to me and to the University of Saskatchewan in any scholarly use which may be made of any material in my thesis.

DISCLAIMER

References in this thesis to any specific commercial product(s), process(es), or service(s) by trade name(s), trademark(s), manufacturer(s), private company(ies), or otherwise, does not constitute or imply its(or their) endorsement, recommendation, or favoring by me or the University of Saskatchewan.

Requests for permission to copy or to make other uses of materials in this thesis in whole or part should be addressed to:

Head	OR	Dean
Department of Geological Sciences		College of Graduate Studies and Research
University of Saskatchewan		University of Saskatchewan
114 Science Place		107 Administration Place
Saskatoon, Saskatchewan, S7N 5E2		Saskatoon, Saskatchewan, S7N 5A2
Canada		Canada

ABSTRACT

During the Late Pliocene and early Pleistocene, when the paleo-Orinoco delta system transited over the Amacuro Shelf and reached the paleo-shelf-break along the southeastern shoreline of Trinidad. At this time onwards, the shelf-edge delta clinoforms developed further eastward. These deltaic clastic wedges serve as the unique analog in the geological record for an accommodation-driven inner-shelf and shelf-edge delta, developed at an oblique foreland tectonic setting situated at a tropical-equatorial paleogeographic setting. These deposits were influenced by strong Atlantic longshore current, tropical storms, and phytodetrital pulses, and with an exceptionally high sediment accumulation rates. These four aspects make the clastic wedges unique candidates for sedimentological, ichnological, and stratigraphic investigation. The primary objectives of this thesis are to: (a) collect, analyze, and integrate outcrop data on lithofacies, trace fossils, and discontinuity surfaces into a comprehensive depositional and ichnological model for the first growth-fault-guided shelf-marginal pulse of the paleo-Orinoco delta, as recorded in the Mayaro Formation outcrops in southeast Trinidad; and (b) deduce the dominant sedimentary processes during the across shelf transit and their impacts on the benthic infauna as preserved in the Morne L'Enfer Formation outcrops of southwest Trinidad, which are possibly slightly older than the Mayaro Formation. The basal interval of the Morne L'Enfer Formation has specifically been investigated for this purpose, where the deltaic clastic wedges are preserved directly above shelf deposits.

The entire Mayaro Formation megasequence is categorized into deposits belonging to twelve different subenvironments based on lithofacies associations and ichnological characteristics. Ichnological evidence indicates that the shelf-edge deltas are one of the most extreme marine environments for benthic metazoans to colonize. However, the combinations and ranking of stress factors affecting the colonizing fauna are diverse and distinct in every individual subenvironment indicating the relative dominances of river-influence, waves, and/or sediment-gravity-flows vis-à-vis slope instability. Due to variations in stress factors, the megasequence also displays dual ichnologic and sedimentologic properties of both the shelf-edge delta lobe(s) and the outer shelf delta lobe(s). A minor transient tidal influence can only be observed in the

architectural elements, e.g. elongated interbar embayment and interlobe prodeltaic depocentres, which control topography and enhance tidal effect.

Discovery of an unusual monospecific *Glossifungites* Ichnofacies along an incision surface in the midst of the Mayaro Formation succession enabled a substantial overhaul of the earlier understanding of the formation in terms of its depositional model and stacking pattern. The surface has been re-identified as a canyon/gully cut at the shelf-edge, which possibly acted as a conduit for (a) the mass movements and for (b) the coarse clastic (mostly silt to medium-grained sand) sediment transfer to deep marine settings. The monospecific nature of the *Glossifungites* Ichnofacies suite indicates that the incision surface was under substantial ecological stresses for the colonizing infauna. The stresses might have arisen from slope instability of the steep canyon/gully walls, mass movements above the incision surface, elevated water turbulence, and lowered salinity from river influx. Five different facies tracts have been identified within the canyon/gully-fill, which crosscuts the shelf-edge delta-front. The facies tracts are dominated by different types of sediment-gravity flow deposits, which are systematically stacked and are almost devoid of trace fossils due to rapid sedimentation rates and slope instability. They are also strikingly different from the surrounding deltaic facies. A high-frequency sequence stratigraphic model involving the influence of growth-fault tectonics on the relative sea-level curve has been invoked to explain the incision of the canyon/gully and its sequential filling processes.

On the other hand, the transition from the open shelf to inner-shelf deltaic condition as displayed by the basal members of the Morne L'Enfer Formation is strongly dominated by evidences of river influence with the transient background action of fair-weather waves and storm waves. A peculiar pattern of disappearance of trace fossils produced by irregular sea-urchins highlight that the river influence was quite strong not only at the sediment-water interface but also in the water-column, which affected invertebrate larvae. The initial progradation of the clastic wedge on the shelf was dominated by hyperpycnal flows and waves in contrast to tidal domination in the younger members of the formation.

ACKNOWLEDGEMENTS

First of all, I deeply apologize to every individual member of my family for making this apparently ‘absurd’ decision of leaving a stable well-remunerating career in the oil-and-gas industry and coming to Canada in order to sail on an unfathomed and unchartered academic water. I fully accept the accountability for making that decision, which caused an immense distress for all of them; and I intend here to refrain from pointing a finger towards any bureaucratic institution. I deeply acknowledge the initiatives and ingenuities of Carlos Zavala, especially for introducing me to Luis Buatois and Gabriela Mángano, to both of whom I will remain immeasurably indebted. Repsol E&P T&T Limited provided continuous support for the fieldwork in Trinidad, for which I deeply thank Livan Blanco Valiente, Rafael Vela, Yrma Vallez, Anderson Arjoon, Jivanti Ramdular, Jose Luis Huedo Cuesta, and their entire subsurface group. Field assistance by Marlon Bruce and Balázs Törő was vital for the success of this study and I cannot fully express my gratitude in any word. I thank Ron Steel, Jasper Knight, Franz Fürsich, Andrea Fildani, James MacEachern, Shahin Dashtgard, Korhan Ayranci, and seven anonymous reviewers for their valuable comments, suggestions, and critical observations on the manuscripts. I acknowledge the diligent review of the project and my thesis by Stephen Hubbard, Brian Pratt, Alec Aitken, James Merriam, Samuel Butler, and Matt Lindsay. Logistic and additional assistance in the field from Dinelle Medina, Ann Marie Singh, Michael, Ragoo and health and safety department of Repsol are highly appreciated. Additional financial support was provided by an NSERC Discovery Grant to Luis Buatois. The Graduate Teaching Fellowship, the Devolved Scholarship from the Department of Geological Sciences, the AAPG Foundation Merrill W. Haas Memorial Grant, the Saskatchewan Innovation and Opportunity Award from the Provincial Government of Saskatchewan and University of Saskatchewan, the Dr. Rui Feng Graduate Studies Award, and the travel grants from the University of Saskatchewan, the Geological Society of America, and the International Ichnological Association to me have proven to be crucial for this study. I will remain deeply thankful to Ven Kolla, Liviu Giosan, Octavian Catuneanu, Dennis Meloche, Andreas Wetzel, Tony Ekdale, Renata Netto, Koji Seike, Juan Jose Ponce, Noelia Carmona, Silvio Casadio, Robin Renaut, Irene Espejo, Patricio Desjardins, Luis Quiroz, Pablo Alonso, Raju Hossain, Sara Worsham, Christopher West, Sandra Duarte, Sarah

Grummett, Zain Belaústegui, Jenny Scott, Davinia Diez-Canseco Esteban, Solange Angulo, Krisztina Pandur, Setareh Shahkarami, Adrienne Bangsung, Neeraj Sinha, Anand Kale, Kyle Reid, Elizabeth Schatz, Sidhartha Sinharay, Williams Rodriguez, Luc Chabanole, Andrei Ichaso, Kai Zhou, Liya Zhang, Sudipta Tapan Sinha, Santanu Banerjee, Soumyajit Mukherjee, Manasij Santra, Arun Saraf, Brahma Parkash, Nancy White, John Martin, Mary Jean Verrall, Satyajit Chowdhury, Nabarun Pal, Vincy Yesudian, Sudipta Basu, Chantal Strachan-Crossman, Michelle Howe, Tim Prokopiuk, Jim Rosen, Roy Rule, Olena Ponomarenko, Soo In Yang, Marcelina Łabaj, Mohamed Gouiza, Michael Cuggy, Soumya Das, Husham El Taki, Sandor Sule, Late Jordi de Gibert, Late Tripti Banerjee, Shreyosi Dasgupta Chowdhury, my parents Pankaj and Ranjana Dasgupta, and my brother Mainak Dasgupta for their gracious help, encouragement, and discussions.

To

Luis and Gaby

(And to whomsoever around the globe the curse of bigotry of any kind,
either ‘ugly’ and overt or ‘nice’ and covert, torments alike in everyday life)

TABLE OF CONTENTS

PERMISSION TO USE ……. i

DISCLAIMER ……..... i

ABSTRACT ……... ii

ACKNOWLEDGEMENTS ……... iv

DEDICATION ……... vi

TABLE OF CONTENTS …… vii

LIST OF TABLES ……..... xii

LIST OF FIGURES …… xiii

CHAPTER 1: INTRODUCTION AND LITERATURE REVIEW …….. 1

CHAPTER 2: TRANSITION …… 6

CHAPTER 3: EVALUATING THE IMPACT OF STRESS FACTORS ON …….. 8
ANIMAL-SEDIMENT INTERACTIONS WITHIN SUBENVIRONMENTS OF A
SHELF-MARGIN DELTA, THE MAYARO FORMATION, TRINIDAD

3.1 Introduction …….. 9

3.2 Geologic setting ……... 11

3.2.1 Columbus Basin …… 11

3.2.2 Study area …….. 13

3.3 Methods …… 15

3.4 Sedimentary facies, ichnology and depositional model ……... 23

3.4.1 Shelf-attached Mass Transport Complex (MTC) …….. 23

3.4.2 Shelf-edge delta lobe ……. 25

3.4.2.1 Active subaqueous feeder channel-fill – river- …….. 27
dominated wave-influenced delta-front
3.4.2.2 Abandoned subaqueous feeder channel-fill and ……. 28
internal levee – river-dominated wave-influenced delta-front
3.4.2.3 Proximal overbank and crevasse complex ……. 31
– river-dominated wave-influenced delta-front
3.4.2.4 Distal overbank ……..... 31
– river-dominated wave-influenced delta-front
3.4.2.5 Amalgamated terminal mouth-bar – …….. 34
river- and wave-influenced delta-front
3.4.2.6 Proximal/attached wave-modified subaqueous …….. 36
barrier bar system of delta-front
3.4.2.7 Distal/discrete wave-modified subaqueous barrier … 39
bar system of delta-front
3.4.2.8 Proximal prodelta or prodeltaic inter-lobe ……. 44
embayment
3.4.3 Outer shelf delta lobe …… 48
3.4.3.1 Wave-modified fringing barrier bars (outer shelf ….. 48
shoals)
3.4.3.2 Proximal prodelta and/or inter-lobe embayment on ... 53
outer shelf
3.4.4 Incised canyon fill ……. 55
3.5 Discussion …… 62
3.5.1 Uniqueness of animal-substrate interaction in the paleo- …… 62
Orinoco Shelf-edge Delta
3.5.1.1 Extreme effects of stress factors on the ecology of … 62
benthic animals
3.5.1.2 Diverse permutations (i.e. combination + ranking) … 63
of stress factors corresponding to the sedimentary processes

specific to depositional subenvironments

3.5.1.3 Ichnological duality of shelf-edge delta system ……. 63

3.5.2 Evaluation of stress factors in depositional subenvironments .. 65

3.5.2.1 Stress factors on the upper-slope and within …….. 65
incised canyon/gully

3.5.2.2 Stress factors at the shelf-edge ……... 66

3.5.2.2.1 Stress factors in river dominated……. 66
subenvironments

3.5.2.2.2 Stress factors in wave-dominated …… 69
subenvironments

3.5.2.2.3 Stress factors in shelf-edge prodelta …… 71

3.5.2.3 Stress factors in the outer shelf delta …….. 72
subenvironments

3.5.2.4 Depositional model based on the integration of ……. 73
ichnological and sedimentological datasets

3.6 Conclusions …….. 75

3.7 Acknowledgements …….. 76

CHAPTER 4: UNUSUAL OCCURRENCE AND STRATIGRAPHIC ……... 78
SIGNIFICANCE OF THE *GLOSSIFUNGITES* ICHNOFACIES IN A
SUBMARINE PALEO-CANYON – EXAMPLE FROM A GELASIAN SHELF-
EDGE DELTA, SOUTHEAST TRINIDAD

4.1 Introduction …….. 79

4.2 Depositional Setting of the Gelasian Mayaro Formation ……. 81

4.3 Ichnology and sedimentology of the paleo-canyon wall and fill …….. 86

4.4 Discussion …… 90

4.4.1 The *Glossifungites* Ichnofacies in the Mayaro Formation …… 90

4.4.2 Sequence stratigraphic implications …….. 92

4.5 Conclusions …….. 97

4.6 Acknowledgements …….. 98

CHAPTER 5: HIGH-FREQUENCY STACKING PATTERN AND ……... 99
STAGES OF CANYON/GULLY EVOLUTION ACROSS A FORCED
REGRESSIVE SHELF-EDGE DELTA-FRONT

5.1 Introduction …….. 100

5.2 Geology of the Canyon System(s) within the Mayaro Formation …… 103

5.2.1 Geologic Background …… 103

5.2.2 Facies tracts and sedimentary processes within the Mayaro … 105
incised canyon/gully

5.2.2.1 FT-A ……... 108

5.2.2.2 FT-B ……... 110

5.2.2.3 FT-C ……... 111

5.2.2.4 FT-D ……... 115

5.2.2.5 FT-E ……... 116

5.2.2.6 FT-F ……... 117

5.3 Discussion …… 120

5.3.1 The Mayaro Formation — advent of accommodation-driven ... 120
delta-front at the shelf-edge

5.3.2 Sequence-stratigraphic order and frequencies of controlling … 121
factors

5.3.3 Derivation of growth-tectonics-influenced local base-level …. 123
curves

5.3.4 Incision and sedimentation cycle in response to local base- … 125
level curve
5.3.5 Application of sequence-stratigraphic order in subsurface ….... 127
analogs of the Mayaro Formation megasequence
5.4 Conclusions …….. 128
5.5 Acknowledgments …… 128
CHAPTER 6: ICHNOLOGY OF A LATE PLIOCENE HYPERPYCNAL ……. 130
SYSTEM, MORNE L'ENFER FORMATION, FULLARTON, TRINIDAD:
IMPLICATIONS FOR RECOGNITION OF AUTOGENIC EROSIONAL
SURFACE AND DELINEATION OF STRESS FACTORS ON IRREGULAR
ECHINOIDS
6.1 Introduction …….. 131
6.2 Geologic setting ……... 133
6.3 Sedimentological and ichnological observations at the Fullarton …… 134
section
6.3.1 Unit FT-L …….. 137
6.3.2 Unit FT-U …….. 143
6.3.2.1 Facies UA ……... 144
6.3.2.2 Facies UB ……... 147
6.3.2.3 Facies UC ……... 148
6.3.2.4 Facies UD ……... 149
6.4 Discussion …… 149
6.4.1 Sequence-stratigraphic status of the erosional …….. 150
contact surface – Autogenic erosional surface on shelf setting
dominated by hyperpycnal flow

6.4.2 The role of stress factors ……... 153

6.5 Conclusions …….. 160

6.6 Acknowledgements …….. 161

CHAPTER 7: CONCLUSIONS …… 162

REFERENCES ……. 164

LIST OF TABLES

Table 3.1. Summary of the depositional subenvironments, their outcrop…….. 15
occurrences, facies associations, and sedimentary processes of the paleo-Orinoco delta as displayed by the Mayaro Formation outcrops.

Table 3.2. Summary of the ichnological characteristics with respect to the stress…. 20
factors and preservational biases as displayed by sediments deposited in different subenvironments of the Mayaro Formation outcrops.

Table 5.1. Summary of the facies tracts classification of the Mayaro Formation…... 106
with description of facies associations, and interpreted sedimentary processes.

Table 6.1. Locations of the outcrop reference points in western ……... 137
Cedros Bay section of the Morne L'Enfer Formation, Fullarton, Trinidad.

Table 6.2. Relative influences of ecological stress factors and their…….. 158
cumulative effects on adult invertebrate endobethos (sea-urchin) community and their planktotrophic larvae (echinopluteus) at the sediment-water interface (SWI) and in the overlying water column in different sedimentary sub-environments on the continental shelf affected by a wave-influenced and fluvial discharge-dominated delta system. Three cases, A, B, and C, of ecological niches listed in Fig. 6.8 are also assigned.

LIST OF FIGURES

Fig. 3.1. General stratigraphy and location of the study areas…… 14

Fig. 3.2. General view of mass transport complex (MTC) deposit in …….. 24
Outcrop 1A (i.e. at the base of the Mayaro Formation exposures).

Fig. 3.3. General view of subaqueous channel and channel-bank…….. 26
deposits of the river-dominated delta-front subenvironments.

Fig. 3.4. Detailed ichnological and sedimentological features of……... 29
the sandy lithosomes in active channel-fills of the delta-front, as exposed in Outcrop 4.

Fig. 3.5. Detailed ichnological and sedimentological features of……... 30
the sandy lithosomes in thin-bedded/laminated sandy heterolithic sediments within abandoned channel-fills of the delta-front, as exposed in Outcrop 4.

Fig. 3.6. General view and sedimentary features of proximal overbank of…… 32
subaqueous channel system in river-dominated delta-front.

Fig. 3.7. General view and sedimentary features of distal overbank deposits…… 33
with thin-bedded/laminated muddy heterolithic sediments of subaqueous channel system in river-dominated delta-front.

Fig. 3.8. Detailed sedimentary features of mouth-bar deposits of…….. 35
shelf-edge delta.

Fig. 3.9. General view of the proximal/attached wave-modified subaqueous…… 37
barrier bar (both amalgamated- and layered- types) system of wave-influenced delta-front and underlying proximal prodelta (or prodeltaic inter-lobe embayment) as exposed in Outcrop 6C-i.

Fig. 3.10. Ichnological and sedimentological features of the……. 38
proximal/attached wave-modified subaqueous barrier bar system at the wave-influenced shelf-edge delta-front.

Fig. 3.11. General view, sedimentological, and ichnological features of distal and 42
discrete barrier bars.

Fig. 3.12. Ichnological and sedimentological features of distal/discrete…… 43
wave-modified subaqueous barrier bar system as exposed in Outcrops 8A-ii and 9.
Fig. 3.13. Ichnological and sedimentological features of distal/discrete…… 44
wave-modified subaqueous barrier bar system as exposed in Outcrops 8A-ii and 9.
Fig. 3.14. Ichnological and sedimentological features of proximal prodelta…….. 46
or prodeltaic inter-lobe embayment at the shelf-edge as exposed in Outcrop 6C-i.
Fig. 3.15. General view and sedimentary features of the outer shelf deltaic…….. 50
lobe as exposed in Outcrop 11.
Fig. 3.16. Ichnological features of wave-modified fringing barrier bars…… 52
or outer shelf shoals.
Fig. 3.17. Ichnological and sedimentological features of proximal prodelta…….. 54
or inter-lobe embayment on outer shelf, as exposed in Outcrop 11.
Fig. 3.18. The canyon/gully-fill succession cutting across the distal/discrete…… 57
wave-modified subaqueous barrier bar system of the shelf-edge delta-front.
Fig. 3.19. Sedimentary features of the canyon/gully-cut and -fill as exposed…… 60
in Outcrops-8B and -C.
Fig. 3.20. Schematic block diagram, modified after Edwards (1981),……... 64
showing different depositional subenvironments of the Mayaro Formation belonging to the shelf-edge delta and outer-shelf delta systems.
Fig. 3.21. Schematic reconstruction of trace fossil distribution in different……... 74
subenvironments of the shelf-edge delta and the associated outer shelf delta.
Fig. 3.22. Cartoon showing lateral and vertical facies associations in the……. 75
Mayaro Formation outcrops.
Fig. 4.1. Location maps. …….. 80
Fig. 4.2. The southern wall or the incision-surface of the paleo-canyon...…… 83
and the associated underlying and overlying sedimentary facies.

Fig. 4.3. Northern wall or the incision-surface of the paleo-canyon and ...…… 84
associated underlying and overlying sedimentary facies.
Fig. 4.4. Trace-fossil suite within delta-front sheet-like sandstone bodies……. 85
in the immediate vicinity of the southern wall (marked by the red arrow) of the paleo-canyon.
Fig. 4.5. Trace-fossil suite within the delta-front heterolithic intervals in the…… 88
immediate vicinity of the southern wall (marked by the red arrow) of the paleo-canyon.
Fig. 4.6. Schematic diagram showing stages of the development of the…… 92
Glossifungites Ichnofacies on the paleo-canyon wall in the succession of Mayaro Formation, Trinidad.
Fig. 4.7. Schematic diagram of the conceptual depositional model in relation…….. 94
to the development of the *Glossifungites* Ichnofacies.
Fig. 5.1. Simplified Pliocene-Quaternary stratigraphic column of 101
southern……...
Trinidad and its eastern offshore vicinity.
Fig. 5.2. (A) Paleographic map of the Gelasian paleo-Orinoco delta system……. 102
showing tentative distribution of the depositional sub-environments in relation to the structural features (modified after Bowman, 2003). (B) The rectangle in Fig. 5.2A is enlarged into the location map of the Mayaro Formation outcrops (marked in red) with the outcrop numbers. (C) The RMS-amplitude slice approximately from the Gelasian horizon of the 3D seismic volume. (D) Vertical TWT section from the 3D seismic volume roughly focused at the Gelasian horizon along the XY straight-line in Fig. 5.2A-C, showing the recurrent canyon/gully activity.
Fig. 5.3. Schematic section perpendicular to the axis of the …….. 108
paleo-canyon/gully and parallel to the depositional strike of the shelf-edge delta.
Fig. 5.4. Photographs of the lithofacies defining the FT-A to -C. ……. 109

Fig. 5.5. Photographs of the lithofacies defining the FT -D……... 113

Fig. 5.6. Photographs of the lithofacies defining the FT-D to -E...…… 114

Fig. 5.7. Photographs of the lithofacies defining the FT-F……. 119

Fig. 5.8. Schematic representation of the different base levels …….. 122
versus the time curves with respect to the 'sixth-order' physiographic events.

Fig. 5.9. (A) Cartoon showing the lateral and the vertical associations……. 124
of subenvironments of shelf-edge delta in the Mayaro Formation outcrops and also the relationship of the canyon/gully-filling facies tracts (FT-A to E) with the deltaic facies tract (FT-F), which chiefly belongs to the delta-front subenvironments. (B) Relationships among the 'fourth-' and 'fifth-order' sequences, and 'sixth-order' system tracts in TWT seismic section interpreted from Fig. 5.2D.

Fig. 6.1. Paleogeography and stratigraphy of the late Miocene – Pliocene…… 135
in the Southern Basin.

Fig. 6.2. Geological and outcrop maps …….... 136

Fig. 6.3. Schematic stratigraphic cross section of the Morne L'Enfer ……... 138
Formation in the westernmost fault block of the Fullarton section (between reference points FL01 and FL08).

Fig. 6.4. Photographs showing five different locations from the exposures of…….. 139
the FT-L and the contact between the FT-L (underlying) and the FT-U (overlying).

Fig. 6.5. Characteristic ichnological features of the unit FT-L..…… 140

Fig. 6.6. Schematic diagram showing composite ichnofabric of the unit……... 143
FT-L, produced by the upward migration of the shallow and middle tiered community in response to vertical aggradation of the shelf floor.

Fig. 6.7. Characteristic ichnological features of the unit FT-U within……... 145
different facies.

Fig. 6.8. Schematic diagram showing different niches of spatangoid……. .. 159
colonization on the shelf and in the presence of advancing clastic wedges deposited in settings influenced by hyperpycnal and hypopycnal discharges and wave actions.

CHAPTER 1: INTRODUCTION AND LITERATURE REVIEW

River-deltas have been defined by many authors since the time of Pliny the Elder (Plinius Secundus, ca. 77-79). I summarise my understanding as follows. *Involving seaward movement of the shoreline, the clastic sedimentary wedges, which develop subaqueously and subaerially, and accumulate at the region wherever rivers encounter standing bodies of water (i.e., oceans or lakes or intra-continental marshland) are known as river-deltas (or simply deltas, in general, unless referring to specific depositional environments, e.g.,, alluvial or colluvial "deltas" or deep-marine "deltas")*. While entering a standing body of water, the kinetic energy of the river required to transport clastic sediments significantly runs out; therefore, the transported materials are deposited at the rivermouth as a 'fanning out' clastic wedge, which systematically varies in terms of the sedimentary facies from proximal to distal areas of the rivermouth and also from the axial part to laterally away from it, depending on the relative dominance of fluvial and oceanic processes (see below). The interaction of bethic animals with these sedimentary facies also varies in terms of the types of colonizers, and their behavioural and feeding habits (see below).

For the last half a century, deltas remained within the focus of geoscientists in both academia and the hydrocarbon industry. Galloway's (1975) seminal triangular classification of deltas based on relative influences of river, waves, and tidal actions has shown the path forward for research in deltaic sedimentology especially for the last 10–15 years, during which the literature became substantially enriched (*e.g.,* Bhattacharya and Walker, 1992; Orton and Reading, 1993; Kuehl *et al.*, 1997; Kolla *et al.*, 2000; Bhattacharya and Giosan, 2003; Sidi *et al.*, 2003; Saller and Blake, 2003; Porębski and Steel, 2003, 2006; Giosan and Bhattacharya, 2005; Giosan *et al.*, 2005; Correggiari *et al.*, 2005; Bhattacharya, 2006; Bhattacharjee *et al.*, 2006; Olariu and Bhattacharya, 2006; Giosan, 2007; Buatois *et al.*, 2008; Bhattacharya and MacEachern, 2009; Li *et al.*, 2010; Olariu *et al.*, 2010; Nageswara Rao *et al.*, 2010; Ashton and Giosan, 2011; Dan *et al.*, 2011; Vakarelov *et al.*, 2012; Purkait and Majumdar, 2014; Nienhuis *et al.*, 2015; Korus and Fielding, 2015; Patruno *et al.*, 2015; Flood *et al.*, 2015). However, the literature is also highly skewed favouring inner-shelf deltas. Moreover, depositional facies modeling for two- and three-dimensional distribution of architectural elements in a deltaic system lacked much emphasis until the beginning of the last decade (Gani and Bhattacharya,

2005). Ichnological evaluation of marginal marine depositional environments, particularly in deltaic-estuarine environments, is also a recently developing field. There have been a limited number of published studies until mid-2000s describing the relationships between trace fossils and deltaic sedimentary processes (*e.g.*, Hobday and Tavener-Smith, 1975; Turner *et al.*, 1981; Pollard *et al.*, 1982; Moslow and Pemberton 1988; Lewis and Ekdale, 1991; Buatois and López Angriman, 1992; Gingras *et al.*, 1998; Siggerud and Steel, 1999; Martinius *et al.*, 2001; Corbeanu *et al.*, 2004; Garrison and van der Berg, 2004; McIlroy 2004; Chakraborty and Bhattacharya, 2005). Identification of ecologic stress factors on benthic animals has recently been employed by integrating sedimentological, ichnological, and stratigraphic data in precisely characterizing different types of sedimentary processes taking place in specific deltaic subenvironments (MacEachern *et al.*, 2005, 2007a, 2007b; Hansen and MacEachern, 2007; McIlroy, 2007; Buatois *et al.*, 2008, 2011, 2012; Carmona *et al.*, 2008, 2009; Bhattacharya and MacEachern, 2009; Jones, 2013; Ayranci *et al.*, 2014).

A shelf-edge or shelf-margin delta is the seaward end member of all kinds of river-deltas with respect to their position on the continental shelf (see *Fig. 1* in Porębski and Steel, 2006). The position of a delta on the shelf is controlled by relative sea-level cycle(s) under the influence of eustasy, plate tectonics, sediment supply and accumulation rate, and the geometrical/physiographic architecture of the shelf. Although development of a shelf-edge delta is not a rare geological phenomenon, its stratigraphic preservation potential, especially as outcropped analog, is poor due to later erosion events, subduction, and collisional orogeny (Ingersoll and Graham, 1983), unless slivers of outer continental shelves get uplifted or obducted. Sedimentological studies of shelf-edge deltas started in the 1980s (Edwards, 1981; Suter and Berryhill, 1985; Neuberger, 1987; Mayall *et al.*, 1992). However, advancements in characterizing the shelf-edge delta deposits have quite recently been made (*e.g.*, Sydow and Roberts, 1994; Mellere *et al.*, 2002; Kolla *et al.*, 2003; Sneider, 2003; Steel *et al.*, 2003; Porębski and Steel, 2003, 2006; Gardner *et al.*, 2005; Cummings *et al.*, 2006; Uroza and Steel, 2008; Moss-Russell, 2009; Covault *et al.*, 2009; Flint *et al.*, 2011; Rouby *et al.*, 2011; Sonibare *et al.*, 2011; Dixon *et al.*, 2012a, 2012b, 2013; Moscardelli *et al.*, 2012; Sánchez *et al.*, 2012; Olariu *et al.*, 2013; Bourget *et al.*, 2014; Bowman and Johnson, 2014; Schwartz and Graham, 2015). Also very recently, researchers have documented trace fossil occurrences from outcrop and core data

while characterizing facies and understanding the stratigraphic context of ancient shelf-margin delta deposits (Larsen and Surlyk, 2003; Vincent *et al.*, 2007; Uroza and Steel, 2008; Covault *et al.*, 2009; Flint *et al.*, 2011; Dixon *et al.*, 2012a, 2012b, 2013; Bowman and Johnson, 2014). However, no detailed ichnological analysis delineating the stress factors on colonizers is available. Sedimentological and especially detailed ichnological studies on inner-shelf deltas, which rapidly transited on the shelf towards the shelf-break before assuming the shelf-edge delta stage, are also rare (*e.g.,* Olariu *et al.*, 2012).

The Neogene and Pleistocene of the Southern Basin in Trinidad and the adjoining Columbus Basin, originally defined by Michelson (1976) and Leonard (1983) in immediate eastern offshore situated off the SE shoreline of Trinidad Island, provide an opportunity to study uplifted outcrops and subsurface preservation of the transiting inner-shelf and shelf-margin deltaic lobes of the paleo-Orinoco River system (see *Fig. 1* in Wood, 2000; *Fig. 18.1* in Gibson *et al.*, 2012). The NE margin of the South American Plate was a passive margin setting during the Jurassic to Early Oligocene (Gibson *et al.*, 2012). The basin afterwards evolved as a large, structurally complex, Neogene-Pleistocene oblique foreland depocenter filled with siliciclastic sediments delivered by the paleo-Orinoco River. In the Late Oligocene, the transformation of the basin from passive margin to foreland setting had also been associated with fundamental changes in the paleo-Orinoco River in terms of its sedimentary provenance and drainage system (Xie and Mann, 2014): (a) The Andean Cordillera contributed more sediments in addition to the Precambrian Guyana Shield; (b) The transformation also included the paleo-Orinoco becoming a major drainage system replacing the pre-existing smaller drainages into the ocean. Evolution of the Columbus Basin vis-à-vis its tectonic and structural geological setting is debated as one of the most complex Cenozoic basins of the world due to the juxtaposition of rotated and faulted blocks (for structural and plate tectonic configuration of southern Trinidad and Columbus Basin, see Dunham *et al.*, 1996; Algar, 1998; Pindell *et al.*, 1998; Babb and Mann, 1999; DiCroce *et al.*, 1999; Wood, 2000; Pindell & Kennan, 2009; Garciacaro *et al.*, 2011a, 2011b; Gibson *et al.*, 2012). In fact, the *"graveyard of geologists"* is the term that was applied even by the famous Trinidadian geologist and former Honourable Prime Minister of Trinidad, Patrick Manning, indirectly referring to the complex stratigraphic juxtaposition of crustal blocks making correlation of strata at the regional scale extraordinarily difficult (Manning, 2003). Due to the

oblique convergence between the Caribbean and South American Plates, the Columbus Basin initially developed as a transpressional foreland basin in response to the fold-thrust belt along Serranía del Interior-Central Range system until the Early Tortonian, after which the basin attained a thin-skinned pull-apart stage during Pliocene. During Early Pleistocene (Gelasian) the transpression tectonics reinitiated and ensued, resulting in (i) Southern Range uplift, (ii) renewed uplift of the Central Range-Darien Ridge system, and (iii) uplift of the Galeota and Teak Ridges (Gibson *et al.*, 2012). Due to this uplift, parts of the deltaic sediments deposited during on-shelf transit of the paleo-Orinoco river-mouth and during its first shelf-edge phase(s) are exposed as outcrops in southern Trinidad. In this doctoral research project, the scope of work has been narrowed down to the study the sedimentological, ichnological, and sequence stratigraphic characteristics of those uplifted outcrops of two specific formations in the Southern Basin – the Mayaro and the Morne L'Enfer formations. The stratigraphic ages of both formations are a highly disputed topic. The Mayaro Formation is devoid of any peer-reviewed published biostratigraphic data. Also, all the recent references to the Mayaro Formation in the literature do not follow the reassignment of Gelasian Age into the Pleiscocene Icehouse (Gibbard *et al.*, 2010). Referring to unpublished industrial proprietary palynological data, Bowman (2003) reported the age to be 2.3±0.3 Ma (*i.e.,* Gelasian). Later retracting from previous estimation after correlating proprietary subsurface data from offshore hydrocarbon fields with published geological maps, Bowman and Johnson (2014) reported the age to be ca. 3.5 Ma (*i.e.*, Piacenzian/late Pliocene). The samples collected from the outcrops of the formations during the course of this study yielded no microfossil or macrofossil (except a few intact fossilized plant leaves belonging to the Combretaceae family in the Mayaro Formation; see Section 3.4.2.6). The barren nature of the deposits can possibly be attributed to the acute dilution of body fossils by the very high sediment accumulation rates and the post-depositional dissolution of calcareous fossils. We assume the age of the shelf-edge deltaic deposits of the Mayaro Formation to be Gelasian (explained in Section 3.2.1), whereas the age of the inner-shelf deltaic counterpart in its on-shelf transit phase before reaching the shelf-break belonging to the Morne L'Enfer Formation to be slightly older (*i.e.,* late Pliocene) (Kugler, 1956, 2001; Saunders and Kennedy, 1965; Donovan and Jackson, 1994; Wach *et al.*, 2003; Vincent *et al.*, 2007; Vincent, 2008; Wach and Vincent, 2008; Osman, 2006; Winter, 2006; Steel *et al.*, 2007; Chen *et al.*, 2014). Further details on the geological settings of study areas are provided in each chapter.

The primary objectives of the doctoral research project are to collect sedimentological, ichnological, and basic structural data from the study areas in order to characterize the ecological stress factors and the sedimentological processes acting within each subenvironment of the on-transit inner-shelf and the shelf-edge deltaic deposits. The study is the first of its kind to comprehensively evaluate the sedimentary processes taking place at the shelf-edge and on the shelf during the transit of a prograding clastic wedge through integration of sedimentological, ichnological, and sequence-stratigraphic understandings. How the integration of ichno-sedimentological characteristics helped in this project in terms of preparation of the constituent manuscripts (Chapters 3–6) has been furnished in the following chapter (Chapter 2: Transition).

CHAPTER 2: TRANSITION

During a couple of field seasons in 2011 and 2013, the entire section of Mayaro Formation outcrops in Mayaro-Guayaguayare area in SE Trinidad and the basal section of the Morne L'Enfer Formation outcrops in the Fullarton area in SW Trinidad were measured (Figs. 3.1B-C, 4.1A-B, 4.2A-B, 6.2A-B). Sedimentological, ichnological, and basic structural data were collected and interpreted. By integrating the sedimentological and ichnological data in Chapter 3, the ecological stress factors on infaunal colonization and preservation potential of trace fossils vis-à-vis the intrinsic sedimentary processes have been characterized for all the twelve depositional subenvironments of the shelf-edge delta system (Tables 3.1 and 3.2; Figs. 3.20 and 3.21). During this process, the canyon/gully incision surface in the Mayaro Formation was identified through delineation of the unique monospecific *Glossifungites* Ichnofacies suite (see Chapter 4). Initially the previous interpretation of 'prodelta on upper shelf' by Bowman (2003) was retained while constructing a stratigraphic model for the sediments filling the inside of canyon/gully cutting across the shelf-edge delta-front (Fig. 4.7). While further characterizing each individual subenvironment, no stratigraphically significant discontinuity surface was found separating them except the incision surface itself. Therefore, except for the canyon/gully-fill, the entire Mayaro Formation was found to be lateral associations of deltaic subenvironments (as discussed in Chapter 3), whereas the canyon-gully-fill was found to be a series of facies tracts comprising almost entirely of different types of sediment-gravity flow deposits. In Chapter 5, the stratigraphic model for the canyon/gully-fill has been revisited by explaining the systematic variations of the facies tracts through the hypothesis of high-frequency interference pattern between regional glacio-eustatic curve and subsidence curve by the growth-fault tectonics and associated ductile 'shale'-kinesis (Figs. 5.8A-C, 5.9A-B). As in Chapter 3, the same exercise is repeated for the basal part of Morne L'Enfer Formation outcrops, where the open shelf to deltaic transition is displayed by the first pulse of the inner-shelf deltaic clastic wedge overlying directly on the shelf deposits along an erosional surface. High fluvial influence on infaunal colonization has been found in this clastic wedge. Chapter 6 furnishes the case of a drastic change in sedimentary regime (from open shelf below to delta-front above) across this autogenic erosional surface and the responses arising from this regime change on ichnological characteristics

(particularly the responses of the irregular sea-urchin burrowers) in different delta-front subenvironments influenced by hyperpycnal, and also possibly hypopycnal, discharges.

CHAPTER 3: EVALUATING THE IMPACT OF STRESS FACTORS ON ANIMAL-SEDIMENT INTERACTIONS WITHIN SUBENVIRONMENTS OF A SHELF-MARGIN DELTA, THE MAYARO FORMATION, TRINIDAD

Dasgupta, S., Buatois, L.A., and Mángano, M.G., 2015, Living on the edge: evaluating the impact of stress factors on animal-sediment interactions within subenvironments of a shelf-margin delta, the Neogene Mayaro Formation of Trinidad: *Journal of Sedimentary Research*, accepted and revision submitted.

Keywords: Shelf-edge delta, stress-factor(s), ichnology, bioturbation, animal-substrate interactions.

Abstract

Integrating sedimentological and ichnological characteristics of the Gelasian Mayaro Formation along the SE coast of Trinidad allows recognition of a river-dominated to wave-influenced shelf-edge deltaic succession of the paleo-Orinoco River developed under strong slope instability. Four main sedimentary settings and twelve subenvironments developed on and beyond the outer shelf (*i.e.*, at the shelf-margin) have been identified. Extreme paleoenvironmental conditions make the succession rarely and sporadically colonized. The subenvironment-specific stress factors acting upon the colonizers are diverse in terms of their combinations and rankings (in terms of degree of influence). Ichnological evidence suggests that shelf-edge deltas are among the most stressful marine environments, due to a combination of physicochemical factors in response to the intrinsic sedimentary processes and the relative hierarchy of their influences specific to every subenvironment. Within any particular subenvironment, the relative dominance of the fluvial feeder system, the action of waves (and rare influence of tides), and slope-instability determine the combinations and ranking of stress factors. Fluvial-dominated shelf-edge subenvironments demonstrate the extreme influence of stress factors related to channel activity (*e.g.*, salinity changes, high sedimentation and erosion rates, flocculation of mud, seasonal variations of river flux), whereas wave-/storm-/oceanic

swell-dominated subenvironments away from the axial feeder(s) are mostly influenced by barform morphodynamics and their effects on local physiography. The paleo-Orinoco delta is not only represented by the delta lobe(s) developed at the shelf-edge, but by delta lobe(s) formed on the outer shelf as well. Outer shelf deltaic subenvironments manifest typical ichno-sedimentological signatures of a 'normal' (wave-influenced in this case) inner-shelf delta. Being susceptible to extensive gravitational instabilities characteristic of the shelf-margin and upper-slope, the delta system suffered from canyonization/gullying and subsequent filling (see Chapter 5). The shelf-edge delta system was also associated with 'shelf-attached' mass transport systems. Such depositional subenvironments dominated by slope-instability and gravity flows appear to be the most unconducive for benthic colonization, resulting in the almost complete absence of bioturbation. Characterization of the stress factors, as the functions of parameters arising from specific sedimentary/oceanographic processes, chemical conditions, and preservational constraints specific to each subenvironment, leads to the construction of a comprehensive ichnological and depositional analog model for shelf-edge deltas in general, and for the accommodation-driven low-latitude shelf-edge deltas at an active oblique foreland setting in particular.

3.1 Introduction

A shelf-edge delta (also known as shelf-margin delta) is the basinward end member of all kinds of river-deltas (see *Fig. 1* in Porębski and Steel, 2006) with respect to their position on the continental shelf, being controlled by the relative sea-level cycle, sediment accumulation rate and the architecture of the shelf. Delta construction at or beyond the shelf-edge by a river is not a rare phenomenon, but is rarely preserved in the geological record due to ensuing transgressive erosion and/or later subduction (Ingersoll and Graham, 1983). Sedimentological understanding of processes taking place in shelf-edge deltas started developing in the 1980s (Edwards, 1981; Suter and Berryhill, 1985; Neuberger, 1987). Over the last decade, there has been a great advancement in constructing depositional and stratigraphic models for deltas forming at the shelf-break and beyond (Kolla *et al.*, 2003; Sneider, 2003; Steel *et al.*, 2003; Porębski and Steel, 2003, 2006; Gardner *et al.*, 2005; Cummings *et al.*, 2006; Uroza and Steel, 2008; Moss-Russell,

2009; Covault *et al.*, 2009; Flint *et al.*, 2011; Rouby *et al.*, 2011; Sonibare *et al.*, 2011; Dixon *et al.*, 2012a, 2012b, 2013; Moscardelli *et al.*, 2012; Sánchez *et al.*, 2012; Olariu *et al.*, 2013; Bowman and Johnson, 2014; Bourget *et al.*, 2014). However, the ichnology of marginal marine settings, particularly of deltaic depositional environment, is a more recently developing field. There was a relatively limited number of published studies until the mid-2000s describing the relationships between trace fossils and deltaic sedimentary processes (*e.g.*, Hobday and Tavener-Smith, 1975; Turner *et al.*, 1981; Pollard *et al.*, 1982; Moslow and Pemberton 1988; Lewis and Ekdale, 1991; Buatois and López Angriman, 1992; Gingras *et al.*, 1998; Siggerud and Steel, 1999; Martinius *et al.*, 2001; Corbeanu *et al.*, 2004; Garrison and van der Berg, 2004; McIlroy 2004).

Since 2005, delineation of ecologic stress factors on deltaic benthos has been successful in characterizing different delta types and their subenvironments by integrating sedimentological and ichnological datasets (MacEachern *et al.*, 2005, 2007a, 2007b; Hansen and MacEachern, 2007; McIlroy, 2007; Buatois *et al.*, 2008, 2011, 2012; Carmona *et al.*, 2008, 2009; Bhattacharya and MacEachern, 2009). Being guided by Galloway's (1975) seminal triangular classification of deltas, stress factors have been delineated for river-dominated, wave-, and tide-influenced deltas. Even more recently, emphasis has been placed on mixed deltas in order to discriminate the variable influences of river, wave and tidal processes (*e.g.*, Vakarelov *et al.*, 2012). Stress factors including intensified sediment accumulation and erosion rates, turbidity (concentration of suspended particles) and turbulence, salinity fluctuations, occasional sediment-gravity flows of different genesis (*i.e.*, "ignitive" or instantaneous surge-type and sustained; see *Chapter 4* in Weimer and Slatt, 2007) and rheological types (*i.e.*, from plastic to Newtonian), and phytodetrital pulses are characteristics of fluvial dominance. In tide-influenced deltaic settings, clay flocculation, fluid-mud deposition, and subaerial exposure are the primary factors affecting animal-substrate interactions. Stresses induced by longshore current and storm activity in wave-influenced deltas affect the colonizers in the same way as they do in other wave-dominated settings, *e.g.*, in shallow marine environments, although the effects are more intense in deltas due to additive factors of fluvial and/or tidal influences. Waves results in an elevated energy condition affecting morphodynamics (*i.e.*, both sedimentation rate and bar migration) of the large bedform or barform deposits, wave scouring, and longshore drift. [*N.B.* The term 'barform' has

been used, often interchangeably with bedform deposits, throughout the thesis implying the large, often elongated, and low-gradient bedform or dune deposits. Although initially in the literature, especially in text books, it had been used with braided fluvial and tidal geomorphic connotation, in recent years the term has also been abundantly used for elongated and low-gradient dunes developed in shallow, marginal, and deep marine environments (e.g., Hickson and Lowe, 2002; Arnott, 2003; Hubbard et al., 2008; Pemberton et al., 2015).]

The existing literature has dealt with ichnological characterization of inner-shelf deltas. While describing, characterizing and modelling ancient shelf-edge deltas, researchers have mentioned trace fossil occurrences (Vincent *et al.*, 2007; Uroza and Steel, 2008; Covault *et al.*, 2009; Flint *et al.*, 2011; Dixon *et al.*, 2012a, 2012b, 2013; Bowman and Johnson, 2014), but no detailed ichnological analysis is available. The present study is the first to characterize and rank ecologic stress factors on animal-substrate interactions in shelf-edge deltas utilizing the Gelasian Mayaro Formation in SE Trinidad Island as an analog. Ease of accessibility, conducive logistics and weather, and the availability of published studies on the sedimentological characteristics make the Mayaro Formation a type locality for ichnological studies of shelf-edge deltas developed in low latitudes.

3.2 Geologic setting

3.2.1 Columbus Basin

The Columbus Basin, originally defined by Michelson (1976) and Leonard (1983), is situated off the SE coastline of Trinidad. The basin evolved as a structurally complex Mio-Plio-Pleistocene depocenter filled with clastic sediments delivered by the paleo-Orinoco River (Wood, 2000). Detailed discussion on the tectono-structural evolution of the Columbus Basin has been presented by many scholars (*e.g.*, Dunham *et al.*, 1996; Algar, 1998; Pindell *et al.*, 1998; Babb and Mann, 1999; DiCroce *et al.*, 1999; Wood, 2000; Pindell and Kennan, 2009; Garciacaro *et al.*, 2011a, 2011b; Gibson *et al.*, 2012). Due to the oblique convergence between the Caribbean and South American Plates, Columbus Basin initially developed as a transpressional

foreland basin between the Oligocene and Tortonian, after which the basin attained a thin-skinned pull-apart stage during the Pliocene. During the Early Pleistocene the transpressional uplift re-ensued (Gibson *et al.*, 2012). Sometime during the Pliocene-Early Pleistocene, the paleo-Orinoco River delta reached the shelf-margin and started forming its delta-front along the shelf-break controlled by growth fault tectonics with extremely high sediment accumulation and/or accommodation creation rates (*i.e.*, 5-10 m/ka in Wood, 2000 and Bowman and Johnson, 2006, 2014; or 10 m/ka in Alvarez, 2008). With the successive growth faulting and progradation of the delta, the shelf-break moved basinwards (Wood, 2000; Sydow *et al.*, 2003; Garciacaro *et al.*, 2011b; Gibson *et al.*, 2012). There is a series of NNW-SSE oriented growth faults (*e.g.*, Cedar Grove Growth Fault) (Fig. 3.1C; also see *Figs. 3-4, 6* in Garciacaro *et al.*, 2011b). The depositional strike was possibly guided by the orientation of the growth faults. The Gros Morne Formation and the younger Mayaro Formation constitute the first two pulses of delta-front sedimentation at/near the shelf-edge (Fig. 3.1A-C). However, the Mayaro Formation represents the first undisputed shelf-edge delta-front development, being guided by a growth fault (which is possibly the Cedar Grove Fault). Porębski and Steel (2006) estimated the Quaternary Orinoco River delta to be an accommodation-driven one, which thereby invariably requires relative sea-level fall in order to attain shelf-edge stage. There is no other stratigraphic record throughout the late Oligocene to Pliocene of the paleo-Orinoco delta reaching the shelf-edge. This implies that the delta possibly remained consistently accommodation-driven throughout its geological record. Sometime in the Piacenzian-Gelasian ages the inner-shelf paleo-Orinoco delta completed its transit of the wide paleo-shelf and reached the shelf-edge due to relative sea-level fall, when the Gros Morne Formation and Mayaro Formation sediments were deposited. With the deposition of the Mayaro Formation, the paleo- Orinoco delta kept on prograding with the eastward prograding shelf-edges beyond the SE shoreline of Trinidad (Wood, 2000; Sydow *et al.*, 2003; Bowman, 2003; Uroza, 2008; Bowman and Johnson, 2014).

The age of the Mayaro Formation is controversial due to the lack of published biostratigraphic data. Based on palynologic data, Bowman (2003) reported the age to be 2.3±0.3 Ma (*i.e.*, Gelasian/Early Pleistocene). Correlating proprietary subsurface data from offshore hydrocarbon fields with published geological maps (*e.g.*, Kugler, 1959, 1996, 2000), Bowman and Johnson (2014) later reported the age to be ca. 3.5 Ma (*i.e.*, Piacenzian/late Pliocene). We

found the entire Mayaro Formation to be barren of body-fossils, after analyzing 48 samples collected from almost all the thick (thickness > 5 m) mudstone and muddy heterolithic intervals. Renewal of transpressional tectonic uplift during Gelasian and afterwards, and the Pleistocene Icehouse, which started in Gelasian (the Pretiglian), are likely to be the reasons for the relative sea-level fall that caused the accommodation-driven delta to remain at the shelf-edge. Notably, the onset of those two events corresponds the age of the Mayaro Formation to the previously estimated age (*i.e.,* ca. 2.3±0.3 Ma) as reported by Bowman (2003).

3.2.2 Study area

The Quaternary transpressional uplift exposed the Mayaro Formation outcrop as the southern limb of a synclinorium between Galeota Point and Mayaro (Fig. 3.1B). The outcrops exposed as small cliffs of different heights and lengths along the 4.6 km stretch of SE shoreline of Trinidad constitute our study area (Fig. 3.1B-C). Structurally, the strata are tilted northerly (dip towards north from avg. 45° in Outcrops 1A-1B to avg. 14° in Outcrop 11). Approximately 765 m of true thickness of discontinuous outcrops is exposed. Bowman (2003) postulated that the thick mud-rich units being eroded out comprise the gaps in continuity of outcrops. That assumption is not supported by – (1) the sands being semi-consolidated to unconsolidated and (2) more than 100 m thick mud-dominated exposed interval (Outcrops 8B-8C) being more resistant to erosion than semi-consolidated sandstones. It is strangely improbable that, in a series of gently dipping outcrops parallel to depositional strike, substantially thick mud-rich intervals never get exposed except at one long stretch (*i.e.*, Outcrop 8B-8C).

Considering the stratal inclination and total stretch of exposures along the true dip direction, the total stratigraphic thickness of Mayaro Formation is ca. 2 km from Outcrop 1A to Outcrop 12. The upper 65 m succession at Radix Point Hill (Fig. 3.1B) resembles Outcrops 10-11 in ichnological and sedimentological characteristics. However, because Radix Point is located within the intense tectonic deformation zone of the Darrien Ridge, paleogeographic reconstruction and correlation of Radix Point outcrops are not possible with respect to Outcrops 10-11 or younger unexposed strata of Mayaro Formation (Bowman, 2003).

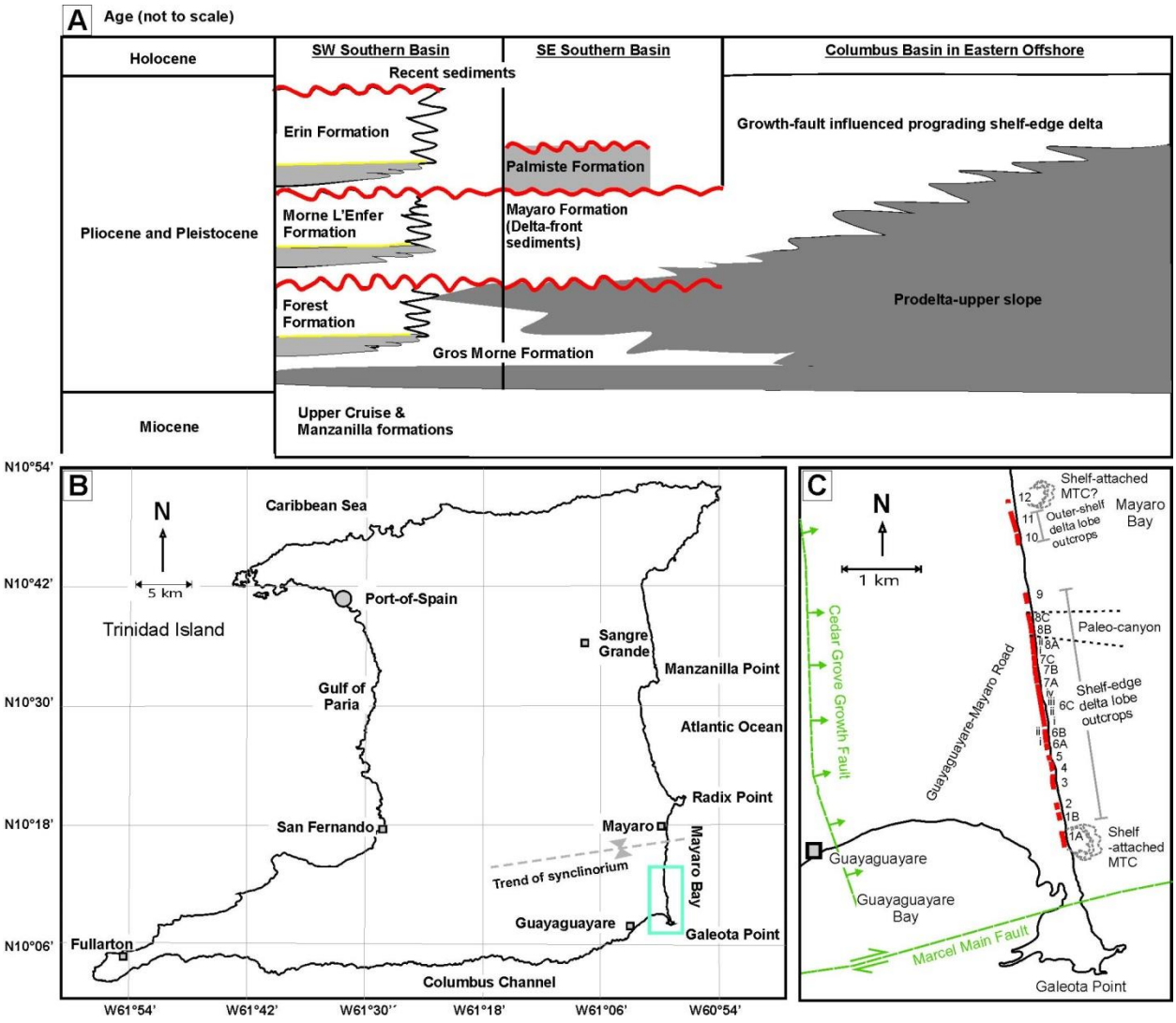

Fig. 3.1. General stratigraphy and location of the study areas. (A) Simplified chronostratistratigraphic position of the Mayaro Formation and its depositionally equivalent sedimentary successions in southern Trinidad and its eastern offshore vicinity (Dasgupta and Buatois, 2015). (B) Location of the Mayaro Formation outcrops shown by the blue rectangle on the map of Trinidad. The trend of the southern synclinorium is shown with the dotted line (following Saunders, 1997). (C) Map showing the Mayaro Formation outcrops along with their depositional settings. The depositional strike is along the Cedar Grove Growth Fault, which is roughly parallel to the contemporary shelf-break, also coinciding with the SE coastline of Trinidad.

3.3 Methods

All the twelve outcrop segments have been measured and described in the field taking grain-size, physical sedimentary structures, facies associations, ichnodiversity, bioturbation intensity, degree of lithification, and discontinuity surfaces into account. Accordingly, all the outcrop images are interpreted using a graphic drafting and design software. Some of the interpreted images are presented in this article. The interpreted images and associated mesoscopic photographs of the outcrops are utilized here to arrive directly at the depositional model. The facies descriptions are summarized in the 'Sedimentary facies association' column of Table 3.1. In the following section we address the depositional environment avoiding separate facies descriptions for each of the subenvironments in order to avoid redundancy. The sedimentological and ichnological datasets are integrated (as in Tables 3.1 and 3.2) to derive the possible ecological stress factors. For the convenience of potential application of the subenvironments in static reservoir modelling, the types of heterolithic sedimentary facies are kept to only three (*i.e.*, "upscaled"), using the sandstone net-to-gross ratio (NTG): viz. 10-30%, 30-60%, and 60-85%. Lithofacies having < 10% net sandstone are considered 100% net mudrocks, whereas those having > 85% are considered as 100% net sandstone.

Table 3.1. Summary of the depositional subenvironments, their outcrop occurrences, facies associations, and sedimentary processes of the paleo-Orinoco delta as displayed by the Mayaro Formation outcrops.

Subenvironments	**Outcrop distribution**	**Sedimentary facies association**	**Sedimentary processes**
Shelf-attached Mass Transport Complex (MTC)	Outcrops 1A, 12 (?)	Cohesive silt-rich muddy matrix-supported debris flow deposit. Rafted blocks of HCS-SCS sands and sandy heterolithic sediments common.	Arcuate collapse of the shelf-edge region onto upper slope as slump/mass debris flow and ensuing en-masse deposition. Physiographically funnelled through a feeder canyon in the proximal areas.
Incised canyon and canyon-fill	Outcrop 8B-8C	Clearly defined lateral canyon walls: 1) a southern wall (northerly 30°-40° slope after structural dip correction) at the top of Outcrop 8A succession, and 2) lateral termination and pinch-out on an irregular northern wall (southerly 15°-40° slope after structural dip correction). Canyon-fill	The Outcrops 8B-8C succession having more prominent architecture of an incised canyon-fill encased within wave-influenced barrier bar setting. Re-establishment of the delta-front at the top of succession with erosional bases. Sediment bypass dominates the filling phase.

		succession deposited from systematically varying types of sediment gravity flows – cohesive debris flow followed progressively sandier muddy sediment gravity flows until re-establishment of the delta-front. Therefore, the muddy canyon-fill is encased within the canyon being vertically and laterally surrounded by delta-front sediments.	
Active subaqueous feeder channel-fill	The upper 8-10 m interval of Outcrops 2; lower 12 m and 20-29 m interval from the base of Outcrop 4; Outcrops 3, 5 and 7A	Channels filled with TCS medium-grained lenticular to tabular sandy bedform deposits, intermittently intercalated with HCS-SCS beds. Wave-rippled, intermittently wrinkled top of the barforms also with localized parting lineations. Barforms with transient coarsening up grain-size trend. Localized gutter-casts and cut-and-fill structures in the thickest sand intervals.	Seasonal formation of sandy bedform deposits under unidirectional channelized flow on muddier slope showing signs of progradation within the channels. Modification by large oceanic waves and storm waves.
Abandoned/ avulsed channel-fill, internal levee	Upper ca. 15 m interval of Outcrop 4, upper 10 m interval of Outcrop 6A	Dominated by thin-bedded/laminated sandy heterolithics. Individual thin-beds/laminations commonly exhibiting inverse overlain by normally graded grain-size trends indicating possible sustained underflow (likely hyperpycnal). Gutter-casts, syneresis and other shrinkage cracks are abundant. Double mud laminations are sporadic within the heterolithic sediments. Abundant soft sediment deformation like layer-confined domino faults, ball-and-pillow, flame structures, fluid escape structures common.	Heterolithic-dominated channel-fill possibly reflects deposition away from channel axis or gradual avulsion or internal levee formation. Deposition is from sustained gravity flow or underflow, which is likely to be seasonal hyperpycnal flow. Transient tidal action suggested by double mud-laminations. Tidal energy dissipation possibly enhanced by topography. Thin mud laminations may have been deposited from quasi-laminar plug flow of mud precipitated from rapid flocculation.
Proximal overbank and crevasse complex of subaqueous channel	Lower 8.5 m interval of Outcrop 2; Outcrop 6A; lower ca. 40 m interval of Outcrop 6B-ii	Proximal overbank dominated by thin-bedded/laminated heterolithic sediments, layer-parallel slumps, slumps at the channel bank, sandy crevasse splays and crevasse channels. Numerous cut and fill structures, post-depositional neptunian injections, large gutter-casts, flame structures and background wave reworking as envisaged by HCS-SCS in medium-grained sandy intervals. Muddier heterolithic intervals locally with	Seasonal increase in flow volume and energy and centrifugal force at the channel bends causing proximal overbank formation. Slumping caused by oversteepened banks as a result of lateral scouring. Seasonal pause of channel activity manifested by modification of bedform deposits by large wave actions. Dominance of outsized gutter-casts, layer-parallel slumps, m-thick soft-sedimentary deformation structure indicating steep slope.

		shrinkage cracks.	
Distal overbank of subaqueous channel	Outcrop 1B, ca. 12-20 m interval of Outcrop 4 above its base	Laminated, silt-dominated muddy heterolithic deposits with intermittent HCS and 5-30% NTG ratio. Small scale soft-sediment deformation structures like layer-parallel ptygmatic folding, combined-flow ripples and synsedimentary domino faults.	Spilt over fine-grained sediments deposited away from the subaqueous feeder channel. Lamination-bound ptygmatic folding implying poor competency difference between competent sand layers and incompetent mud layers indicating fluidized soupy substrate with background moderate to low wave reworking.
Amalgamated terminal mouth bar	Outcrop 6C-i to lower part of 6C-ii; Outcrop 7B	Coarsening up grain-size variation from mud-dominated proximal prodelta deposits to medium-grained sandy amalgamated deposit, where the interface shows intense and large (metres scale) soft-sediment deformation structures, namely ball-and-pillow and flame structures, and a few gutter-casts. Systematic variation in lithofacies along the depositional slope from west to east: a) The upslope bedform deposits are large TCS, climbing dune stratified sand. b) The downslope deposits are sandy turbidite-grainflow deposit (Bouma Ta-Tb-Td). c) Transition zone between these modes of depositional style where climbing dunes tranform into small TCS and then into turbidite-grainflow.	The facies variation along the depositional slope indicative of terminal mouth bar. Amalgamation due to high sediment accumulation and wave action within and laterally with wave-influenced barrier bar complex along depositional strike.
Proximal wave-modified, subaqueous barrier system: Amalgamated and layered barrier bar complex	Parts of Outcrop 6C-ii; Outcrops 6C-iii and 6C-iv. Parts of Outcrop 7B. Outcrop 7C. Lower ca. 30 m interval of Outcrop 8A-i	Chiefly SCS (intermittently HCS) and tabular medium-grained sand bodies, either amalgamated 7-8 m thick (rare thickness amounts up to 25 m) or discrete 1-2 m thick layers separated by silty heterolithic sediments. The reactivation surfaces commonly containing gutter-casts, brecciated silty intraclasts and dm-thick debris flow deposits, soft sediment deformation like ball and pillows, flame structures. Exposed top surfaces of the bedform deposits contain signatures of microbial stabilization (wrinkle marks) and wave-ripples.	The paleocurrent directions of the feeder system in associated terminal lobe (*i.e.*, dominantly along 030° and weakly along 000°) indicate forced orientation of the feeder system along the longshore drift. Tabular sandy lithosomes interpreted to be elongated sand bodies along the longshore current direction. The large size of the SCS beds and grain-size indicate direct interaction between the shelf-edge and large oceanic waves and tropical storm waves.
Distal wave-	From middle	Chiefly SCS (intermittently	Sandy lithosomes interpreted to be

modified subaqueous barrier bar system of delta-front: Spit-bars and associated tidally influenced interbar shoals	interval of Outcrop 8A-i, through Outcrop 8A-ii to Outcrop 9 (while Outcrop 8B-8C documents the canyon-fill cutting across)	HCS) and tabular medium-grained sand bodies of discrete 1-3 m thick beds separated by thin-bedded/laminated silty heterolithic sediments with varying NTG ratio. Reactivation surfaces containing gutter-casts, brecciated silty intraclasts and dm-thick debris flow deposits, soft sediment deformation like ball and pillows, flame structures. Evidences of post depositional fluidization and fluid escape within the SCS bodies. Bar-tops showing wave-ripples and ladder-back wave-ripples with ripple crests parallel to 085-095° and 110-120°.	spit-like discrete subaqueous barrier bars with heterolithic intervals being deposited at the tidally influenced shoals at the periphery of interbar areas shielded by spit-bars. With relatively more marine influence, spit-bar and interbar system situated further away from the feeder system compared to the amalgamated and layered barrier splays. Shallower-water (*i.e.*, above the fair weather wave base) than the proximal barrier splays with bar-tops being exposed to swash action, rip currents and tidal incision into inlet formation. Wave reworking at the bar-tops and along the inter-bar areas. Heterolithic intervals reworked by wave-energy dissipation guided by the orientation of barforms. Bar-tops reworked by longshore drift. Sporadic occurrence of high colonization of *Ophiomorpha nodosa* associated with incised inlets indicative of relatively longer colonization window, as a result of relatively slower sediment accumulation compared to proximal barrier system, or as localized bar abandonment, or as overall slowing down of aggradation vis-a-vis basin subsidence.
Proximal prodelta	Outcrop 6B-i and lower 14 m interval from the base of Outcrop 6C-i	Coarsening up grain-size variation from a) laminated organic fragment-bearing silt and massive mud flow beds to b) thin-bedded/laminated sheet-like silt-sand intercalation gradually varying into sand bodies belonging to mouth bar and/or barrier splay. Abundant syneresis and other shrinkage cracks. Intermittent double mud laminations, mud-draped ripples, lenticular current-rippled sand and intermittent tidal bundles. Combined flow ripples abundant in coarser grained silt-sand intervals. Foundered ripples and mantle-and swirl structure in muddy intervals.	Stratigraphic superposition of prodeltaic sediments over delta-front deposits explained by 2 hypotheses: 1) autogenic retrogradation related to autobreak or autoretreat; 2) allogenic retrogradation caused by changes either in reduced sedimentation rate or faster subsidence (or both). In absence of any characteristics of transgressive surface at the base and the prodeltaic interval being very short, the change in depositional sub-environment is likely an autogenic one.
Wave-modified fringing barrier bars (outer shelf shoals)	Outcrops 10 and 11 (and also at the upper 65 m interval of the	SCS-HCS medium-grained metre(s)-thick tabular sand beds associated with intermittent layers of sand-rich heterolithic deposits (60-85 % NTG ratio)	Wave-influenced shoreface (rarely foreshore) barrier bar setting of delta-front under the influence of strong longshore drift on outer shelf under a regular marginal marine

	outcrops of Radix Point headland)	and non-cohesive debris flow deposits. Common layer parallel convolutions and slumps, and layer-confined soft sediment deformation structures like ball-and-pillows and flame structures. Gradual coarsening and thickening up trend with respect to underlying prodeltaic deposits in Outcrop 11. Lateral scouring surfaces also common. Rare swash cross stratification and swash-related liquefaction. Large nodules, commonly elongated or layer-parallel, are common with rare septarian clefts.	deltaic condition on a steep and narrow shelf near the shelf-edge. Relatively less gradient than shelf-edge and presence of at least a narrow sliver of shelf are manifested through the similarities with regular wave-influenced delta-front or inner-shelf shoals. Seasonal variation of weather interpreted from lam-scram stratification fabric. Limited subaerial exposure at the foreshore as evidenced by swash cross stratification and swash-related liquefaction.
Proximal prodelta and/or inter-lobe embayment on outer shelf	From 4 m to11 m interval from the base of Outcrop 11 (and also at the middle 30 m interval 65 m below the top of the succession of Radix Point outcrops)	Sheet like laminated silt-rich muddy interval and then gradually coarsening up into the sandy barforms. Sparse preservation of syneresis cracks and other shrinkage cracks. Gutter or chutes filled with TCS fine-medium grained sand with basinward 125°±5° paleocurrent direction and ca. 1:1.5 aspect ratio. Layer parallel slickensides, syn-sedimentary thrusts. Sparse preservation of tidal bundles. Intermittent organic fragment-rich thin beds are common. The transition from prodelta to delta-front is marked by increasing wave and directional flow influence as documented by increased number of lenticular beds, combined flow ripples and gutter-casts.	Deposited at areas of deltaic abandonment (autobreak) by switching delta-front lobes. Transient tidal influence a possible indication of deposition within embayment. Absence of any sedimentary feature suggesting hyperpycnal flow or wave-influenced underflow implies the system to be more buoyancy-driven than friction- and density-driven as in shelf-edge condition.

Table 3.2. Summary of the ichnological characteristics with respect to the stress factors and preservational biases as displayed by sediments deposited in different subenvironments of the Mayaro Formation outcrops.

Subenvironments	**Ichnological characteristics (ichnotaxa listed in order of decreasing abundance)**	**Stress factors and preservational biases (listed in order of decreasing importance)**
Shelf-attached Mass Transport Complex (MTC)	No bioturbation; BI = 0. Rare *Ophiomorpha nodosa* preserved within sandy HCS-SCS rafted blocks.	Rapid surge-type mobilization and deposition en-masse does not favour any colonization due to slope and substrate instability, and also because of trailing fluid mud activity after the deposition en-masse.
Incised canyon and canyon-fill	A) Southern wall (SCW) of the incision colonized by monospecific firmground *Thalassinoides* isp. (*Glossifungites* Ichnofacies) crosscutting the pre-existing softground trace fossil assemblages belonging to the distal wave-modified, subaqueous barrier system. Enormous incisional exhumation of firm sand overlain by cohesive debris flow deposits is demonstrated by the firmground burrows. B) Northern incision surface (NCW) not colonized, showing evidences of regular collapse as wedges of noncohesive cohesive debris flow deposits. C) Canyon-fill grossly unbioturbated (BI = 0) except very rare mottles or simple structures like *Planolites* isp. towards the top.	1) Cohesive debris flows unfavourable for any benthic animals to colonize due to substrate instability and fluid mud activity immediately after deposition en-masse. 2) Silty and organic rich underflow deposits having poor preservation potential due to lack of much lithological contrast. 3) Decomposition of organic materials after deposition triggering dysoxic-anoxic conditions. 4) Turbidity and turbulence along with rapid sediment accumulation rate associated with the sand-rich sediment gravity flows. 5) Lack or limitation of bedding parallel view at the outcrops effectively causing sampling bias.
Active subaqueous feeder channel-fill	Chiefly unbioturbated; BI = 0. Top surfaces of the barforms seldom moderately to highly colonized (BI = 3–4) with low ichnodiversity suite of vertical to horizontal burrows of opportunistic vermiform (*Skolithos* isp., *Planolites* isp., *Cylindrichnus* isp.) and bivalve (*Solemyatuba ypsilon*) colonizers. Downward decrease of intensity of bioturbation from top of the dunes. Vary rare intense (BI = 5) bioturbation at a reactivation surface at the base of Outcrop 5 with colonization of clay-lined *Thalassinoides* isp. and *Planolites* isp.	1) Morphodynamics of barform migration directly controlling the colonization of the bar-top, while sediment accumulation rate being very fast. 2) Salinity changes likely remains a background stress factor due to fluvial discharge. 3) Seasonal changes from hyperpycnal to hypopycnal stage. 4) Channel topography.
Abandoned/ avulsed channel-fill, internal levee	1) Rarely bioturbated; BI = 0–1. 2) Very low ichnodiversity suite of *Diplocraterion* isp., *Planolites* isp., *Rhizocorallium* isp. *Arenicolites* isp. 3) Extreme size reduction.	1) Salinity fluctuation is interpreted to be the main stress factor. 2) Fluid mud activity as tidally influenced quasi-laminar plug flow and rapid flocculation of mud may have acted as a hindrance for suspension feeders. 3) Tidal energy dissipation enhanced by the negative channel topography at the shelf-edge. 4) Seasonal changes from hyperpycnal to hypopycnal stage. 5) Channel topography.

Proximal overbank and crevasse complex of subaqueous channel	No bioturbation; BI = 0.	1) Freshwater influx. 2) Rapid rates of erosion and deposition narrowing colonization window. 3) Unstable slope.
Distal overbank of subaqueous channel	No bioturbation; BI = 0. Rare mottles.	1) Prevalent fluid mud activity and unstable soupy substrate as a taphonomic barrier. 2) Rapid flocculation rate. 3) Water turbidity as a hazard for suspension-feeders.
Amalgamated terminal mouth bar	No bioturbation; BI = 0.	1) Very rapid sediment accumulation and erosion. 2) High turbidity at the sediment-water interface. 3) High turbulence. 4) Freshwater discharge at the time of mouthbar formation.
Proximal wave-modified, subaqueous barrier system: Amalgamated and layered barrier bar complex	1) Localized bioturbation. 2) Low intensity of bioturbation (*i.e.*, BI = 0–1). 3) Paucispecific (*i.e.*, having composed of a few ichnospecies) colonization by decapod crustaceans, polychaetes and rarely sea-anemones. 4) Common forms documented are *Cylindrichnus* isp. and 3D gallery of *Ophiomorpha nodosa* in sandy lithosomes (*Skolithos* Ichnofacies). Heterolithic intervals with paucispecific suites (*Cylindrichnus* isp., *Skolithos* isp., *Teichichnus* isp., *Asterosoma* isp., *Bergaueria* isp., *Planolites* isp. and escape trace fossils). 5) Intensity and ichnodiversity grossly higher than in channel-filling sand bodies, but substantially less than in distal barrier system and analogous wave-modified shoals of outer shelf delta.	Transient and gradual change from fluvial dominance to more oceanic wave influence is evidenced by elevated ichnodiversity, ichnoabundance and occurrence of marine decapod and sea-anemone burrows. 1) Rapid sediment accumulation concomitant with subsidence. 2) Morphodynamics of bedform migration limiting colonization window in barforms. 3) Turbulence responsible for suspended particles detrimental to suspension feeders, whereas peripheral or inter-bar areas with less turbulence documents colonization of suspension feeders like sea-anemones.
Distal wave-modified subaqueous barrier bar system of delta-front: Spit-bars and associated tidally influenced interbar shoals	Different from amalgamated barrier splay system as follows: 1) Trace-fossil abundances are strikingly higher. Unbioturbated to sparsely bioturbated (BI = 0–1) within barforms, but low to highly bioturbated (BI = 2–4). 2) Ichnodiversity significantly higher and gradually increasing further away from the feeder system. The trace fossils in the sandy barforms are: *Ophiomorpha nodosa*, *Scolicia* isp., large escape trace fossils, *Macaronichnus* isp. and *Sinusichnus sinuosus*; whereas the heterolithic intervals are colonized with the following ichnotaxa: softground *Thalassinoides* isp., *Cylindrichnus concentricus*, *Scolicia* isp., *Teichichnus* isp., *Asterosoma* isp., *Rosselia* isp., *Conichnus* isp., *Bergaueria* isp., *Planolites* isp. and small escape trace fossils. 3) Outcrops 8A and 9 respectively record the striking appearance of *Scolicia* isp. and *Macaronichnus* isp. 4) Colonization by paucispecific suites only. 5) Specific bar-top with metres-wide tidal inlet incision and high colonization of *Ophiomorpha nodosa* (BI = 4). 6) Localized development of lam-scram features within	1) Alternate changes between brackish and normal marine salinity, especially at the heterolithic tidally influenced interbar shoals. 2) Morphodynamics of barforms limiting colonization window (only the inactive and abandoned bar-tops are highly colonized). 3) Rapid erosional scouring rate by tidal and rip currents, and high sediment accumulation rate. 4) Fluid mud activity in the tidally influenced interbar areas. 5) Mantle-and-swirl structures and difference types of shrinkage cracks indicate interchanging substrate condition from soupground to softground in the tidally influenced heterolithic sediments. 6) Restricted occurrence of *Macaronichnus* isp. indicating rare nutrient-rich cold water upwelling.

	heterolithic intervals.	
Proximal prodelta	1) Abundant mantle-and-swirl structures in association with foundered ripples in mud-dominated intervals evidencing soupy substrate being colonized by vermiform organisms 'swimming' within the substrate. 2) Relatively stabilized softground muddy substrate showing sparse bioturbation (BI = 0–2), increasing upward towards sandier heterolithic intervals, and paucispecific suites by polychaetes and bivalves -. 3) Ichnogenera present are: *Planolites* isp., *Asterosoma* isp., *Siphonichnus* isp., *Teichichnus* isp. *Cylindrichnus* isp.	1) Fluid mud activity as a hindrance for suspension feeders in the soupground substrate. 2) Diurnal or seasonal changes of substrate from soupground to softground and *vice versa* allowing only a few opportunistic colonizers for a limited span of time. 3) Lowered Eh (dysoxia) due to decomposition of organic fragments delivered as phytodetrital pulses as an ecological stress for organic-rich laminations which are grossly unbioturbated. 4) Salinity fluctuations as background stress factor. 5) Scarcity of bedding parallel field of observation as a bias due to semi-consolidated nature of the outcrop. 6) Preservation potential due to lithological contrast in muddier intervals.
Wave-modified fringing barrier bars (outer shelf shoals)	1) Stressed '*Skolithos-Cruziana* ichnofacies': *Scolicia* isp., *Teichichnus* isp., *Ophiomorpha nodosa*, softground *Thalassinoides* isp., *Diplocraterion* isp., *Conichnus* isp., *Bergaueria* isp., *Skolithos* isp., *Cylindrichnus* isp., *Planolites* isp., escape trace fossils. 2) Dominance of echinoids, decapod crustaceans, sea-urchins and polychaetes as colonizers. 3) Intense to complete bioturbation at the shoaling bar-tops, *i.e.*, BI = 5–6, whereas bar interiors being sparsely colonized by deep tier suites. 4) Zones of repeatedly churned deposit-feeding behaviour by echinoids. 5) Deep tier burrows like *Ophiomorpha nodosa*, *Thalassinoides*, *Teichichnus* isp., and *Cylindrichnus* isp. crosscut shallow-tier *Scolicia* isp.; rare and sporadic occurrences of *Bergaueria* isp.	Very close resemblance with normal shoreface depositional setting, with minor stresses possibly arising from 1) Normal marine to brackish salinity fluctuations, 2) Colonization window being limited by seasonal variations and morphodynamics of the rapid deposition, erosion and migration of barforms. Escape trace fossils indicative of rapid sedimentation and erosion. 3) Episodic water turbidity at the sediment-water interface is underscored by the sporadic and rare occurrence of *Bergaueria*. 4) Slope instability due to relatively steeper gradient than inner shelf. 5) Temporal changes in energy condition influencing both sedimentation rate and colonization window, as indicated by lam-scram fabric.
Proximal prodelta and/or inter-lobe embayment on outer shelf	1) Stressed *Cruziana* Ichnofacies' characterized by *Chondrites* isp., *Phycosiphon incertum*, *Siphonichnus* isp., *Asterosoma* isp., *Rosselia* isp., *Schaubcylindrichnus* isp., *Thalassinoides* isp., *Cylindrichnus* isp., "*Terebellina"* isp., *Planolites* isp., *Palaeophycus* isp., *Solemyatuba ypsilon*, *Diplocraterion* isp., *Rhizocorallium* isp.(?), *Nereites* isp. (?). 2) Dominance of bivalves, polychaetes and other vermiform organisms as colonizers. 2) No to sparse bioturbation (BI = 0–1) in general. At places, moderate to intense bioturbation (BI = 3–5). 3) Mostly simple and rarely composite ichnofabric with prominent absence of deep tier colonization. Dominance of shallow infaunal and semi-infaunal deposit-feeding and chemosymbiotic trophic behaviour. Occurrence	1) Occasional fluctuations between brackish and normal marine salinity as the background stress factor limiting colonization of strictly marine traces like *Phycosiphon incertum* and *Chondrites* isp. 2) Decomposition of organic material resulting in localized dysoxia and anoxia deep within the substrate, acting as a stress factor. Beds deposited under local dyoxia documents colonization by chemosymbionts *e.g.*, *Chondrites*. 3) Fluid mud activity is possibly another stress factor limiting epibenthic colonization. 4) Episodic slowing down of sedimentation causing localized dysoxia. 5) Transient tidal activity influencing both sedimentation rate and

	of *Chondrites* isp. restricted within individual thin-beds.	fluid mud activity.

3.4 Sedimentary facies, ichnology and depositional model

There are four main types of depositional settings and twelve subenvironments that are characterized and described in detail below, all of them being exclusively subaqueous without any evidence of subaerial exposure. Table 3.1 lists all the depositional subenvironments with their sedimentological characteristics (*i.e.*, facies associations and interpretation of sedimentary processes). Table 3.2 shows the ichnological characteristics of every subenvironment with respect to the stress factors and preservational biases. Estimation of bioturbation intensity as the Bioturbation Index (BI) follows scheme proposed by Taylor and Goldring (1993).

3.4.1 Shelf-attached Mass Transport Complex (MTC)

The 65 m long Outcrop 1A interval at the base of Mayaro Formation exposures is a mass transport complex mobilized from the shelf-edge delta and deposited possibly on the upper-slope (Fig. 3.2A-E). The stratigraphic occurrence immediately below the overlying shelf-edge delta-front succession suggests this interval to be a 'shelf-attached MTC' following the classification schemes by Moscardelli and Wood (2008) and Romero-Otero *et al.* (2010), who reported similar subsurface MTCs overlain by delta-front sediments in regional seismic data from the Atlantic Ocean offshore of Trinidad. Within a cohesive silt-rich muddy matrix, the entrained rafted blocks show relic hummocky and swaley cross-stratifications (HCS-SCS) (Fig. 3.2D), wave-ripples, and to a lesser degree soft-sediment deformation within the blocks than the slickensided and sheared surrounding zones which envelop the blocks. The rafted blocks show a more gentle overall contortion and rigid-body block rotation (Fig. 3.2C-D). The cohesive matrix, however, shows a range of deformation from absolutely fluidized mud flow character to sheared as well as blocky brittle-ductile deformation of silty mudstones (Fig. 3.2E). Numerous discontinuity surfaces and indicators of ductile to brittle-ductile shearing (within sedimentary regime) point toward eastward and northward directions of flow of the mass movement. Apart from rare

occurrences of *Ophiomorpha nodosa* within sandy HCS-SCS rafted blocks, the MTC is unbioturbated (BI = 0).

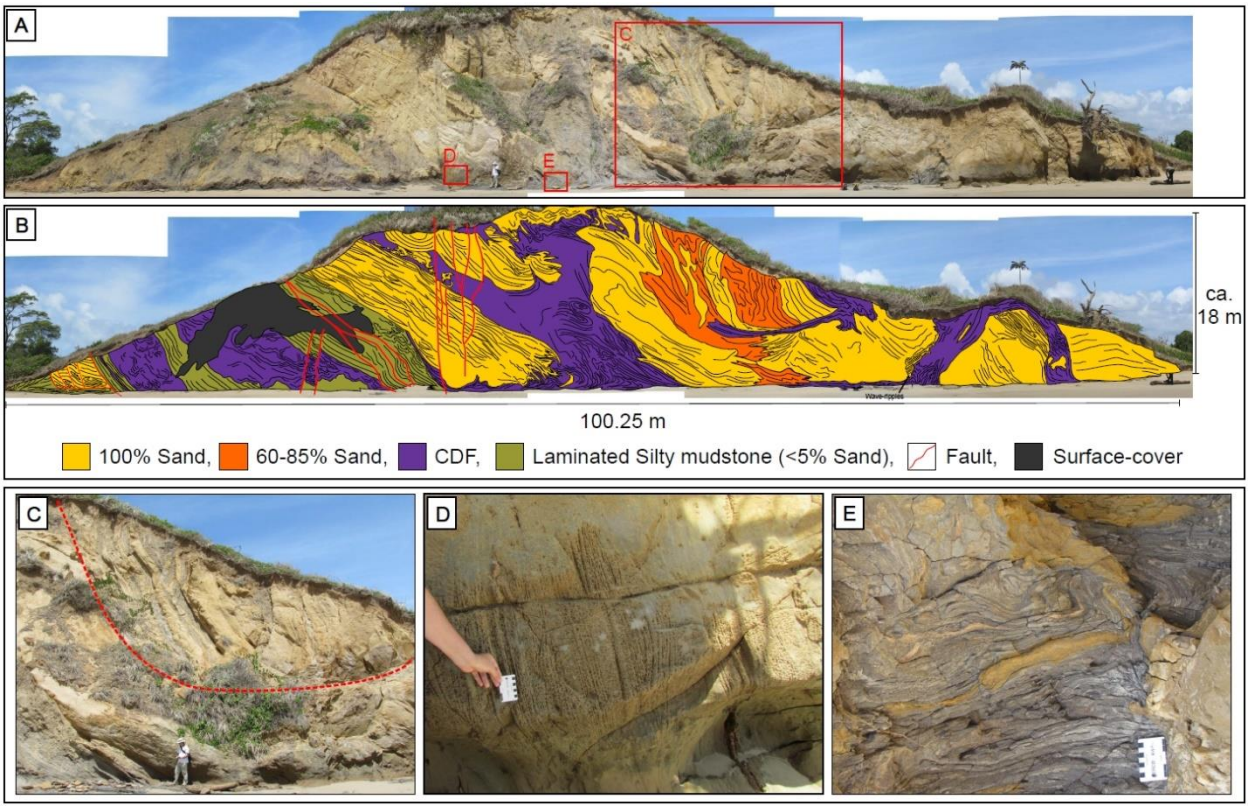

Fig. 3.2. General view of mass transport complex (MTC) deposit in Outcrop 1A (*i.e.*, at the base of the Mayaro Formation exposures). (A) and (B) Respectively the stitched and the interpreted photographs of the attached MTC. The colour indices are used at the bottom for sandy and sandy-heterolithic allochthonous blocks, cohesive debris flow deposit (CDF), silty mudstone, faults and the surface debris-cover. Rectangles C, D, and E in Fig. 3.2A are enlarged in Fig. 3.2C-E. (C) Rafted sandy heterolithic block. Red dashed dotted curve approximately follows the detachment/shear surface. (D) HCS sandstone in a rafted block. (E) Complex ductile deformation within fluidized cohesive silt-rich muddy matrix of the CDF.

The shelf-attached MTC is interpreted to be the result of arcuate and basinwardly concaving system of failures at the shelf-break region onto upper-slope as slumps, which were deposited (‘froze’) en-masse after the kinetic forces fell below the plastic strength. In the literature, shelf-attached MTCs are, in a landward direction, reported to be funneled downslope through paleocanyons, with development of aggradational or progradational clinoforms off the

paleoshelf break; and such basin-margin slumps are common features along any shelf-edge, especially wherever influenced by tectonism and/or high sedimentation rates (Shanmugam *et al.*, 1994; Weaver *et al.*, 2000; Nixon and Grozic, 2007; Moscardelli and Wood, 2008; Moscardelli *et al.*, 2010; Silva *et al.*, 2010). Therefore, it preserved the sedimentary features of en-masse deposition, *e.g.*, chaotic distribution, orientation and deformation of rafted blocks, and the shear fabrics. Rafted blocks of HCS-SCS sands and sandy heterolithic sediments are exhumed and mobilized potentially from relatively older delta-front deposits by slumping. The cohesive silty mud is interpreted to be remobilized from (1) relatively older prodelta deposits at the shelf-edge and outer-shelf, and (2) shelf and upper-slope mud. Mass movements at the shelf-break can be triggered by a combination of many factors that cause oversteepening and slope instability, *e.g.*, earthquakes, relative sea-level fluctuations, high sediment accumulation rates, clathrate dissociation (causing the release of enormous amount of methane resulting in collapse of strata, liquefaction, sedimentary diapirism and 'volcanism'), and large waves (Moscardelli and Wood, 2008; Alfaro and Holz, 2014).

Outcrop 12 is another ca. 9 m thick small exposure of cohesive debris-flow deposit of unascertained depositional affinity. This deposit contains allochthonous blocks from delta-front deposits within a cohesive muddy matrix. The deposit also may belong to a part of a shelf-attached MTC. Outcrop 12 subcrops northwards. It may also be a much smaller scale MTC related to basinward collapse of shoaling delta-front bars (for an analog example, see Dixon *et al.*, 2013).

3.4.2 Shelf-edge delta lobe

From Outcrops 1B to 9 (excluding 'out-of-trend' Outcrops 8B-8C; discussed in Section 3.4.4), the entire interval represents the succession of sediments deposited in one of the prograding delta-front lobes of the paleo-Orinoco delta system. The transect along the Outcrops 1B to 9 is ca. 1400 m thick and 3000 m long along the depositional strike. The following depositional subenvironments have been identified in view of their sedimentary facies associations and ichnological characteristics:

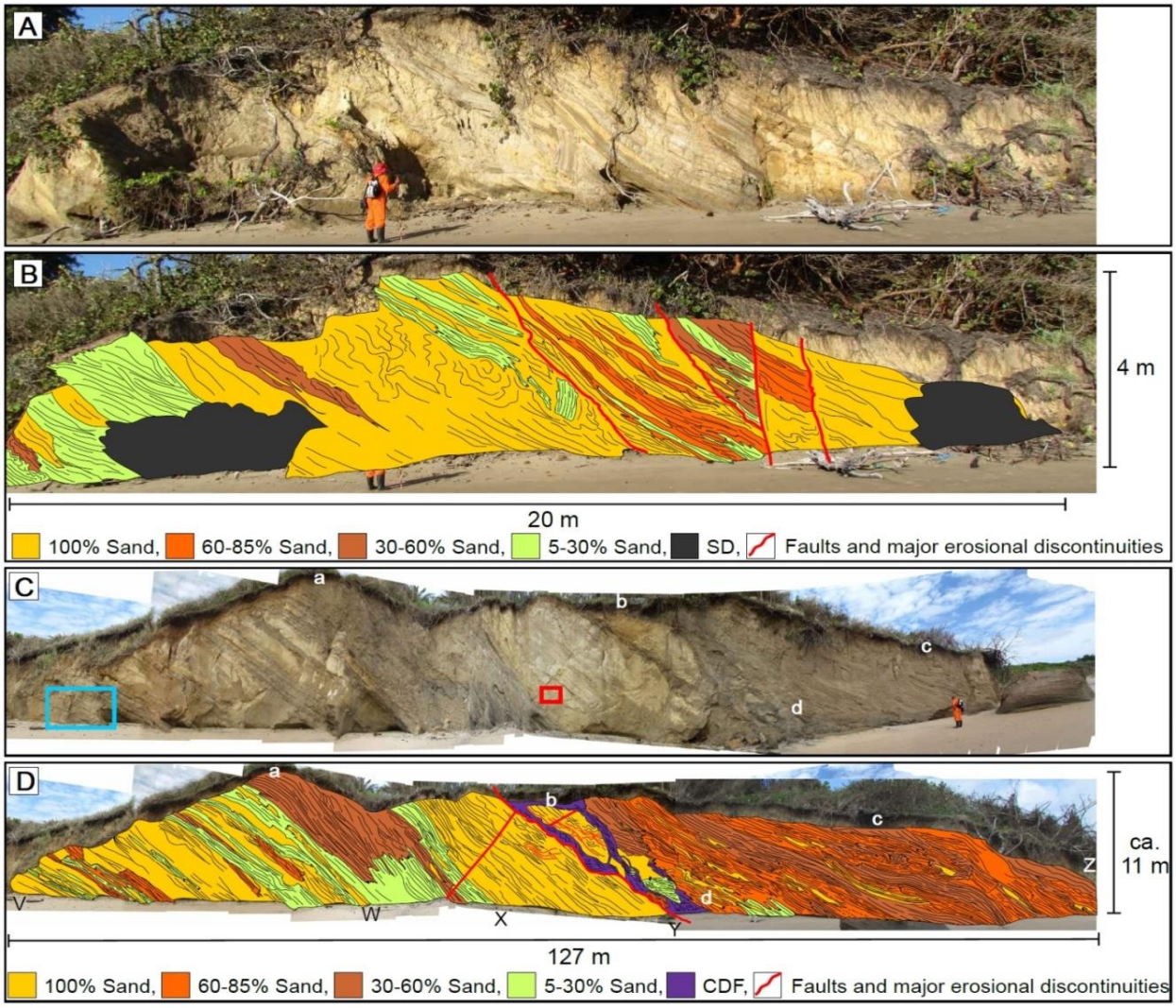

Fig. 3.3. General view of subaqueous channel and channel-bank deposits of the river-dominated delta-front subenvironments. (A) and (B) Respectively the stitched and the interpreted photographs of Outcrop 2. Beds pinch out on the cut-surface. The chaotic nature of the sand containing large clasts below the cut-surface(s) denotes the localized slumping along the erosional channel bank. (C) and (D) Respectively the stitched (not corrected for distortion) and interpreted (with corrections for the distortions) photographs of the intervals exposed in Outcrop 4: active subaqueous channel-fills (intervals V-W and X-Y), internal distal overbank (interval W-X), channel-bank slumps (immediately above the erosional cut-surface at Y) and abandoned subaqueous channel-fills (interval Y-Z). In Fig. 3.3C, the large blue and the small red rectangles have been enlarged in Fig. 3.4A and 4C respectively. Points a, b, c, and d indicate the same location-points on the outcrop in Figs. 3.3C and D. [*N.B.* Lateral erosional cut-surface(s) and synsedimentary fault surface(s) parallel to the cut-surfaces are marked in red. The colour indices are used at the bottom for surface debris-cover (SD), TCS-SCS sandstone and heterolithic intervals with varying sand-contents, cohesive debris flow deposit (CDF) at the slumped channel bank, and faults.]

3.4.2.1 Active subaqueous feeder channel-fill – river-dominated, wave-influenced delta-front

Channel-fills are trough cross stratified (TCS), lenticular to tabular medium-grained sandstone bedforms/barform deposits, which are deposited within the incised geometry of the channels. Channel depth or width cannot be ascertained because of partial and inclined exposures. The channels can be identified by the concave-up geometry of the incision surfaces, the domination of TCS, cut-and-fill structures, large gutter-casts, and debris-flow deposits and convolutions associated with slumping of the channel-banks (Figs. 3.3A-D; 3.4A, C). The subaqueous nature of the channels is manifested by the background wave influence, as the interplay of unidirectional to oscillatory flow is preserved as SCS beds intercalated with TCS beds (Fig. 3.3C-D) and combined-flow ripples (Fig. 3.4B). The tops of the barforms are wave-rippled with localized parting lineations and wrinkle marks. This implies that during the time of reduced influx through the feeder channel, the sandy lithosomes are reworked by fair-weather waves at the top and subjected to microbial substrate-stabilization. At the sediment-water interface on top of the barforms, supercritical unidirectional grainflow patterned the interface with parting lineations with basinwards paleocurrent directions (avg. 100°). Paleocurrent direction of wave-reworking (*i.e.,* avg. 030°↔210° as shown by the wave-ripples), which is different from the parting lineation orientation, indicates that directions of fair-weather wave movements were possibly controlled by local physiography (*e.g.,* channel morphology and orientation, orientation of the delta lobe itself), not by the local depositional slope. Barforms intermittently show coarsening up grain-size trend (*e.g.,* interval from below X to Y in Fig. 3.3C-D). Formation of sandy bedforms under unidirectional channelized flow is possibly seasonal on top of a muddier slope showing signs of progradation within the channels themselves, whereby the bedform deposits were also being modified by large oceanic waves and storm waves. Table 3.1 lists the intervals that have been identified as active channel-fill deposits.

Sandstone lithosomes, particularly their interior parts, are grossly unbioturbated (BI = 0). The top surfaces of the barforms are moderately to highly bioturbated (BI = 3–4) with low ichnodiversity suites of simple vertical to horizontal burrows of opportunistic vermiform (*e.g., Skolithos* isp., *Planolites* isp., *Cylindrichnus concentricus*) and bivalve (*Solemyatuba*

subcompressa) producers (Fig. 3.4C-F) (for more on trace makers, see *e.g.*, Seilacher, 1990, 2007; Belaústegui and Gibert, 2013). The intensity of bioturbation decreases downward from the top of the dunes. Only one rare instance of intense bioturbation (BI = 5) is observed at a reactivation surface at the base of Outcrop 5 with colonization of clay-lined *Thalassinoides* isp. and *Planolites* isp.

3.4.2.2 Abandoned subaqueous feeder channel-fill and internal levee – river-dominated, wave-influenced delta-front

Within the incised channel geometry, as in the upper ca. 15 m interval of Outcrop 4 (Y-Z interval in Fig. 3.3D) and the upper 10 m interval of Outcrop 6A, the channel-fills are dominated by thin-bedded/laminated heterolithic sediments with varying sand content (30-85% NTG). This reflects possible geomorphic processes, such as: (1) deposition away from the channel axis, (2) gradual avulsion, or (3) internal levee formation. [*N.B.* The term 'internal levee' used here denotes geomorphic similarity with the deepwater channel-complexes with multiple cut-and-fill stages]. As shown in Fig. 3.5A-B, individual thin-beds/laminations commonly exhibit reverse and normal grading indicating possible sustained underflow, which is likely to be the result of seasonal hyperpycnal discharge with or without being aided by wave-action. Gutter-casts, shrinkage cracks (syneresis), and soft-sediment deformation structures (*e.g.*, layer-confined domino faults, ball-and-pillow structures, flame structures, and fluid escape structures) are abundant (Fig. 3.5A). Transient tidal action is suggested by double mudstone drapes, which are localized within the heterolithic sediments (Fig. 3.5C). In tidally influenced depositional environments, double mudstone laminations occur in the subtidal settings (Dalrymple, 2010). Tidal energy dissipation is possibly enhanced by the channelized physiography at the shelf-edge, especially at the relatively inactive parts within a channel. However, the sharp mud laminations might also have been deposited from quasi-laminar plug flow of mud, which was precipitated from rapid flocculation.

These deposits are sparsely bioturbated (BI = 0–1) with a very low ichnodiversity and paucispecific suites (*i.e.*, having composed of a few ichnospecies) of *Diplocraterion* isp.,

Planolites isp., *Rhizocorallium* isp. and *Arenicolites* isp. Burrow sizes are extremely reduced (as shown in Fig. 3.5C).

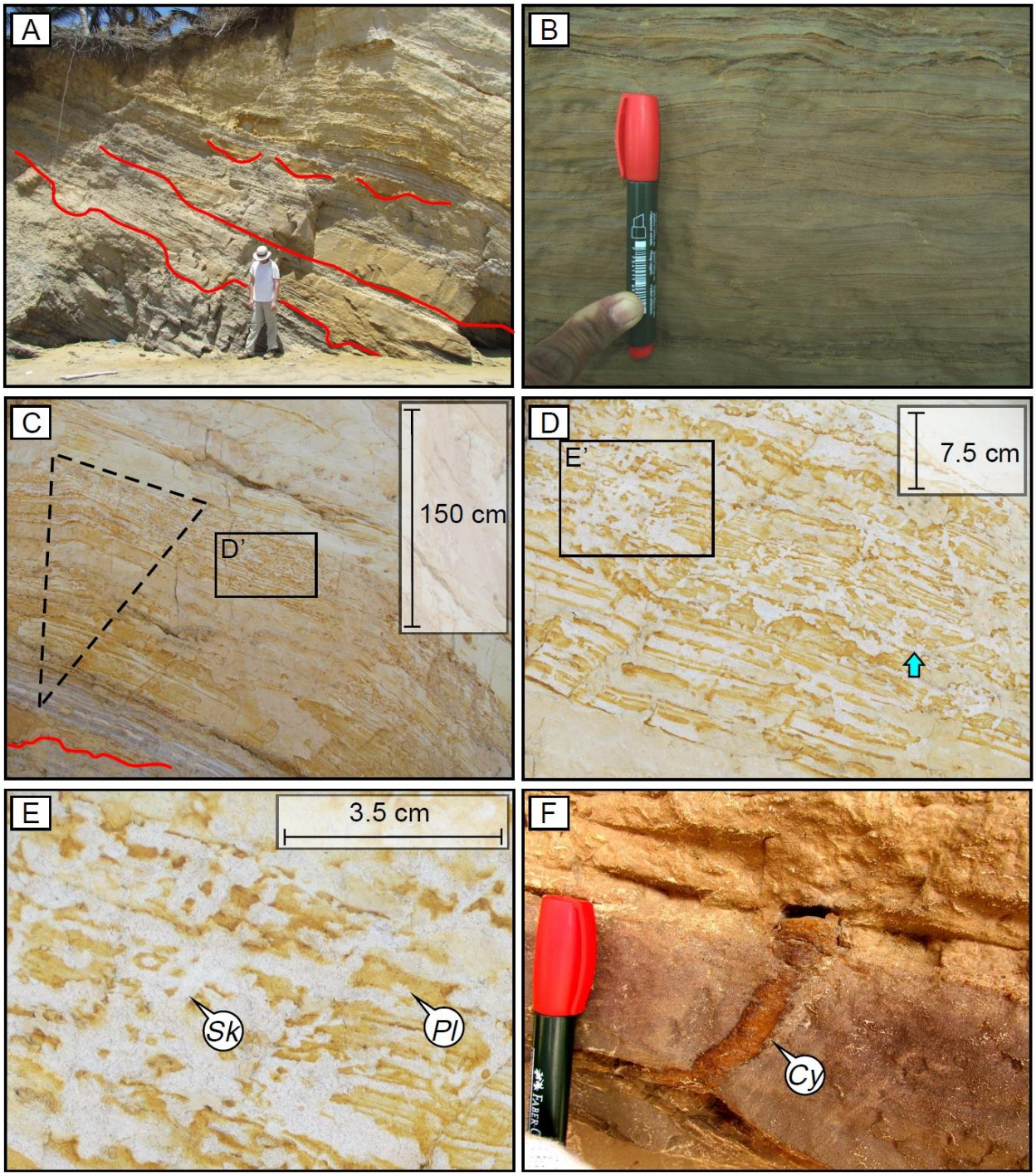

Fig. 3.4. (*N.B.* Figure caption is intentionally moved to the next page due to the large size of the figure)

Fig. 3.4. Detailed ichnological and sedimentological features of the sandy lithosomes in active channel-fills of the delta-front, as exposed in Outcrop 4. (A) Enlarged from the large blue rectangle from Fig. 3.3C, the photograph shows lensoid shaped small channel bodies filled with SCS-TCS with guttercasts at the erosional bases. (B) Combined-flow ripples within SCS-TCS sandstone in channel-fills. (C) Enlarged from the small red rectangle from Fig. 3.3C, the photograph shows coarsening-up trend, erosional base and top, and high-to-intense bioturbation at the top of the barform within channel-fill. An isolated gutter-cast is shown (defined by the red curve) below the barform. (D) Closer view of the rectangle D' in Fig. 3.4C showing intensifying-upward and paucispecific ichnofabric, containing *Skolithos* isp. *(Sk)*, *Planolites* isp. *(Pl)* and possibly *Solemyatuba* isp. (as shown by the blue arrow). (E) Closer view of rectangles E' in Fig. 3.4D. (F) *Cylindrichnus concentricus (Cy)* in TCS sandstone.

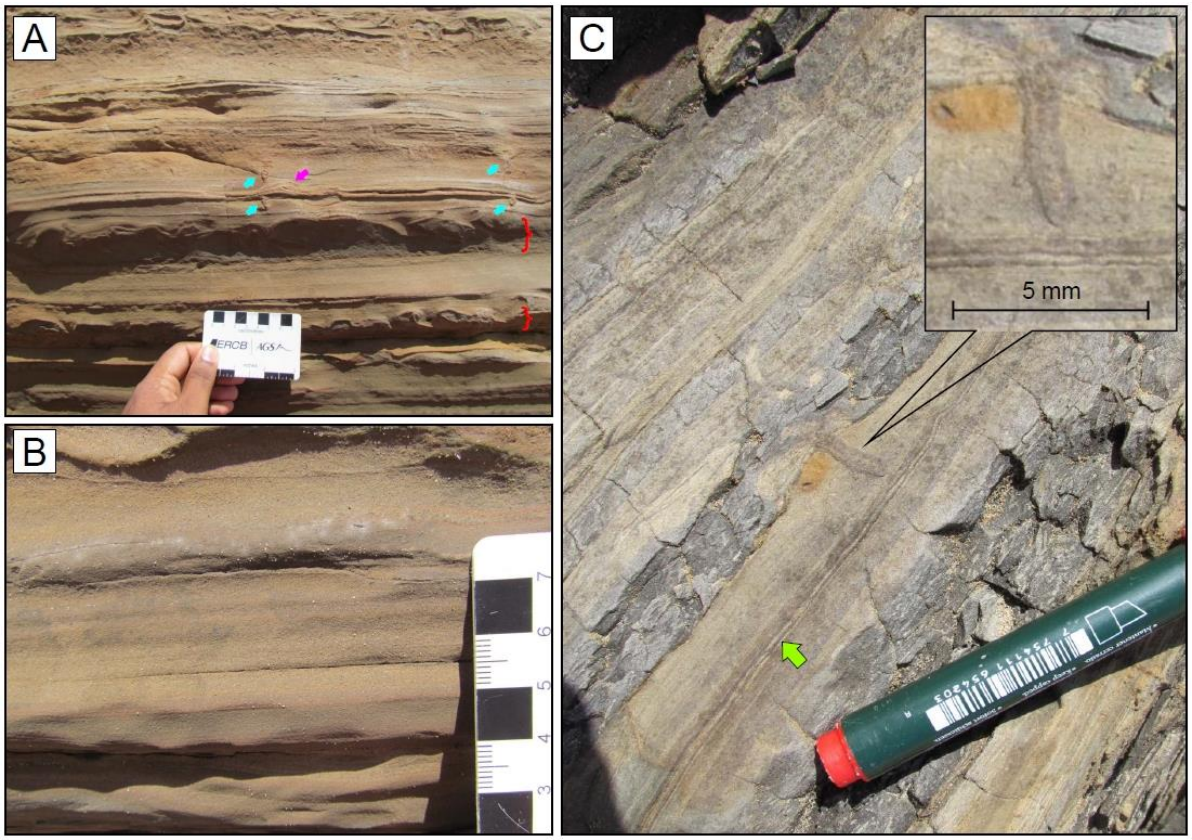

Fig. 3.5. Detailed ichnological and sedimentological features of the sandy lithosomes in thin-bedded/laminated sandy heterolithic sediments within abandoned channel-fills of the delta-front, as exposed in Outcrop 4. (A) The blue arrows show the shrinkage cracks (syneresis) and the purple arrow shows synsedimentary thrust due to shrinkage. The red braces demarcate the layers with intense soft-sediment deformation structures, such as ball-and-pillow and flame structures. (B) Waxing-waning (or reverse and normally graded) grain-size trends indicative of sustained underflows. (C) Alternate deformed muddy heterolithic and laminated less-deformed sandy heterolithic layers. The zoomed inset shows a single *Diplocraterion* isp., which is extremely reduced in size. The green arrow denotes a 'double mudstone-laminae', indicative of tidal influence.

3.4.2.3 Proximal overbank and crevasse complex – river-dominated wave-influenced delta-front

Overbank sediments immediately adjacent to the channel deposits are dominated by thin-bedded/laminated heterolithic sediments, layer-parallel slump deposits (*i.e.*, subparallel to the bedding surfaces), slump deposits at the channel bank, sandy crevasse splays and crevasse channels (Fig. 3.6A-D). The outcrop intervals are listed in Table 3.1. The heterolithic deposits show strikingly higher but variable NTG ratio than distal overbank deposits (see section 3.4.2.4 below) and no bioturbation (BI = 0). The intervals are also characterized by post-depositional neptunian injections (Fig. 3.6C), numerous cut and fill structures (Fig. 3.6D), large gutter-casts (Fig. 3.6A), flame structures, ball-and-pillow structures (Fig. 3.6D), and reworking by large oceanic swell and storm waves as envisaged by HCS-SCS in medium-grained sandy intervals. Muddier heterolithic intervals locally contain shrinkage cracks. Unequivocal levee architecture (*i.e.*, the convex-up deposit in the immediate geomorphic vicinity of the channel-cut) cannot be identified. Increase in flow volume and energy as well as centrifugal force at the channel bends are responsible for spilling over, breaching and overbank deposition. Slumps are the result of oversteepened banks possibly due to lateral scouring. Seasonal pause of channel activity can be interpreted from the gross modification of the bedform deposits by large waves into HCS-SCS. Dominance of chutes and gutter-casts, layer-parallel slumps, large-scale sedimentary deformation structure indicate a steep slope, perhaps steeper than the shelf-edge due to levee formation, with the levee being larger than the scale of observation in outcrop.

3.4.2.4 Distal overbank – river-dominated wave-influenced delta-front

In association with the channel-overbank complex, the silt-rich heterolithic sediments with poor sand content (NTG ratio below 30%) are parallel-laminated, locally showing HCS, grossly unbioturbated (BI = 0; except for rare mottles), and devoid of large soft-sediment deformation structures unlike the proximal overbank deposits (Fig. 3.7A-D). The sand grains defining the lighter-coloured laminations are medium to fine in size. Small-scale soft-sediment deformation structures (*e.g.*, ptygmatic folding confined within thin-beds, synsedimentary domino faults) and combined-flow ripples are common (Fig. 3.7C-D).

It is interpreted that these fine-grained sediments were deposited, possibly during seasonal high fluvial flux, away from the subaqueous feeder channels. Lamination-bound ptygmatic folding suggests very a high competence contrast between stiffer sandier layers and incompetent muddier layers indicating a fluidized soupy substrate (for mechanism of ptygmatic folding with respect to competence contrast or viscosity ratio, see Ramsay and Huber, 1987). Moderate to low background wave reworking is manifested by the localized HCS and combined-flow ripples.

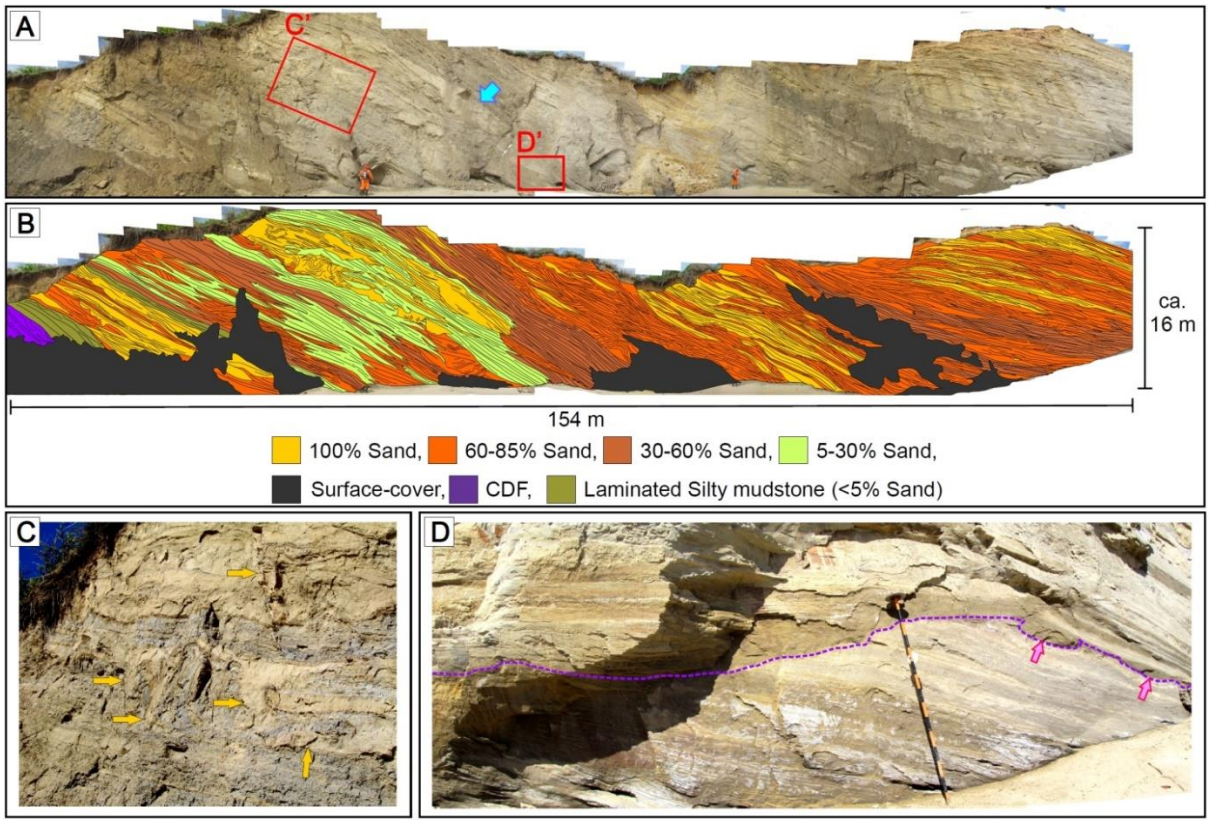

Fig. 3.6. General view and sedimentary features of proximal overbank of subaqueous channel system in river-dominated delta-front. (A) and (B) Respectively the stitched and interpreted photographs of Outcrop 6B showing thin-bedded/laminated heterolithic sediments, layer-parallel slumps, numerous injections, and sandy crevasse chutes (or large guttercast, as indicated by the blue arrow in Fig. 3.6A). The colour indices are used in Fig. 3.6B at the bottom for sandy lithosomes and heterolithic intervals with varying sand-contents, cohesive debris flow deposit (CDF), laminated silty mudstones, and the surface debris cover. (C) Neptunian sandstone injections (indicated by the yellow arrows) – dykes and sills, enlarged from rectangle C' in Fig. 3.6A. (D) Cut and fill structure enlarged from rectangle D' in Fig. 3.6A. The

Jacob's stuff is 1.5 m in length. The cut surface is marked by dashed purple curve. The pink arrows show ball-and-pillow structures.

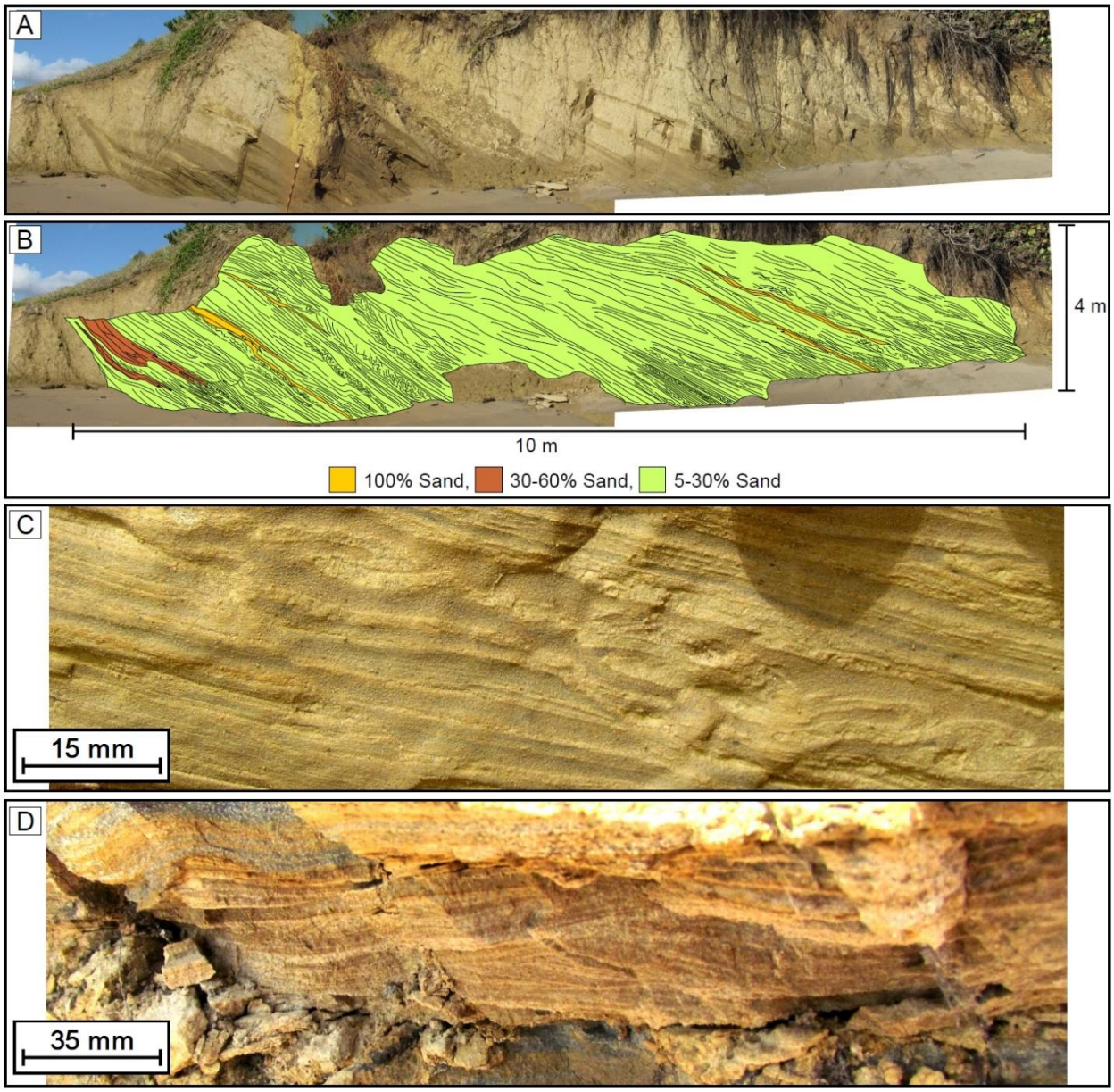

Fig. 3.7. General view and sedimentary features of distal overbank deposits with thin-bedded/laminated muddy heterolithic sediments of subaqueous channel system in river-dominated delta-front. (A) and (B) Respectively the stitched and the interpreted photographs of Outcrop 1B. The Jacob's stuff in Fig. 3.7A is 1.5 m in length. The HCS and absence of any large soft-sediment deformation are notable. The colour indices are used in Fig. 3.7B at the bottom for rare sand beds and heterolithic intervals with varying and low sand-contents. (C) Ptygmatic folds. (D) Combined-flow ripples.

3.4.2.5 Amalgamated terminal mouth-bar – river- and wave-influenced delta-front

Although the mouthbar deposits are amalgamated and fused with those of the associated wave-influenced barrier system (*e.g.,* Outcrop 6C-i to lower part of 6C-ii; Outcrop 7B), there is a systematic variation in lithofacies along the depositional slope from west to east, as envisaged along the east-west trending modern natural ravinements, confirming sedimentation as mouth-bar(s) (Fig. 3.8A; Ahmed *et al.*, 2014). The upslope back-bar bedform deposits consist of the large TCS sandstones, followed by climbing-dune-stratified sandstone (Fig. 3.8A-B). The downslope terminal splay deposits are bedded sandy turbidites and grainflow deposits (massive sandy beds, Bouma Ta or Lowe S3, and laminated sandstone Bouma Tb units and detrital plant leaf fragment-rich laminated Bouma Td units) (Bouma, 1962; Lowe, 1982) (Fig. 3.8A, D-E). There is a transition zone between these modes of depositional style where climbing dunes transform into small TCS and then collapse into turbidite-grainflow deposits (Fig. 3.8A, C-E). Intervals are all unbioturbated (BI = 0). There is an overall coarsening up grain-size trend from mud-dominated proximal prodelta deposits to medium-grained sandy amalgamated deposits, where the transitional interval shows intense and large (meters scale) soft-sediment deformation structures (*e.g.,* ball-and-pillow structures and flame structures, and a few gutter-casts) indicating rapidly deposited mouth-bar sediments and resultant loading. Along the depositional strike (*i.e.,* on the outcrop section) the entire interval appears to be an intercalation of large and small TCS and sandy gravity flow deposits reflecting repeated aggradation and lateral accretion of terminal mouth-bars with basal mud-clasts and gutter-casts at the reactivation surfaces. Though the facies variation along the depositional slope is indicative of a terminal mouth-bar, high sediment accumulation rate and wave-reworking amalgamated the mouth-bar facies with the wave-modified barrier complex in the vertical, lateral and along the depositional slope directions, thus making it impossible to draw a tentative boundary for delineating and characterizing the two specific depositional subenvironments.

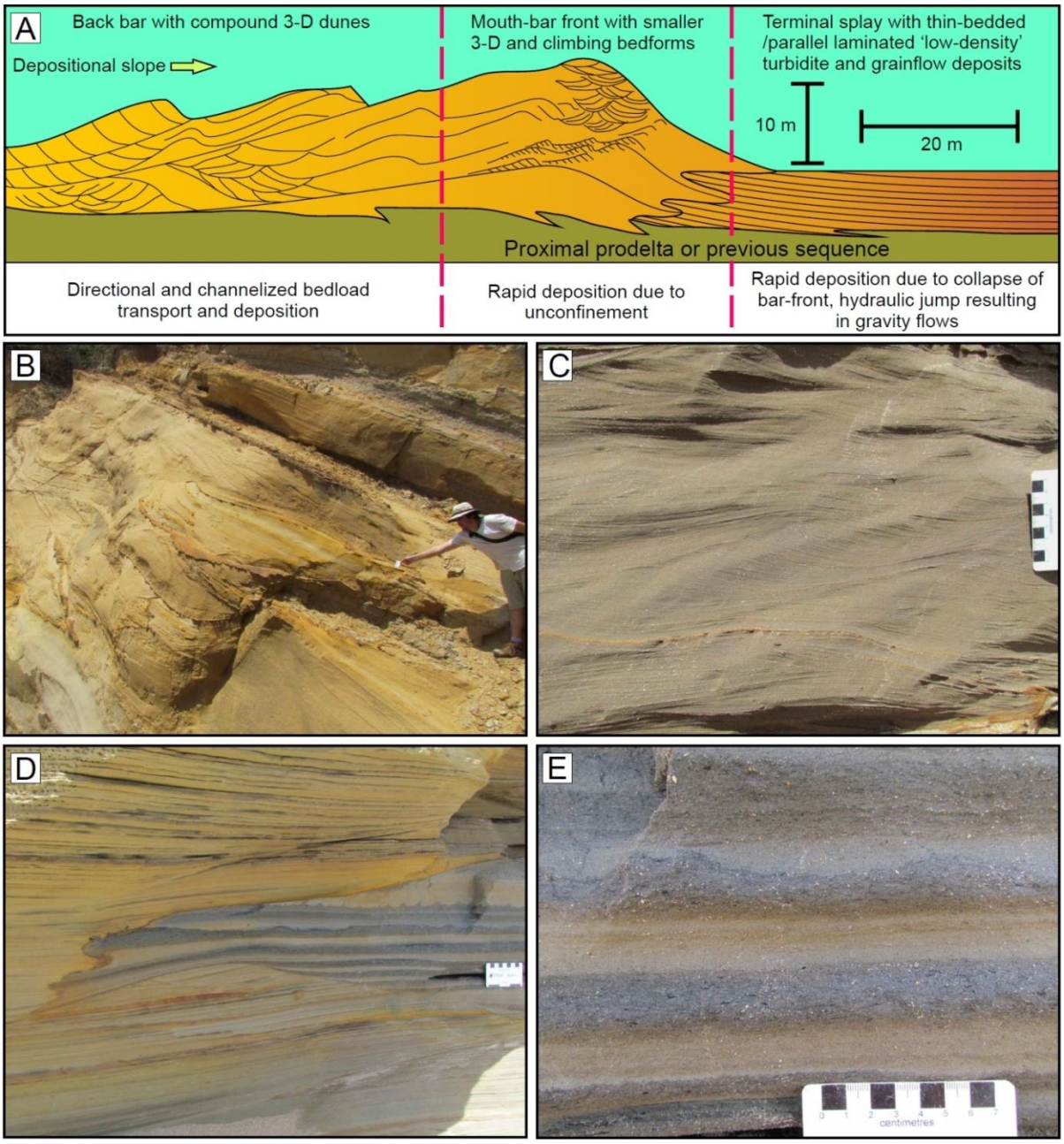

Fig. 3.8. Detailed sedimentary features of mouth-bar deposits of shelf-edge delta. (A) Schematic model for the mouth-bar showing its dimension and sedimentary features as exposed along the depositional slope in Outcrop 6C (modified after Ahmed *et al.*, 2014). (B) Large TCS in depositional upslope characteristic of back-bar settings. (C) Climbing ripples and smaller TCS (at the top), which are characteristic of transition between bar-crest and bar-front. (D) Transition from cross-stratified sand at the bar-front to 'low-density' (sensu Lowe, 1982) turbidite beds in terminal splay. (E) Closer view of the 'low-density' turbidite beds, which, in this photograph, are defined by sharp base with flame structures at places, laminated sand (Bouma Tb) as basal unit, and laminated organic fragment-rich silt unit at the top (Bouma Td) (sensu Bouma, 1962).

Although in Outcrop 6C-i the re-establishment of delta-front mouth-bar above the proximal prodelta (see section 3.4.2.8) can be interpreted both as an autocyclic (*i.e.*, simple facies variation following Walther's law; see Middleton, 1973) or an allocyclic process (*i.e.*, result of extra-basinal factors influencing falling relative sea-level), apart from a few gutter-casts (as pointed by Bowman, 2003; Bowman and Johnson, 2014) there is no convincing diagnostic evidence of a regressive surface of marine erosion (RSME), as a sequence stratigraphic surface, as postulated by Bowman and Johnson (2014). The ubiquitous presence of gutter-casts throughout can be observed in all delta-front deposits in the Mayaro Formation, except in the feeder-dominated distal overbank subenvironment.

3.4.2.6 Proximal/attached wave-modified subaqueous barrier bar system of delta-front

Outcrop 6C-ii displays a gradual transformation of the terminal mouth-bar deposits into the wave and storm dominated barrier system into Outcrops 6C-iii and 6C-iv. The poorly exposed outcrop series of 7 shows the same possible changes from Outcrop 7B to 7C and up to the lower ca. 30 m interval of 8A-i. The attached barrier bar deposits consist of SCS (intermittently HCS) and tabular medium-grained sandstone bodies. The tabular sandy lithosomes are either amalgamated, 7-8 m thick (rarely up to 25 m thick), or discretely layered, 1-2 m thick beds separated by silty heterolithic intervals (Figs. 3.9A-B; 3.10A-B). The sandstone bodies are interpreted to be bar deposits sub-parallel to the longshore current direction. The heterolithic intervals are interpreted to be deposited at the inter-bar areas and in peripheral areas of the barrier bars with lower energy conditions. The reactivation surfaces commonly contain gutter-casts, brecciated silty intraclasts and dm-thick debris flow deposits, soft-sediment deformation, such as ball-and-pillow structures, and flame structures (Fig. 3.10C). Also within the SCS bodies, evidence of post-depositional fluidization and fluid escape structures are common. Intact fossilized leaves of flowering trees belonging to the Combretaceae family (common in present-day Venezuela and Trinidad) within the SCS beds refer to coeval and rapid wave remobilization of phytodetrital pulses from the laterally adjacent feeder system (Fig. 3.10D). Approximately 150-200 m of aggradation of the barrier splays in Outcrop 6C-ii to 6C-iv with common instances of amalgamation indicates very rapid subsidence, concomitant with rapid

sedimentation. The length of the barrier splays cannot be ascertained because of the tilted nature of the outcrops, although maximum 100-120 m long segments are exposed implying the lengths to be in km scale. The large size of the SCS beds and the grain-size indicate direct interaction between the shelf-edge and large oceanic waves and tropical storm waves. Exposed top surfaces of the bedform deposits contain signatures of microbial stabilization (wrinkle marks) and are wave-rippled with ripple-crests being along ca. 075° and 140°. Paleocurrent directions of fair-weather wave reworking indicate that the general wave energy dissipation was oblique to the depositional strike, guided by longshore drift and also possibly influenced by local paleotopography. In the Mayaro Formation outcrops only the downdrift preservation of barrier bars is exposed, considering the position of the feeder system. No evidence of subaerial exposure during deposition is observed. Interpreted bathymetry is below fair-weather wave base and above the wave base of oceanic swells and storm waves at the shelf-slope break, with only bar-tops being exposed to shallower wave action and microbial stabilization (for the exmples of wrinkle marks related to subtidal barrier bars, see *cf.* Draganits and Noffke, 2004; Schieber et al., 2007).

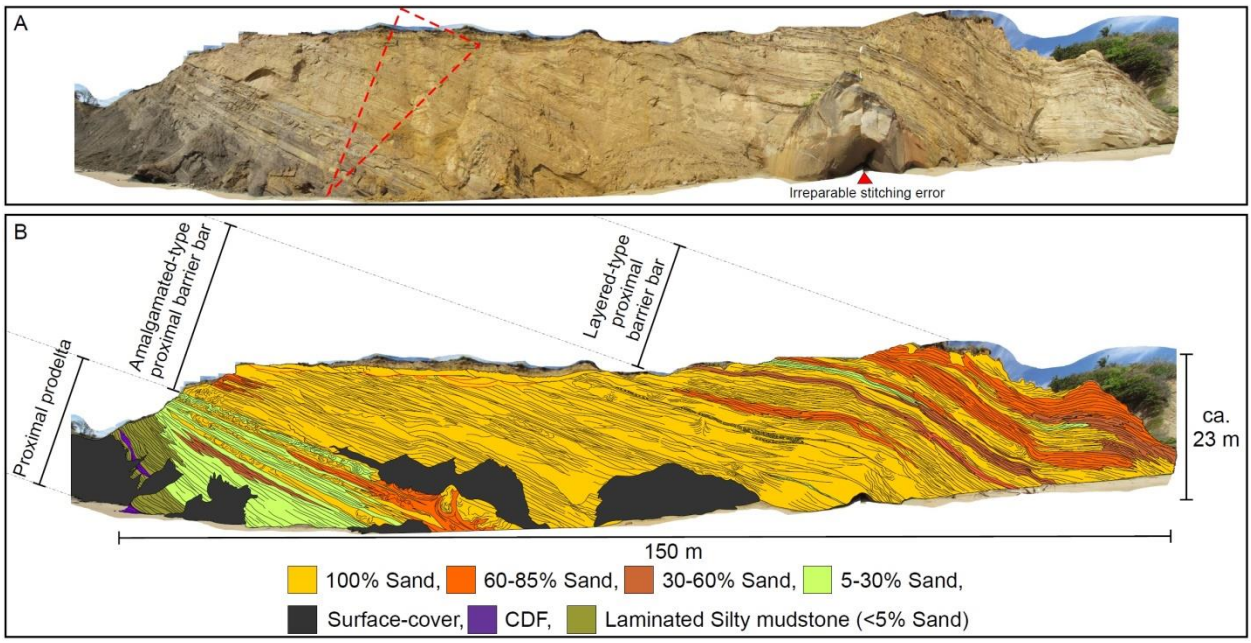

Fig. 3.9. General view of the proximal/attached wave-modified subaqueous barrier bar (both amalgamated- and layered- types) system of wave-influenced delta-front and underlying proximal prodelta (or prodeltaic inter-lobe embayment) as exposed in Outcrop 6C-i. (A) and (B) Respectively the stitched and the interpreted photographs of the outcrop. The dashed triangle in Fig. 3.9A indicates grain-size coarsening and thickening upward trend.

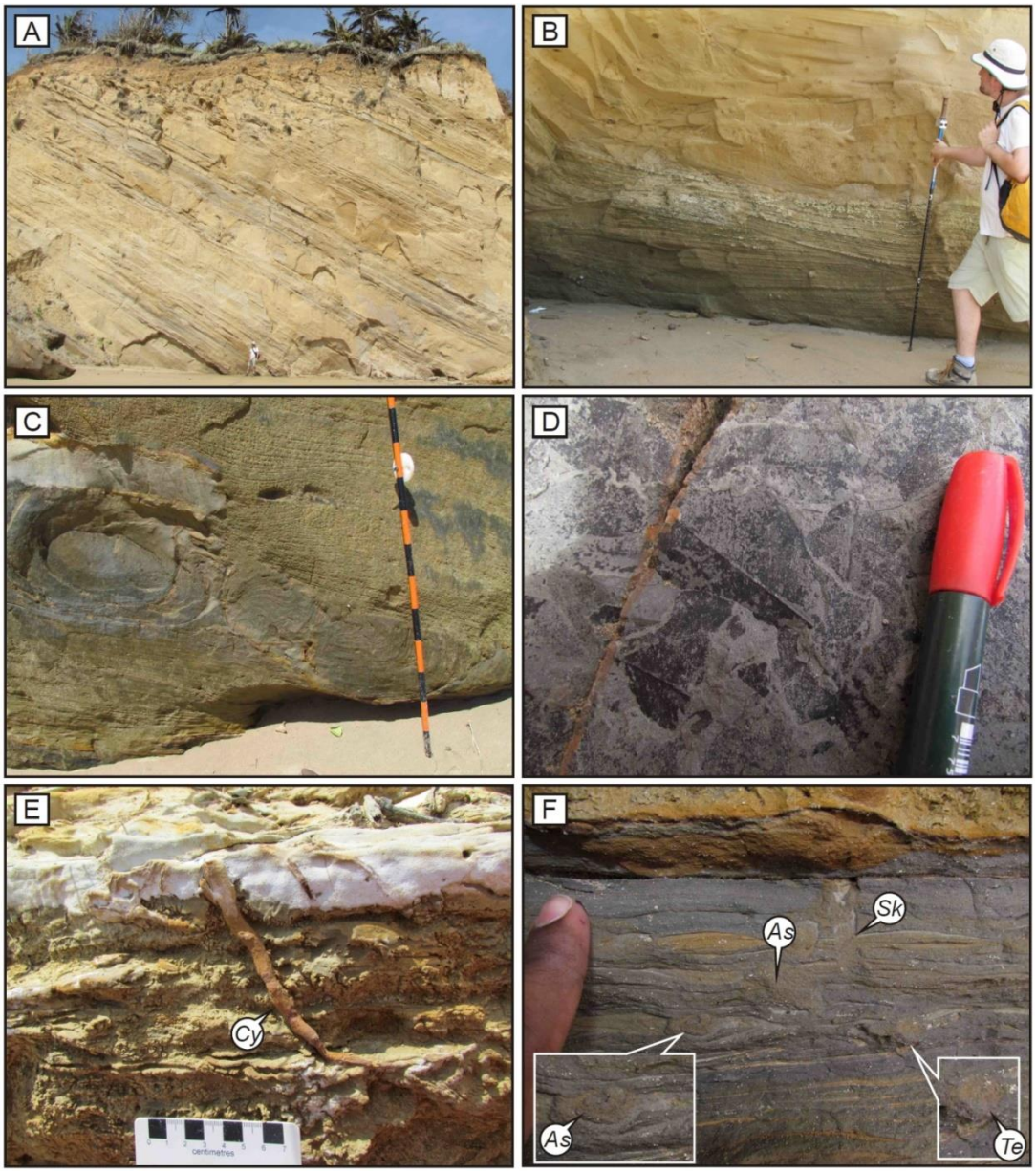

Fig. 3.10. Ichnological and sedimentological features of the proximal/attached wave-modified subaqueous barrier bar system at the wave-influenced shelf-edge delta-front. (A) Layered-type thick HCS-SCS sand beds separated by silty heterolithic intervals in Outcrop 6C-ii. (B) Closer view of the amalgamated-type SCS beds. (C) Guttercasted reactivation/amalgamation surface between two SCS beds. The top of the lower bed contains ball-and-pillow structures manifesting soft-sediment deformation. (D) In bedding-parallel view, intact fossilized leaves of flowering plants belonging to the Combretaceae family within SCS beds and pointing towards wave-remobilization of phytodetrital pulses from laterally situated river-dominated feeder system. (E) Isolated *Cylindrichnus* isp. burrows (marked as *Cy*) in SCS beds. (F) Rare, localized, and paucispecific colonization in heterolithic sediments containing *Skolithos* isp. *(Sk),* *Asterosoma* isp. *(As),* and *Teichichnus rectus (Te).* Zoomed inset shows *Asterosoma* isp. and *T. rectus.*

Localized and low intensity (BI = 0–1), monotaxic and rarely bitaxic colonization by decapod crustaceans, polychaetes and rarely sea-anemones characterize the barrier bars (for references on colonizers, see *e.g.*, Alpert, 1973; Monaco *et al.*, 2007; Seilacher, 2007; Gingras *et al.*, 2008; Belaústegui and Gibert, 2013). Common ichnotaxa documented are *Cylindrichnus concentricus* (Fig. 3.10E), and locally three-dimensional galleries of *Ophiomorpha* isp. in some sandy lithosomes. Therefore sandbodies display characteristics of the *Skolithos* Ichnofacies, whereas heterolithic intervals display a mixed highly stressed *Cruziana* Ichnofacies and *Skolithos* Ichnofacies, characterized by paucispecific trace fossil suites (*Cylindrichnus concentricus, Skolithos* isp., *Teichichnus rectus, Asterosoma* isp., *Bergaueria* isp., *Planolites* isp. and escape trace fossils) (Fig. 3.10F). Abundance and ichnodiversity both are higher than in channel-filling sandy lithosomes, but substantially less than in (1) distal barrier system and (2) analogous wave-modified shoals of the outer shelf delta.

3.4.2.7 Distal/discrete wave-modified subaqueous barrier bar system of delta-front

In the outcrops stretching from the middle interval of Outcrop 8A-i, through Outcrop 8A-ii, up to Outcrop 9 (excluding the Outcrops 8B-8C *i.e.,* the incised canyon/gully-fill cutting across, see below), the wave-modified barrier bar system of the delta-front shows ichno-sedimentological evidence favouring more marine and less fluvial influences (Fig. 3.11A-G). The tabular medium-grained SSC-HSC sand-bodies of discrete 1-3 m thick beds are separated by thin-bedded / laminated silty heterolithic sediments with varying NTG ratio (Fig. 3.11A-C). The facies association is similar to the proximal layered barrier bar complex. However, the striking differences are: (1) evidence of strong tidal reworking (*e.g.*, flaser laminations, tidal bundles, double mudstone drapes), within the inter-bar heterolithic deposits (Fig. 3.11G). In tidal bundles, the bidirectional current ripples show a N-S paleocurrent (*i.e.*, parallel to the depositional strike) likely to be defined by the bar orientations, (2) passively filled, prominently incised channels and gutter-casts eroded by tidal and/or rip currents, parallel to the basinward slope (E-W), cutting across inactive bars / bar-tops exposed for relatively longer time sufficiently enough for extensive decapod colonization (popularly known as "*Ophiomorpha* paradise") (Fig. 3.11C-E), (3) sparse intervals of flow transformation from wave-influenced oscillatory movement into directional SE-ward movement (100°-120°), possibly triggered by rip currents as exhibited by a

combination of SCS-TCS, and (4) organic fragment-rich, wave-rippled laminations in the heterolithic intervals with ripple crests perpendicular to depositional strike indicate wave energy dissipation being guided by the orientation of the barforms (Fig. 3.11F). The bar-tops are also wave-rippled, locally ladder-back wave-rippled, with crests parallel to 085-095° and 110-120°, denoting directions of fair-weather waves being controlled by topography. The common occurrence of mantle-and-swirl structures (*i.e.*, biogenic structures produced by sediment-swimming organisms that disrupt and deform sediments having high interstitial fluid contents along their swimming paths; see Lobza and Schieber, 1999) and syneresis cracks in muddier heterolithic intervals point out interchanging substrate condition from soupground to softground in the tidally influenced heterolithic sediments (Fig. 3.13C).

Compared to the proximal barrier bar system, the ichnological characteristics also differ conspicuously as follows: (1) trace-fossil abundances are strikingly higher with no to sparse bioturbation (BI = 0–1) inside the barforms, but low to high bioturbation (BI = 2–4) at the inactive and abandoned bar-tops and also in heterolithic intervals (Fig. 3.11C-D); (2) ichnodiversity is significantly higher (see below), and gradually increases further away from the feeder system. The ichnogenera in the sandy barforms are: *Ophiomorpha nodosa*, *Scolicia* isp., large escape trace fossils, *Macaronichnus segregatis*, and *Sinusichnus sinuosus*. The heterolithic intervals are colonized by the producers of softground *Thalassinoides* isp., *Cylindrichnus concentricus*, *Scolicia* isp., *Teichichnus rectus*, *Asterosoma* isp., *Rosselia* isp., *Conichnus* isp., *Bergaueria* isp., *Planolites* isp., and small escape trace fossils (Figs. 3.12A-D; 3.13D); (3) outcrops 8A and 9, respectively record the first (or earliest) appearance of *Scolicia* isp. and *Macaronichnus segregatis* in the Mayaro Formation succession. This definitely proves more normal marine conditions similar to the highly oxygenated upper to lower shoreface. However, the abundance of trace fossils is still quite lower than in a typical shoreface environments (see *e.g.*, MacEachern and Pemberton, 1992; Pemberton and MacEachern, 1997; Pemberton *et al.*, 2001, Mángano et al., 2005; Buatois *et al.*, 2007); (4) paucispecific suites typify the colonization. Only at rare locations more than two forms occur together (Fig. 3.12B); (5) the same bar-top containing a meters-wide tidal inlet incision is highly colonized with *Ophiomorpha nodosa* (BI = 4) (Fig. 3.11B-E); and (6) localized development of lam-scram fabric (or laminated-to-scrambled; see *e.g.*, Howard, 1978; MacEachern and Pemberton, 1992) within heterolithic

intervals indicates certain degree of seasonal variations of sedimentation rates selectively restricting and enabling colonization window (Fig. 3.13A).

In comparison with the amalgamated and layered barrier splays, the relatively more ichnological similarity with normal marine condition in these sandy lithosomes indicates that the sandstone bodies were deposited further away from the feeder channels as the spit-like discrete subaqueous barrier bars. The heterolithic intervals were deposited at the tidally influenced shoals at the periphery of inter-bar areas shielded by the distal barrier bars / spit-bars. Paleobathymetry is interpreted to be shallower than the proximal barrier splays (*i.e.,* mostly above the fair-weather wave base) with bar-tops being exposed to swash action of the breaking waves, rip currents and tidal incision into inlet formation. As the ichnological characteristic in Outcrop 9 indicates, the sediment accumulation rate is relatively lower than in the proximal barrier system resulting in longer colonization windows. The restricted occurrence of *Macaronichnus segregatis* indicates nutrient-rich cold water upwelling (Quiroz *et al.*, 2010) and adequate enough oxygen under the swash zone of breaking waves (Pemberton *et al.*, 2001) (Fig. 3.13B). Though smaller architectural elements of tidally influenced shoals cannot clearly be delineated and characterized in the limited two-dimensional outcrop view, their stressed ichnological signature can be observed. Sporadic occurrence of the "*Ophiomorpha* paradise" associated with incised tidal channels is indicative of relatively longer colonization windows, which can be the result of relatively slower sediment accumulation compared to the proximal barrier system, or as localized bar abandonment, or as overall slowing down of aggradation vis-à-vis basin subsidence.

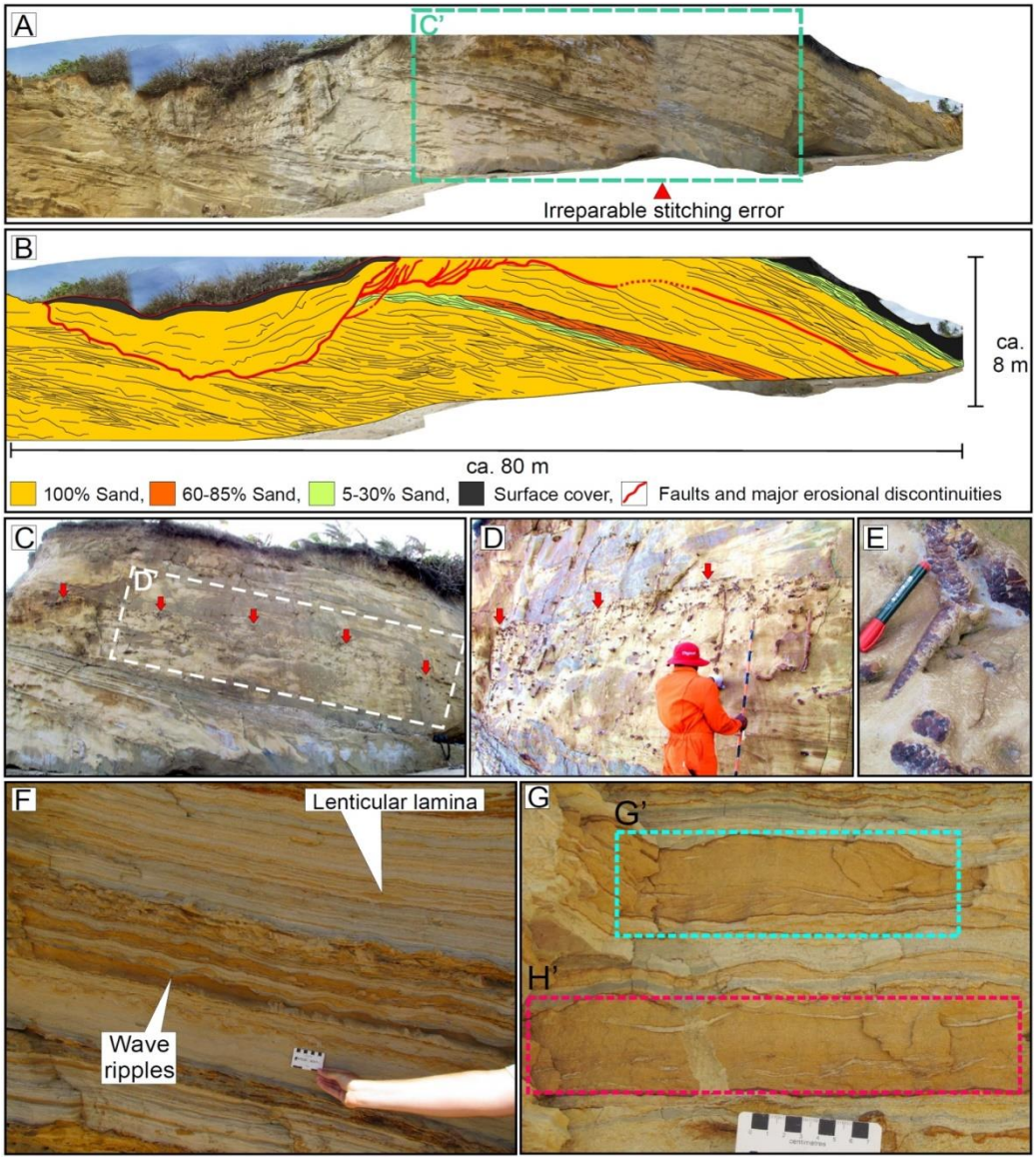

Fig. 3.11. General view, sedimentological, and ichnological features of distal and discrete barrier bars. All photographs are roughly taken looking towards west, *i.e.,* showing north-south sections parallel to the depositional strike. (A) and (B) Respectively the stitched and the interpreted photographs of distal barrier bars with SCS, cut by an inlet as exposed in Outcrop 8A-i. The inlet cutting orthogonal to the barform(s) and the extensional rupture surfaces referring to collapse of its bank are marked in red curves in Fig. 3.11B. (C) The enlarged view of rectangle C' from Fig. 3.11A showing the bar-top colonization of *O. nodosa.* (D) The rectangle D' from Fig. 3.11C is further enlarged to show the *O. nodosa* galleries. The red arrows in Fig. 3.11C-D indicate the erosional bar-top that serves as colonization-surface for the decapods. (E) The close-up view of *O. nodosa.* (F) Wave-reworking along depositional strike with crests of wave ripples being oriented along 085-095°. Lenticular laminae show tidal reworking along north-south. (Outcrop 8A-ii) (G) The rectangles G' and H' respectively showing bidirectional current ripples and flaser laminae, deciphering tidal reworking along the depositional strike (*i.e.,* along the elongated interbar depocentre). (Outcrop 8A-ii).

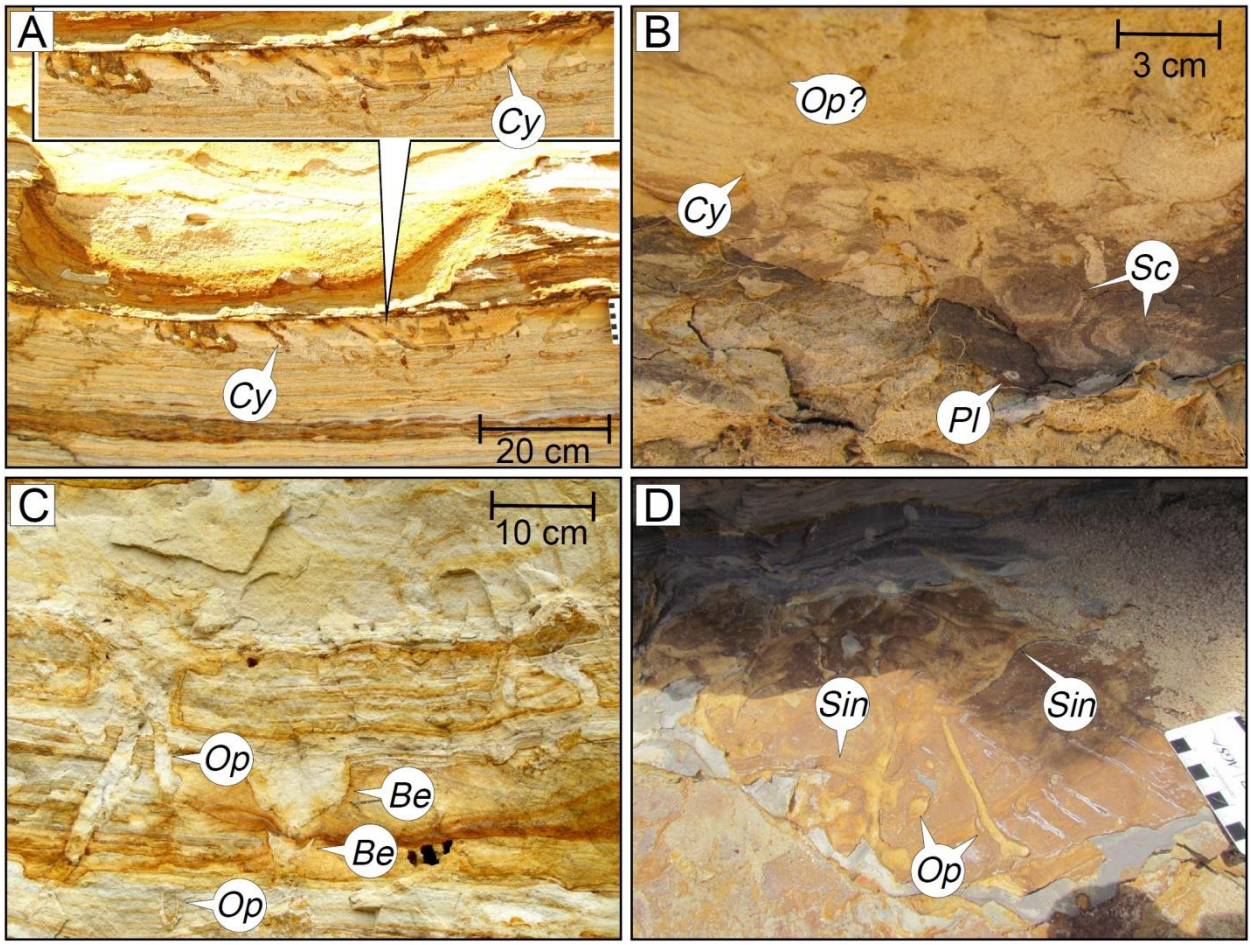

Fig. 3.12. Ichnological and sedimentological features of distal/discrete wave-modified subaqueous barrier bar system as exposed in Outcrops 8A-ii and 9. All photographs (except Fig. 3.12D) are taken looking towards west, *i.e.*, showing north-south sections parallel to the depositional strike. (A) Guttercast cutting across orientation of the barform. Monospecific colonization of *Cylindrichnus concentricus (Cy).* The view is enlarged in the inset. (Outcrop 8A-ii) (B) Low bioturbation showing *Cylindrichnus* isp. *(Cy)*, *Planolites* isp. *(Pl)*, *Scolicia* isp. *(Sc)*, and possibly *Ophiomorpha nodosa (Op).* Outcrop 8A-ii marks first occurrence of *Scolicia* isp. in Mayaro Formation succession. (C) Suite of *Bergaueria* isp. *(Be)* – *O. nodosa (Op)*, where retrusive *Bergaueria* isp. increase in size in successive beds. The later-formed deep-tier *Ophiomorpha* isp. burrows originating from younger colonization-surface colonize older beds and laminations. (Outcrop 9) (D) The *Sinusichnus sinuosus (Sin)* with rare crosscutting relationship with *O. nodosa.* (Bedding plane view in Outcrop 9)

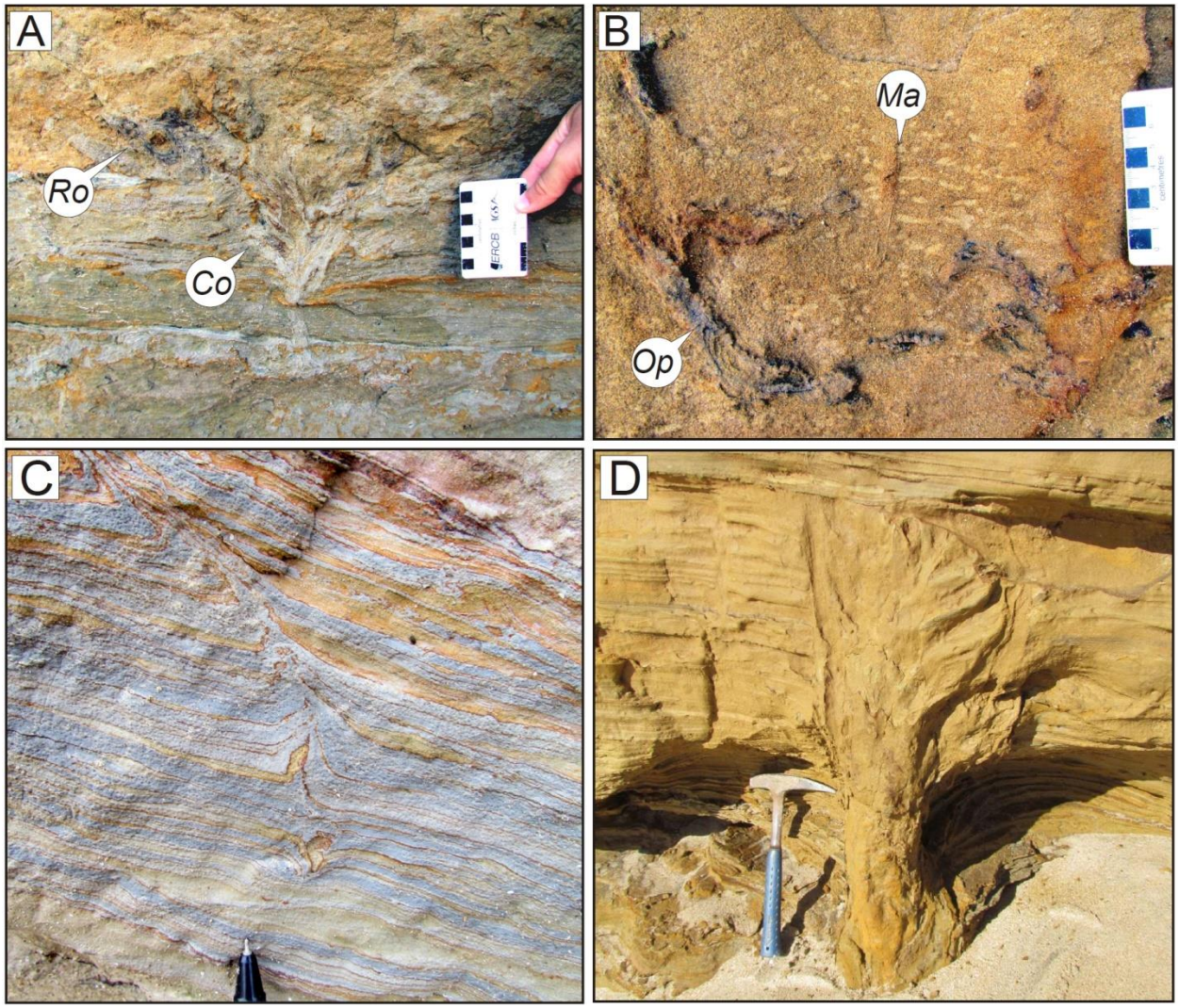

Fig. 3.13. Ichnological and sedimentological features of distal/discrete wave-modified subaqueous barrier bar system as exposed in Outcrops 8A-ii and 9. (A) Localized lam-scram-like feature within heterolithic interval with *Conichnus* isp. *(Co)* – *Rosselia* isp. *(Ro)* suite. (Outcrop 9) (B) Suite defined by shallower tier *Macaronichnus segregatis (Ma)* and deeper tier *Ophiomorpha nodosa (Op)* within SCS bed. (Outcrop 9) (C) Shrinkage crack propagating from maximum shrinkage in clay-rich silty laminations upwards as well as downwards *i.e.*, towards sandier layers. (Outcrop 8A-ii) (D) Large escape trace fossil. (Outcrop 9).

3.4.2.8 Proximal prodelta or prodeltaic inter-lobe embayment

Both the Outcrop 6B-i and the lower ca. 14 m interval of Outcrop 6C-i show a similar trend of silty mud dominated sediments gradually coarsening and transitioning upward into the sandier deposits. Both the intervals display coarsening up grain-size variation from (1) an

intercalated interval of parallel-laminated and massive-appearing organic fragment-bearing silty mudstone into (2) the thin-bedded/laminated sheet-like siltstone-sandstone (fine to medium grain-size) intercalations, silty heterolithic lensoid to tabular barforms, and then gradually varying into delta-front sand bodies – belonging to proximal overbank in Outcrop 6B-ii and mouth-bar and/or barrier splay in Outcrop 6C-i (Fig. 3.9A-B). In these mud-dominated intervals, the occurrences of double mudstone drapes, mud-draped ripples, lenticular current-rippled sands (combined-flow ripples), and intermittent tidal bundles indicate background tidal activity (Fig. 3.14A-C, H). Combined-flow ripples are more abundant in coarser grained siltstone-sandstone intercalations (Fig. 3.14C).

The parallel-laminated and massive-appearing mudstones in the lower interval were deposited by suspension settling of mud partcles and fluid cohesive mud flows respectively. The heterolithic, lensoid to tabular barforms display the typical sedimentary structures of subtidal bars (De Mowbray and Visser, 1984), *e.g.*, slight changes in gradient of the cross-bed sets within the same barform across a mud-draped erosional surface (*i.e.*, reactivation surface, *sensu* Visser, 1980; Fig. 3.14D). Also the syneresis cracks can be observed (Fig. 3.14B, E). Foundered ripples and mantle-and-swirl structures in muddy intervals indicate: (1) the fluid mud substrates and quasi-laminar plug flow resulting from rapid flocculation, and (2) the recurrent coarser-grained clastic sediments being deposited and getting foundered on the soupy substrate (Fig. 3.14B, F-G). Changes (possibly seasonal) from tidal influence into fine-grained fluvial plume activity might have resulted in rapid flocculation and increased quasi-laminar plug flow.

Mantle-and-swirl structures in association with foundered ripples are abundant in mudstone-dominated intervals, which are evidence of a soupy substrate being colonized by vermiform organisms 'swimming' within the substrate (Lobza and Schieber, 1999). Relatively stabilized softground muddy substrate show sparse (BI = 0–2) burrows with simple forms. The BI increases upward towards sandier heterolithic intervals, although trace fossil suites remain paucispecific throughout, with polychaetes and bivalves being common trace-makers with more common shallow-tier deposit feeding and rarer suspension feeding types (for references on colonizers, see *e.g.*, Seilacher, 2007; Gingras *et al.*, 2008; Dashtgard, 2011; Dashtgard and Gingras, 2012; Belaústegui and Gibert, 2013). The ichnogenera identified are *Planolites* isp.,

Asterosoma isp., *Siphonichnus* isp., *Teichichnus rectus*, and *Cylindrichnus concentricus* (Fig. 3.14F-H).

Stratigraphic superposition of prodeltaic deposits above underlying delta-front sediments (*e.g.*, the sediments of Outcrops 6B-i above the Outcrops 6A sediments, and the sediments of 6C-i above the Outcrop 6B-ii sediments) can be explained by two hypotheses:

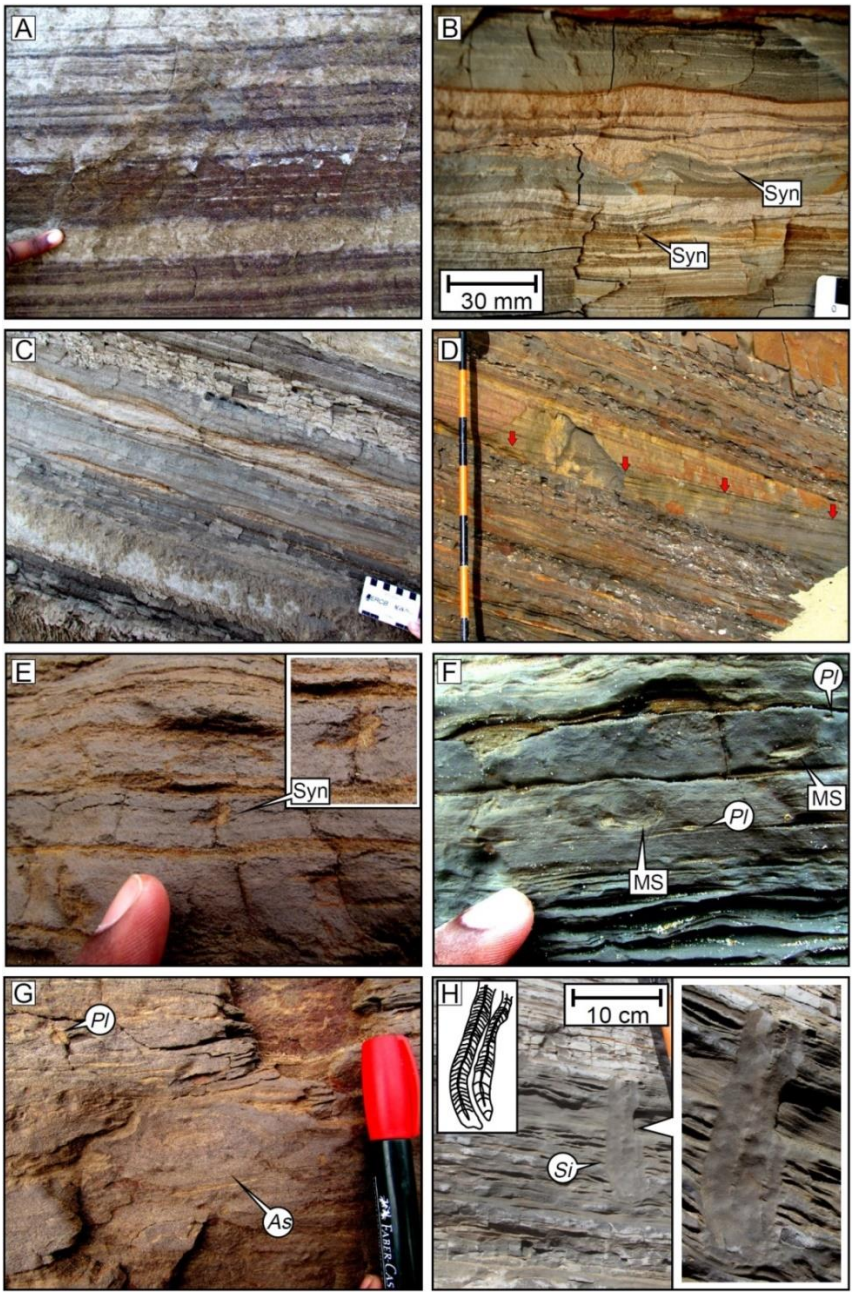

Fig. 3.14. (*N.B.* Figure caption is intentionally moved to the next page due to the large size of the figure)

Fig. 3.14. Ichnological and sedimentological features of proximal prodelta or prodeltaic inter-lobe embayment at the shelf-edge as exposed in Outcrop 6C-i. (A) Series of double mudstone laminae in silty heterolithic tidal rhythmite. (B) Mud-draped and locally foundered ripples with syneresis cracks (Syn). (C) Tidal rhythmite defined by alternating silt-sand thin-beds/laminations and quasi-laminar mud flow layers, showing apparent neap-spring cycles. The sandy thin-bed in the middle shows combined-flow ripples. (D) Tidal rhythmite defined by alternating silt-sand thin-beds/laminations and quasi-laminar mud flow layers, showing apparent neap-spring cycles. The thickest bed is a lensoid shaped, subtidal, and mud-draped planar cross-bedded sand-silt bar. The red arrows indicate the most prominent mud-draped surface of "mild erosion" by "subordinate current" (see text). The orange and black intervals of the Jacob's stuff are individually 10 cm long. (E) Syneresis crack (Syn) in sand-draped clayey silt thin-beds. Inset shows zoomed view. (F) Mantle-and-swirl structures (MS) in thin-beds of clayey silt containing a few rare *Planolites* isp. *(Pl).* A foundered current ripple can be observed in the top left corner. (G) A closer view of isolated specimens of *Asterosoma* isp. *(As)* and *Planolites* isp. *(Pl).* Foundering of ripples partially deformed the left periphery of *Asterosoma* isp. (H) A couple of isolated *Siphonichnus* isp. *(Si)* colonizing a thinbedded/laminated interval of sandy siltstone laminations and very fine-grained sandstone. The larger inset shows the zoomed view of the trace fossils. The smaller inset shows a schematic drawing of the traces.

(1) Autocyclic processes: Autoretreat, *i.e.*, retreating shoreline after continuous progradation of the delta-front, and autobreak, *i.e.*, abandonment of a delta-front lobe with continuing background subsidence can create a prodeltaic depositional suite (Muto *et al.*, 2007). The second situation results in embayment. Tidal energy dissipation tends to get enhanced by the presence of an embayment.

(2) Allocyclic processes associated with the increase in subsidence rate and/or the diminishing sediment supply causing retrogradation from the paleo-Orinoco system itself. These apparently allocyclic processes can potentially be indirectly related to quasi-autogenic growth fault tectonics (see Fig. 5.8A-B in Chapter 5).

Without any diagnostic evidence of a transgressive surface at the interface between the underlying delta-front deposits and overlying prodeltaic intervals, the change in depositional subenvironment is most likely an autogenic facies variation with ongoing background basin subsidence.

3.4.3 Outer shelf delta lobe

Outcrops 10 and 11 are situated ca. 730 m away from the northernmost outcrop (*i.e.*, Outcrop 9) of the main series of exposures of the Mayaro Formation (*i.e.*, Outcrops 1A–9). Moreover, the bedding surfaces (dipping ≤ 15° towards ca. 025°-035°) have a strikingly different structural orientation compared to the consistently northerly-northwesterly dipping strata of the shelf-edge delta-front sediments in Outcrops 1B-9, with dip-angles ranging between 15°-35°. Although this change in structural orientation may or may not be purely tectonic, the sedimentological and ichnological characteristics of Outcrops 10 and 11, as summarized in Tables 3.1 and 3.2 and also detailed below, are conspicuously different from similar facies counterparts of the shelf-edge, resembling 'normal' wave-influenced deltas developed on the shelf. Therefore, Outcrops 10 and 11 are interpreted to be a deltaic lobe deposited on the outer shelf. The same deltaic system near the shelf-slope break has the potential to simultaneously form different lobes at/near the shelf-margin and on the outer shelf away from the shelf-margin. Two sedimentary subenvironments have been identified based on the sedimentological and ichnological characteristics as follows:

3.4.3.1 Wave-modified fringing barrier bars (outer shelf shoals)

Except for a limited interval (for which, see section 3.4.3.2; Fig. 3.15A-B) in Outcrop 11, the entire Outcrops 10 and 11 consist of meter(s) thick, medium-grained, tabular SCS-HCS sandstone beds intercalated with intervals of thin-bedded/laminated sand-rich heterolithic sediments (60-85 % NTG ratio), and slump deposits consisting of blocks of sandstone and heterolithic sediments remobilized for short distances (Fig. 3.15C-E). Some of the sandstone beds lack internal fabric or bedforms due to intense soft-sediment deformation (*e.g.*, convolutions, ball-and-pillow structures, flame structures) (Fig. 3.15D, F). The tabular beds of slump deposits and sandstones with convoluted laminations are common indicating unstable slope condition and possibly frequent earthquakes (Fig. 3.15C-D). However, sizes of the bedforms and soft-sediment deformation structures are not as large as to those of the previously mentioned shelf-edge equivalent architectural elements. A gradual coarsening and thickening up trend from prodelta to delta-front can be observed in Outcrop 11 (Fig. 3.15B). Heterolithic

intervals commonly show either (1) scoured lateral termination causing amalgamation of sandstone beds or (2) gradual lateral variation into sandstone beds (Fig. 3.15C). This implies that the heterolithic intervals represent the lateral/peripheral parts of the sand bars. Along the depositional dip (*i.e.*, across the barforms), there are indications of erosion and transportation as documented by gutter-casts and transformation of SCS into TCS with E-SE paleocurrent directions at some intervals. Swash cross stratifications are rarely exposed indicating sporadic transition of shoreface into foreshore or at least into the swash zone (Fig. 3.15G). Sporadic occurrence of the large (upto 120 cm in diameter) , elongated or oblate-shaped septarian ferroan dolomitic nodules parallel to bedding surfaces displaying septaria or clefts can be observed, which also may be indicative of synsedimentary earthquakes (Pratt, 2001). [*N.B.* Septarian concretions or septarian nodules are concretions containing angular extentional fractures (the clefts) that are called "septaria"]. The clefts are secondarily filled with calcareous cement.

The tabular sandstone bodies display characteristics of the *Skolithos*-stressed *Cruziana* Ichnofacies (*cf.* Gingras et al., 1998, Coates and MacEachern, 1999; Buatois *et al.*, 2005, 2011; Fielding *et al.*, 2006). The shoaling bar-tops are intensely or completely bioturbated (BI = 5–6) mostly by echinoids, and also sparsely by decapod crustaceans, sea-anemones, and polychaetes (*Scolicia* isp., *Teichichnus rectus*, *Ophiomorpha nodosa*, softground *Thalassinoides* isp., *Diplocraterion* isp., *Arenicolites* isp., *Conichnus* isp., *Bergaueria* isp., *Skolithos* isp., *Cylindrichnus concentricus*, *Planolites* isp.) (Fig. 3.16A-D) (for references on colonizers, see *e.g.*, Alpert, 1973; Smith and Crimes, 1983; Monaco *et al.*, 2007; Seilacher, 2007; de Gibert and Goldring, 2008; Gingras *et al.*, 2008; Dashtgard, 2011; Dashtgard and Gingras, 2012; Belaústegui and Gibert, 2013). Escape trace fossils can also be sparsely observed. At the bar-tops, zones of several episodes of bioturbation by deposit-feeding echinoids are common (Fig. 3.16A-C). Interiors of the barforms are sparsely colonized (BI = 0–2). Deep- to mid-tier deposit-feeder burrows (*e.g.*, *Ophiomorpha nodosa*, *Thalassinoides* isp., *Teichichnus rectus*, and *Cylindrichnus concentricus*) sporadically crosscut shallow-tier *Scolicia* isp. (Fig. 3.16C-E), whereas rare and sporadic occurrences of suspension-feeder or predator burrows (*Bergaueria* isp.) emphasize the presence of turbidity at the sediment-water interface. Escape trace fossils indicate sporadic rapid sedimentation rates.

The upper 65 m of the isolated Radix Point succession exhibit almost identical ichnological and sedimentological characteristics to the shoaling sandstone beds of Outcrops 10 and 11. The lam-scram fabric is better developed in these outcrops at intermittent intervals than in the Outcrops 10-11 referring to seasonal variation of storm and fair-weather alternations (Fig. 3.16F).

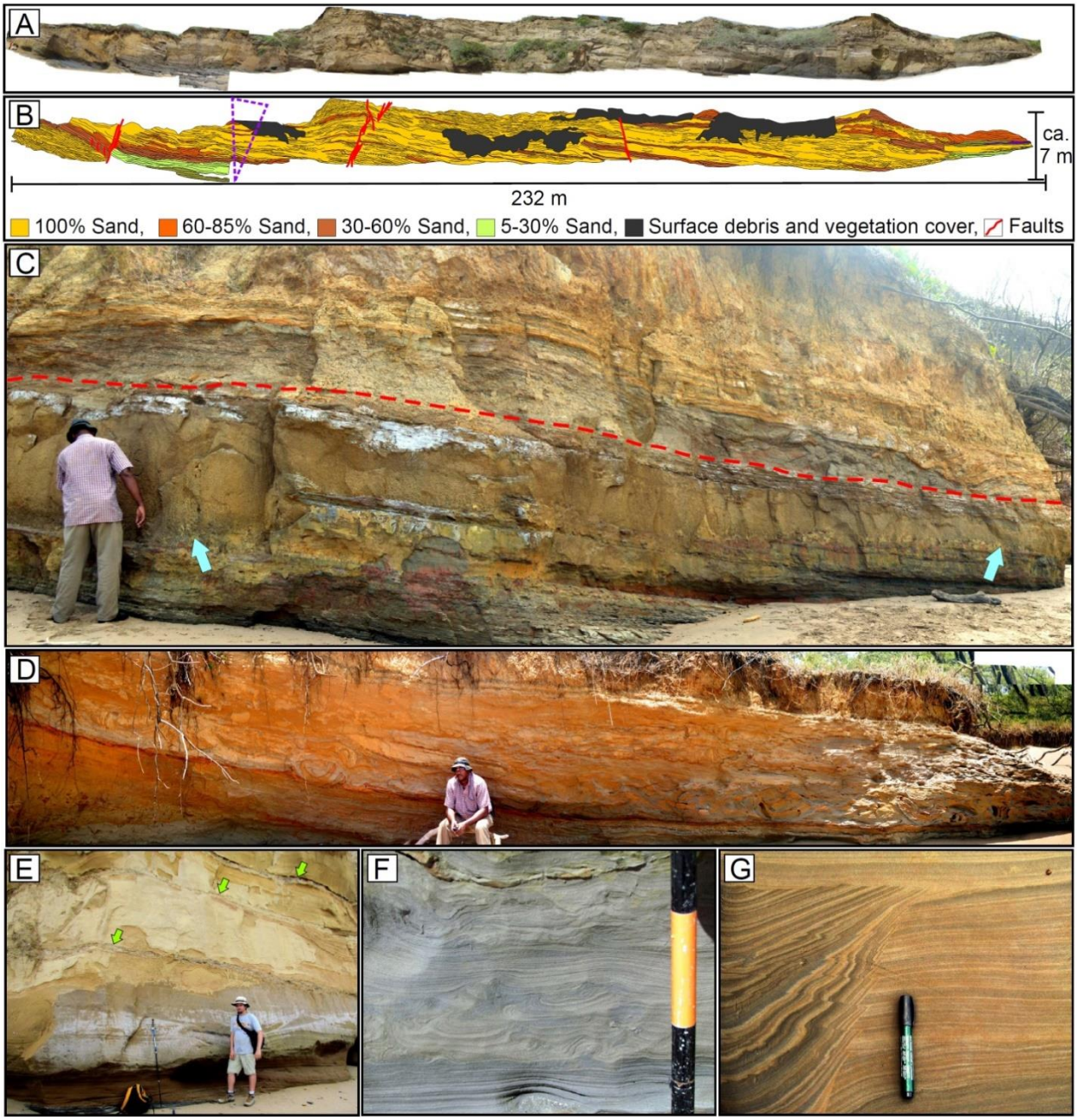

Fig. 3.15. (*N.B.* Figure caption is intentionally moved to the next page due to the large size of the figure)

Fig. 3.15. General view and sedimentary features of the outer shelf deltaic lobe as exposed in Outcrop 11. (A) and (B) Respectively the stitched and the interpreted photographs of the Outcrop 11. The entire outcrop is interpreted to be deposited as the wave-modified fringing barrier bars or outer shelf shoals, except the lower portion of the second fault-block from the left, which shows a coarsening-up grain-size trend is interpreted to be deposited at the proximal prodelta and/or embayment on outer shelf. (C) Lateral thickness variation of the SCS sandy thick bed (*i.e.,* the barform, between two blue arrows) of the wave-modified fringing barrier bars or outer shelf shoals. Sharp erosional cut near the left arrow contrasts with gentler erosional and gradual facies variation near the right-arrow. Dashed red curve marks the base of a slump bed. Above the slump bed and also below the sandy thick bed are the intervals of thin-bedded heterolithic sediments. (D) Alternate intervals of slumps and undeformed beds. Slump layers consisting of non-cohesive debris flow deposits contain soft-sedimentary deformation structures like rafted blocks, clasts, and ball-and-pillow structures. (E) Localized amalgamation of SCS sandy thick beds with non-cohesive sandy debris flow deposits containing heterolithic intraclasts at the reactivation/amalgamation surfaces. (F) Alternate parallel laminations and convolute-laminations within swash cross-stratified sand. (G) Swash cross-stratified sand.

The tabular sandstone beds show the same characteristics of the equivalent wave-influenced delta-fronts developed on the inner shelf or the shoreface (and rarely foreshore) depositional subenvironments of wave-influenced shorelines. The sands were deposited as barrier bars under the influence of a strong longshore current on a narrow shelf close to the shelf-break. The presence of at least a narrow sliver of shelf was likely as evidenced by the similarities with regular wave-influenced inner-shelf delta-front or inner-shelf shoals and by the dissimilarities with respect to the shelf-edge counterparts as previously discussed. Sediment accumulation was high, but relatively slower than in shelf-edge counterparts resulting in more lateral scouring and accretion of barforms creating longer colonization windows at the bar-tops. As indicated by the sandstone beds with convoluted laminations and bedded slump deposits, either the depositional slope might have been substantially steep or synsedimentary seismic activities were quite common. The outcrop sections along the depositional slope are not available. Limited subaerial exposure at the foreshore is evidenced by swash cross stratification and swash-liquefaction (*i.e.*, liquefaction by means of introduction of water into the sediments by breaking waves). The type of delivery mechanism cannot be ascertained in the absence of outcrops of the feeder-dominated delta-front lobe.

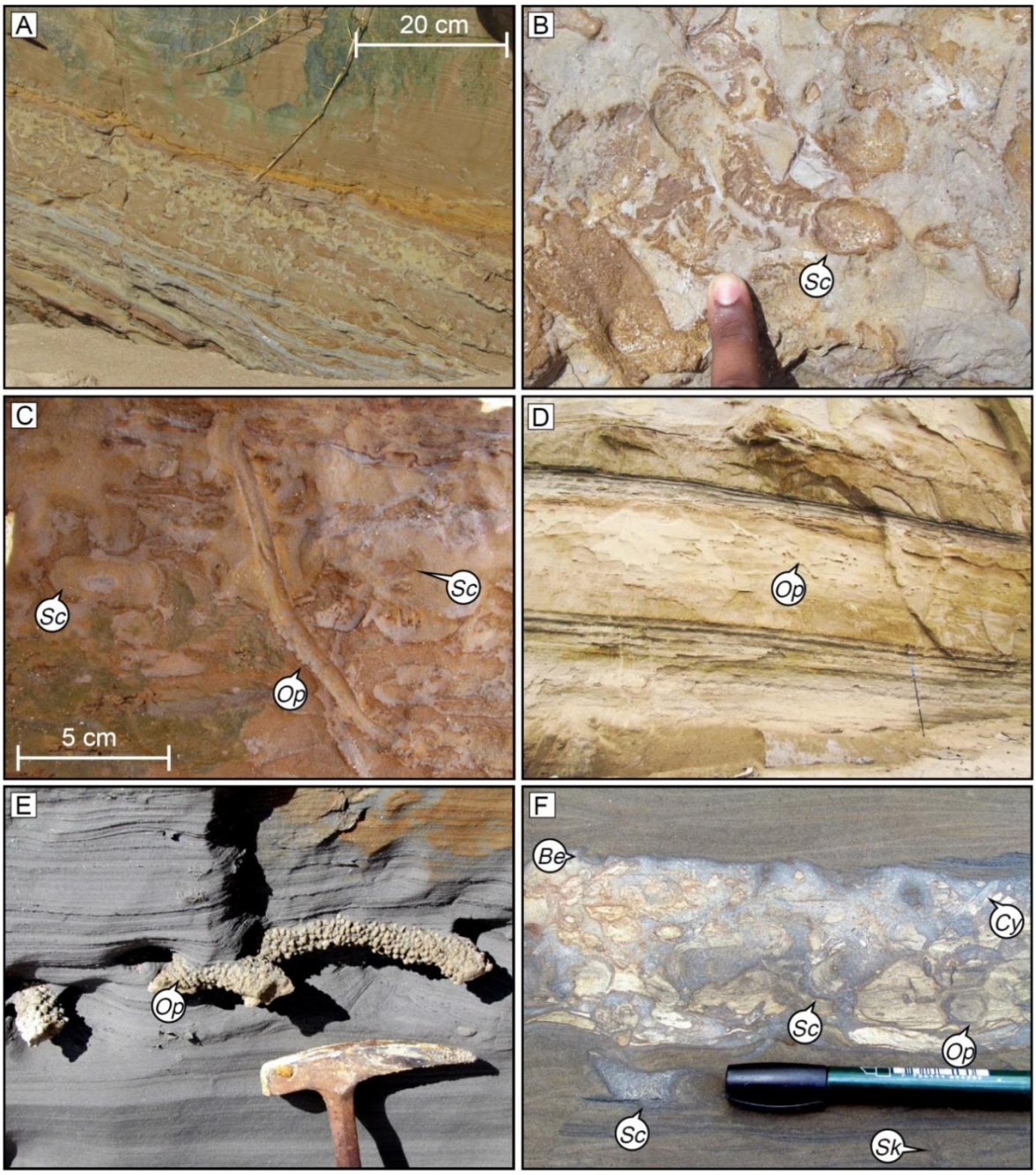

Fig. 3.16. Ichnological features of wave-modified fringing barrier bars or outer shelf shoals. (A) and (B) Respectively side and bedding-plane views of bar tops showing intense to complete bioturbation by echinoids *i.e., Scolicia* isp. *(Sc).* (C) Deep tier *Ophiomorpha nodosa (Op)* crosscutting shallow tier intense bioturbation of *Scolicia* isp. *(Sc).* (D) and (E) Distant and close-up views of interior of the sandstone beds sparsely colonized by deep tier *Ophiomorpha nodosa (Op).* The Jacob's stuff in Fig. 3.16D is 1.5 m long. (F) Lam-scram fabric. The bioturbated zone is intensely bioturbated with *Scolicia* isp. *(Sc), Ophiomorpha nodosa (Op), Cylindrichnus concentricus (Cy), Skolithos* isp. *(Sk), Bergaueria* isp. *(Sk),* whereas surrounding zone is sparsely bioturbated or completely not colonized.

3.4.3.2 Proximal prodelta and/or inter-lobe embayment on outer shelf

There is a very limited 7 m interval in Outcrop 11 (from 4 m to 11 m interval from the base) which shows characteristics of a proximal prodelta (see below) (Figs. 3.15A-B, 3.17A). Also, the middle 30 m interval (65 m below the top) of the Radix Point succession exhibits similar ichno-sedimentological features. The interval consists of sheet like parallel-laminated silt-rich muddy sediments, which gradually coarsen and thicken up into the sandy barforms belonging to the outer shelf shoals (Fig. 3.17A). Syneresis cracks occur sparsely. Gutter-casts or chutes crosscut the interval, more commonly towards the top. The gutter-casts are filled with TCS fine-to medium-grained sandstone with basinward 125°±5° paleocurrent directions (Fig. 3.17B). An aspect ratio of 1:1.5 reveals deep scouring on a high gradient slope by these sub-meter scale gutters. Bedding-parallel slickensides and syn-sedimentary thrusts within siltstones also indicate penecontemporaneous shearing parallel to bedding planes developed on a steep slope. Transient tidal influence is documented by sparse preservation of tidal bundles and isolated tidal bars near the prodelta-delta-front transition (Fig. 3.17C). Intermittent organic fragment-rich thin-beds are common. The transition from prodelta to delta-front deposits is marked by topward increasing wave influence and directional flows as indicated by the increased number of lenticular beds, combined-flow ripples and guttercasts. The absence of any feature denoting evidence of hyperpycnal flow or wave-influenced underflow implies the system to be more buoyancy-driven than friction- and density-driven, in sharp contrast to the shelf-edge deltaic counterparts.

The proximal prodeltaic deposit presents features of a stressed *Cruziana* Ichnofacies characterized by *Chondrites* isp., *Phycosiphon incertum*, *Siphonichnus* isp., *Asterosoma* isp., *Rosselia* isp., *Schaubcylindrichnus* isp., *Thalassinoides* isp., *Cylindrichnus concentricus*, "*Terebellina*" isp., *Planolites* isp., *Palaeophycus* isp., *Solemyatuba ypsilon, Diplocraterion* isp., *Rhizocorallium* isp. (?), and *Nereites* isp. (?) (Fig. 3.17D-F). Bivalves, crustaceans, and vermiform organisms dominated as colonizers. Moderate to intense (BI = 3–5) but localized bioturbation is observed with no to rare background bioturbation (BI = 0–1). Ichnofabrics are

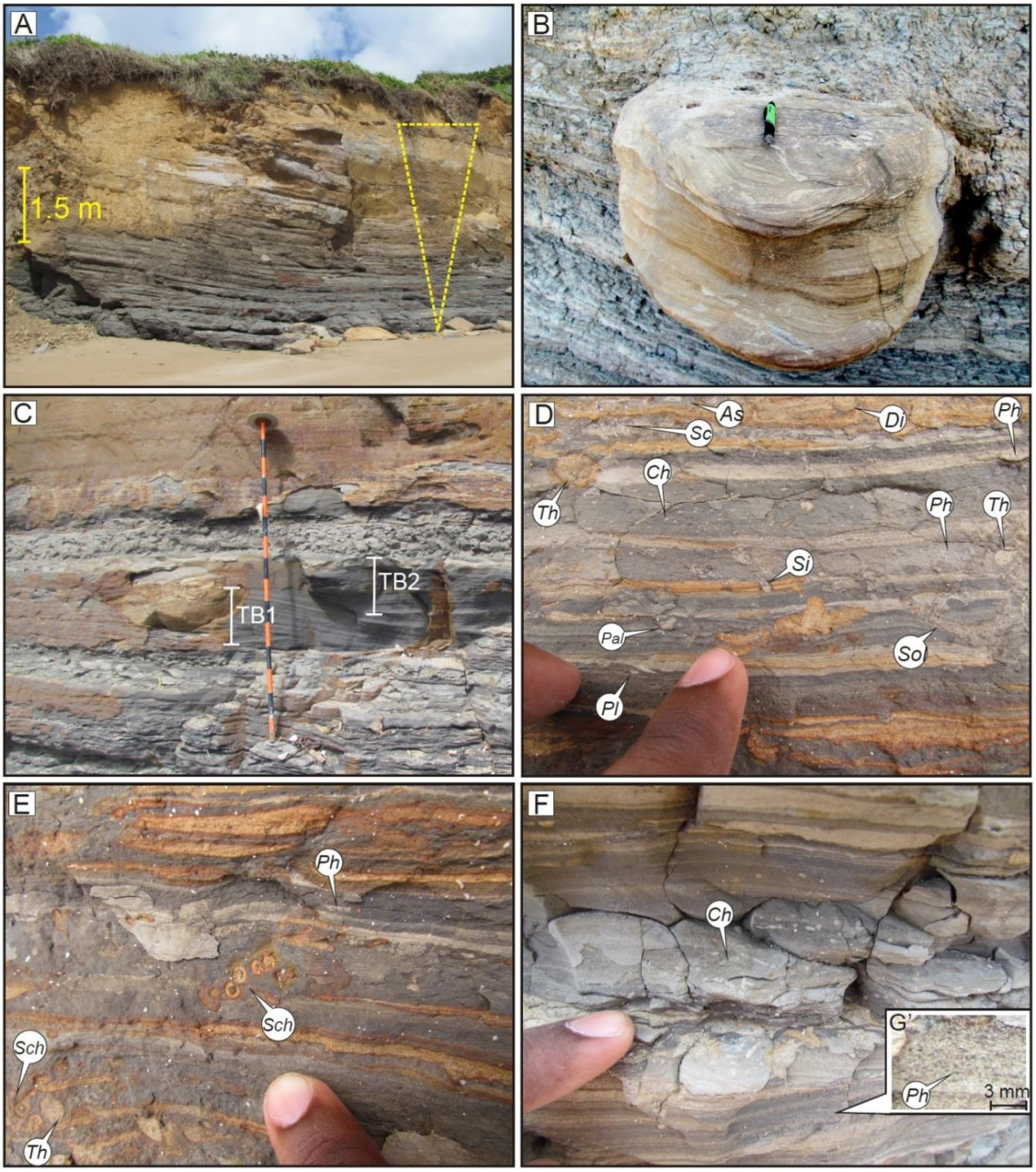

Fig. 3.17. (*N.B.* Figure caption is intentionally moved to the next page due to the large size of the figure)

Fig. 3.17. Ichnological and sedimentological features of proximal prodelta or inter-lobe embayment on outer shelf, as exposed in Outcrop 11. (A) Upward coarsening grain-size and thickening of beds in transition from prodeltaic sediments to delta-front. (B) TCS sandstone filling guttercast crosscutting prodeltaic facies. (C) Lens-shaped tidal bar at the prodelta-delta-front transition showing tidal-bundles (TB1 and TB2). (D) Moderate bioturbation within heterolithic sediments showing increased ichnodiversity compared to any other subenvironments of Mayaro Formation. Still the assemblage is depauperate and consists of individual ichnotaxa that are highly reduced in size; *e.g.*, *Phycosiphon incertum (Ph)*, *Thalassinoides* isp. *(Th)*, *Diplocraterion* isp. *(Di)*, *Siphonichnus* isp. *(Si)*, *Solemyatuba ypsilon (Sol)*, *Chondrites* isp. *(Ch)*, *Asterosoma* isp. *(As)*, and *Scolicia* isp. *(Sc)*. (E) The ichnodiversity and abundance changes laterally as shown here with relatively deeper-tier *Schaubcylindrichnus* isp. *(Sch)* and *Thalassinoides* isp. *(Th)* colonizing zone with shallow-tier *Phycosiphon incertum (Ph)*. (F) Along with *P. incertum (Ph)* (a closer view in inset G'), localized occurrence of *Chondrites* isp. *(Ch)* confined within the vicinity of the thin-bed (indicated by the finger), which is rich in organic-fragments.

mostly simple and rarely composite with (1) prominent absence of deep-tier colonization, (2) dominance of shallow infaunal and semi-infaunal deposit-feeding, and (3) chemosymbiotic trophic behaviour. *Chondrites* isp. burrows are confined within individual thin-beds signifying localized dysoxia from decaying organic fragments and intervals of very slow sedimentation (Fig. 3.17F) (for relationship between oxygenation and *Chondrites* colonization, see *e.g.*, Bromley and Ekdale, 1984; Ekdale and Mason, 1988; Bromley and Asgaard, 1991; Martin, 2004).

3.4.4 Incised canyon fill

At the top (*i.e.*, at the northern tip) of the Outcrop 8A succession, the delta-front sediments terminate against a discontinuity surface, referred to hereafter as SCW (or southern canyon/gully wall) (Figs. 3.18A-B; 3.19B). The SCW is irregular and inclined at 45°-58° towards 345°-035° (*i.e.*, ca. 30°-40° paleoslope after structural dip correction). Bowman (2003) and Bowman and Johnson (2014) described the SCW as a tectonic fault (see MB8 succession in *Fig. 3* of Bowman and Johnson, 2014). However, Dasgupta and Buatois (2012, 2015) reported the SCW being colonized by firmground *Thalassinoides* isp. demonstrating it to be an incision surface defining an example of the *Glossifungites* Ichnofacies. The decapod crustaceans colonized the SCW where firmground sands of the delta-front were exhumed. Their burrows penetrated at right-angle near the SCW, colonized up to a meter depth and crosscut the pre-existing softground trace fossils in the delta-front sand (Figs. 4.4-4.6 in Chapter 4). Silt-rich

muddy sediments deposited later above the incision surface filled the open firmground burrows during subsequent sedimentation.

Sediments deposited above the SCW are exposed as ca. 130 m thick interval in Outcrops 8B-8C (Fig. 3.18A-D). An almost meter thick listric normal fault-zone with undeterminable net-slip amount and containing lithified fault-gauge in Outcrop 8B has resulted in omission of an unknown thickness from the actual thickness of the interval (Fig. 3.18C). The succession is vertically overlain by gradual re-establishment of delta-front sediments as seen at the top of Outcrop 8B cliff (Fig. 3.18C). Those delta-front packages have intermittent erosional scour surfaces as their bases.

Towards the northern end of Outcrop 8C, the supra-SCW sediments abut as well as pinch out against another discontinuity surface, referred as NCW (or northern canyon/gully wall), which separates the supra-SCW succession from relatively older delta-front sediments (Figs. 3.18D; 5.19A). Compared to the SCW, the NCW is more irregular in nature with ca. 15°-40° paleoslope towards the SSE (after structural dip correction) and is characterized by slump-scars and associated cogenetic noncohesive debris flow deposits.

Therefore, the sediments in Outcrops 8B-8C were deposited within an east-west trending topographic furrow, which is interpreted to be a canyon/gully, flanked by two steep incision surfaces, interpreted to be canyon/gully walls: (a) the SCW, which was deep enough to exhume firmground sand to be colonized later, and (b) the NCW, which is unbioturbated for having rheologically unstable slope for colonization.

The canyon/gully-fill successions are dominated by systematically varying (from bottom to top) facies tracts (FT) of sediment-gravity flows as follows: (for detailed descriptions and explanations, see Chapter 5)

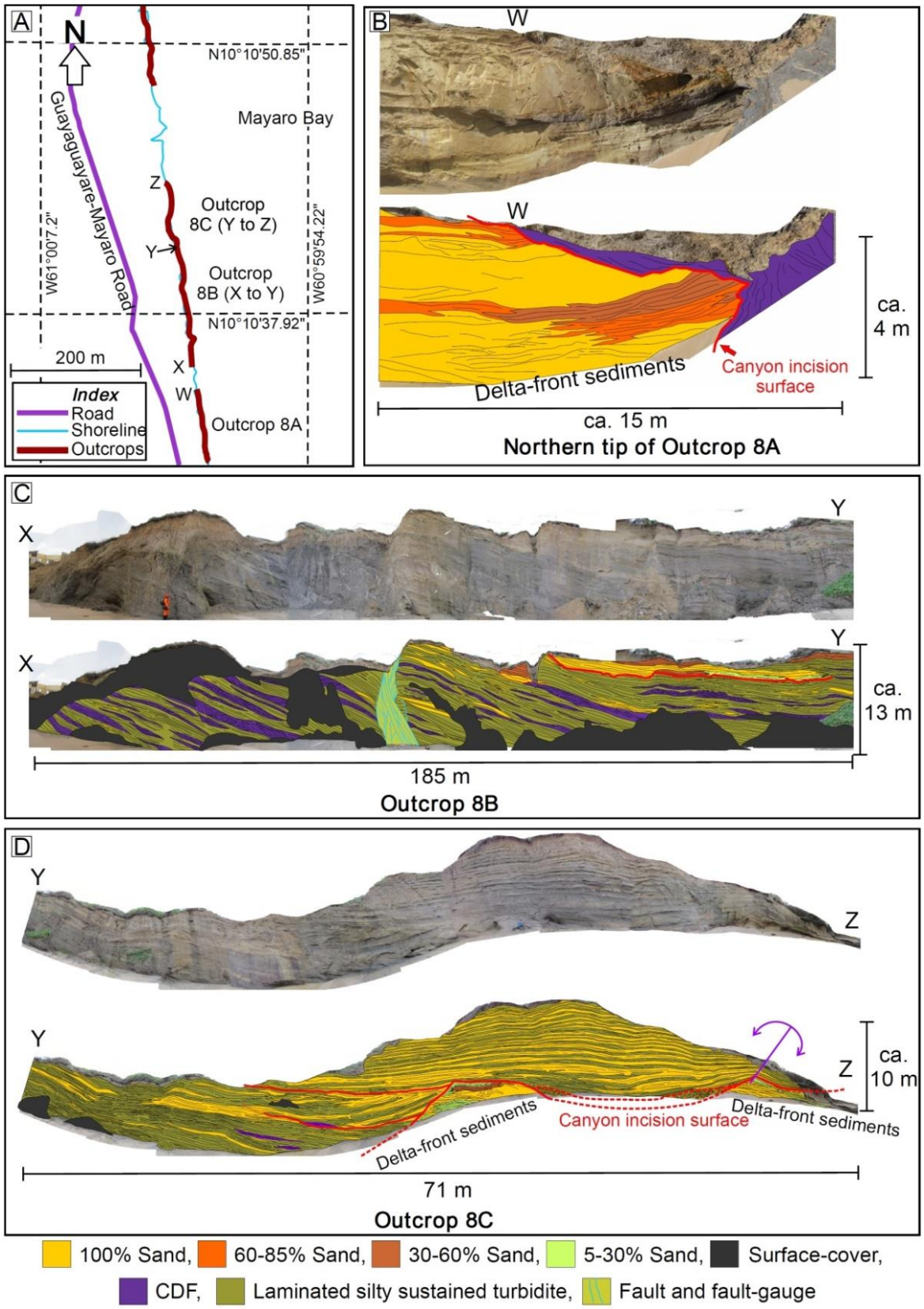

Fig. 3.18. (*N.B.* Figure caption is intentionally moved to the next page due to the large size of the figure)

Fig. 3.18. The canyon/gully-fill succession cutting across the distal/discrete wave-modified subaqueous barrier bar system of the shelf-edge delta-front. See section 3.4.4 (also Dasgupta and Buatois, 2015) for details. All the erosional cut-surfaces are marked in red. All the fault surfaces are marked in blue. (A) The map showing continuity of the canyon/gully-fill outcrops marked by points W, X, Y, and Z. (B) Stitched and interpreted photographs of the southern tip of the canyon/gully-fill. The SCW separates the delta-front (SCS barforms and heterolithic) sediments below and FT-A and -B (in blue) above. (C) Stitched and interpreted photographs of the sediments belonging to FT-C (southern block) and -D (northern block) separated by normal fault contact (with fault gauge). The southern block is upthrown. The delta-front sediments get re-established in pulses on top of FT-D with erosional bases (marked as red curve at the right-top corner). (D) Stitched and interpreted photographs of the sediments belonging to the FT-D and -E above and SCS sand beds belonging to the delta-front below the canyon/gully cut surface (NCW). Multiple secondary cut-surfaces are also shown here in red curves. The curved purple double arrow on a purple straight-line marks the axial trace of a supratancous fold, originating from differential compaction. Between the two dashed curves of canyon/gully incision surface lies the FT-A sediments originating from collapse of the primary canyon/gully-wall (see Fig. 3.19A).

FT-A: Cohesive and non-cohesive debris flow deposits derived from canyon/gully-wall collapse, which are locally deposited as dm to m thick lenses or wedges at or near the canyon/gully-wall, thereby not accounting into the total thickness of the canyon/gully-fill (Fig. 3.19A).

FT-B: at the base, ca. 30 m thick silt-rich cohesive debris flow deposit with landward rotated, allochthonous glided blocks derived from relatively older delta-front SCS-HCS sands (Fig. 3.19B-C). The FT-B is interpreted to be the proximal tail of a shelf-attached MTC thus evidencing progradation of contemporaneous shelf-edge compared to that of Outcrop 1A.

FT-C: ca. 45 m thick intercalation of lithological couplets defined by a) cm to dm thick beds of laminated silty sustained turbidite, interpreted to be hyperpycnite and/or underflow deposits, and b) slope-healing (*i.e.*, the debris flows healed their basal irregular topographic slopes by filling the irregular depressions) cohesive debris flow deposits derived in-situ from the silty turbidite (Fig. 3.19D).

FT-D: ca. 35 m thick interval consisting of physiographic units that correspond to bypassing of coarse clastic sediments along channels and their terminal and crevasse splays at slope breaks within canyon/gully as follows (Fig. 3.19E-H). (a) The 1-2 m thick channels containing medium-grained sand with planar and trough cross-stratification (TCS) and scoured

bases. Imbricated and intermittently armoured rip-up intrabasinal mud-clasts occur at the bases of the channels. Only bedload being preserved reflects the bypassing nature of the channels (Fig. 3.19G-H). (b) The 1-2 m thick sharp-based tabular-lenticular beds consisting of medium-grained sand-rich hybrid sediment-gravity flow deposits (Haughton *et al.*, 2009) (Fig. 3.19E-F). These sandstone beds associated with cohesive 'linked debrites' are interpreted to be the overbank and crevasse splays of the channels. The background sediments are similar to FT-C. [*N.B.* Linked debrites are deposited within turbidite units as a result of flow transformation from turbulent Newtonian flow to viscoplastic flow due to the increasing amount of clay in the flow; see Haughton *et al.*, 2003; also see section 5.2.2.4 for further elaboration and explanation.]

FT-E: Massive to parallel-laminated, tabular dm-thick sandy turbidite (*i.e.*, Ta-Tb; *sensu* Bouma, 1962) intercalated with background FT-C sediments (Fig. 3.19A, G-H). The thickness of the splays decreases upward. The base of this 20 m thick FT-E package is a gently curved scoured surface. The sandbodies are interpreted to be terminal splays of channels of FT-D, possibly showing a backfilling trend within the canyon/gully.

The 130 m silty mud-rich interval of Outcrops 8B and 8C are interpreted as a succession of prodeltaic sediments deposited within an incised canyon/gully (Dasgupta and Buatois, 2012, 2015). Bowman (2003) and Bowman and Johnson (2014) interpreted the same interval as distal prodelta on upper-slope. Based on the following points, the interval is interpreted to be a canyon/gully-fill:

i) The interval is flanked by irregular incision surfaces – SCW and NCW, incision being deep enough to exhume firmground sand.

ii) The interval is encased within underlying, overlying and laterally occurring wave-influenced delta-front deposits.

iii) All the FTs are deposited by different types of sediment-gravity flows.

iv) The FTs appear to be backfilling the canyon/gully.

v) None of the FTs are bioturbated, except a few very rare mottles or simple structures like *Planolites* isp.

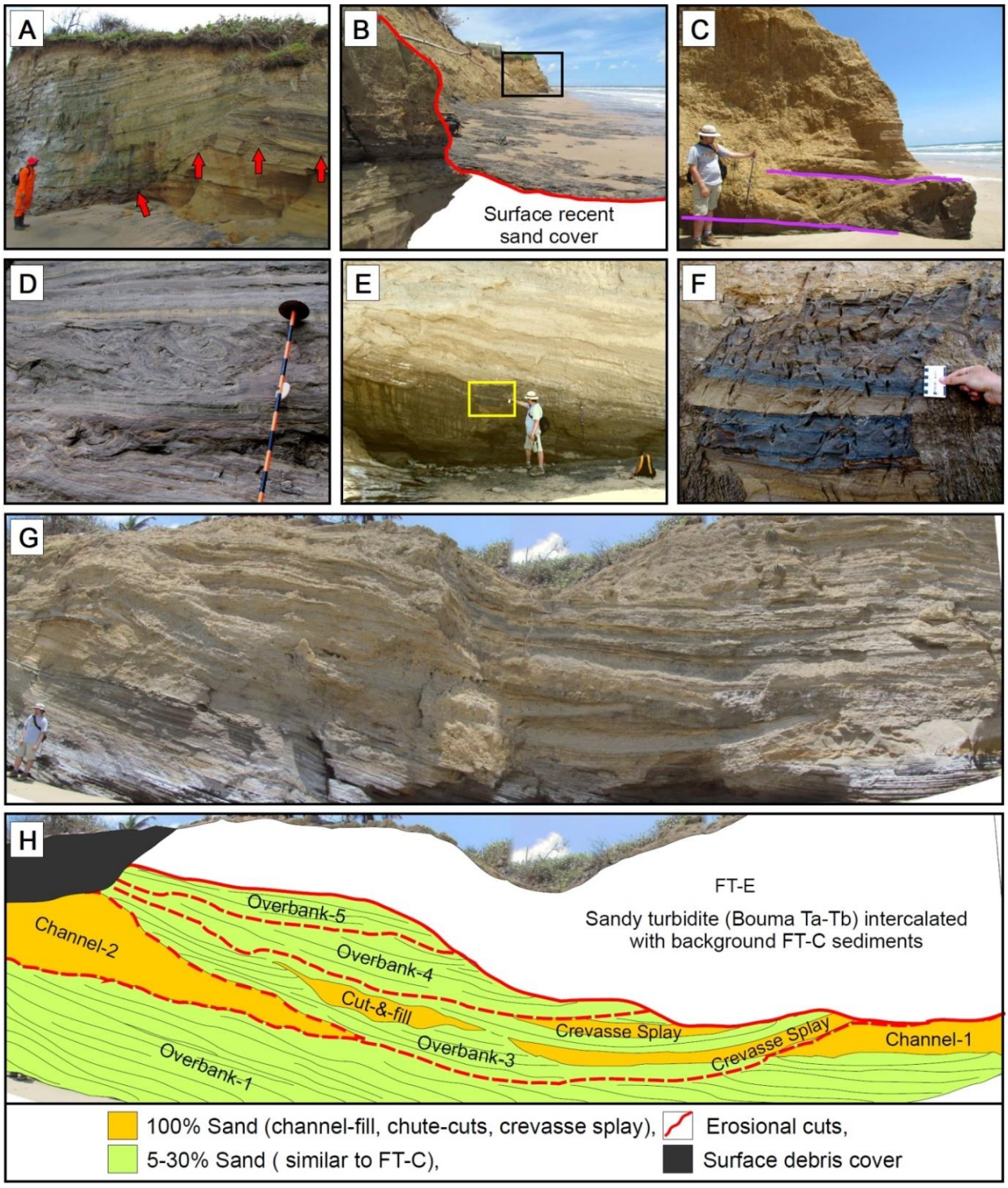

Fig. 3.19. (*N.B.* Figure caption is intentionally moved to the next page due to the large size of the figure)

Fig. 3.19. Sedimentary features of the canyon/gully-cut and -fill as exposed in Outcrops-8B and -C. (A) Red arrows marking the NCW, which separate the delta-front sediments below and FT-A veneer on top it. The FT-E sediments with suprataneous fold are above both the NCW and FT-A package. (B) The red curve showing the SCW, which separate the delta-front sediments below and FT-A and -B packages above. The rectangle marks the glided block. (C) Closer view of the glided block marked in Fig. 3.19B. The purple curves demarcate two glide-surfaces. (D) Lithological couplets of FT-C defined by intercalation of the laminated silty sustained turbidite (hyperpycnite and/or underflow deposit) and the cohesive debris flow deposits. (E) The FT-D package defined by the tabular beds (splays of bypassing channels) of hybrid-type gravity flow deposit consisting of combinations of the turbidite and 'linked debrites'. (F) Closer view of the hybrid gravity-flow deposits in the FT-D. The darker beds are the clay-bearing silty 'linked debrite'. The lighter coloured beds consist of the 'Bouma-type' turbidite units. (G) and (H) Stitched and interpreted photographs of FT-D and FT-E packages. [*N.B.* For detailed discussion and illustrations, see Dasgupta and Buatois (2015)].

The incision and filling of the canyon/gully is likely the result of local accommodation creation and filling in response to interactions between glacio-eustasy and growth faulting (see Fig. 5.8A-C in Chapter 5). Gullying on the shelf-edge, in general, may also be related to initiation of large scale shelf-edge collapse into attached MTC on the deeper slope (see section 3.4.1). During the filling and healing of the canyon/gully, the sediments were derived by longshore currents and hyperpycnal and wave-induced underflows. Characterizing the sediments as distal prodelta deposits on the upper-slope is also conceptually valid, although any regional allocyclic changes like landward regional shoreline movement or autocyclic delta-lobe switching is ruled out in view of paleocanyon/gully incision and filling. The delta-front depositional processes remained unchanged immediately outside the canyon/gully below and above the canyon/gully-fill. Coarser-grained sediments were mostly bypassing through the canyon/gully into the deep-water, until the delta-front was re-established at the top.

Similar shelf-edge incisions and healing of comparable but varying dimensions have been reported by Dixon *et al.* (2013) and Covault *et al.* (2009) from a few examples of shelf-margin delta deposits around the globe; although the sequence-stratigraphic controls and contexts of those cuts and subsequent healing phases may vary. However, their depositional trend can be analogous to the succession of FTs mentioned above (also see Dasgupta and Buatois, 2015).

3.5 Discussion

3.5.1 Uniqueness of animal-substrate interaction in the paleo-Orinoco Shelf-edge Delta

Ichnological aspects of the Paleo-Orinoco shelf-edge delta system point towards some unique characteristicss of the system, which are as follows:

3.5.1.1 Extreme effects of stress factors on the ecology of benthic animals

At a first look, the outcrops appear grossly devoid of trace fossils, with the exception of large and localized *Ophiomorpha nodosa* on the sandy cliffs. Smaller burrows require meticulous exploration to be found, not only for the reason that they are localized, but also due to their diminutive sizes and low abundance. Ichnodiversity is also so low, except among outer-shelf delta deposits, that recognition of discrete ichnotaxa in very low-abundance suites requires prolonged rigorous observation. Also, the lack of lithological colour contrast, particularly in mud-dominated prodeltaic facies associations, and poor consolidation of the sediments are responsible for the extreme taphonomic or preservational biases, where both ichnodiversity and abundances of trace fossils are already depauperated by ecologic stress factors. Poor consolidation not only hinders visualization, it also strongly influences the visibility in different moisture and light conditions resulting in challenges in estimating of ichnodiversity and ichnoabundance. In regular inner-shelf deltas, stress factors do have similar effects on ichnodiversity and intensity of bioturbation (MacEachern *et al.*, 2005, 2007a, 2007b; Hansen and MacEachern, 2007; McIlroy, 2007; Buatois *et al.*, 2008, 2011, 2012; Carmona *et al.*, 2008, 2009; Bhattacharya and MacEachern, 2009), but in the case of this shelf-edge delta, the effects are extreme and colonization is highly restricted, being confined to very narrow temporal and spatial colonization windows juxtaposed with the ambient and specific (to depositional subenvironments) stress factors (see section 3.5.2 and Table 3.2). On the other hand, tiering structure is very simple and in most cases burrows do not show any crosscutting or recolonization feature.

3.5.1.2 Diverse permutations (*i.e.*, combination + ranking) of stress factors corresponding to the sedimentary processes specific to depositional subenvironments

Salinity change is the sole ambient stress factor, whereas the combined effects of stress factors (*e.g.*, turbidity, turbulence, fluid mud activity, rapid erosion and deposition restricting colonization window) associated with tidal activity, sediment accumulation rate and morphodynamics are quasi-ambient (*i.e.*, ambient specific to certain group of subenvironments only as explained below) stress factors. Being a deltaic system, salinity fluctuations remain the background ecological stress, although the intensity of changes are likely to be different in various subenvironments – from extreme freshet conditions in feeder dominated settings (*e.g.*, subaqueous channel-overbank system) to very feeble in wave-influenced barrier bars on the outer shelf. Similarly tidal influence left no signature on thick-bedded sandy lithosomes, but tidal energy dissipation is ambient in all embayment conditions – from moderate in inter-bar areas in the barrier bar system and very low in shelf-edge prodelta. Sediment accumulation in response to fast creation of accommodation by growth-tectonics and shale-kinesis (*i.e.*, subsurface ductile shale creep movement) is always high – one of the extremes in the world (*i.e.*, 5-10 m/ka) (Wood, 2000; Bowman and Johnson, 2006, 2014). Morphodynamics of bedform deposits (*i.e.*, span of bedform formation, its collapse or erosion and migration rates) also has a strong influence on colonization windows on top and within all sandstone bedform deposits. All the other remaining stress factors (slope instability, flow turbulence, water turbidity, nutrient dispersion and upwelling, diurnal or seasonal changes in sediment flux, soupy substrate condition, oxygenation content) are not ambient, *i.e.*, relevant to specific subenvironments in terms of the presence and order of importance of individual stress factors (see Table 3.2).

3.5.1.3 Ichnological duality of a shelf-edge delta system

A large equatorial river like the paleo-Orinoco should be able to form a multi-lobate delta system both at the shelf-edge and also on the outer shelf, thereby demonstrating two distinct ichnological characters for the same system responding to two different degrees of strength of the stress factors – being very high at the shelf-edge and regular (similar to inner shelf deltas) on the outer shelf. Being disposed to to the extreme slope instability, erosion or gullying, direct

interaction with the breaking large-wavelength oceanic swelles, and fast sediment accumulation rates due to the substantial accommodation space available can be the explicable reasons making a shelf-margin delta lobe more stressed for the colonizers. The scenario of the same large river-delta system forming multiple lobes – some at the shelf-margin and others on the shelf – is the most plausible cause to explain both the extremely stressed (*e.g.*, as in Outcrops 1A to 9) and the regularly stressed (*e.g.*, as in Outcrops 10 and 11) deltaic ichnological signatures. This reaffirms the initial depiction of a multi-lobe shelf-edge delta depositional model by Edwards (1981) for the Wilcox Group (Paleocene-Eocene) of southern Texas (Fig. 3.20).

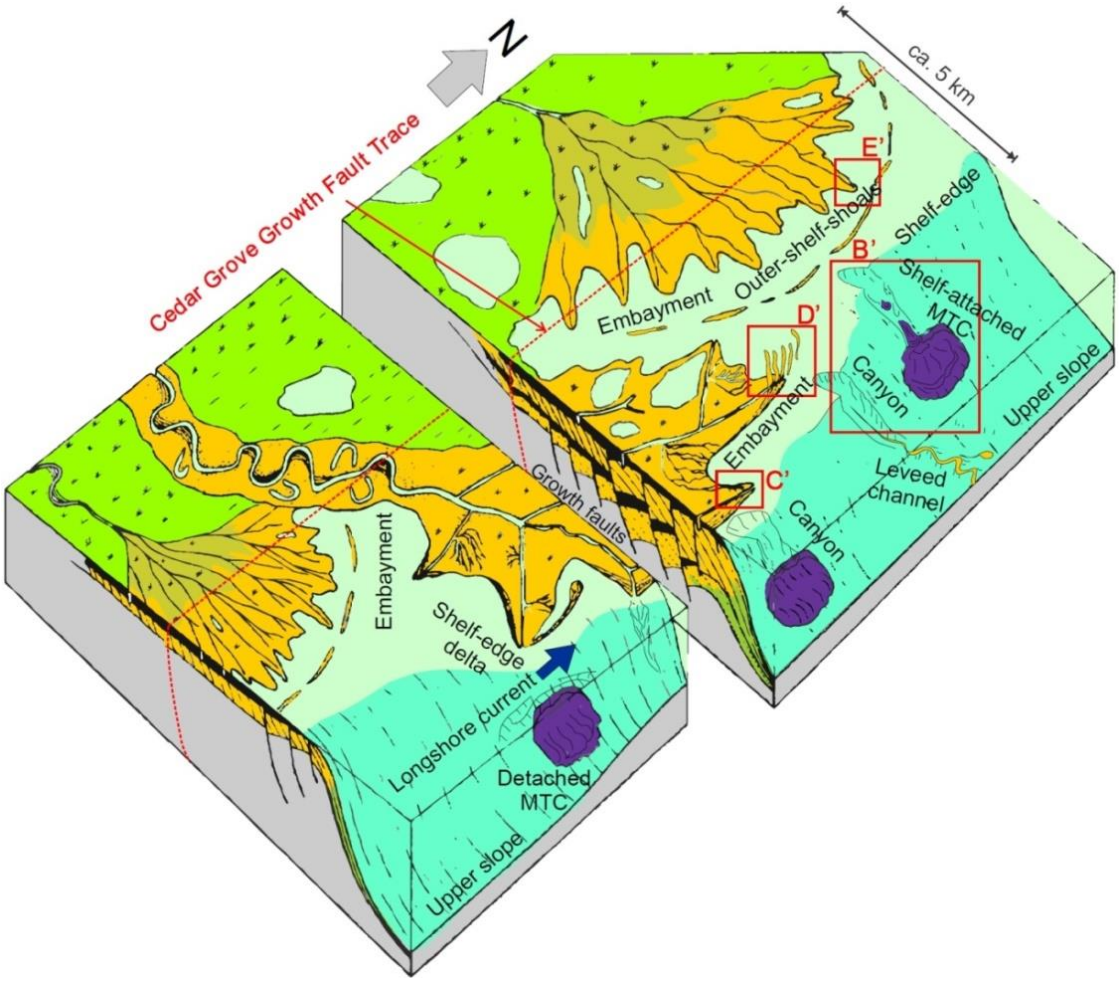

Fig. 3.20. Schematic block diagram, modified after Edwards (1981), showing different depositional subenvironments of the Mayaro Formation belonging to the shelf-edge delta and outer-shelf delta systems. Rectangles B', C', D', and E' are elaborated in Fig. 3.21.

3.5.2 Evaluation of stress factors in depositional subenvironments

Table 3.2 summarizes the ranking of the stress factors in each of the twelve depositional subenvironments. In this section we address the role of stress factors in the outer shelf, the shelf-edge, the upper-slope and the incised canyon/gully settings associated with the paleo-Orinoco delta system.

3.5.2.1 Stress factors on the upper-slope and within incised canyon/gully

Upper-slope deposits are completely devoid of trace fossils. Both the attached MTC and the canyon/gully-fill are deposits of diverse types of sediment-gravity flows, of which silt-rich cohesive debris-flows were dominant, followed by deposits of silt- and fine-grained sand-rich sustained turbidity currents, sand-rich 'high-density' turbidity currents, and hybrid flows. Therefore, the stress factors are direct results of the rheology of the flows. First, the steep gradient of upper-slope and its further steepening by rapid deltaic sedimentation are the precursors of prevailing high slope instability, the consequent gravity flows, and their frequencies. Sediment-gravity flows themselves are precursors of turbulence and water turbidity. While high slope instability and turbulence are the factors causing uninhabitable substrate conditions for all potential colonizers, water turbidity is a hindrance for suspension feeders like some of the worms, cnidarians, bivalves, and brachiopods (*cf. section 3.1.1* in Buatois and Mángano, 2011). Most sediment-gravity flows being erosional at their bases are thereby capable of removing varying thicknesses of sediment at the sediment-water interface, thus removing any traces of epifaunal and shallow infaunal colonization. Also reworking on top of the muddy sediment-gravity flow deposits by internal waves and tides create fluid mud acting as another stress factor (for mobilization of fine-grained sediments by internal waves and tides, see *e.g.*, Shi, 1998; Petruncio *et al.*, 1998; Puig *et al.*, 2003; Liu and Lin, 2004; Pomar *et al.*, 2012). Topography, especially at the canyonized/gullied shelf-edge and upper-slope, plays an important role in enhancing the strength of internal baroclinic bottom currents. All sediment-gravity flow deposits as exposed in the Mayaro Formation outcrops are bearing plant debris – either as disseminated fragments or as rare coaly laminations within sustained turbidity-current deposits. There is possibly no way to ascertain whether disseminated organic fragments were refractory

organic substances (*i.e.,* without any nutrition value) or decomposing ones during sedimentation. However, the sheet-like laminated organic materials are derived from phytodetrital pulses into the sustained turbidity currents, representing decaying plant materials, which consume and reduce the oxygen content under burial conditions. This fact also explains the absence of any deeper infaunal colonization. Preservational/taphonomic and observational biases are also responsible for the low diversity and abundance of trace fossils in the muddy upper-slope deposits.

Selective colonization at the canyon/gully-wall is caused by the further heightened instability of the slope due to very steep gradient, as estimated to be > 15° in both SCW and NCW. The NCW clearly contains signatures of repeated mass-wasting processes, whereas the SCW preserves localized *Glossifungites* Ichnofacies. This is because during the colonization, the slope of the SCW possibly was more stable at that location or higher up on the wall away from axial activity of the canyon/gully. Still the colonization is monotaxic, suggesting bioturbation under high stress or by highly opportunistic colonizers. Therefore, slope instability under steep gradient remains the possible stress factor influencing colonization window, as well as a preservational hazard, along with salinity changes and turbulence. The sand substrate was exhumed deep enough to be rheologically firm, because experimental observations (*e.g.,* Niemeijer *et al.*, 2009) suggest that same volumetric strain to attain firmness in coarser grain-size (sand in this case) requires much longer burial history than finer ones.

3.5.2.2 Stress factors at the shelf-edge

Stress factors at the shelf-edge vary according the depositional subenvironments established by the delta lobes vis-à-vis their autogenic movements. The primary controlling factor is the domination of either river-influenced processes or wave action.

3.5.2.2.1 Stress factors in river dominated subenvironments

In feeder-dominated (*i.e.,* dominated by channel and proximity to a channel/conduit) subenvironments (*i.e.,* the channels-overbanks-crevasses complex and mouth-bars), salinity

fluctuations and very high rates of sedimentation and erosion are two primary ambient stress factors. The distinctive diagnostic characters of the feeder system (*e.g.*, facies association and channel geometry) and occurrences of syneresis cracks are possible evidences of salinity changes, especially wherever they are associated with interchanging substrate condition between soupground and softground in muddy heterolithic substrates (as in section 3.4.2.7).

Likewise the grain-size trend defined by reverse grading overlain by normal grading within beds and phytodetrital debris in sand (commonly intact leaves) refer to pure and wave-aided 'hyperpycnal' sustained turbidity current (Mulder *et al.*, 2003; Bhattacharya and MacEachern, 2009; Zavala *et al.*, 2012). Steep gradients favour underflows at the shelf-edge, especially near a river mouth along where the hyperpycnal discharges are amplified by convective instability provided by the wave action (see *Fig. 1* in Bhattacharya and MacEachern, 2009). Buatois *et al.* (2011) identified distinctive ichnofabrics for the subenvironments of inner shelf, river-dominated deltaic deposits influenced by hyperpycnal flows in the Upper Cretaceous Magallanes Formation of the Austral Basin, Argentina. However, in the case of the paleo-Orinoco delta system, the extreme effects of stress factors were responsible for the lack of clear development of analogous ichnofabric in subenvironments dominated by river-processes.

For active channel-fills, the morphodynamics of the sandy barforms within the channel primarily and locally controls the colonization window. No bioturbation inside the barforms implies that the ambient stress factors (*i.e.*, sedimentation rate and salinity fluctuations) heavily prevailed during the active phases of channels, which were possibly related to flooding seasons. Seasonal drop in discharge and sediment load (or possible switching over from hyperpycnal to hypopycnal phase) fully or partly restored marine salinity. As a result, opportunistic colonization of vermiform organisms and bivalves within a limited time-window ensued at the top of the bars during the inactive phases of channels, thus forming a rare paucispecific suite of moderate–high BI of *Skolithos* isp., *Planolites* isp., *Cylindrichnus concentricus* and *Solemyatuba subcompressa*. Rare intense bioturbation recorded by *Thalassinoides* isp. and *Planolites* isp. perhaps points toward the channel being on the verge of abandonment with a prolonged colonization window and deeper-tier infaunal colonization.

For channels filled with silty heterolithic sediments deposited outside the axial sediment supply (*i.e.*, internal levee/ overbank) or for channels filled after their avulsive abandonment, the flocculation of clays and the deposition of fluid mud from quasi-laminar plug flow aided by tidal reworking constrained the colonization (in addition to ambient salinity changes). Fluid mud should be an unfavourable substrate condition particularly for suspension-feeders due to increased concentration of clay and silt particles practically clogging the feeding apparatus of these organisms (Gingras *et al.*, 1998; MacEachern *et al.*, 2005), and also for both detritus- and deposit-feeders preferring softground substrates. The infauna is incapable of excavating into fluid mud or stabilizing their burrow walls (Potter *et al.*, 2005). Channelized topography across the shelf-break zone enhances the effects of surface tides and internal tides along the channel(s), especially when the river-dominance is subdued during low discharge. Size reduction and simple morphology of individual trace fossils are obvious (*e.g.*, Fig. 3.5C), as well as overall low ichnodiversity.

Both proximal and distal overbank deposits are unbioturbated but likely due to various permutations of stress factors. The heterolithic deposits of the distal levee show intrastratal ptygmatic folding of thin-beds/laminations, which points toward the highest possible rheological difference between stiffer or more competent (silty medium-lower to fine-grained sand) and incompetent (clay-bearing silt) layers (Ramsay and Huber, 1987). For the lower viscosity fine-grained substrate, this indicates a dominantly soupy condition, but competent enough to prevent foundering of the coarser grains from sand laminations. The suspended sediment load, which spilled over and away from the feeder channels during high discharge activity, suffers from rapid flocculation by interacting with the ambient sea water and triggers both cohesive quasi-laminar plug flow and turbulent flow to deposit the distal overbank heterolithic sediments. A turbid water column near the sediment-water interface and associated soupy substrates created by the seasonal rapid flocculation completely suppress any possibility of colonization by benthic organisms. On the other hand, the proximal overbank deposits are highly influenced by salinity changes and high sedimentation rates due to immediate proximity to the feeder system. Regular breaching and scouring as well as bank collapse or slumping make the niche absolutely unfavourable for colonizers.

Mouth-bar deposition likely takes place during the high discharge seasons. The large dimensions of the TCS, climbing dune cross-stratification, soft-sedimentary deformation structures, and architectural amalgamation are suggestive of the depositional element being deposited by the fastest sedimentation rate among all the subenvironments encountered in the Mayaro Formation. In addition to high turbulence and freshwater influx, a rapid sediment aggradation rate is not favourable for any colonization. Even the distal sediments accumulated due to the collapse of the aggrading mouth-bar are deposited by surge-type sediment-gravity flows thereby implying also very high sedimentation rate.

Overbank and mouth-bar deposits are completely barren of trace fossils, whereas the sediments within the active and abandoned channels, where seasonal salinity fluctuations are supposed to be maximum, are colonized by opportunistic communities. This observation leads to the hypothesis that, in relative terms, channels are bathymetrically deeper than the surrounding overbank and terminal mouth-bar and evade salinity fluctuations during the seasonal hypopycnal stage of the fluvial discharge, thereby paving the short time span for opportunistic colonization. In addition to the rapid sedimentation and erosion rates at the mouth bars, the hypopycnal plumes affect the overbank and terminal mouth-splays alike in maintaining low salinity, high flocculation and water turbidity, consequently making the deposits completely barren of trace fossils.

3.5.2.2.2 Stress factors in wave-dominated subenvironments

The sandy barrier bar complex exhibits the direct influences of wave action as indicated by the SCS-HCS beds. However, the thickness (commonly amalgamated to multi-meter scale) of the SCS and HCS beds, their constituent medium-grained sand, and long wave-length (2–8 m) – all point towards the waves being very large in dimensions compared to the regular storm waves on the shelf. This supports the hypothesis that direct interaction of the oceanic swells and shelf-break causes the large surface waves at the shelf-margin deltas (Galloway and Hobday 1996; Porębski and Steel, 2006). According to Dumas *et al.* (2005) and Dumas and Arnott (2006), to remain symmetrical but unidirectional and to attain enough shear strength at the bottom to move medium-grained sands, the large oceanic waves require significantly high sedimentation rate,

very long wave-period and substantially large and fast wave orbitals of oscillatory flow and oscillatory-dominant combined flow. Thus, the modified "storm" wave-base (oceanic swell wave base?) for large waves applicable to the shelf-break is likely to be relatively deeper (≫ 50 m) than regular storm wave-base (*i.e.*, 13-50 m; Dumas and Arnott, 2006). The modified "storm" wave-base is sufficiently so deep that it explains the absence of any sedimentological or ichnological evidence of subaerial exposure within the barrier bar deposits of the Mayaro Formation. The primary ambient stress factor in the wave-influenced subenvironments (*i.e.*, very high sediment accumulation and erosion rates) results in the derivative stresses like pace of morphodynamic movements of barforms, rip currents, extreme dilution of nutrients within sediments, turbulence, and water turbidity.

The attached barrier bars proximal to the feeder system and the mouthbars seem to be deposited under very high rates of sedimentation restricting any colonization window. The morphodynamic movements of the barforms under longshore drift provided the rare time windows for the low intensity and paucispecific colonization by decapods, polychaetes and rarely sea-anemones. Therefore, amalgamated barrier bars and mouthbars both are completely barren of trace fossils, whereas layered barrier bars with heterolithic intercalations still show sporadic bioturbation due to the limited availability of colonization window. The paleocurrent directions measured from the TCS within the feeder system demonstrate that the feeder system was oriented northwards 000°–030°. In comparison with the N-S regional depositional strike, it may imply a strong longshore drift influencing the shape of the lobe. Therefore, turbulent instability above the sandy softground substrate remains a strong stress factor as a derivative of wave action. As a result, *Bergaueria* isp., a burrow produced by suspension-feeding or predator sea-anemones, can be found rarely and only in the heterolithic intervals deposited in inter-bar areas with reduced energy condition.

Moving laterally along the depositional strike distant to the feeder system, the barrier bars are developed as discrete sand bodies like spit-bar and barrier-inter-bar systems under more marine conditions as a departure from the fluvial-feeder influence, which resulted in reduced salinity fluctuations, and relatively reduced rates of sedimentation as well as erosion. The paucispecific nature of colonization points toward the ambient stress factors. The same barform

is intensely colonized by *Ophiomorpha nodosa*, only where it is also cut by a tidal inlet (Fig. 3.11A-E). This indicates that more inactive barforms are not only subjected to inlet incision, also their tops get densely colonized by decapods. Distal barrier bars mark the first occurrence of fully marine trace fossils, such as *Scolicia* isp. and *Macaronichnus segregatis*, in the Mayaro Formation outcrop, thereby indicating a departure, at least seasonally, from brackish-water influence (Figs. 3.12B, 3.13B).

The discrete occurrence of barrier barforms likely had created elongated depocenters, which are shielded from direct wave action. Such a restricted depocenters can be prone to more seasonal salinity fluctuations, influx of sediments (sand and silt) during the hyperpycnal phase of the feeder system, elevated tidal influence due to topographic effect, and clay flocculation and fluid mud activity during the hypopycnal phase. These depocenters are likely filled with inter-bar shoals – flood-tidal and ebb-tidal shoals. The tidal bundles, combined-flow ripples, and wave ripples indicate sediment transport along these elongated depocenters (*i.e.*, N-S) by tidal currents (Fig. 3.11F-G). The ichnodiversity in these heterolithic deposits (softground *Thalassinoides* isp., *Cylindrichnus concentricus, Scolicia* isp., *Teichichnus rectus, Asterosoma* isp., *Rosselia* isp., *Conichnus* isp., *Bergaueria* isp., *Planolites* isp. and small escape trace fossils) is conspicuously higher than in sandy barforms (*Ophiomorpha nodosa, Scolicia* isp., large escape trace fossils, *Macaronichnus segregatis*, and *Sinusichnus sinuosus*). This is presumably due to protection from the large wave action and increased colonization windows within these elongated depocenters. However, localized occurrence of mantle-and-swirl structures in muddier intervals do indicate possible seasonal variation not only in sedimentation rate and lowering of salinity, but also changes in substrate rheology from softground to soupground and *vice versa*.

3.5.2.2.3 Stress factors in shelf-edge prodelta

The outcrop record of the shelf-edge prodelta shows temporal fluctuations of substrate rheology as the main stress, which acts both as a hindrance for colonization and a preservational hazard. Fluid mud activity is evidenced by mantle-and-swirl structures, foundered ripples, transient tidal influence as shown by double mudstone drapes, and an absence of trace fossils made by suspension feeders. Only the softground substrates are colonized by the ecologically

resilient polychaetes and bivalves. Rarely does more than one ichnotaxa occur together. This paucispecific opportunistic colonization can be attributed to two additional factors (*i.e.*, oxygenation level and salinity changes). Laminations rich in organic fragments indicate phytodetrital pulses reaching the areas away from deltaic lobes. Their decomposition potentially leads to localized dysoxia or anoxia. Also, the presence of shrinkage cracks (syneresis) may indicate changes in ambient salinity condition. However, because bedding surface views along contrasting lithological boundaries are absent in the outcrop, observational bias may have made the subenvironment appear more stressed than it actually was.

3.5.2.3 Stress factors in the outer shelf delta subenvironments

The limited outcrops (Outcrops 10-11) of sediments deposited at the outer shelf deltaic lobes of the same system display typical ichnological signatures of a wave-influenced deltaic succession (*e.g.*, MacEachern *et al.*, 2005; Buatois *et al.*, 2008; *i.e.*, stressed '*Skolithos*-*Cruziana* Ichnofacies') for the wave-influenced delta-front and stressed '*Cruziana* Ichnofacies' for the proximal prodelta. Apart from the direct fluvial influence, repeated large-wave activity (storm events) is the main controlling factor which influences the bar migration vis-à-vis the colonization window. The abundance of both protrusive and retrusive trace fossils reflects both rapid sedimentation and scouring/erosional removal of sediments, implying contrastingly much lower aggradation rates than the subenvironments in shelf-edge lobe counterparts. Slower aggradation rate is one of the four fundamental differences that caused the outer-shelf sediments to get relatively more bioturbated, in terms of ichnodiversity, abundance, and complexity, than its shelf-edge counterparts. The second difference is the presumed presence of narrow sliver of shelf that influences the attenuation of kinetic energy of the larger waves. Therefore, the sizes of the HCS-SCS beds are much smaller and more discrete than those on the shelf-margin. The gradient must have been gentler than the shelf-edge to preserve bedforms like swash cross-stratifications formed at the foreshore-shoreface transition. However, the gradient is steeper than in inner-shelf deltas, as demonstrated by common slump beds with extensive soft-sediment deformation. Although the sediments show sparse colonization and depauperate assemblages, strictly marine ichnotaxa, such as *Chondrites* isp. and *Phycosiphon incertum*, are exclusive to the outer shelf prodelta, being absent in the shelf-edge counterparts. This demonstrates substantial

restoration of marine lower-shoreface to offshore conditions at certain intervals possibly due to seasonal variations. Moreover, sporadic occurrences of *Chondrites* isp. limited within single beds refer to localized dysoxia by slow sedimentation as well as decomposition of plant fragments, thus leading to the colonization by the chemosymbionts. Similar to the shelf-edge prodelta counterparts, fluid-mud deposition remains the stress factor on epibenthic colonization.

3.5.2.4 Depositional model based on the integration of ichnological and sedimentological datasets

Traversing from south to north, *i.e.*, 4.6 km lateral stretch and 2 km vertical thickness, the outcrops exhibit the record of facies variations moving obliquely upward through the succession in paleogeographic space. Fig. 3.20 illustrates an idealized depositional model (modified after Edwards, 1981). Fig. 3.21 shows all the depositional subenvironments irrespective of their occurrences in the succession and their corresponding trace fossil distributions. Integration of ichnological and sedimentological datasets records the autogenic spatial adjustments of the depositional subenvironments and corresponding facies variations. While moving from the base to top of the Mayaro Formation succession, the vertical and lateral occurrences of subenvironments vis-à-vis the depositional history of the succession are illustrated in Fig. 3.22. The system grossly and steadily progrades. The shelf-attached MTC at the top of the upper-slope is the basinward-most depositional setting that occurs at the base of the Mayaro Formation succession. The MTC was likely to be connected to a canyon/gully that incised upon a contemporaneous shelf-margin and was fed by the further landward occurring delta-lobe (Moscardelli and Wood, 2008). With continued progradation, the accommodation space got filled with sediments delivered and deposited by a friction-dominated subaqueous feeder system of the shelf-edge delta, overlain by autogenic facies variation into the wave-influenced barrier-system. With further progradation of the shelf-edge delta and ensuing basinward movement of the shore-line, an outer-shelf delta-lobe of the same system developed towards north of the locus of shelf-edge lobe. There is a conspicuous absence of any outcropping stratigraphic surface with allogenic connotation, except the canyon/gully-cut, which may be a result of localized relative sea-level changes triggered by growth-tectonics (Chapter 5; Dasgupta and Buatois, 2015).

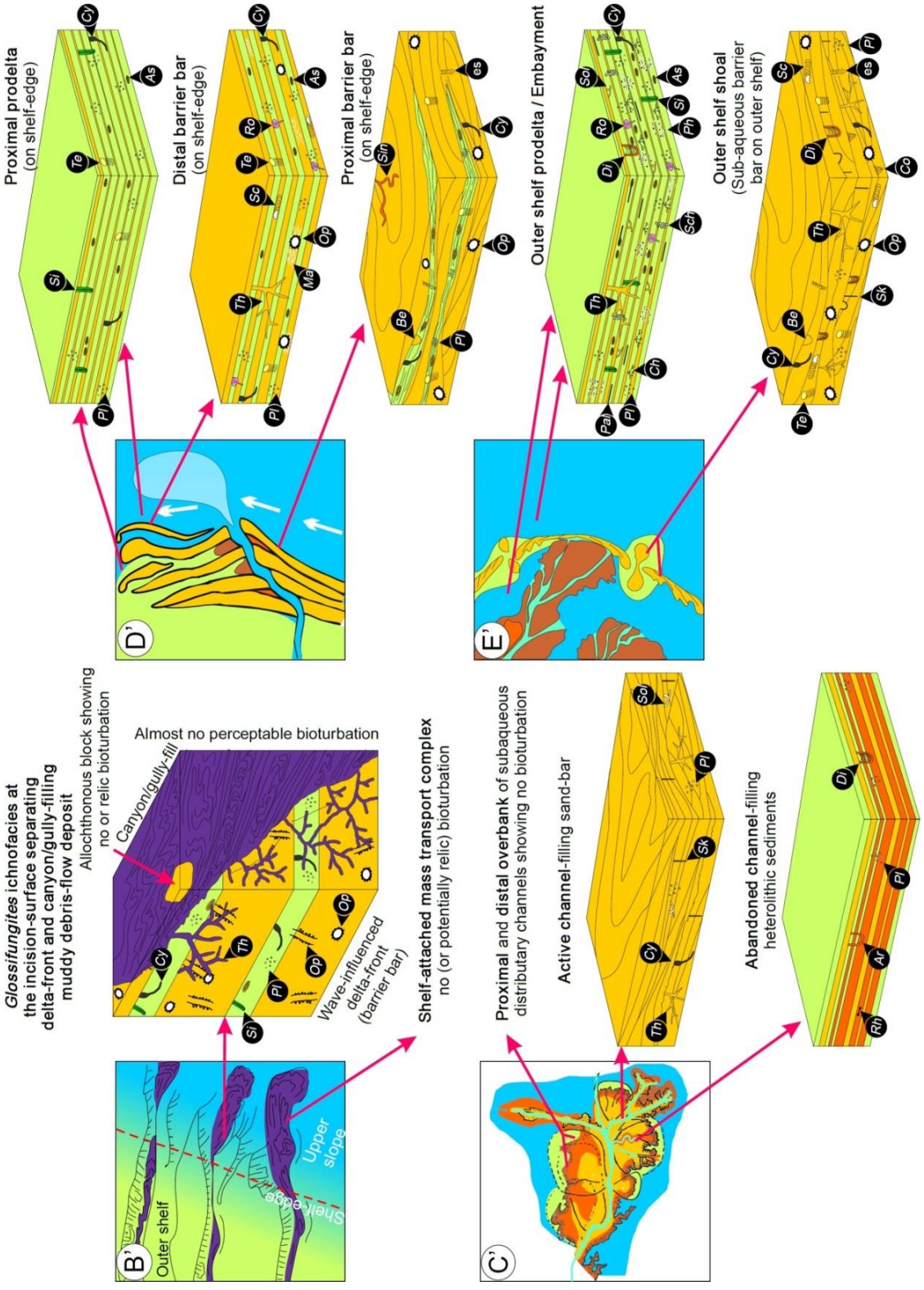

Fig. 3.21. (*N.B.* Figure caption is intentionally moved to the next page due to the large size of the figure)

Fig. 3.21. Schematic reconstruction of trace fossil distribution in different subenvironments of the shelf-edge delta and the associated outer shelf delta. Elaborated from rectangles B', C', D', and E' in Fig. 3.20 (modified after Boyd *et al.*, 1989; Bhattacharya and Walker, 1992; Bhattacharya and Giosan, 2003), Rectangles B'-E' respectively show schematic plan-views of canyon/gully-cut and connected shelf-attached MTC, subaqueous friction-dominated river-influenced channel-overbank-crevasse-mouth-bar system, wave-influenced delta-front system, and outer shelf shoals. The block diagrams elaborate the trace fossils within sediments in each sub-environments. The ichnogenera shown are as follows: *Ophiomorpha* isp. *(Op), Skolithos* isp. *(Sk), Diplocraterion* isp. *(Di), Planolites* isp. *(Pl), Cylindrichnus* isp. *(Cy), Scolicia* isp. *(Sc), Thalassinoides* isp. *(Th), Teichichnus* isp. *(Te), Schaubcylindrichnus* isp. *(Sch), Palaeophycus* isp. *(Pal), Asterosoma* isp. *(As), Rosselia* isp. *(Ro), Conichnus* isp. *(Co),* escape trace fossils (es), *Arenicolites* isp. *(Ar), Siphonichnus* isp. *(Si), Bergaueria* isp. *(Be), Solemyatuba* isp. *(Sol), Macaronichnus* isp. *(Ma), Chondrites* isp. *(Ch), Phycosiphon* isp. *(Ph),* and *Sinusichnus sinuosus (Sin).*

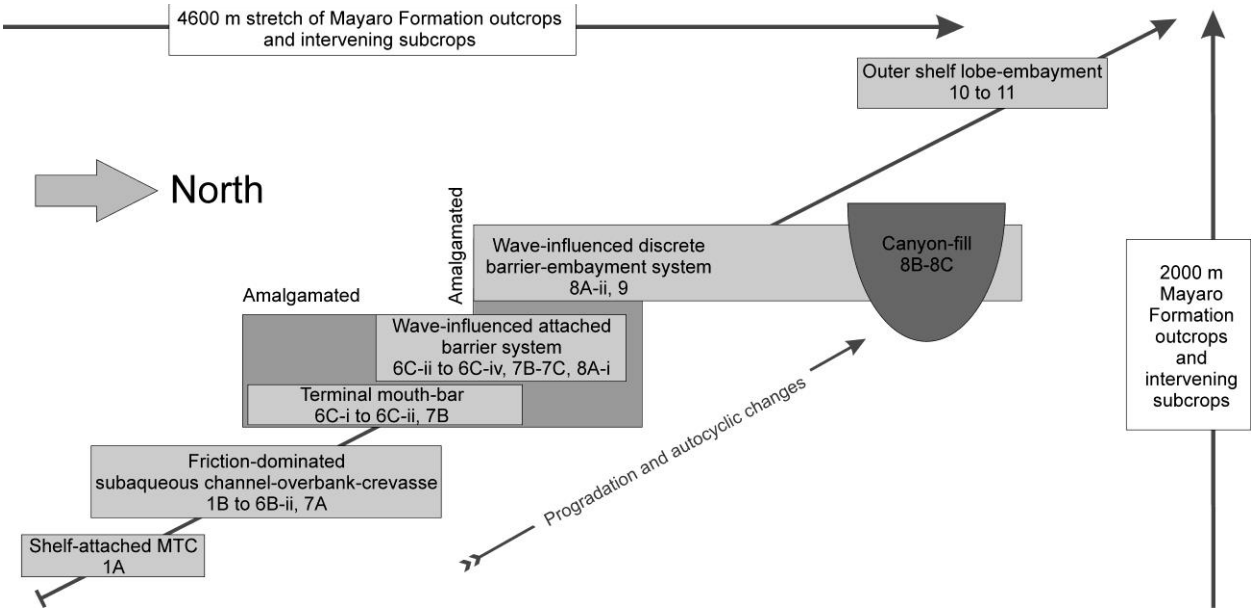

Fig. 3.22. Cartoon showing lateral and vertical facies associations in the Mayaro Formation outcrops. See also (or Chapter 5).

3.6 Conclusions

The Mayaro Formation succession outcropping along the SE coast of Trinidad was deposited in a river-dominated to wave-influenced deltaic environment at/near the shelf-break; the slope-instability related to relatively high gradient and growth-tectonics was an additional

controlling factor on this delta system. Ichnological evidence suggests that shelf-edge deltas are one of the most extreme marine environments. However, like the diverse physical sedimentological processes taking place in every distinct subenvironment, the corresponding ichnological characters and the combinations of controlling stress factors are also diverse and distinct. The apparent ranking (permutations) of the stress factors are also distinct and diverse, so is the preservation potential of trace fossils. Likewise the ichnological and sedimentological characteristics of the shelf-edge delta system also strikingly vary in geographic three-dimensional space and exhibit characters of upper-slope, shelf-margin, and outer shelf components as well as of canyon(s)/gully(ies) cutting across shelf-edge delta-lobe. Especially the delta-lobes themselves can demonstrate dual characters of an extremely stressed shelf-edge properties and regularly stressed on-the-shelf properties. The present study, therefore, furnishes a combined ichno-sedimentological comprehensive model for a low-latitude, accommodation-driven, shelf-edge delta of a large river system like the paleo-Orinoco developed on an active continental margin (oblique foreland). Autogenic changes along with overall continued progradation appear to be the controlling stratigraphic factors for distribution of sedimentary facies and corresponding ichnological characteristics in the oblique succession of the Mayaro Formation outcrops. Integrated sedimentological and ichnological characterization of every individual subenvironments of the system will serve as a guideline for other shelf-edge deltas in space and time.

3.7 Acknowledgements

The authors are immensely indebted to the profound support and encouragements by Carlos Zavala, Livan Blanco Valiente, Rafael Vela, and Yrma Vallez. We are grateful to James MacEachern, Shahin Dashtgard, Korhan Ayranci, and the anonymous reviewer for the meticulous scrutiny of the article, valuable recommendations, and comments. We also deeply acknowledge the cordial helps and inputs from Marlon Bruce, Anderson Arjoon, Jivanti Ramdular, Jose Luis Huedo Cuesta and the entire subsurface group of Repsol E&P T&T Limited. Logistic and onsite support and assistance from Dinelle Medina, Ann Marie Singh, Michael, and Siewchan Ragoo are highly appreciated. Field assistance by Balázs Törő in 2013

was invaluable to fill up the remaining gaps in the study. Financial supports provided are as follows: Canadian Natural Sciences and Engineering Research Council (NSERC) Discovery Grant to Buatois; funding for fieldwork by Repsol E&P T&T Limited, and Graduate Student Scholarship and Teaching Assistantship from Department of Geological Sciences, University of Saskatchewan, Dr. Rui Feng Graduate Studies Award, the AAPG Foundation Merrill W. Haas Memorial Grant, and the Saskatchewan Innovation and Opportunity Awards from the Provincial Government of Saskatchewan and University of Saskatchewan to Dasgupta. The authors are thankful to Liviu Giosan, Ven Kolla, Juan José Ponce, Brian Pratt, Noelia Carmona, Alec Aitken, Dennis Meloche, Luis Quiroz, Pablo Alonso, Andreas Wetzel, Renata Netto, Davinia Diez-Canseco Esteban, Siddhartha Sinharay, Shreyosi Dasgupta, and Late Tripti Banerjee for meaningful discussions and inspirations.

CHAPTER 4: UNUSUAL OCCURRENCE AND STRATIGRAPHIC SIGNIFICANCE OF THE *GLOSSIFUNGITES* ICHNOFACIES IN A SUBMARINE PALEO-CANYON – EXAMPLE FROM A GELASIAN SHELF-EDGE DELTA, SOUTHEAST TRINIDAD

Dasgupta, S., and Buatois, L.A., 2012, Unusual occurrence and stratigraphic significance of the *Glossifungites* ichnofacies in a submarine paleo-canyon – Example from a Pliocene shelf-edge delta, Southeast Trinidad: *Sedimentary Geology*, v. 269–270, p. 69–77.
(*N.B.* See Chapter 3 for the controversy involving the age of Mayaro Formation)

Keywords: *Glossifungites* Ichnofacies; submarine canyons; Paleo-Orinoco; shelf-edge delta; firmground.

Abstract

Sedimentary rocks belonging to the shelf-margin delta of the Paleo-Orinoco River are present at the southeast coastline of Trinidad in the Columbus Basin. The Gelasian Mayaro Formation, exposed as foreshore cliffs, represents the wave-influenced delta-front and mouth bar of this system. These deposits consist of thick to very thick hummocky cross-stratified sandstone beds and thin-bedded to laminated heterolithic sediments. They also contain abundant soft-sediment deformation structures and sparse well-preserved softground burrows (*e.g.*, *Ophiomorpha nodosa*). Towards the north-central part of the outcrop, the delta-front deposits are cut across by a paleo-canyon filled with younger mud-dominated prodeltaic sediments. The rare exposure of the canyon-wall exhibits an unusual preservation of *Glossifungites* Ichnofacies. Contrastingly distinct from archetypal examples, this monospecific suite contains a low abundance of firmground *Thalassinoides* filled with mud rather than sand. The tracemakers burrowed into a firm medium-grained sandy substrate of the delta-front, and the burrows were subsequently passively filled by the mud from the overlying the canyon-fill. The deep-tier firmground *Thalassinoides* suite crosscuts the pre-existing softground trace fossils. Integration of ichnological, sedimentological, and sequence-stratigraphic datasets indicates that the older delta-front sediments are separated from the canyon-fill deposits by distinct episodes of fluctuating

relative sea-level controlled by the basin-bounding growth-fault activities and the development of the canyon. Whereas the entire shelf-margin megasequence might have been deposited through a regional scale sea-level lowstand, the local fluctuations in accommodation resulting from the growth-fault movements and the incision of the canyon were responsible for the shifting positions of the depositional architectural elements of the shelf-edge delta.

4.1 Introduction

The *Glossifungites* Ichnofacies (Seilacher, 1967) is a substrate-controlled ichnofacies which has been extensively used in sequence stratigraphy to identify and characterize discontinuity surfaces (MacEachern *et al.*, 1992, 2007; Pemberton *et al.*, 1992, 2001, 2004; Buatois and Mángano, 2011). Development of the *Glossifungites* Ichnofacies in siliciclastic sediments invariably involves erosional removal of sedimentary layers. The *Glossifungites* Ichnofacies is commonly conspicuous in outcrops and cores, and is preserved at lithological interfaces, typically mudrocks overlain by coarser-grained clastic sediments. In such cases, the unlined burrows occurring in mudrock are passively filled with coarser grains from the overlying stratum. This reveals that the burrows remained open after the tracemaker relinquished the structure, thereby permitting sand grains from subsequent depositional events to pervade into the open, stable burrows. In a few cases, occurrences of burrows filled with sand and emplaced in compacted sand have been documented (*Fig. 5* of Pemberton *et al.*, 2004; *Fig. 14* of Buatois *et al.*, 2008). The *Glossifungites* Ichnofacies develops in a wide variety of sequence-stratigraphic contexts (MacEachern *et al.*, 1992, 2007; Buatois and Mángano, 2011), but the majority of documented case studies are from shallow-marine settings. Only a few examples are known from deep-marine contexts, such as incision of submarine canyons during relative sea-level falls (*e.g.*, Hayward, 1976) or possible autogenic erosional episodes by turbidity currents and bottom currents (*e.g.*, Savrda *et al.*, 2001; Hubbard and Schultz, 2008; Gérard and Bromley, 2008).

The outcrop of the walls of a paleo-canyon in the Gelasian Mayaro Formation from southeast Trinidad Island of Trinidad and Tobago (Fig. 4.1) serves as a unique example of the development of the *Glossifungites* Ichnofacies, as the only known example of this ichnofacies

developed on a canyon incision surface, which separates the underlying delta-front sandy sediments from the overlying prodelta mudrocks. The incision surface identified on the basis of the development of *Glossifungites* Ichnofacies marks a co-planar stratigraphic surface in the shelf-edge delta setting of the Gelasian Paleo-Orinoco River. It indicates striking changes in accommodation vis-à-vis changes in the loci of deposition for the sandy lithosomes of the shelf-edge delta system before and during the formation of canyon, colonization of the firm substrate exhumed by the incision and also during the subsequent filling of the canyon, involving the passive filling of the burrows. The aims of this paper are: (1) to characterize the major incision surfaces of the paleo-canyon in terms of sedimentary and ichnological characteristics; (2) to establish the relative chronological order of the series of ichno-sedimentological events taking place in relation to the development of the paleo-canyon; and (3) to refine the sequence-stratigraphic context from the integration of ichnological and sedimentological datasets.

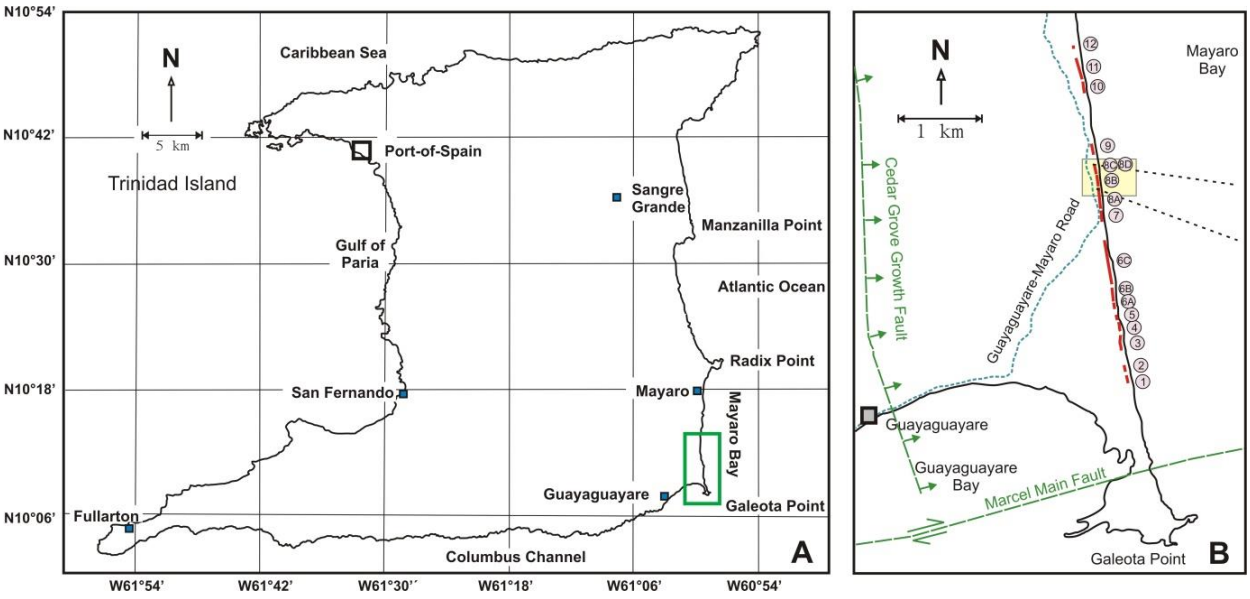

Fig. 4.1. Location maps. (A) Location of the Mayaro Formation outcrops along the southeastern shoreline of Trinidad Island shown with the green rectangle. (B) Locations of the Mayaro Formation outcrops as foreshore cliffs (marked by red) with the outcrop numbers (circles). The paleo-canyon incised within the delta-front sediments discussed in this paper is delineated with a rectangle. Two dashed straight lines indicate the approximate orientation of the flanks of the canyon.

4.2 Depositional Setting of the Gelasian Mayaro Formation

The Gelasian Mayaro Formation of the Columbus Basin is exposed as foreshore cliffs along the north-south trending southeast coastline of Trinidad Island between two prominent headlands – Radix Point in the north and Galeota Point in the south (Fig. 4.1). The ca. 702 m thick Mayaro Formation outcrops represent an almost strike-parallel sliver of the growth-fault-bounded shelf-edge deltaic sediment belonging to the Gelasian Paleo-Orinoco River. The Columbus Basin is bounded towards the North by the Central Ridge-Darien Ridge Lineament, on the South by the Amacuro Platform of the present-day Orinoco Delta, offshore Venezuela, and on the West by the Cedar Grove growth-fault; towards the East, the basin continues into the hydrocarbon-rich offshore part of the basin on the present-day Trinidad shelf and deeper offshore (Wood, 2000; Sydow *et al.*, 2003; Callec *et al.*, 2010). The approximately north-south trending Cedar Grove growth-fault, which limits the Mayaro Formation sediments towards the west as its down-thrown side, passes parallel to the outcrops near Guayaguayare town within ca. 3 km away from the exposures (Fig. 4.1).

Bowman (2003) categorized the Mayaro succession into a hierarchy of complex five-level stratigraphic cycles – from (i) a hundreds to thousands of metre thick lower-order regressive shelf-edge delta megasequence, to (ii) hundreds of metre thick higher-order regressive-transgressive cycles and (iii) tens to hundreds of metre thick further higher-order progradational, aggradational or retrogradational subcycles, and to (iv) tens of metre thick progradational or retrogradational packages that intermittently comprise (v) less than a metre to several metre thick hummocky and swaley cross-stratified sandy strata. Uroza (2008) reinterpreted parts of the outcrop and constructed a conceptual depositional architectural model for this shelf-edge delta.

As estimated by Porębski and Steel (2006), the present-day Orinoco delta is an accommodation-driven one, which implies that the delta-front requires relative sea-level fall to reach the shelf margin. This suggests that the delta-front of the Paleo-Orinoco River migrated towards and stacked up at the shelf-edge during the relative sea-level lowstand of the Plio-Pleistocene icehouse and perhaps also during the following rise. The fluctuations of relative sea

level in the Columbus Basin are both influenced by eustasy and tectonism, whereby the regionally extensive repeated growth-fault movements have always influenced the accommodation available for sedimentation of the north-eastward prograding Paleo-Orinoco delta (Wood, 2000).

The Mayaro Formation is interpreted to have been deposited by fluvially influenced hyperpycnal-flow sedimentation, and further remobilization of the sediments took place by wave-action. The sand-filled gutter-casted chutes of substantial thickness (up to ca. 2-3 m) bear evidence for hyperpycnal flow bypassing the areas of the delta-front deeper onto the continental slope. The chutes are cut through the wave-remobilized sheet-like deltaic mouth-bar sediments characterized by stacked thickness of the hummocky cross-stratified medium-grained sandstone (comparable to the S2h hyperpycnite facies of Zavala *et al.*, 2011), locally amounting up to 25-30 m in thickness, and intervening thinly laminated heterolithics composed of alternate laminations of silty sand and mud. The thickness of the delta-front megasequence (ca. 702 m in outcrop) and the deeply incised large gutter-casts suggest that sedimentation took place in a setup with substantially high delta-front gradient and high accommodation space, which are characteristic of the transition from the outer shelf to the upper slope. Seismic data from the adjoining hydrocarbon fields also support a shelf-margin setup for the Mayaro Formation (Wood, 2000; Sydow *et al.*, 2003).

The delta-front is cut across by an ESE-WNW trending incised paleo-canyon, later filled by prodeltaic sediments. The southern wall of the paleo-canyon is exposed towards the northern end of outcrop 8A (Figs. 4.2-4.3). This southern cut-surface strikes approximately at S55°E, dipping ca. 58° north-easterly. The northern wall of the paleo-canyon can be located in outcrops 8C and 8D and is more irregular, from gently dipping towards SSW to almost sub-horizontal (Figs. 4.2, 4.4A). The prodeltaic sediments filling the paleo-canyon chiefly consist of organic fragment-bearing alternate layers of undeformed laminated siltstone / shale, and highly deformed cohesive debris flow (CDF) deposits (Fig. 4.2C). The organic fragment-bearing CDF deposits contain internal synsedimentary deformation features, such as shear fabrics, slickensides on the slip surfaces, and reoriented mica flakes.

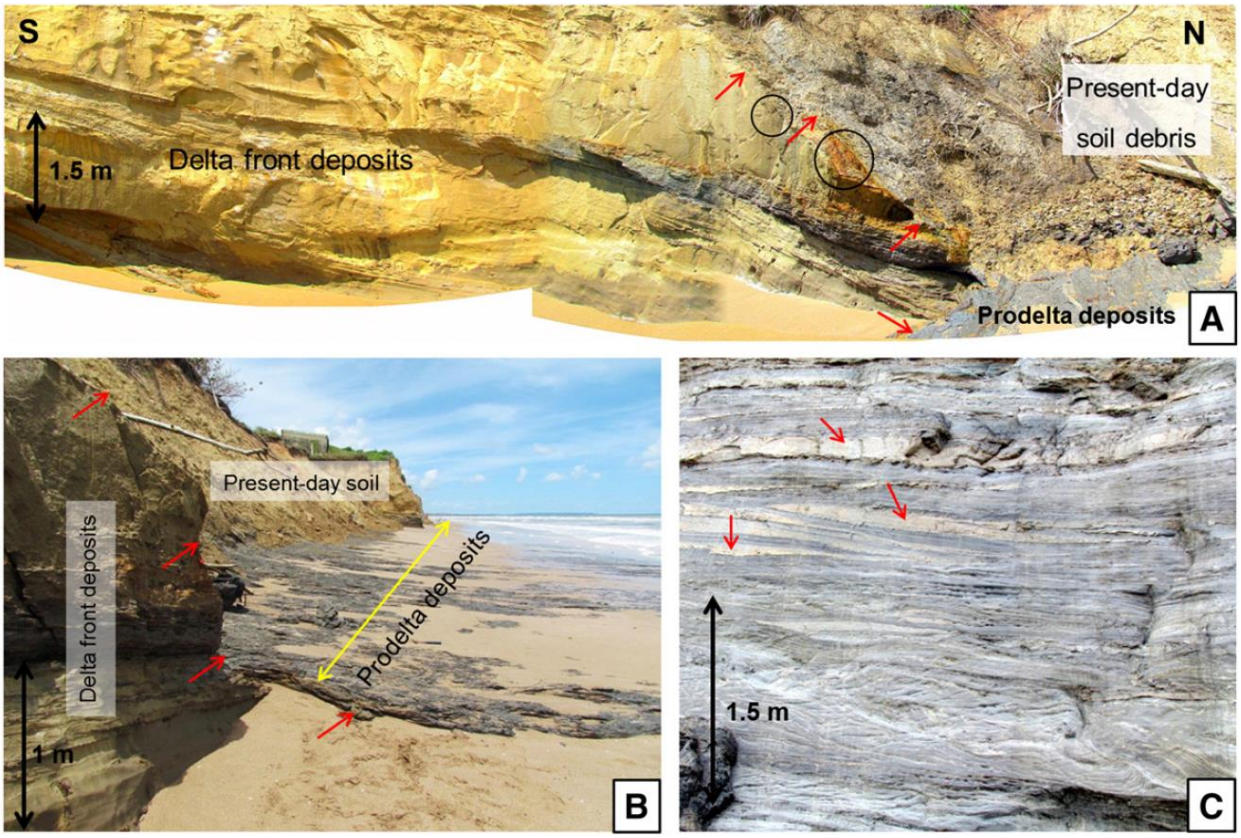

Fig. 4.2. The southern wall or the incision-surface of the paleo-canyon and the associated underlying and overlying sedimentary facies. (A) Stitched photograph showing the southern incision-surface of the paleo-canyon, marked by the red arrows, separating the delta-front sandstone with the thinly laminated heterolithic sediments from the prodeltaic mudrocks. The circles mark tensional fractures associated with the wall of the canyon. (B) Photograph, looking towards north, showing prodeltaic canyon-filling mudrocks and the southern incision-surface (marked by the red arrows). (C) The prodeltaic mudrocks, in outcrop 8B of Fig. 4.1, filling the paleo-canyon. Layers of cohesive debris flow and laminated or thinly bedded silty hyperpycnites, locally cut across by lenses of sandy turbidites, are indicated by red arrows.

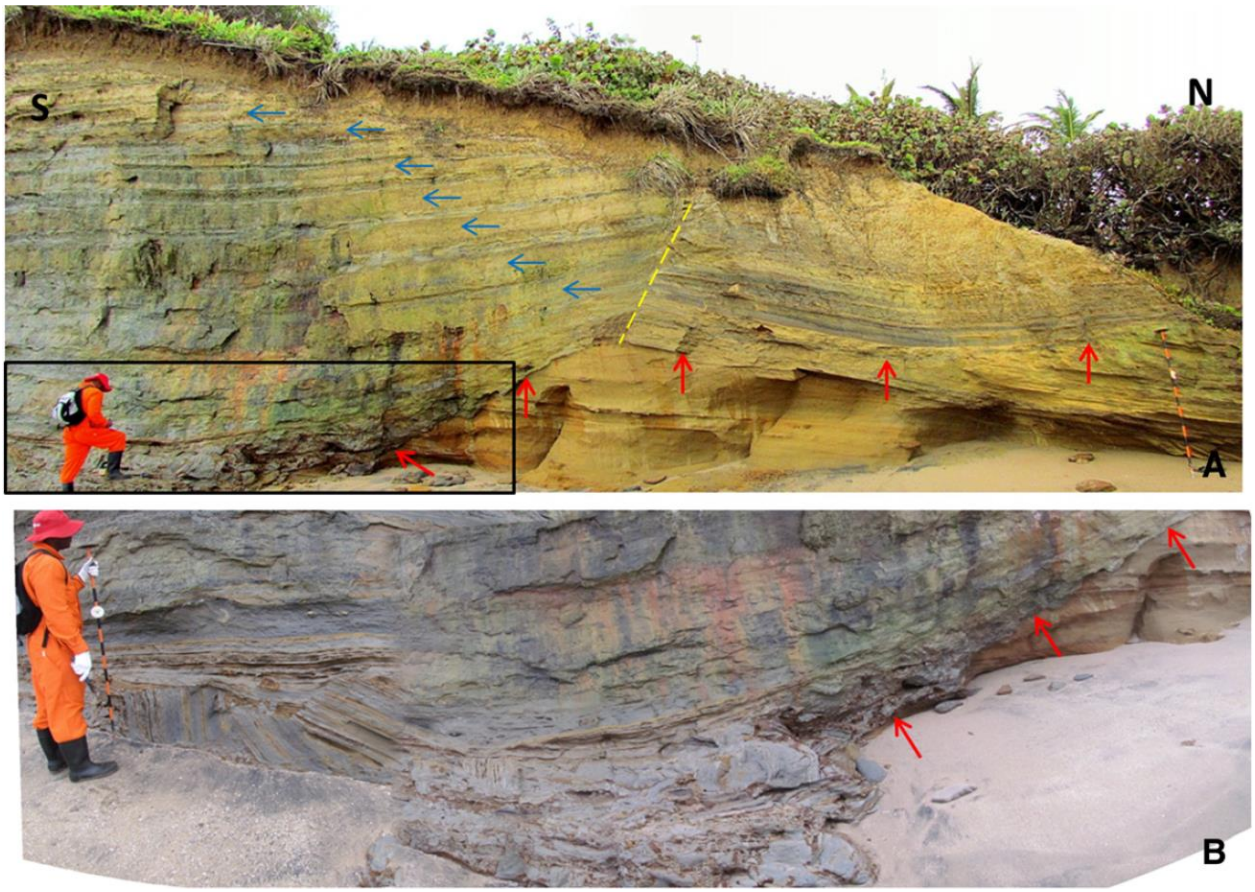

Fig. 4.3. Northern wall or the incision-surface of the paleo-canyon and associated underlying and overlying sedimentary facies. (A) Stitched photograph of the northern incision-surface of the paleo-canyon, marked by the red arrows, separating the yellow-coloured delta-front sandstone with the thinly laminated heterolithic sediments from the alternate layers of dark grey-coloured prodeltaic mud-rocks and sheet-like sandy turbidite beds marked by blue arrows. The clast-supported mudrock breccia with sandy matrix, on which the man is standing, characterizes the debris flow originating from the collapse of the canyon wall. The axial trace of the synsedimentary suprateneous monocline is marked by the dashed yellow line. The Jacob Stick at the extreme right corner is 1.5 m long. (B) Close-up photograph of the slumped debris-flow deposit marked by the rectangle in Fig. 4.3A. The canyon-wall is marked by the red arrows.

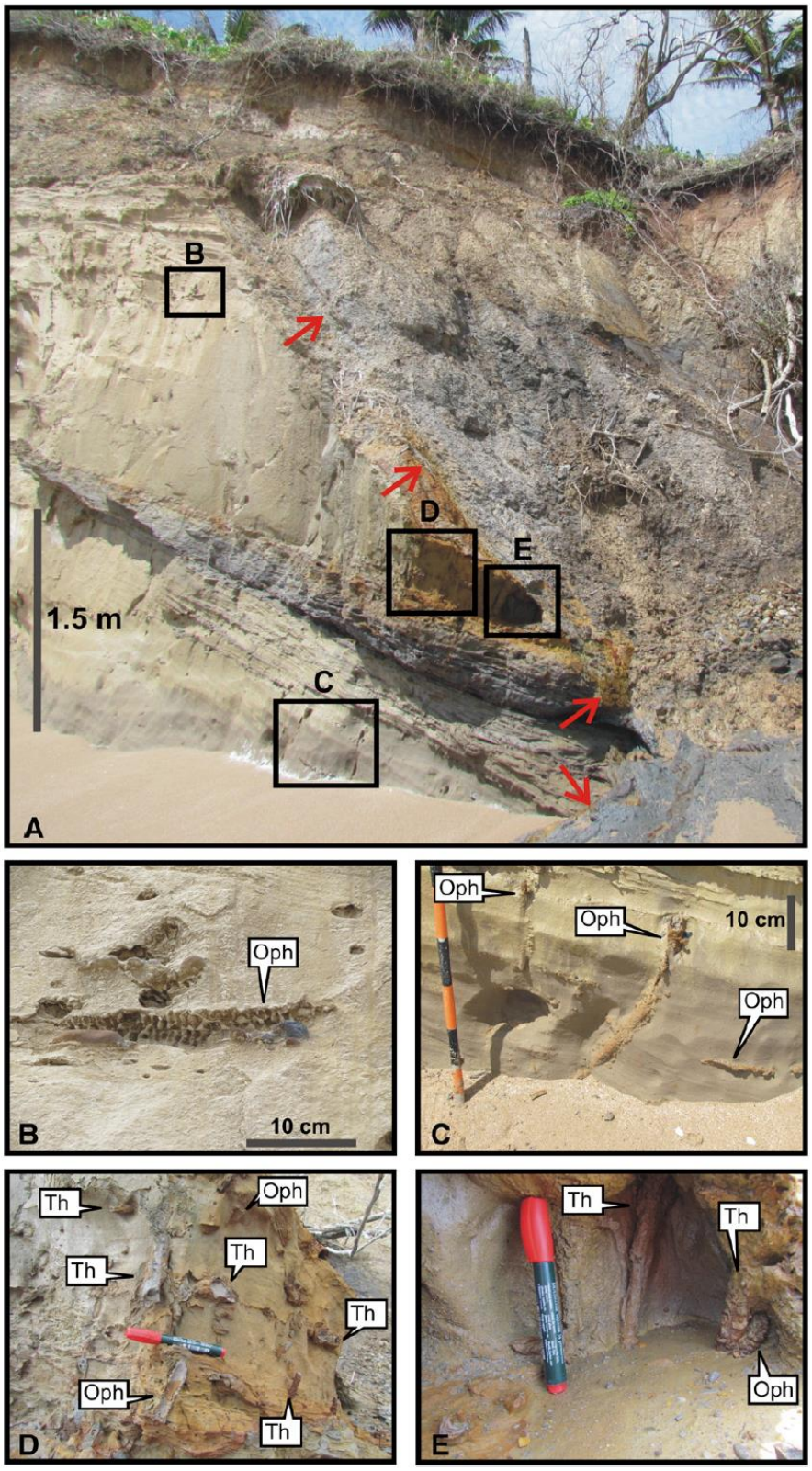

Fig. 4.4. (*N.B.* Figure caption is intentionally moved to the next page due to the large size of the figure)

Fig. 4.4. Trace-fossil suite within delta-front sheet-like sandstone bodies in the immediate vicinity of the southern wall (marked by the red arrow) of the paleo-canyon. (A) Colonization by softground *Ophiomorpha nodosa* (Oph) (marked by B and C rectangles) and firmground *Thalassinoides* (Th) (marked by D and E rectangles). (B) Close-up of rectangles B in Fig. 4.4A. (C) Close-up of rectangle C in Fig. 4.4A. (D) Close-up of rectangle D in Fig. 4.4A showing firmground *Thalassinoides*, filled with mud from the prodeltaic canyon-fill. The marker pen is 14 cm long. (E) Close-up of rectangle E in Fig. 4.4A showing firmground *Thalassinoides* cross-cutting softground *Ohiomorpha nodosa* (Oph) on the right side of the photograph. The marker pen is 14 cm long.

The couplets of deformed and undeformed layers are locally cut by centimetres-thick, massive, sandy turbidite lenses (Fig. 4.2C) and approximately a metre-thick chutes or channels filled with tractional load with imbricated rip-up clasts deposited from the bypassing hyperpycnal turbidity current (comparable to the B1s and B2s hyperpycnite facies of Zavala *et al.*, 2011). Since the entire growth-faulted block of the Mayaro Formation outcrop is non-homogeneously tilted (varying from sub-horizontal to less than 30°) towards north by later complex tectonic processes, the outcrop of the northern wall of the paleo-canyon should be relatively younger in age and gentler in dip than the older and steeper southern wall. The canyon-fill near the northern wall is more heterogeneous in terms of lithology, whereby the prodeltaic mudrocks are intercalated with alternating sandy turbidite sheets and slumped sediments originating from the collapsing wall of the paleo-canyon (Fig. 4.3A-B). Fig. 4.4A also shows the synsedimentary monocline of suprateneous type developed by the differential compaction of sediments, because the muddy canyon-fill suffered from greater compactional sagging away from the flank of the paleo-canyon towards the canyon axis.

4.3 Ichnology and sedimentology of the paleo-canyon wall and fill

The delta-front sediments cut across by the southern wall of the paleo-canyon (outcrop 8A in Fig. 4.1B) are sheet-like sandstone bodies and thinly laminated heterolithics, consisting of alternate mud and fine-to-medium-grained sand laminations. The sandstone thickness to the total thickness ratio (*i.e.*, the net-to-gross or NTG) is approximately 84.3 % in the outcrop 8A. The individual sandstone sheets are 0.7 to 3.5 m thick and laterally vary in thickness. The sandstone sheets are either amalgamated or intercalated with the heterolithic sediments, which are laterally discontinuous due to erosional cuts in places making the sandstone bodies amalgamated locally.

The sheet-like bodies consist of faintly hummocky cross-stratified medium-grained sandstone. Deposits are sporadically and sparsely bioturbated (bioturbation index or BI is 0-1). BI reflects the visual estimation of the degree of bioturbation (Taylor and Goldring, 1993). These sandstone bodies are interpreted as the wave-modified mouth-bar lobes of the shelf-edge delta-front. The sands were deposited by the hyperpycnal flows after crossing a possible slope-break generated by the active shoulder of the growth-fault scarp (Cedar Grove growth-fault), and were coevally modified by wave-action. The bulk of the sand budget is stored in a north-south trending linear belt near the shelf-edge defined by the growth-fault (Uroza, 2008). The mechanically resistant sandstone bodies form the present-day foreshore cliffs. These deposits are comparable to the S2h hyperpycnite facies of Zavala *et al.* (2011).

The heterolithic layers are composed of parallel-laminated medium-grained sandstone and starved current-rippled- to parallel-laminated clayey siltstone, locally containing lenticular thin sand beds / laminations. The lithological contacts are sharp in general and gradational in rare instances. These fine-grained deposits are moderately bioturbated (BI 3-4). They are interpreted to be distal parts of the lobate sheets, and are inferred to be deposited from the low-density lofted part of the hyperpycnal flow. These deposits are comparable to S2/L and S3/L hyperpycnite facies of Zavala *et al.* (2011).

The sandy delta-front deposits contain a trace-fossil suite consisting of *Ophiomorpha nodosa* emplaced in softground. *S*pecimens are 2-6 cm in diameter, displaying low abundance (BI = 0 to 1, locally 2) (Fig. 4.4A-E). Burrow segments are both vertically and horizontally arranged (Fig. 4.4B-C). Burrow-walls are reinforced with pellets (0.2-0.7 cm in diameter). Reinforcements may have allowed burrow stabilization in loose sand. Sparse bioturbation of the deposits and the monospecific nature of the trace-fossil suite suggest environmental stress factors due to the lowered salinity, high sedimentation rate and increased turbidity by the hyperpycnal flows. The heterolithic intervals also contain a trace-fossil suite consisting of *Planolites* isp, *Skolithos* isp. and *Thalassinoides* isp. emplaced in softground and with lateral variation of abundance (BI = 1 to 4, rare patches of BI = 6). The same delta-front sediments are exposed beyond the northern wall of the paleo-canyon, where they are completely devoid of any perceptible bioturbation. Abundance of large wave generated sedimentary structures such as

swaley and hummocky stratification, exceptionally high thickness of sandstone beds (more than a metre in general) and large dewatering structures imply high rates of sedimentation and concomitant subsidence. The individual beds and laminations within the heterolithic sediments commonly show typical signatures of hyperpycnites such as coarsening and then fining upward rhythmic grain size variation (waxing-waning cycles of flow), internal scouring between a single waxing episode and its following waning event, abundance of organic fragments and shrinkage cracks influenced by frequent salinity changes.

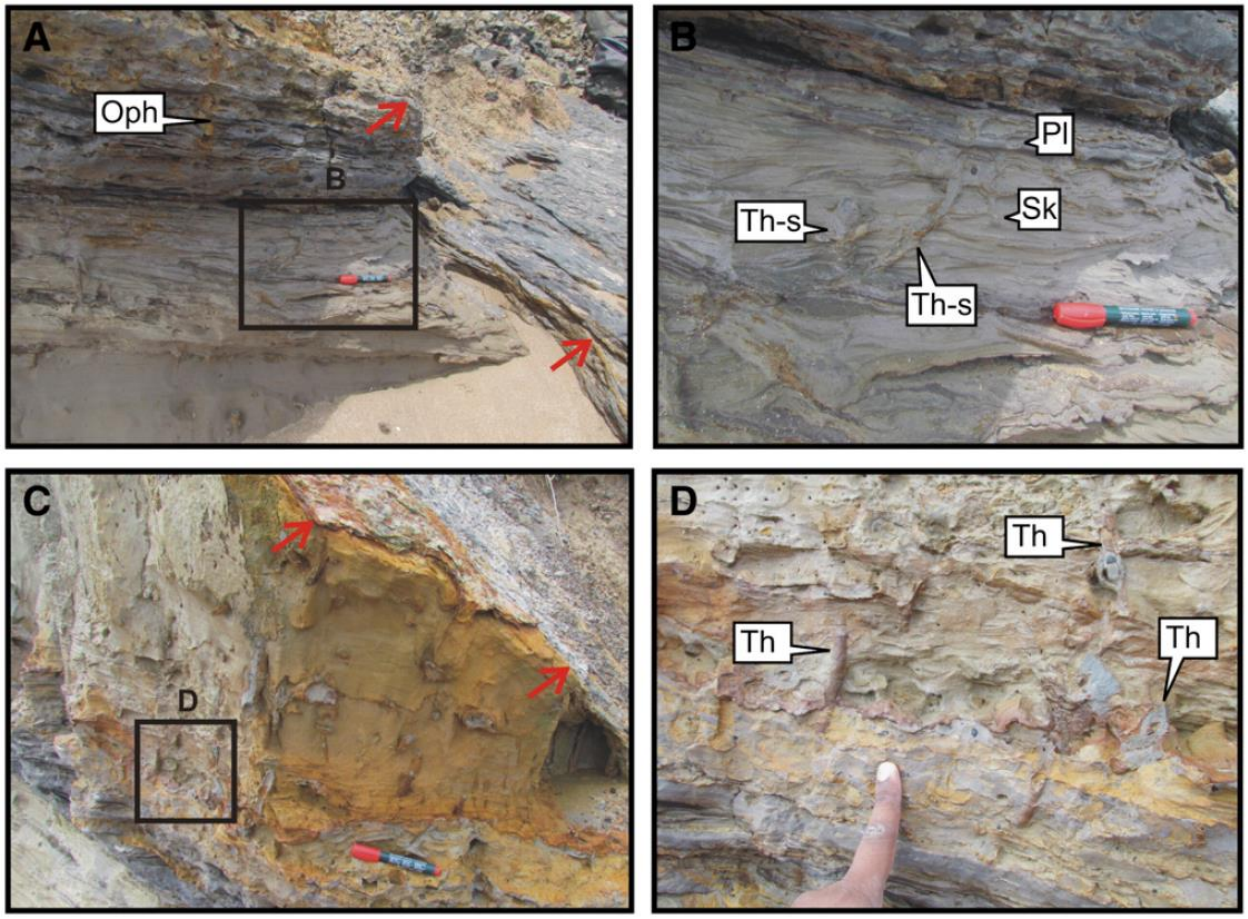

Fig. 4.5. (*N.B.* Figure caption is intentionally moved to the next page due to the large size of the figure)

Fig. 4.5. Trace-fossil suite within the delta-front heterolithic intervals in the immediate vicinity of the southern wall (marked by the red arrow) of the paleo-canyon. The marker pen is 14 cm long. (A) Softground colonization (marked by B rectangle). (B) Close-up of rectangle B in Fig. 4.5A showing softground lined *Thalassinoides* (Th-s), *Skolithos* (Sk) and *Planolites* (Pl). (C) Intense softground colonization (marked by D rectangle) cross-cut by the firmground *Thalassinoides* in the heterolithic interval underlying immediately below the delta-front sandstone shown in Fig. 4.4A, D-E. (D) Close-up of rectangle D in Fig. 4.5A.

Both the delta-front sandstone and the heterolithic sediments, which are in contact with the southern wall of the paleo-canyon in outcrop 8A, exhibit secondary firmground colonization evidenced by *Thalassinoides* isp. (*Glossifungites* Ichnofacies) penetrating from the incision surface (Figs. 4.4A, D-E; 4.5D) and cross-cutting the pre-existing softground suites (Figs. 4.4E, 4.5D). The firmground suite is monospecific and of low density, containing a three-dimensional maze of *Thalassinoides*. Burrows are 1-5 cm in diameter, unlined, passively filled with mud from the overlying prodelta, and surrounded by diagenetic dolomitic halo. The firmground *Thalassinoides* adjoining the colonization surface (*i.e.,* the canyon wall) are more sub-orthogonal to this surface (Fig. 4.4D), and become oblique and also concordant with bedding planes of the delta-front sediments away from the canyon-wall. Passive infill and absence of wall reinforcement indicate that both the sandstone and the heterolithic sediments were compacted prior to secondary colonization event. The rocks suffered further lithification so that the infill became mudrock, which is more resistant to mechanical erosion than the surrounding sandstone and heterolithic units to make burrow casts protruding out of the delta-front sediments (Figs. 4.5D-E, 4.6D).

The sediments filling the paleo-canyon near its southern wall are prodeltaic couplets of alternating organic fragment-bearing, undeformed, parallel-laminated siltstone and shale, and highly deformed CDF deposits. The bed thicknesses are highly variable, but rarely exceed 50 cm. The undeformed siltstone bears the characteristics of typical mud-rich hyperpycnal flows with faint gradational coarsening-up and then fining-up grain-size profiles (*e.g.,* Mulder *et al.*, 2003; Bhattacharya and MacEachern, 2009). Due to the high gradient of the paleo-slope of deposition, the prodeltaic muddy sediments were remobilized as cohesive debris flow limiting the thickness of the muddy hyperpycnite layers and also healing the instability of the slope inside the paleo-canyon. Therefore, facies change from the undeformed hyperpycnite to the debris-flow

deposit can be documented. Neither of these is bioturbated except for some localized rare mottles. This implies very high environmental stress possibly caused by the hyperpycnal influx into the paleo-canyon. Towards the north of the outcrop, near the northern wall of the paleo-canyon, the prodeltaic couplets are locally cut by one to a couple of metres-wide chutes or channels containing the cross-bedded medium-grained sandstone with imbricated armoured clasts of the prodeltaic muddy couplets and without any perceptible bioturbation. This facies seems to be similar to the B2s hyperpycnite facies of Zavala *et al.* (2011), implying bypassing of coarser-grained clastic sediments as high-density hyperpycnal turbidity current onto the deeper slope, while depositing only from the tractional bedload. Just in the vicinity of the northern wall of the paleo-canyon, the prodeltaic couplets are almost rhythmically intercalated with sheet-like non-bioturbated, faintly normally graded to massive high-density turbidite sandstone that is possibly the product of remobilization of sand from the overbank of the paleo-canyon (Fig. 4.3A). This is supported by the local presence of a muddy clast-supported breccia with medium-grained sand matrix, interpreted as non-cohesive debris-flow sediments deposited as a result of mass-wasting from the unstable canyon-wall (Fig. 4.3A-B). Unlike the southern wall of the paleo-canyon, the northern wall of the paleo-canyon in outcrops 8C and 8D does not show similar development of the *Glossifungites* Ichnofacies. Perhaps it did not survive the collapse and remobilization of the unstable canyon banks at these particular localities.

4.4 Discussion

4.4.1 The *Glossifungites* Ichnofacies in the Mayaro Formation

The *Glossifungites* Ichnofacies develops in a wide range of environments displaying firm but unlithified substrates, which commonly consist of dewatered mud and more rarely compacted, unlithified sand (Pemberton and Frey 1985; MacEachern *et al.*, 1992, 2007; Pemberton *et al.*, 1992, 2004; Buatois *et al.*, 2008). The firmness in dewatered mud arises from increased viscosity and cohesion, whereas in case of sand, compaction enhances the surficial contact among sand grains, thus increasing the frictional strength. A firmground tracemaker can still be able to burrow through the firm substrate by mechanically removing particles without

reinforcing the burrow wall. In order to reach the firm substrate, the tracemakers require the substrate to be exhumed by mechanical removal of loose unconsolidated overburden (MacEachern *et al.*, 1992; Buatois and Mángano, 2011). Therefore, the *Glossifungites* suite develops during a hiatus limited between an erosional event responsible for the exhumation of the firm substrate and the deposition of the overlying younger sediments. The erosion has to be sufficiently deep enough to expose the firmground siliciclastic substrate for recolonization. Therefore, the substantiality of erosion should have sequence stratigraphic importance, if the surface characterized by *Glossifungites* Ichnofacies has regional areal extent and / or it represent incision of sufficient depth of statigraphic significance (*e.g.*, a canyon cut).

The *Glossifungites* Ichnofacies developed on the wall of the Mayaro paleo-canyon incised into a shelf-edge delta-front is a unique example of this ichnofacies, because there are only three known occurrences of this ichnofacies from the walls of incised submarine canyons, with one outcrop example (Hayward, 1976) and two subsurface examples (Pemberton *et al.*, 2004; Buatois and Mángano, 2011). None of those three examples are from a shelf-edge delta setting. Moreover, the occurrence of this ichnofacies in Mayaro outcrops also serves as a rare case of its development under stressed ecologic conditions during colonization. Unlike the high abundance and low ichnodiversity archetypal examples of the firmground ichnofacies developed in fully marine environments, the *Glossifungites* Ichnofacies from the Mayaro Formation is monospecific, colonized only by *Thalassinoides*, and also low in abundance (BI = 0 to 2). The stressful conditions make the Mayaro example of the ichnofacies more similar to incised estuarine valleys than to incised submarine canyons in ecologic terms. Possible stress factors include slope instability due to steepness of the gradient of the wall, and elevated turbidity and lowered salinity of the erosional and / or bypassing hyperpycnal flow inside the canyon. The stressed environment not only reduced the degree of bioturbation, but was also responsible for the monospecific nature of the trace fossil suite. The branching of the burrows is rarely exposed on the outcrop walls due to low BI. The archetypal examples of the *Glossifungites* Ichnofacies are generally preserved at the boundary between underlying mudrocks and overlying coarser-grained sediments. Therefore, such burrows of those typical examples are filled with coarser-grained sediment, such as sand and granule. This is because clay particles compact faster than coarser-grained clastic sediments to reach the firm rheological state and shallow erosional

exhumation is enough for exposing the clayey firm substrates. Exhumation of firm sandy substrate, in contrast, requires deeper exhumation. Contrary to archetypal occurrences, the firmground substrate in our instance is delta-front sandstone and heterolithic strata separated by the incision surface from the overlying prodeltaic mudrocks. These firmground burrows, therefore, are filled with mud, rather than sand, coming from the top.

4.4.2 Sequence stratigraphic implications

After deposition of the Paleo-Orinoco delta-front sediment and subsequent softground colonization (Fig. 4.6A), the sediments underwent burial and compaction and turned into a mechanically firm substrate. The delta-front megasequence was incised by a canyon, exhuming the firm substrate (Fig. 4.6B), allowing colonization by the firmground *Thalassinoides* (Fig. 4.6C). While the paleo-canyon was getting filled later with prodeltaic mud, the fine clastic particles infiltrated the vacant burrows and filled them thereby preserving the burrows (Fig. 4.6D).

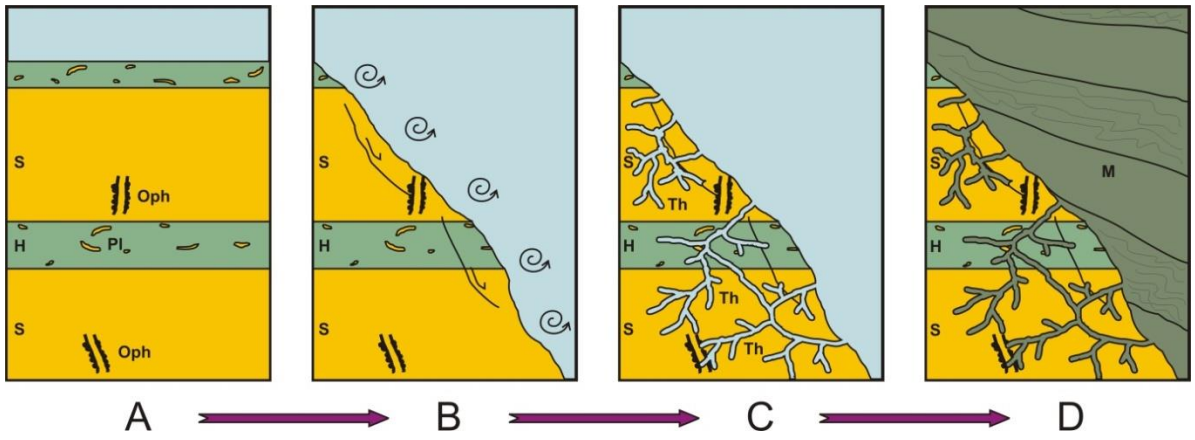

Fig. 4.6. Schematic diagram showing stages of the development of the *Glossifungites* Ichnofacies on the paleo-canyon wall in the succession of Mayaro Formation, Trinidad. (A) Deposition of the delta-front sediments, *i.e.*, sandstones (S) and heterolithic sediments (H), softground colonization such as *Ophiomorpha* (Oph) and *Planolites* (Pl) in the diagram and their burial. (B) Canyon incision and widening. (C) Firmground colonization by *Thalassinoides* (Th) crosscutting pre-existing softground suite. (D) Canyon getting filled by prodeltaic muddy couplets (M) and passive filling of the firmground *Thalassinoides* by the prodeltaic mud. The canyon-filling sediments show higher compaction towards the axial zone of the canyon making the bedding surfaces inclined near the canyon wall.

The steep canyon-walls remained metastable with well-developed zones of weakness. Therefore, the preservation of the canyon-wall containing the *Glossifungites* Ichnofacies is a rare phenomenon and only patches of such surface remained undisturbed from the mass-wasting processes. The northern wall of the paleo-canyon shows the indications of slumping and remobilization during the filling of the canyon as evident from the non-cohesive debris-flow deposits associated with the northern canyon-wall (Fig. 4.3A-B), thereby destroying preservation potential of any firmground suite.

The incision surface of the paleo-canyon characterized by *Glossifungites* Ichnofacies was initially identified as a fault-plane belonging to the regional growth-fault system (Bowman, 2003), based possibly on the occurrences of shear-fabrics in the overlying prodeltaic sediments and tensional rupture surfaces in the underlying delta-front sediments (marked by circles in Fig. 4.2A). However, the shear-fabrics and slickensides on the slip-surfaces are associated with the cohesive debris-flow deposits, which are ubiquitous throughout the canyon fill. The tensional rupture surfaces, sub-parallel to the canyon wall, are interpreted to be related to the slope instability of the canyon-wall. Gradual slumping events along the tensional surfaces of weakness widen the width of a canyon. Similar tensional rupture surfaces can be located sub-parallel to the wall of another minor ravinement surface in outcrop 8A. Such erosional gullies are common on the shelf-margin, and a few of them eventually may evolve into a full-fledged canyon as the major loci of the incision processes. The discovery of the *Glossifungites* Ichnofacies at the lithological interface between the delta-front and prodeltaic sediments confirms the nature of the surface implying a significant erosional event.

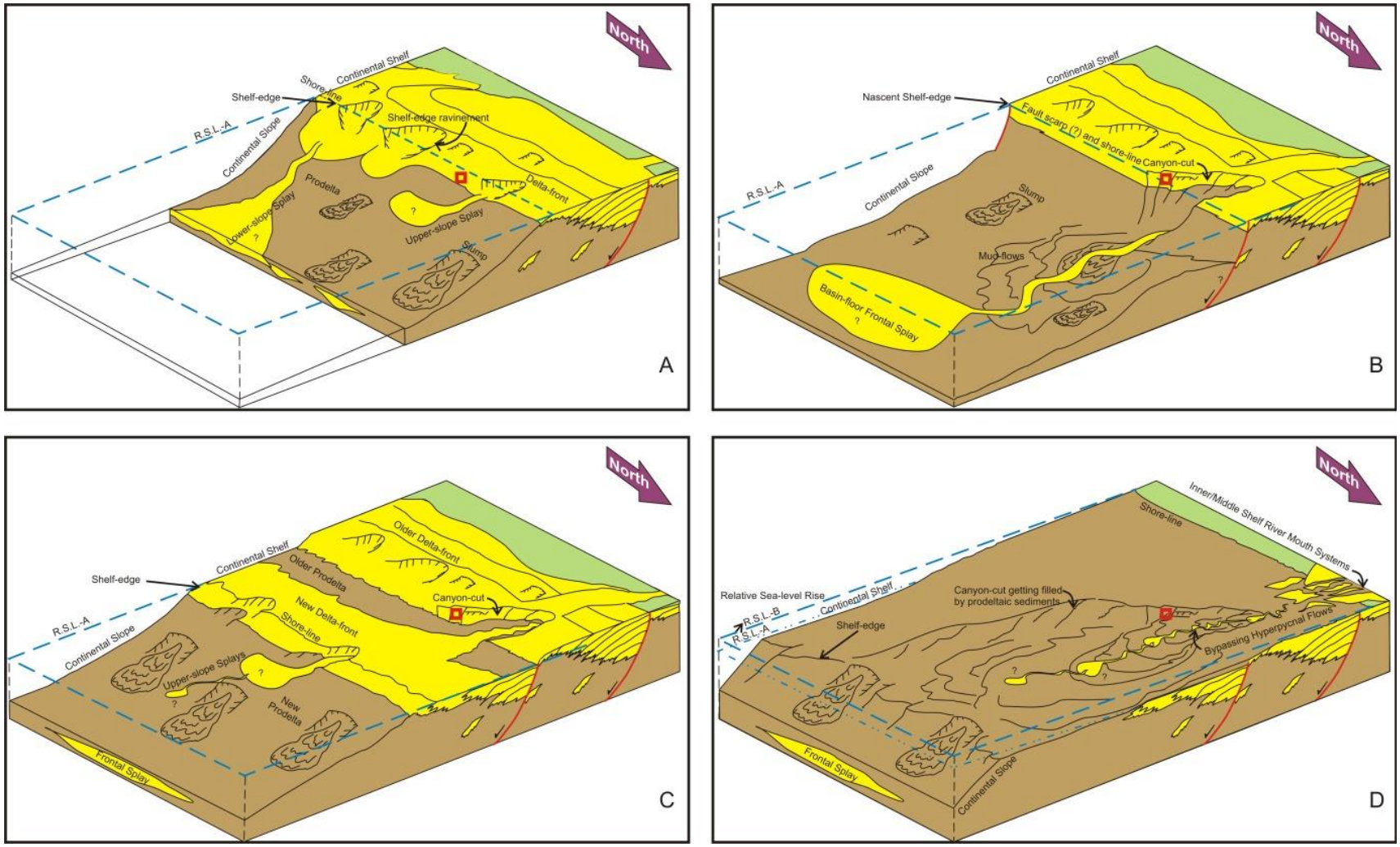

Fig. 4.7. (*N.B.* Figure caption is intentionally moved to the next page due to the large size of the figure)

Fig. 4.7. Schematic diagram of the conceptual depositional model in relation to the development of the *Glossifungites* Ichnofacies. The red rectangle delineates the position of the Gelasian Mayaro Formation outcrop 8A in present-day context. (A) Deposition of the Paleo-Orinoco delta-front sediments (*i.e.,* those presently exposed along Mayaro-Guayaguayare Beach) along the slope-break caused by the preceding growth-fault event. (B) Incision of canyon along a pre-existing ravinement, possibly being triggered by the slope instability caused by the basinward development of new growth-fault. Sediments mostly bypass into deep-water at this time as the different types of gravity flows. (C) Re-establishment of the delta-front basinward (Several subsequent growth-faults developed farther basinward are not shown in this schematic diagram for simplicity). (D) Subsequent rise of relative sea level and sediment starvation during the rise due to sediments getting trapped landward. This is also the time for the firmground colonization during transgression. Finally the canyon along with the firmground burrows on the canyon wall gets filled by prodeltaic mud during the next highstand normal regression. [*N.B.* The depositional and stratigraphic models have been modified after the publication of this manuscript. See chapters 3 and 5.]

On the basis of the occurrence of the *Glossifungites* Ichnofacies, the recognition of a discontinuity between the delta-front sediments and the prodeltaic deposits allows redefining the Gelasian Mayaro Formation megasequence into two clearly distinct stratigraphic units – the relatively older delta-front succession and the younger canyon-fill prodelta succession – with the canyon-wall as the an important stratigraphic surface. A sequence stratigraphic model is proposed as follows and explained in Fig. 4.7 A-D.

The wave-influenced hyperpycnal flows dumped a major portion of its sandy bed load along the shelf-break created by the basin-bounding Cedar Grove growth-fault (Fig. 4.7A). The enormous stack of the delta-front sediments underwent burial and compaction and became firm. During that time, a substantial portion of the sand-budget may have been transported onto deeper slope, as implied by the presence of the enormous gutter-casts / channels / chutes (see *Figs. 3.14-3.16* in Uroza, 2008). With progradation and build-up of the Paleo-Orinoco delta, a series of growth-faults kept on developing progressively basinward (*i.e.,* eastward) (Wood, 2000; Sydow *et al.,* 2003). The development of new growth-fault(s) towards the east of Cedar Grove fault created accommodation in the hanging wall side of the Mayaro sub-basin and also developed a nascent shelf-margin along the shoulder of the new growth-fault. Resulting from the readjustment of accommodation, the new slope instability was generated and sediments were more susceptible to get mobilized into a deep-water setting as different types of gravity-flows (Fig. 4.7B). Canyon-incision and augmentation acted as a conduit for the gravity flows. One or a

few pre-existing shelf-edge gullies or gutters perhaps have evolved into the fully developed canyon. The firm substrates were exposed, as the canyon kept on widening and incising through the pre-existing delta-front deposit. The new delta-front got re-established basinward beyond the new shelf-edge. As evident from subsurface data of hydrocarbon fields, the progressive re-establishment of delta-front, following every new growth-fault development resulting in the progradation of the Paleo-Orinoco shelf-edge delta, has been well documented in the Columbus Basin (Fig. 4.7C).

Subsequently, with the rise of relative sea level, the loci of deposition of the sand-budget of Paleo-Orinoco shifted landward (Fig. 4.7D) and the accommodation within the canyon was filled up with prodeltaic mud of the same system. The canyon-fill setup still kept on receiving coarser-grained clastic sediments as evident from the localized outcrops of the bypassing chutes within the prodeltaic canyon-fill. The southern sub-basin (Mayaro sub-basin) in Trinidad was subjected to farther burial under the Quaternary sediments (Wood, 2000), and the Mayaro Formation sediments have been exposed by the erosional processes along the shoreline of south-eastern Trinidad Island.

The canyon-walls, being major surfaces of erosion and sediment bypass, serve as surfaces of sequence-stratigraphic significance, as the creation of accommodation and also the slope instability caused by the growth-fault activity is responsible for the sediment mobilization onto the deeper slope. The Paleo-Orinoco shelf-edge delta kept on prograding farther basinward, and the basin derived sediments from the hinterland most likely through such major surfaces of sediment bypass. The same canyon-wall must have also acted as the transgressive surface while shifting the shoreline landward. It was only after the landward shift of the shoreline that the prodelta sediments filled up the canyon during the following highstand.

Erosional and bypass surfaces of similar stratigraphic importance can be found in a completely different depositional environment as incised valleys in shallower-marine settings (Pemberton *et al.*, 1992; Zaitlin *et al.*, 1994; Buatois and Mángano, 2011), where during the relative sea-level fall the fluvially cut, subaerial unconformity is formed. In incised valleys, fluvial deposits accumulate along the axis of the incised valley during a late phase of sea-level

fall. During the subsequent transgression, estuarine sediments tend to accumulate along the valley axis towards the downstream side and onlap the interfluves where they form a co-planar surface marking the juxtaposition of the lowstand and the transgressive erosional events. Following the analogy of the co-planar surfaces of two successive lowstand and transgressive events, the canyon-wall incised into the shelf-edge delta-front and filled with prodelta sediments can be considered as another type of co-planar surface marking two distinct regressive and transgressive events, although unlike the fluvially incised valleys, the overlying sediments above the canyon-wall belong to the prodelta setting of the immediately subsequent highstand. (For further details and later improvements of the sequence stratigraphic model, see Chapter 5).

4.5 Conclusions

The ichno-sedimentological study of the Mayaro Formation has revealed the importance of the *Glossifungites* Ichnofacies in delineating a paleo-canyon wall, which hitherto was considered as a growth-fault contact. The sedimentary facies associations outside and inside the paleo-canyon correspond to two different suites of depositional environments, viz. delta-front and prodelta of the shelf-edge delta system of the Paleo-Orinoco. Therefore, the previously suggested Mayaro Formation megasequence should be divided into two distinct stratigraphic units – the forced regressive delta-front succession and the following highstand prodeltaic succession – with the canyon-wall as the new type of co-planar surface marking the superimposition of two regressive and transgressive events. Being strikingly different from the archetypal *Glossifungites* Ichnofacies, the limited development of the monospecific *Glossifungites* Ichnofacies highlights the ecological stress factors such as a steep gradient of the canyon-wall, rapid sediment mobilization, elevated water turbulence and lowered salinity by the hyperpycnally influenced gravity-flows.

4.6 Acknowledgements

The authors deeply acknowledge Carlos Zavala, without whom this project would have been impossible to undertake. Carlos showed us the outcrops and provided valuable feedback and information on the geology of Trinidad. We thank Repsol YPF, Port-of-Spain, Trinidad and Tobago, especially Livan Blanco Valiente, for arranging, supporting and funding the entire field study of the Mayaro-Guayaguayare outcrops. We also appreciate the relentless logistic support by Dinelle Medina. We also express our appreciations to Yrma Vallez, Maria Gabriela Mángano and Brian Pratt for the insightful discussions and to Jim Merriam, Head of the Department, Geological Sciences, University of Saskatchewan, for his encouragements. The field assistance by Marlon Bruce has been indispensable for the authors, and we are delighted to express our profound gratitude towards him. Reviews by Franz Fürsich and an anonymous referee and editorial comments by Jasper Knight helped to improve our manuscript. We also express thanks to Shreyosi Dasgupta, Blaine Novakovski, Luis Quiroz, Solange Angulo, Kyle Reid, Siew Chan Ragoo, and the management and employees of Queen's Beach Hotel in Mayaro, Trinidad.

CHAPTER 5: HIGH-FREQUENCY STACKING PATTERN AND STAGES OF CANYON/GULLY EVOLUTION ACROSS A FORCED REGRESSIVE SHELF-EDGE DELTA-FRONT

Dasgupta, S., and Buatois, L.A., 2015, High-frequency stacking pattern and stages of canyon/gully evolution across a forced regressive shelf-edge delta-front: *Marine and Petroleum Geology*, http://dx.doi.org/10.1016/j.marpetgeo.2015.08.003, in press.

Keywords: Shelf-edge canyon/gully; paleo-Orinoco delta; growth faulting; stacking pattern; high-frequency sequence-stratigraphy; accommodation-driven delta; facies tract.

Abstract

The succession of varying facies tracts filling within a canyon, or a deep incised gully, cutting across the delta-front lobes at the shelf-edge requires to be explained by high-frequency allocyclic and/or autocyclic events. A ‘fifth- and sixth-order’ sequence-stratigraphic model for the shelf-edge canyon-fill or gully-fill is here proposed for the first time. The first Gelasian cold phase and the renewal of transpressional uplift of basin-margin occurring at the same time enforced regressive transit of the inner-shelf paleo-Orinoco delta onto the paleo-shelf-edge. Its delta-front developed along the shoulders of the major successive basin-bounding growth faults. The delivery of clastic sediments into the deeper slope and beyond in the Columbus Basin was through the gullies and canyons that incised and cannibalized across the shelf-edge delta. The Mayaro Formation of southeast Trinidad furnishes the role of growth faulting during the first phase of delta-front development at the paleo-shelf-edge. Thereby, it serves as an example of several ‘fifth-order sequences’, within a ‘fourth-order’ equivalent episode, which is contemporaneous to both the glacio-eustatic episode, the Pretiglian, and the renewal of transpressional uplift after a pause during the Pliocene. Thus, large incision and subsequent filling within the Mayaro Formation cover a passage of time (‘fifth-order’ equivalent) that is unequivocally shorter than the span of the falling Pretiglian eustatic sea-level and second renewed phase of transpression tectonism. The categorization of sedimentary facies of the

canyon-fill or gully-fill and the encasing delta-front outside the it into a series of 'sixth-order' genetic facies tracts shows variations of geomorphic stages of the canyon/gully evolution – from accommodation creation to the stages of filling. These stages, therefore, should be attributed to the 'sixth-order' equivalent autogenic changes influenced by high-frequency growth-tectonics, instead of assuming the stages to be related to the relatively lower-frequency glacio-eustatic allocyclicity of the earliest Pleistocene.

5.1 Introduction

Growth-fault tectonism in unconsolidated to semi-consolidated stack of sediments can be considered intrabasinal in nature. It has an additive effect on accommodation creation during falling relative sea-level, thereby countering the diminutive effects of base-level fall on accommodation. Compared to other normal allogenic stratigraphic controls (*e.g.,* eustasy, thick-skinned lithospheric tectonism), growth-fault tectonics has distinctly different periodicities and frequencies of activity. The high-frequency 'slip-stick-slip' (or 'slide-hold-slide') activities of growth-faulting have mostly been underestimated as the major drivers of 'high-order' cycles especially in the settings with very high sediment accumulation rates (*e.g.,* the shelf-edge deltas). There are a very limited number of published examples, particularly from rift-basins, which relate the growth-fault tectonics with high-frequency sequence stratigraphy (*e.g.,* Young *et al.,* 2003; Zecchin *et al.,* 2006; Răbăgia *et al.,* 2011). The present example is an attempt to make a sequence stratigraphic model showing effects of growth-fault activity on the stacking pattern within gullies and canyons cutting across a shelf-edge delta-front.

The Plio-Pleistocene paleo-Orinoco delivery system of the Columbus Basin has a classic example of growth fault-influenced shelf-edge delta with a very high sediment accumulation rate (*i.e.,* 5-10 m/ka in Wood, 2000, and Bowman and Johnson, 2006, 2014; or 10 m/ka in Alvarez, 2008) in a complex, obliquely colliding and transpressional foreland basin between the Caribbean and South American plates. The tectonic and structural history of the southeast Trinidad and offshore Columbus Basin has been elaborated elsewhere in detail (*e.g.,* Dunham *et al.,* 1996; Algar, 1998; Pindell *et al.,* 1998; Babb and Mann, 1999; DiCroce *et al.,* 1999; Wood,

2000; Boettcher *et al.*, 2003; Pindell and Kennan, 2009; Garciacaro *et al.*, 2011a, 2011b; Gibson *et al.*, 2012). From the basin margin of Columbus Basin at the present-day southeast coastline of Trinidad, successive growth faults provided with the primary shelf-breaks consecutively basinwards, as documented in the published seismic data (Wood, 2000; Sydow *et al.*, 2003; Garciacaro *et al.*, 2011b). The delta-fronts of the paleo-Orinoco River developed along the shelf-breaks. The Gros Morne Formation and the younger Mayaro Formation (Fig. 5.1), exposed in southeast Trinidad, record the first two pulses of delta-front sedimentation near and at the shelf-edge. The Mayaro Formation, however, unambiguously records the first pulse of shelf-edge delta-front defined by an associated growth fault (the Cedar Grove Fault) (Fig. 5.2A-B).

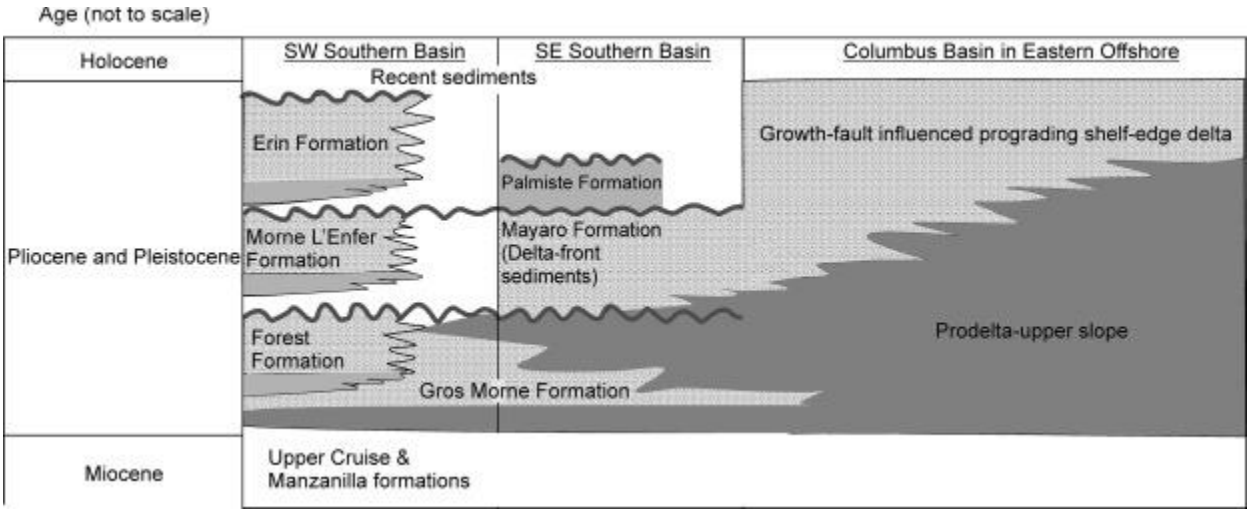

Fig. 5.1. Simplified Pliocene-Quaternary stratigraphic column of southern Trinidad and its eastern offshore vicinity. The vertical axis for age (Ma) is not according to scale.

The deposition of the Mayaro Formation megasequence corresponds to two important events – (1) the onset of global Pretiglian cold climate (or Marine Isotope Stage/MIS 103) of Gelasian Age (Rio *et al.* 1998; *cf.*: Gibbard *et al.*, 2010; Cohen *et al.*, 2013), and (2) the renewal of transpression between Caribbean and South American Plates alongside the margin of deep-water Columbus Basin (Gibson *et al.*, 2012). Both events happened at the same time enabling forced regression of the accommodation-driven paleo-Orinoco delta system by relative sea-level fall (Porębski and Steel, 2006). Previous studies suggested that the Mayaro Formation megasequence was deposited within Milankovitch periodicities (Bowman, 2003; Sydow *et al.*,

2003; Bowman and Johnson, 2014). Therefore, any facies tract level variations in stacking pattern caused by physiographic changes within the Mayaro Formation 'megasequence' must be the response of autogenic or allogenic changes (or the combinations of both) pertaining to the shorter periodicities and the higher frequencies, compared to Milankovitch cycles.

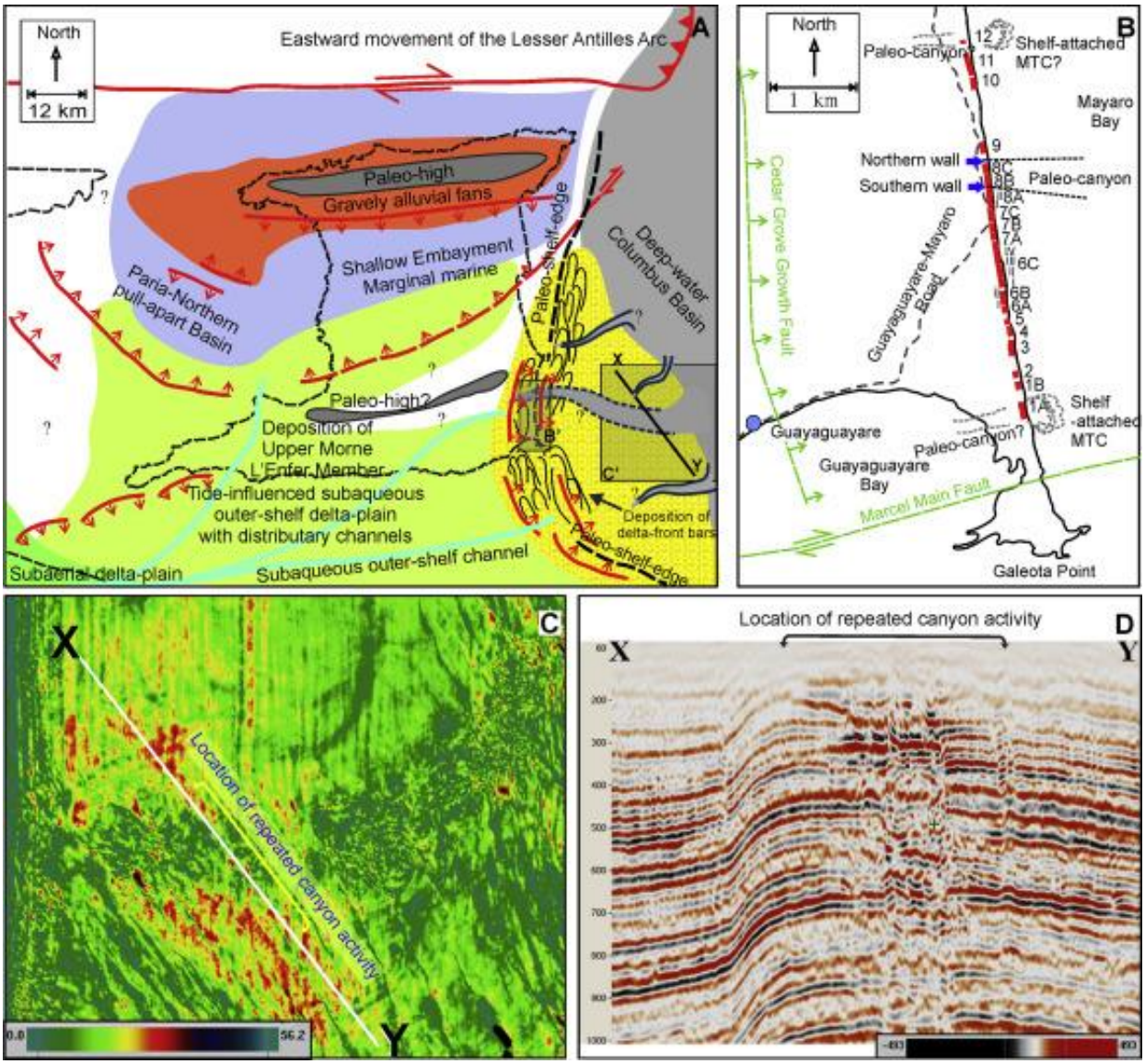

Fig. 5.2. (*N.B.* Figure caption is intentionally moved to the next page due to its length)

Fig. 5.2. (A) Paleographic map of the Gelasian paleo-Orinoco delta system showing tentative distribution of the depositional sub-environments in relation to the structural features (modified after Bowman, 2003). The arrows indicate the direction of movement of the faults following the conventional symbols for thrust, normal fault and strike-slip movement. The rectangle B' shows the location of the Mayaro Formation outcrops in Fig. 5.2B. The rectangle C' shows the area of the stratal amplitude slice from 3D seismic data in Fig. 5.2C. The location of the gully/canyon in the outcrop and similar features in the offshore at the location with repeated canyon activity is connected by dashed curves. [*N.B.* The connectivity between the two is assumed because of their proximity and apparent spatial juxtaposition in order to show a subsurface example of repeated canyonization. The canyon/gully outcrop may potentially be connected to another shelf-edge invagination in the offshore subcrop areas. (B) The rectangle in Fig. 5.2A is enlarged into the location map of the Mayaro Formation outcrops (marked in red) with the outcrop numbers. The dashed lines indicate the northern and the southern walls of the canyon/gully. (C) The RMS-amplitude slice approximately from the Gelasian horizon of the 3D seismic volume. The area covers the same rectangular area C' in Fig. 5.2A. The colour bar denotes amplitude values. (D) Vertical TWT section from the 3D seismic volume roughly focused at the Gelasian horizon along the XY straight-line in Fig. 5.2A-C, showing the recurrent canyon/gully activity. The vertical scale is in milliseconds. The colour bar indicates amplitude values.

The goal of our study is to propose for the first time a high frequency (higher 'order') sequence-stratigraphic model in order to explain the geomorphologic and corresponding depositional cycles within an incised canyon/gully as the cause of variations of facies tracts. The model is based on detailed field study complemented by a limited study of the seismic data in the immediate offshore vicinity of the field area. Our study underscores the role of growth-faulting-related quasi-autogenic shifting (*i.e.,* downward or upward along the depositional dip direction) of the loci of deposition of the coarser clastic sediments (medium-grained sand in case of the Mayaro Formation) as the controlling factors on stratal stacking patterns.

5.2 Geology of the Canyon System(s) within the Mayaro Formation

5.2.1 Geologic Background

The more than 2000 m thick Mayaro Formation mostly records delta-front sandstones and sandy heterolithic sediments deposited as (i) river-dominated subaqueous distributary channel-overbank deposits, (ii) terminal mouthbar deposits, (iii) a series of wave-modified, hummocky-swaley cross-stratified, amalgamated and discrete barrier bars laterally away from

the feeder system, and (iv) very limited intervals of proximal muddy prodeltaic deposits with mixed influences by river, tides, and waves (Dasgupta *et al.*, 2015). The delta-front deposits are exposed as foreshore cliff outcrops towards the north of the Marcel Main Fault near Galeota Point. The exposures are parallel to the depositional strike and the paleo-shelf-break orientation defined by the Cedar Grove Fault (Fig. 5.2B). The lithofacies variations in different deltaic subenvironments reflect the sedimentary processes showing the varying relative dominances of waves, fluvial processes, and gravity-flow processes with minor tidal influence (Wach *et al.*, 2003; Bowman, 2003; Uroza, 2008; Bowman and Johnson, 2014; Dasgupta *et al.*, 2015). The combinations and relative hierarchy of physical, chemical, and rheological stress factors in different subenvironments of the shelf-edge delta are manifested in terms of the inherent ichnological characters (Dasgupta *et al.*, 2015).

In Outcrops 8B-C (Fig. 5.4A), an irregular discontinuity surface, dipping ca. 45°-58° (or ca. 30°-40° after structural dip correction) towards 345°-035°, was initially described as a tectonic fault contact (Bowman, 2003; *cf.* 'tectonic fault' immediately above datum 1500 m in *Fig. 3* of Bowman and Johnson, 2014). However, integration of ichnological evidence with sedimentological and sequence-stratigraphic datasets clearly revealed that the contact is the southern flank of the primary incision surface of a paleo-canyon/gully on the basis of colonization of a monospecific suite attributed to the *Glossifungites* Ichnofacies (Dasgupta and Buatois, 2012; Dasgupta *et al.*, 2015). This contact surface hereafter is referred to as the southern wall of incision. The *Glossifungites* Ichnofacies is represented by firmground *Thalassinoides* on the canyon-wall penetrating into the underlying delta-front sandy sediments and, therefore, crosscutting previously emplaced softground trace fossils of the delta-front. The canyon was filled with five successive and distinct facies tracts or genetic facies associations and then got healed by the re-establishment of the delta-front facies tract.

Also there are two mass transport deposits exposed at the southern and northern ends of the main outcrops of the Mayaro Formation (respectively Outcrops 1A and 12 in Fig. 5.2B). Given their depositional, paleogeographic, and stratigraphic association, the mass transport deposits are 'shelf-attached mass transport complex' deposits (*sensu* Moscardelli and Wood, 2008; Romero-Otero *et al.*, 2010). The shelf-attached mass transport complexes are known to be

funneled downslope through paleocanyons as well. Therefore, the two locations of shelf-attached mass transport complexes also fall within the axial trends of two separate canyon/gully incisions.

All the outcrops along the shoreline are sub-orthogonally aligned to the axial trend of a regional open syncline, and are situated on the southern limb of the fold (Dasgupta *et al.*, 2015). The syncline has the approximately east-west striking axial surface and the entire succession is gently tilted towards the north. Therefore, due to this tilt, it is possible to study mostly the southern side of the incision and the canyon/gully-fill facies tracts.

Towards the northern end of Outcrop 8C, the canyon/gully-fill sediments abut as well as pinch out against another discontinuity surface, referred to as northern wall of incision, which separates the canyon/gully-fill succession from relatively older delta-front sediments (Fig. 5.4B). The northern canyon/gully wall is more irregular in nature with ca. 15°-40° paleoslope towards SSE (after structural dip correction) and is characterized by slump-scars and associated cogenetic noncohesive debris flow deposits (*i.e.,* FT-A, see below).

5.2.2 Facies tracts and sedimentary processes within the Mayaro incised canyon/gully

There are six principal genetic facies tracts, FT-A to -F, which for the most part can be identified in a systematic stratigraphic order within a cycle. Table 5.1 provides with a summary of the facies tracts classification with their descriptions and explanations on the sedimentary processes. In a zone of repeated canyonization or gullying (*e.g.*, as in Fig. 5.2C-D), the incision surfaces (*e.g.*, the southernand northern walls of incision in Outcrops 8B-C) separate a previous cycle from a new one. FT-A is repeated at any level within the cycle. FTs -B to -F are deposited successively upward within a single cycle (Fig. 5.3).

Table 5.1. Summary of the facies tracts classification of the Mayaro Formation with description of facies associations, and interpreted sedimentary processes.

Facies Tracts	**Sedimentary facies association**	**Interpretation / sedimentary processes**
FT-A	(1) Intraclast-supported and matrix-supported breccia. (2) Distributed locally throughout the canyon/gully-fill, especially in vicinity of incision surfaces, without having any preferred occurrence within the canyon/gully-filling stacking pattern. (3) Limited or no stratigraphic significance in particular. (4) Unbioturbated.	(1) Deposited inside the canyon/gully from cohesive and non-cohesive debris flows (Outcrops 8B-C). (2) Derived from slumped/collapsed steepened unstable slope (*e.g.*, the walls and the head of the canyon/gully under constant erosion). (3) Transported as frictional/collisional (non-cohesive) and cohesive types of debris flows.
FT-B	(1) Intraclast-supported breccia with muddy matrix. (2) Intermittent occurrence of glided allochthonous blocks. (3) Filled the bottom and lower parts of the walls of the canyon/gully. (4) Unbioturbated.	(1) Canyon/gully-filling mass transport complex which mostly consists of silty mud-dominated cohesive debris flow deposits. (2) Sediments deposited inside the canyon/gully geometry (Outcrops 8B). (3) Consists of melange of sediments from prodelta, delta-front, and outer shelf/upper slope of the previous cycle, within a sheared and/or fluidized muddy matrix. (4) Materials derived from previous cycle deposited at the lowest part of the canyon/gully-fill. (5) Transported chiefly as mudflow and deposited en-masse.
FT-C	(1) Consists of the dm-m thick couplets *i.e.*, of two alternating litho-units: (a) thin-bedded/laminated muddy and sandy heterolithic siltstone, (b) intraclasts-supported breccia with muddy matrix, with the same bulk material like the other litho-unit. (2) Thin-beds/laminations contain internal grain-size variation as such that inversely graded layers are overlain by normal graded layers. (3) Intermittent double-mudstone laminae and organic-rich intervals within heterolithic siltstone unit. (4) Unbioturbated.	(1) Deposited inside the canyon/gully (Outcrops 8B). (2) Siltstones deposited from ‘pulsating’ waxing-waning sustained turbidity current cycles. (3) Topographic irregularities healed by short-distance remobilization of the heterolithic siltstones producing the smaller slope-healing cohesive debris flow deposit units. (4) Organic-rich laminations are deposited from phytodetrital pulses. (5) Double mudstone laminae are features of baroclinic bottom current reworking.

FT-D	(1) Same FT-C in the background with intermittent medium-grained sandstone lithosomes. (2) Channel-shaped, and tabular to lensoid shaped geometries of sandstone lithosomes. Channel geometry dominates lower part of FT-D, whereas upper part is dominated by tabular/lensoid geometry. (3) Sharp or erosional bases of sandstones. (4) Thickness of individual sandstone lithosomes = 1-2 m. (5) Planar and trough cross-stratified sandstone with imbricated and intermittently armoured mudstone-intraclasts within channel geometry. (6) Lateral and discrete accretion patterns of channels. (7) Tabular beds and lenses consisting of sandstones of hybrid sediment-gravity flow characters (see text for detailed description of subunits). (8) Unbioturbated.	(1) Deposited inside the canyon/gully (Outcrops 8B-C). (2) Deposition in canyon/gully-confined architectural elements (*i.e.*, bypassing channel-tabular overbank-lensoid crevasse system). (3) Only bedload transport within channels implying that the lower-concentration turbulent suspended load bypassed into the deep-water environment. (4) Lateral and discrete accretions of channels indicating avulsion. (5) Breaching the overbank evidenced by crevasses (both distributary and splays). (6) Hybrid sandy turbidites with 'linked debrites' indicating flow-transformation from turbidity flow to more visco-plastic flows possibly by deflocculation of clay particles into fluid mud. (7) System possibly backfilling within the canyon/gully, because of increasing number of lenses/tabular bedforms of hybrid gravity-flow deposits towards top and decreasing number of channels.
FT-E	(1) Sharp erosional bases or gradual changeover from FT-D to FT-E at different locations. (2) Consisting of alternate cm-m thick tabular beds of: (a) Thin-bedded/laminated siltstone units (*i.e.*,silty sustained turbidity current deposit similar to those in FT-C) and (b) Massive to parallel-laminated medium-grained sandstone turbidite units. (3) Unbioturbated; rare mottles.	(1) Deposited inside the canyon/gully (Outcrops 8B-C). (2) Frontal/terminal splays of the bypassing channels of FT-D consisting of tabular sandy turbidite bodies as seasonal sand-rich pulses. (3) System back-stepping within the canyon/gully because (a) the splays completely replaced the bypassing channels unlike FT-D, and (b) more and more distal parts of the splays are exposed towards the top of the succession with overall thinning of beds.
FT-F	(1) Mostly hummocky-swaley cross-stratified sandstones and sandy heterolithic deposits near the incision. (2) Highly variable ichnological signature. (see text and also Chapter 3)	(1) Deposited at shelf-edge outside the canyon/gully (*i.e.*, all other outcrops, except Outcrops 8B-C). (2) Delta-front with the following subenvironments: Active and abandoned subaqueous feeder channel-fills; proximal and distal overbank and crevasse complex of subaqueous channels; river-

		dominated mouthbars; proximal and distal wave-modified, subaqueous barrier bars and associated tidally influenced interbar shoals; proximal prodelta. (3) Distinctly different from all others FTs in terms of mesoscopic physical appearance, net-to-gross ratio, geometry of architectural elements, and trace-fossil assemblages.

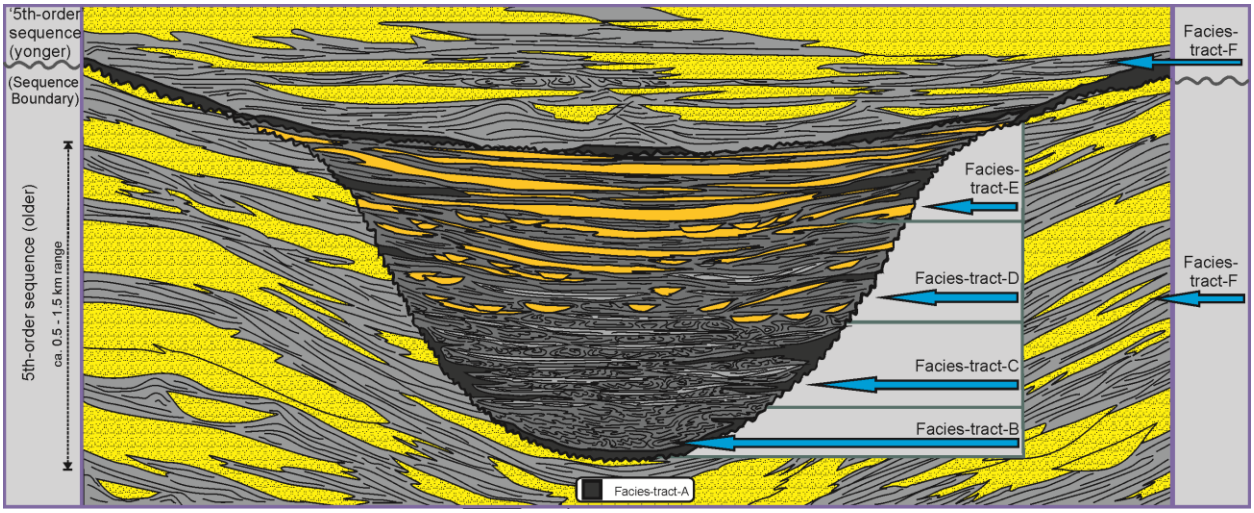

Fig. 5.3. Schematic section perpendicular to the axis of the paleo-canyon/gully and parallel to the depositional strike of the shelf-edge delta. The incision surface separates two 'fifth-order' sequences. The vertical succession of the facies tracts FT-A to -F is schematically depicted. FT-A (the darkest in shade): slump deposits remobilized from the incision surface. FT-B: cohesive debris-flow deposits. FT-C: couplets defined by the alternate beds of the silty sustained-turbidites and the cohesive debris-flow deposits. FT-D: tabular beds, consisting of the hybrid type gravity-flow deposits and the silty sustained turbidity current deposits, crisscrossed by the bypassing channels containing remnant sandy bedload deposits. FT-E: alternate beds of the silty sustained turbidity current deposits and the surge-type sandy turbidites. FT-F: delta-front deposits of sandy distributary channels-overbank, terminal mouthbars, barrier bars, and their silty heterolithic distal and peripheral parts. See text for further details on facies tracts.

5.2.2.1 FT-A

FT-A consists of both intraclasts-supported and matrix-supported breccias with both medium-grained sandstone and clayey siltstone as matrix. The variable sized intraclasts consist of siltstones and heterolithic sediments. The breccias are unbioturbated.

These deposits are interpreted to be deposited from cohesive and non-cohesive debris flows containing (a) blocks of older delta-front deposits from incision surface transported within very short distance and (b) muddy (for cohesive debris-flow deposits) and sandy (for non-cohesive debris-flow deposits) matrix depending upon the bulk of the sediments dislodged (*i.e.*, slided/slumped) and remobilized (Fig. 5.4B). These debris-flow deposits are ubiquitous throughout the canyon-fill, especially near the incision surface (Fig. 5.3). The detrital materials of FT-A were derived as the slided/slumped canyon/gully-walls and also as the mass-wasting detritus delivered along the nascent gully deposited immediately above the incision surface. Nonetheless, the slumping occurred all throughout the different stages of the incision and filling, as long as slope instability was active factor. As a result, FT-A has no preferred occurrence within a canyon/gully-filling cycle and has limited stratigraphic significance in particular.

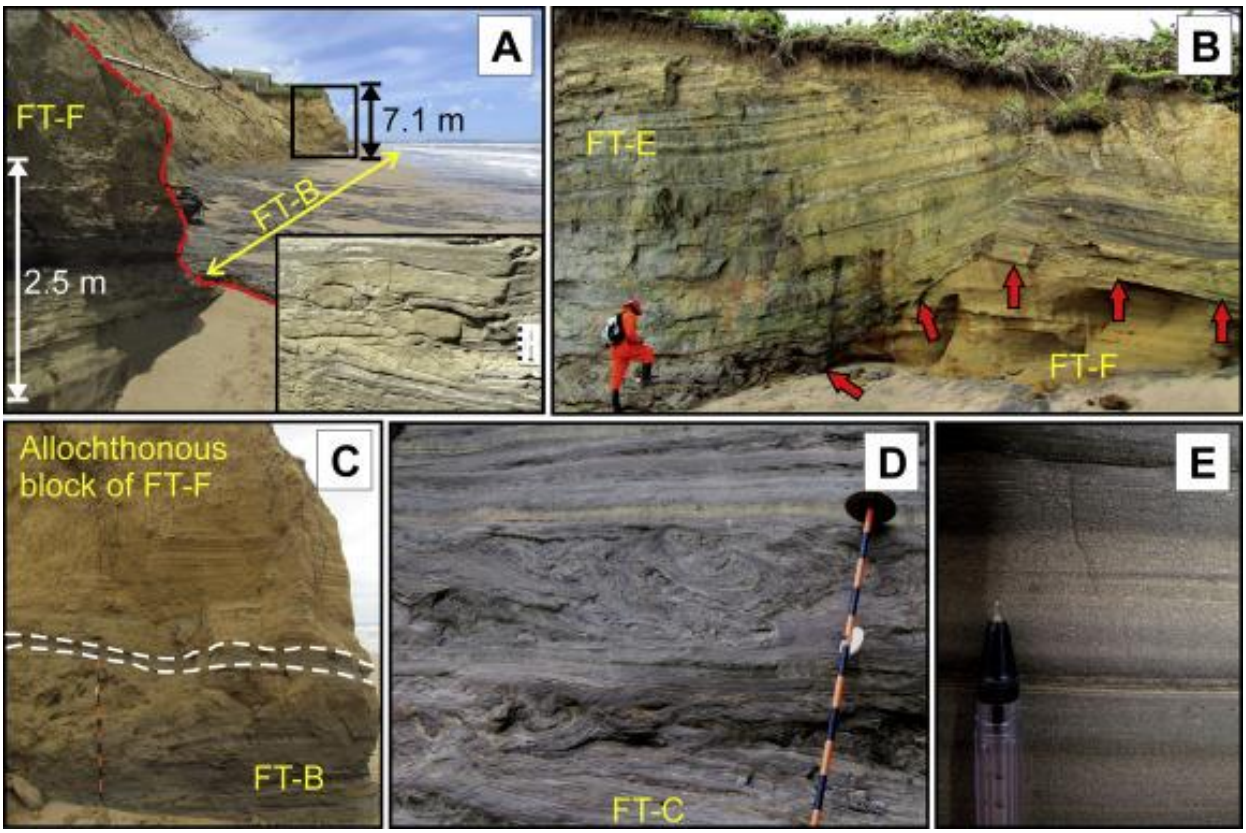

Fig. 5.4. (*N.B.* Figure caption is intentionally moved to the next page due to its length)

Fig. 5.4. Photographs of the lithofacies defining the FT-A to -C. (A) The dashed red curve shows the southern wall of incision, which separates the delta-front sediments (*i.e.*, FT-F) below and FT-B sediments above. The rectangle demarcates a glided block (see Fig. 5.4C). The yellow arrow shows the canyon-filling mass-transport complex deposit deposited above the southern wall of incision. The inset shows the closer view of the mud-flow (canyon-filling mass-transport complex) deposit belonging to FT-B. (B) A non-cohesive debris-flow deposit (FT-A, on which the man is standing) slumped from the incision surface (or the northern wall of incision, marked by the red arrows). Below the incision surface, the sandstone beds of FT-F are exposed. Above the slump-deposit and the incision surface, the alternate beds of the silty sustained-turbidite and the ignitive sandy turbidite are exposed (*i.e.*, FT-E). The slump-deposit contains clasts within a sandy matrix. (C) Closer view of the glided sandstone block marked in Fig. 5.4A. The dashed white curves demarcate decollement/glide surface with sheared muddy gauge. The thin-bedded mud-flow deposit (FT-B) is below the decollement. (D) FT-C defined by couplets (*i.e.*, consisting of two lithofacies units) of the silty sustained turbidity flow deposit and the slope-healing cohesive debris-flow deposit originating from remobilization of the silty sustained turbidity current deposits within short distances. Every orange and black segment of the Jacob stuff is 10 cm long. (E) Closer view of the silty sustained turbidity current deposit showing coarsening- and fining-upward waxing-waning cycles. The sharp 'double mudstone laminations' are formed by background bottom current reworking. The diameter of the pen is 7 mm.

5.2.2.2 FT-B

FT-B consists of intraclasts supported breccia with clayey siltstone matrix. There are large outsized allochthonous blocks of sandstones emplaced within the unit (Fig. 5.4A, C). The matrix is muddy with shearing structures showing varying degrees of shearing – from completely massive mudstone (*i.e.*, signature of complete liquefaction) or clayey siltstone to thin-bedded/laminated mudstones showing sheared, contorted, and rotated blocky appearances (*i.e.*, signature of more brittle shearing). The unit occurs at the base of canyon/gully-fill. FT-B is also unbioturbated.

FT-B represents the canyon/gully-filling mass-transport complex, which mostly consists of cohesive debris-flow deposits. The glided allochthonous blocks appear to be derived from the previously deposited delta-front sediments (FT-F). The fundamental differences with FT-A is that (a) FT-B consists of these allochthonous blocks transported substantial distance because the bulk sedimentary components of these blocks do not have the same sand-to-fine ratio (or in other sense the cohesiveness) with the immediate canyon-wall vicinity, and (b) the canyon/gully-filling mass-transport complexes filled only the bottom and lowest parts of the incision surface, when the canyon/gully was cannibalizing the previous cycle(s).

FT-B sediments are derived as melange of sediments from prodelta, delta-front, and outer shelf/upper slope of the previous cycle, being delivered directly by slope-instability and aided by longshore currents and river-mouth processes. Therefore, the remobilized coarse-grained clastic materials (*i.e.,* medium-grained sand for the case of Mayaro Formation) got partly incorporated within debris flows of the canyon/gully-filling mass-transport complex. However, due to the cannibalization and remobilization of sediments (through the canyon/gully) from the previous cycle(s), the loci of bulk of sand-deposition shifted from shelf-edge delta-front directly to the deep-water environment (see Discussion). The canyon/gully-filling mass-transport complex is unbioturbated owing to the complete instability of substrate during deposition and also possibly due to the decrease in quality of the nutritive substances during the remobilization (Dasgupta *et al.*, 2015).

5.2.2.3 FT-C

FT-C consists of decimeter- to meter-thick couplets (*i.e.,* consisting of two alternating lithofacies units Fig. 5.4D) defined by (1) intraclasts-supported breccia with muddy matrix and (2) thin-bedded/laminated muddy and sandy heterolithic siltstones, which contain internal grain-size variations (*i.e.,* alternating inverse and normal grain-size gradings), intermittent laminations of organic detrital materials, and sharp and rare 'double-mudstone laminations' (Fig. 5.4D-E). Both units are unbioturbated.

The couplets are interpreted to be (1) the small cohesive debris-flow deposit units and (2) the silty sustained turbidity current deposit units respectively (Fig. 5.4D). The latter (*i.e.,* the thin-bedded / laminated, clay-bearing silty sustained turbidity current deposits) testify for 'pulsating' waxing-waning sustained flow cycles (Fig. 5.4E). The organic-rich intervals are interpreted to be the deposits of phytodetrital pulses (MacEachern *et al.*, 2005; Buatois *et al.*, 2011) from the river mouth feeding the canyon/gully or the lofting-related deposits (Zavala *et al.*, 2012). The bases of the FT-C units are sharp and commonly erosional. The background influence of baroclinic bottom current reworking (Dykstra, 2012; Shanmugam, 2013) within the canyon is also sparingly preserved within this unit as sharp 'double mudstone laminations' (Fig. 5.4E).

The silty sustained turbidity current deposits were deposited from the background regular fine-grained underflows (or hyperpycnal flows *sensu lato*), whereas the coarser-grained pulses of the gravity flows bypassed into the deeper slope. This happened when the slope instability at theflanks of incision and at the gully/canyon head was already much reduced, so that sustained gravity flows were possible instead of the ignitive en-masse deposition from mass transport (as in FT-B). The silty sustained turbidity current deposit units exhibit complicated interactions among (a) the waxing-waning stages of sustained turbidity currents, (b) the fluid mud activity vis-à-vis clay flocculation and deflocculation processes, and (c) the background baroclinic currents amplified within the topographic furrow provided by the canyon/gully. The beds are unbioturbated due to the high turbidity, fluid-mud activity, possible dysoxia created by the microbial decomposition of the plant debris and, arguably above all, the low preservation potential of biogenic structures due to poor lithologic contrasts. The topographic heterogeneities are healed by short-distance remobilization of the silty sustained turbidity current deposits thus producing the smaller slope-healing cohesive debris-flow deposit units, which are much less in thickness and areal dimension than the canyon/gully-filling mass-transport complexes in FT-B.

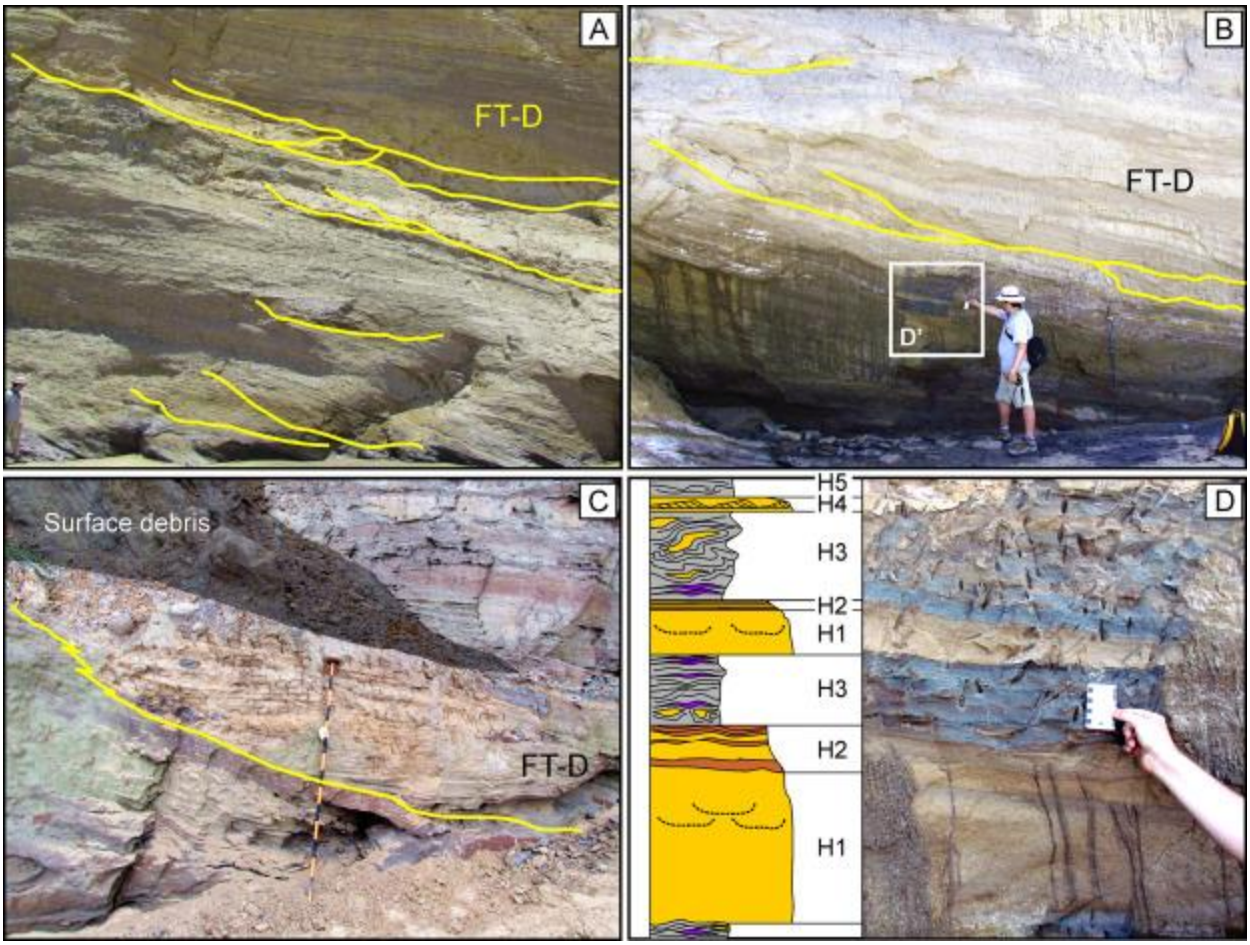

Fig. 5.5. Photographs of the lithofacies defining the FT -D. All channel bases are marked with yellow curves. (A) (B) Lateral and discrete accretion of bypassing chutes/channels crosscutting the tabular beds of hybrid sediment-gravity flow deposits. Rectangle D' is enlarged in Fig. 5.5D. (C) Oblique section of a channel showing planar and trough cross-stratified sandstone with imbricated intrabasinal mudstone clasts. The Jacob stuff is 1.5 m long. (D) Closer view of the hybrid gravity-flow deposits showing lithofacies subunits (after clearing the superficial dirt smeared on all over the outcrop). The schematic sketch on the left side shows the equivalent hybrid sediment-gravity flow deposit subunits, H1-5, after Haughton *et al.* (2009) (see text). The dashed curves and the purple laminations show dish structure and organic debris respectively.

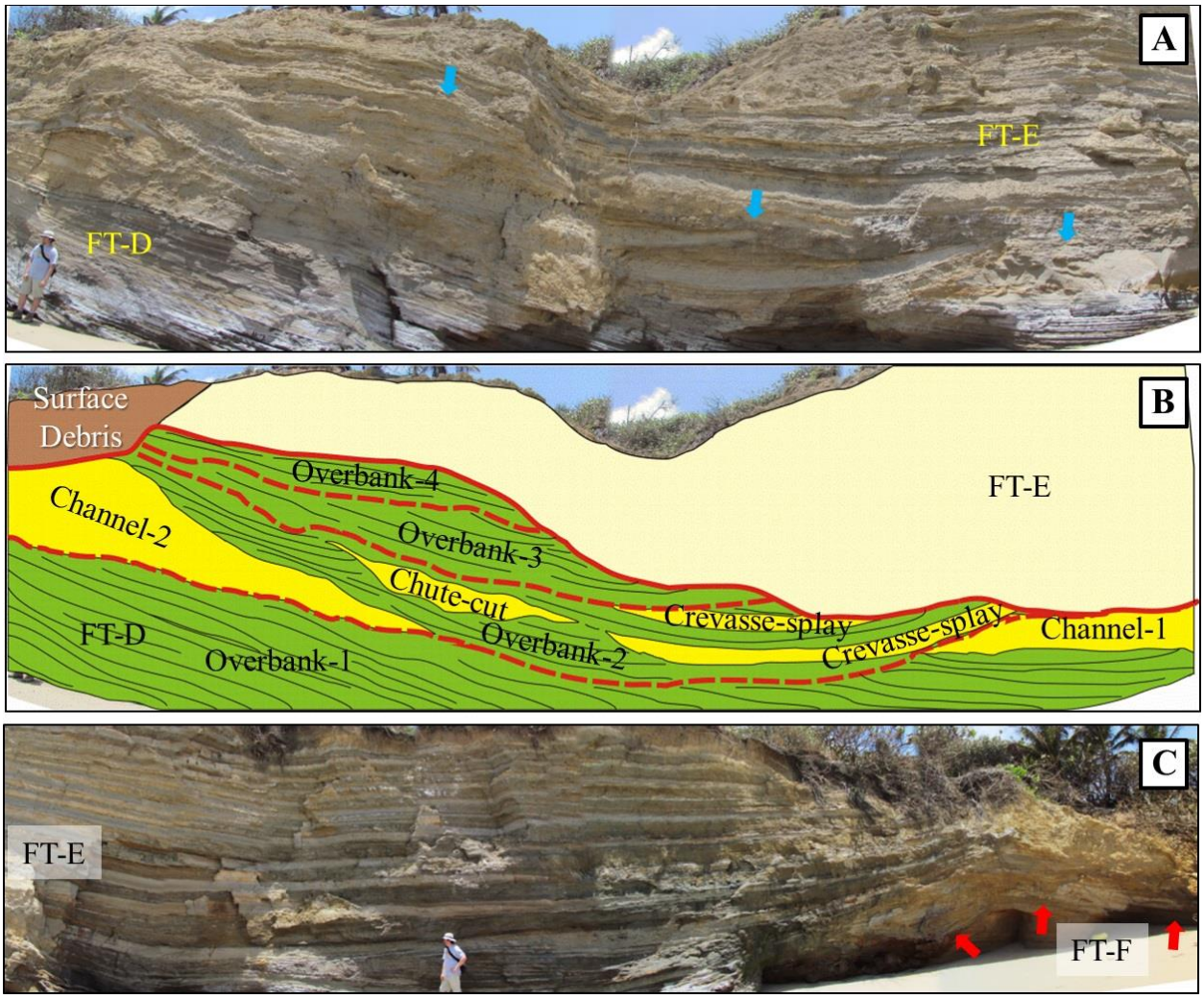

Fig. 5.6. Photographs of the lithofacies defining the FT-D to -E. (A) Photograph of channel-overbank-crevasse splay complex deposit belonging to FT -D overlain by FT-E with sharp erosional base (blue arrows). (B) Schematic interpretation of FT-D architectural elements in Fig. 5.6A. The yellow and green colours indicate sandy lithosomes and heterolithic background (*i.e.*, FT-C in the background) respectively. Four stages of avulsed channel are partly exposed separated by erosional bases, indicated by the dashed red curves. The channel-2 and its proximal to medial overbanks can be identified by the chute cut-and-fill and the crevasse splays, respectively. The lithofacies units of FT-E with sharp erosional base are exposed above. (C) FT-E defined by the alternate beds of the silty sustained turbidity flow deposit and the surge-type sandy 'high-density' turbidite. The beds become thinner near the incision-wall (*i.e.*, the northern wall of incision), marked by the red arrows, and onlap and/or pinch out against it. Below the incision surface, the delta-front sandstone (FT-F) of the older sequence is exposed.

5.2.2.4 FT-D

FT-D is consists of medium-grained sandstones encased within a background of FT-C (*i.e.*, couplets of silty sustained turbidity current deposits and cohesive debris-flow deposits; see above). Figs. 5.5A-D and 5.6A-B demonstrate the geometries and internal features of the sandstone lithosomes of FT-D. There are two geometric types of sandstone lithosomes: arcuate or 'channel-shaped' bodies with planar and trough cross-stratifications and tabular-to-lensoid-shaped bodies with normal grain-size grading (fining upward into siltstone). The erosional-based channel geometry dominates the lower part of FT-D, and the sharp-based tabular to lensoid beds dominate the upper part. Both types of lithosomes are individually 1-2 m in thickness. The foresets of the cross-beds intermittently bear imbricated and armoured mudstone intraclasts (Fig. 5.5C). The sandstone lithosomes with channel-shape show lateral scouring and shifting and discrete reappearance (*i.e.*, lateral and discrete accretions respectively) (Fig. 5.5A-B). Paleocurrent directions measured from the bedform structures appear to be highly variable. FT-D unit is also unbioturbated.

Presence of sedimentary structures only related to bedload transport implies that only the tractional load was deposited within the channels, whereas the turbulent suspended load was bypassing into the deeper-water environment. Variations of paleocurrent directions may indicate the channels to be sinuous. Lateral and discrete accretions of channels are manifestation of sediment bypass and proneness to avulsion of the channels, similar to the deep-marine bypassing sinuous channels of much larger dimension (Kolla *et al.*, 2007). The sharp-based tabular to lensoid sandstone beds consist of the hybrid sediment-gravity flow deposits (*i.e.*, combinations of the sandy turbidites and associated cohesive 'linked debrites') (*e.g.*, Haughton *et al.*, 2003, 2009; Barker *et al.*, 2008; Talling, 2013; Patacci *et al.*, 2014) (Fig. 5.5B, D). Presence of a 'linked debrite' (*i.e.*, cohesive debris-flow deposit subunit), sandwiched between lithofacies similar and comparable to Bouma-type (Bouma, 1962) turbidite subunits (*i.e.*, Ta-Tb below and Td-Te at the top of 'linked debrite') indicates steps of deposition from a hybrid sediment-gravity flow as follows:

a) Deposition of massive (H1 in Fig. 5.5D; equivalent to Bouma Ta subunit) and then parallel-laminated sands (H2 in Fig. 5.5D; similar to Bouma Tb subunit) with banded appearance. The

banded appearance is due to alternating mud-bearing and mud-poor sandstone layers deposited from a 'slurry flow', which is intermediate between turbulent and visco-plastic rheology (Lowe and Guy, 2000; Lowe *et al.*, 2003; Sylvester and Lowe, 2004; Haughton *et al.*, 2009; Talling, 2013).

b) Flow-transformation from turbidity current to visco-plastic flow possibly by deflocculation of clays into cohesive fluid mud and deposition of the 'linked debrite' subunit (H3 in Fig. 5.5D).

c) Deposition from turbulent mud-rich tailing part of the flow (H4 and H5 subunits in Fig. 5.5D, as equivalent to Bouma Tc-Td, and Te subunits respectively). The names of the subunits (H1-5, Fig. 5.5D) are coined after Haughton *et al.* (2009). The tabular or lensoid depositional elements are interpreted as (a) the overbank and crevasse splays of the channels (see above) and (b) the terminal splays of their smaller crevasse-distributaries that evolved from breaching the overbank. Intermittently the tabular beds are crosscut by smaller channels, thereby displaying signatures of crevassing (Fig. 5.5A-B). The lithological heterogeneity has resulted in undulated or warped bedding surfaces after compaction. An individual channel-overbank-crevasse complex, as a complete unit, demonstrates erosional base, channel breach features (*i.e.*, small chute-cuts) adjacent to the main channel bank, and the tabular splays deposited in its medial to distal overbank (Fig. 5.6A-B). The FT-D interval display a possible backfilling character within the canyon/gully, as it contains increasing number of the lenses and tabular bedforms of the hybrid gravity-flow deposits towards top with decreasing number of the bypassing channels. The FT-D is unbioturbated due to the same reasons like FT-C.

5.2.2.5 FT-E

The changeover from FT-D to FT-E is variable in nature, being either sharp or gradual (*e.g.*, the sharp-based FT-E outcrop is shown in Fig. 5.6A-B). FT-E consists of alternate and rhythmic layers defined by (1) centimeters to almost one-meter thick tabular beds of silty sustained turbidity current deposits (as in FT-C) and (2) massive to parallel-laminated medium-grained surge-type turbidite sandstone (*i.e.*, Bouma Ta-Tb facies, Bouma, 1962; high-density turbidite facies S3 -Tb, Lowe, 1982). The northern wall of incision near FT-E outcrop are almost subparallel to the tabular beds of FT-E, where the latter onlap against the former (*i.e.*, northern

canyon/gully wall) and their thicknesses increase away from the walls thereby showing signature of pinching out as well (Fig. 5.6C).

The tabular turbidite bodies are interpreted to be the frontal splays of the bypassing channels of FT-D. Their rhythmic reoccurrence is perhaps manifestation of the seasonal sand-rich pulses. The splays were deposited because of the following possible reasons: (i) the channels progressively came out of the confinement of the overbank at more and more shallower depth and the flows, consequently, underwent hydraulic jump to dump their load as fall-out deposits from the waning pulses, and (ii) with progressive filling of the canyon/gully, the slope instability was getting less, thereby sandy turbidity currents progressively becoming less energetic. The preservation of sediments deposited from the waning pulses predominantly gives appearance of the turbidites deposited from surge-type flows. The splays as well as the entire depositional loci were back-stepping within the canyon/gully, because (i) the splays in FT-E replaced the bypassing channels system of FT-D, and (ii) more and more distal parts of the splays are outcropped towards the top of the succession as manifested by their overall thinning upward (Fig. 5.6C).

The sizes of these terminal splays must be much smaller within the narrow confinement of the canyon/gully at the shelf-edge compared to that of deep-water frontal splays developed either on unconfined slope and abyssal plain, or along the mouth of canyons in lower slope, or in ponded slope basins. Therefore, although quite similar in terms of sedimentary processes to upper-fan lobes (*sensu* Shanmugam and Moiola, 1988), the origin of frontal splays in canyon/gully-confinement at the shelf-edge should be disambiguated from the origin of other deep-water frontal splays on lower slope and abyssal plain. Rather, *"channelized lobe"* (see Nelson *et al.*, 1983) complexes specifically at/near the shelf-break of Mediterranean Ebro Fan may be more approximate analogs for FT-E splays.

5.2.2.6 FT-F

FT-F comprises mostly delta-front and minor proximal prodeltaic sediments. Although lithologically FT-F is grossly sandstone and sandy heterolithic sediments, their geometry,

sedimentary structures, ichnological characteristics, and facies associations are highly variable and can be categorized into multiple subenvironments of the delta-front and prodelta (Bowman and Johnson, 2014; Dasgupta *et al.*, 2015) (Table 5.1). In spite of that, keeping their remarkable sedimentological and ichnological distinctiveness compared to other canyon/gully-fill facies tracts into consideration, all deltaic sediments outside the canyon/gully have been combined together into FT-F for the purpose of this article. In Outcrops 8B-C, immediately below the southern and the northern walls of incision, FT-F consists of the tabular beds of hummocky-swaley cross-stratified, 0.5 to 20 m thick, multistory to amalgamated medium-grained sandstone and heterolithic beds. Further characterization of all the facies within FT-F laterally away from the canyon/gully incision is beyond the scope of this article (see Dasgupta *et al.*, 2015).

FT-F lithosomes are interpreted to be deposited as wave-influenced barrier bars and wave- and tidally influenced interbar regions (Fig. 5.7A-B). The delta-front subenvironments developed primarily outside the confinement of the canyon/gully (Figs. 5.3, 5.6C). The sandstones are sparsely to highly bioturbated with *Ophiomorpha nodosa*, *Scolicia* isp., large escape trace fossils, *Macaronichnus segregatis*, and *Sinusichnus sinuosus*. The heterolithic sediments separating the sandstone bedforms also display similar trends of river and wave influences, with a minor tidal influence within the inter-bar regions (Dasgupta *et al.*, 2015). The heterolithic sediments contain either no bioturbation or sparse to moderate and sporadic colonization by *Thalassinoides* isp., *Cylindrichnus concentricus*, *Scolicia* isp., *Teichichnus rectus*, *Asterosoma* isp., *Rosselia* isp., *Conichnus conicus*, *Bergaueria* isp., and *Planolites montanus*, as well as small escape trace fossils. Erosional 10s of m wide and 8-9 m deep inlets can be found within the upper part of FT-F deposits (Fig. 5.7C). The steepness of the banks and the aspect ratio of the inlets refer to the steep gradient of the shelf-edge, where wave and tidal action gorged out such topographic furrows as the shelf-edge invaginations.

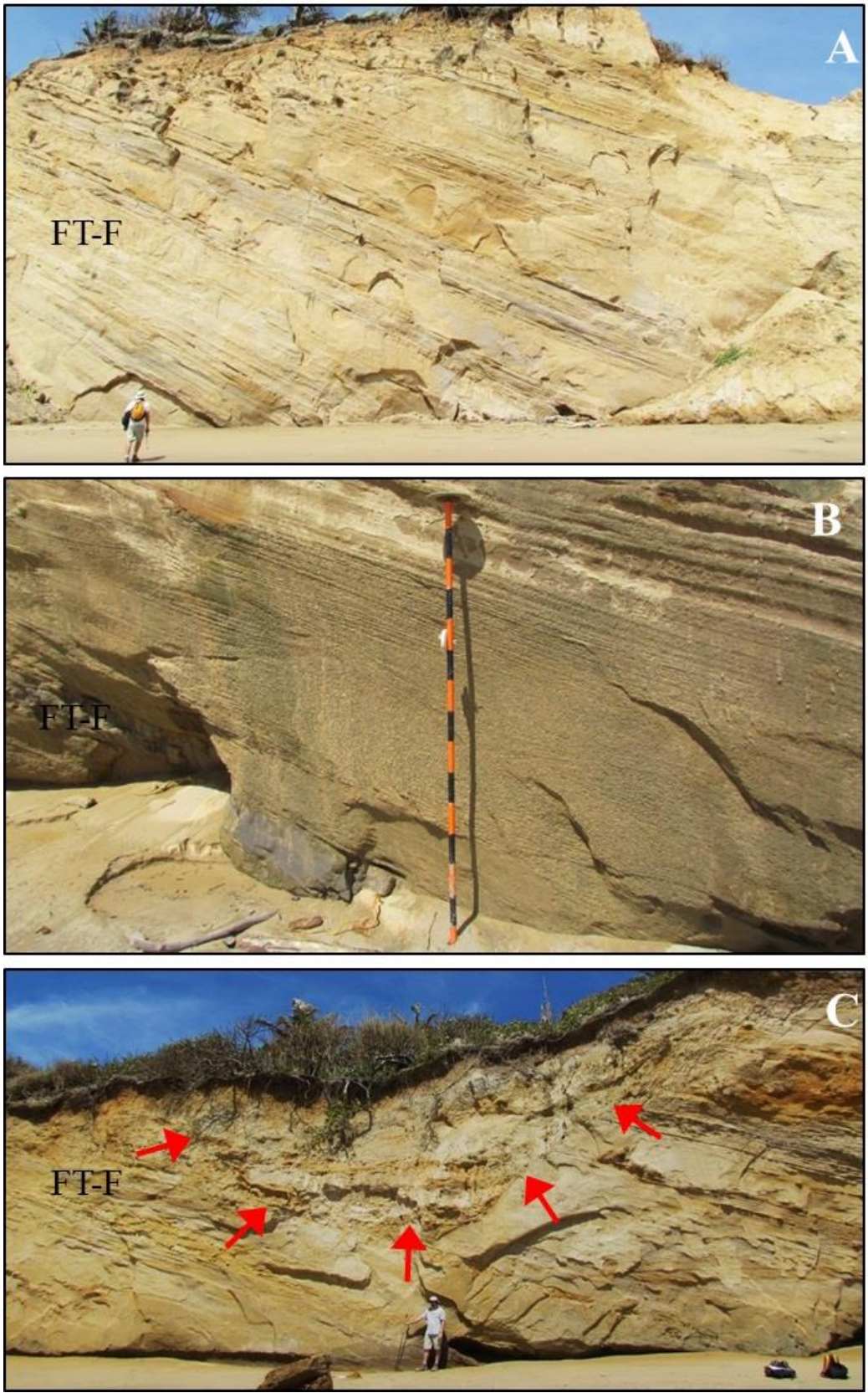

Fig. 5.7. (*N.B.* Figure caption is intentionally moved to the next page due to the large size of the figure)

Fig. 5.7. Photographs of the lithofacies defining the FT-F. (A) Alternate tabular sandstone beds and silty-sandy heterolithic beds defining the barrier-bar complex of the wave-influenced delta-front belonging to FT-F. (B) Close-up of a barrier-bar containing hummocky-swaley cross-stratified sandstone. (C) Inlet or invagination across FT-F. The tidal incision surface is denoted by the red arrows. The invagination is passively filled. There is no lithofacies change above and below the cut surface. The tensional cracks parallel to the cut surface (exposed towards the top right corner of the inlet) manifest steep unstable slope of the invagination.

5.3 Discussion

5.3.1 The Mayaro Formation — advent of accommodation-driven delta-front at the shelf-edge

The NE-ward progradation of the paleo-Orinoco delta-front started in the Early Pliocene from its initial paleo-geographic position ca. 150 km away from the paleo-shelf-edge near the SE coastline of Trinidad (DiCroce *et al.*, 1999; Wood, 2000; Gibson *et al.*, 2012). However, the Quaternary Orinoco delta, being an accommodation-driven system, invariably requires a basinal base-level fall to complete the transit on the shelf and to reach the shelf-edge (Porębski and Steel, 2006). Such a forced regression condition (*sensu* Posamentier *et al.*, 1992; *cf.* Catuneanu, 2006) was provided by the onset of the Pretiglian cold event (or MIS 103) immediately followed by the onset of renewed transpressional uplift of Trinidad resulting in the deposition of the Mayaro Formation, after a pause of transpression tectonics from middle Miocene (ca. 11.4 Ma) until the end of Pliocene (Pindell *et al.*, 1998; Gibson *et al.*, 2012).

The onset of cooling climate (the Northern Hemisphere Glaciation) has been recorded from late Pliocene in higher northern latitudes from different parts of the world. The noticeable effects of truly glacial episode on the equatorial-tropical regions are more conspicuous at the very beginning of Gelasian (*i.e.*, transformation from warm Tiglian to cold Pretiglian climate). Such global low-latitude signatures of this transformation are: (i) the final closure of the Panama Isthmus (Bartoli *et al.*, 2005; Schneider and Schmittner, 2006) and the Great American Biotic Interchange (GABI) (Webb, 2006), (ii) the changes in Asian monsoon (Zhang *et al.*, 2009), and the Pretiglian migration of primates into the previously isolated islands in Southeast Asia across

the exposed Sunda Shelf (Harrison *et al.*, 2006), and (iii) the onset of a long period of strong climatic fluctuations with significant cooling in northern South America (Andriessen *et al.*, 1993; Hooghiemstra and Ran, 1994), where the paleo-Orinoco River had its catchment and delta.

After the regressive transit of the paleo-Orinoco inner-shelf delta all across the subaerially exposed Amacuro shelf, the progradation of the delta continued at/near the outer shelf and shelf-edge. The paleo-Orinoco shelf-edge delta-fronts recurrently developed along the shoulders of growth faults consecutively basinward. The shoulders of the growth faults acted as the newly formed shelf-edges and obviously as the potential sites of rapid sediment accumulation as delta-front, as exposed in FT-F of the Mayaro Formation.

5.3.2 Sequence-stratigraphic order and frequencies of controlling factors

In sequence-stratigraphic hierarchy based on magnitude of base-level changes, the 'order' inversely denotes the hierarchical rank of a sequence-unit and the corresponding episode (*sensu* Vail *et al.*, 1977, 1991; Embry, 1995; Krapez, 1997; Miall, 2010; Catuneanu *et al.*, 2009, 2010; Catuneanu and Zecchin, 2013). Use of cycle duration to assign an 'order' is still debated and is a discretion of the stratigrapher. The entire Mayaro Formation is a 'fourth-order megasequence' deposited during a glacio-eustatic cycle of Milankovitch frequency (Bowman, 2003; Sydow *et al.*, 2003; Bowman and Johnson, 2014). In this article, we have followed the same 'order' for the Mayaro Formation megasequence, just for the sake of assigning a rank without any particular bias towards cycle duration. The Mayaro Formation 'megasequence' is not only estimated to be deposited during a Milankovitch glacio-eustatic period, it also coincides with the anomalously weak orbital forcing of the earth with rather strong marine isotopic response (see below).

However, internal cyclic facies tract variations within the Mayaro Formation (and potentially within analogous subsurface sequences basinward) cannot be explained by further higher-frequency glacio-eustatic fluctuations below the contemporaneous climatic frequency range. This is because the transition between the Tiglian and Pretiglian coincided with prominent, anomalous and systematic variations of 100 ka period cycles in terms of isotopic

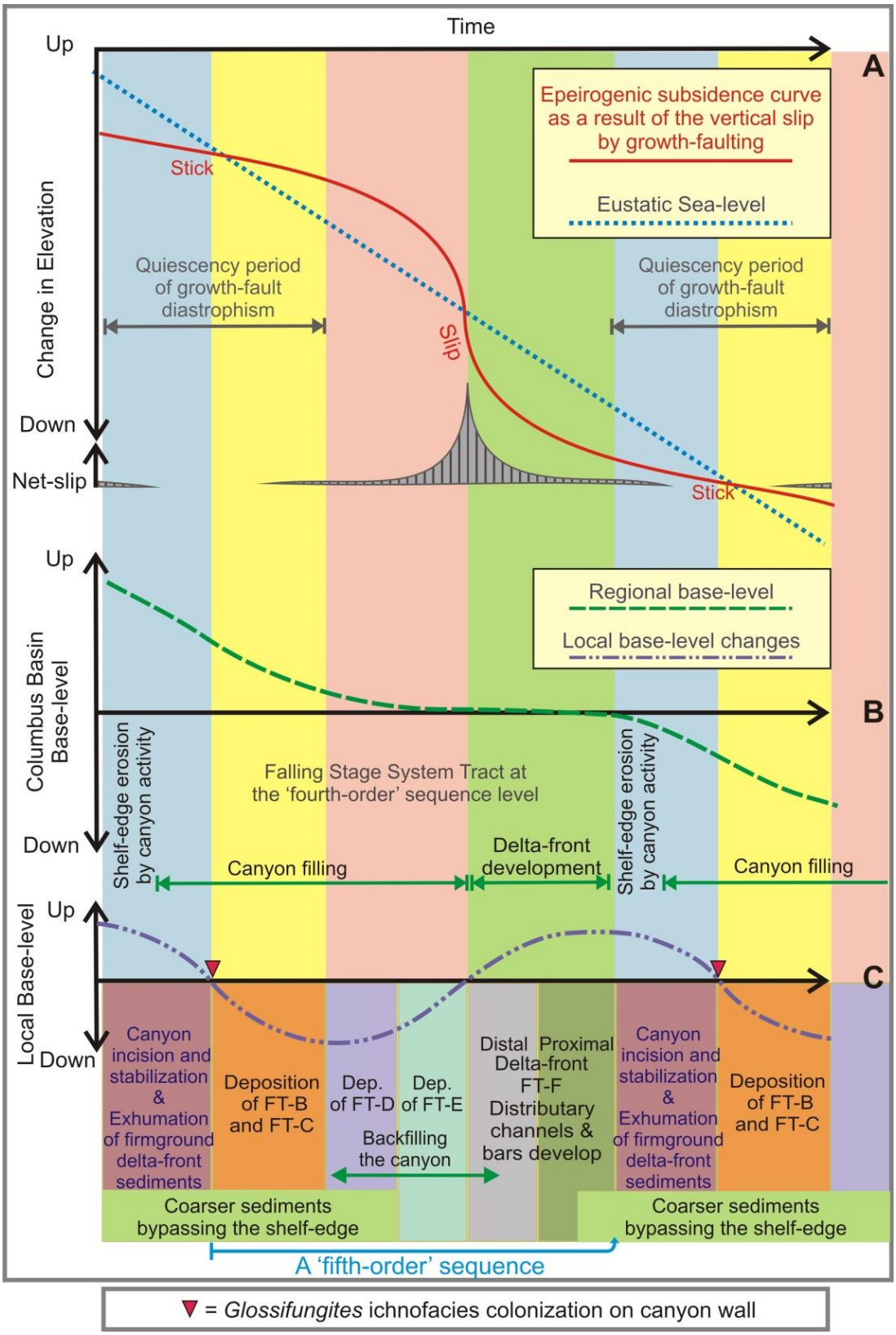

Fig. 5.8. (*N.B.* Figure caption is intentionally moved to the next page due to the large size of the figure)

Fig. 5.8. Schematic representation of the different base levels versus the time curves with respect to the 'sixth-order' physiographic events. (A) The glacio-eustatic sea-level curve and epeirogenic subsidence curve as a result of the vertical slip by the growth fault movements. (B) The regional base-level of the Columbus Basin as a resultant interference of the glacio-eustasy and the growth-tectonics. Shelf-edge incision takes place at every steepening of the curve. (C) The simplified local base-level curve in terms of creation and filling of the accommodation within a canyon/gully at the location of repeated canyonization/gullying activity across the shelf-edge delta-front. The 'sixth-order' facies tracts representing the geomorphic events and defining the 'fifth-order' sequences are depicted in relation to the local base-level curve.

response without much forcing by the earth's orbit (Nie, 2011). In a shelf-edge delta with very high sediment accumulation rate, only the thin-skinned fault-tectonic activity (the slip-stick-slip or the slide-hold-slide phenomenon associated with faulting) has higher frequency than glacio-eustatic cycles. Therefore, fault activity appears to be the only candidate as the controlling factor for effectively explaining the deposition of higher-order (or lower ranking) sequences.

5.3.3 Derivation of growth-tectonics-influenced local base-level curves

Following physical principle of interference of waves in two dimensions, faulting, as a whole, and more frequent growth-faulting in particular, can modulate the regional base-level curve as a resultant curve as shown in Fig. 5.8A-B. Nevertheless, the regional base-level curve has to continue falling to keep the accommodation-driven Orinoco delta static (in relative sense) at the prograding shelf-edge. The falling regional base-level curve, defining the falling stage systems tracts of the 'fourth-order' hierarchy, attains a gentler gradient during the relative active periods (the slip/slide periods) of growth-faulting by relative accommodation-creation by means of subsidence and ductile shale movement away from the older pre-Quaternary sequences below. The relative quiescence periods (the stick/hold periods) of growth-tectonics facilitate steeper fall of regional base level.

For easier visualization of the modified regional base-level at the local scale (*i.e.,* within the canyon/gully crosscutting the delta-front at the shelf-edge), a simplified more-or-less sinuous local base-level curve (Fig. 5.8B-C) can empirically be constructed from the regional base-level curve by slight clock-wise rotation the reference frame. The local base-level curve illustrates alternating absolute accommodation creation and filling cycles within the shelf-edge

invagination (canyon/gully). The slip/slide-phases of the time-axis, however, is supposed to be more constricted in reality than as depicted in Fig. 5.8A-C, as the active phases being faster than stick/hold-phases of stress buildup.

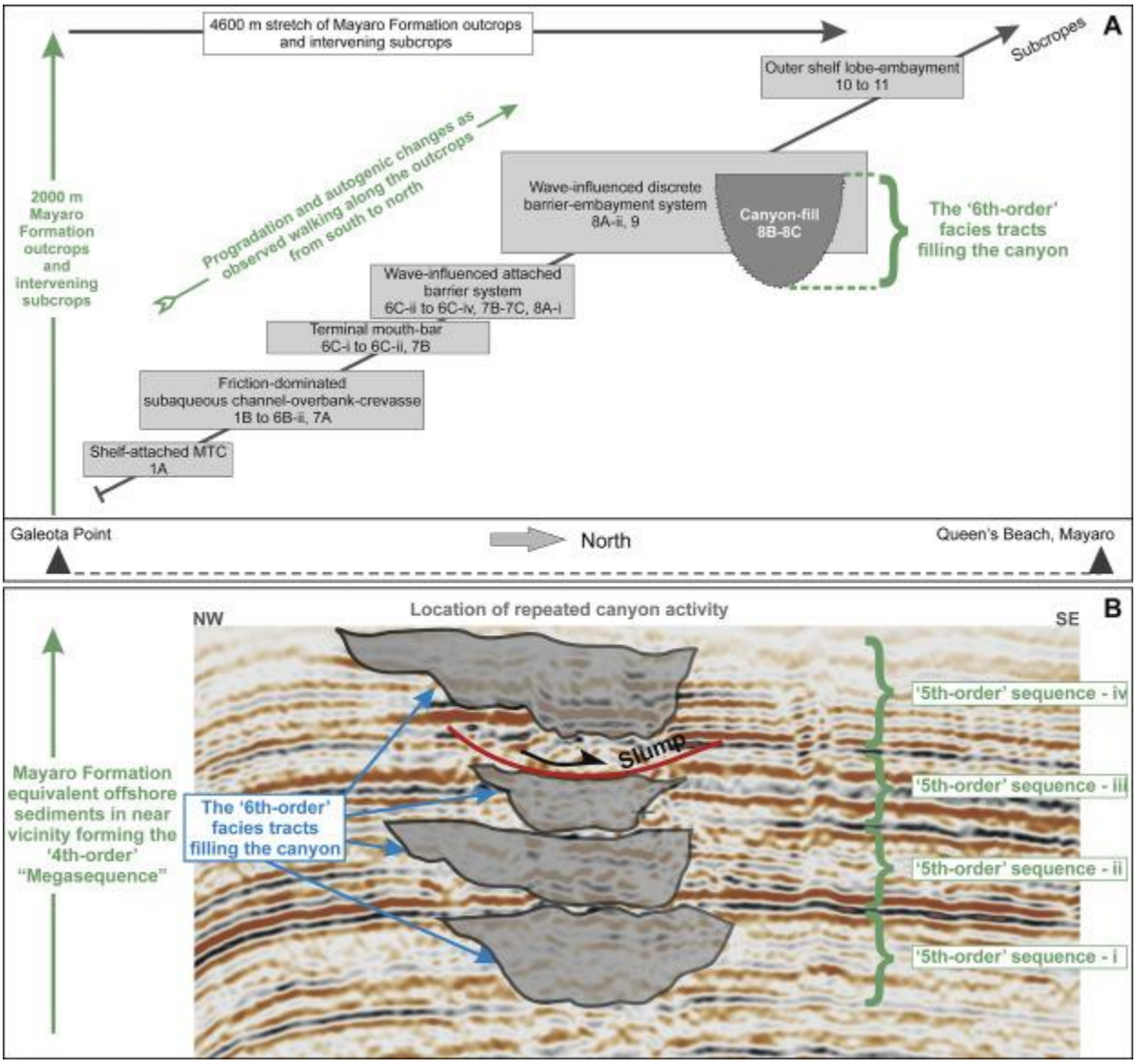

Fig. 5.9. (A) Cartoon showing the lateral and the vertical associations of subenvironments of shelf-edge delta in the Mayaro Formation outcrops and also the relationship of the canyon/gully-filling facies tracts (FT-A to E) with the deltaic facies tract (FT-F), which chiefly belongs to the delta-front subenvironments. (B) Relationships among the 'fourth-' and 'fifth-order' sequences, and 'sixth-order' system tracts in TWT seismic section interpreted from Fig. 5.2D.

5.3.4 Incision and sedimentation cycle in response to local base-level curve

In view of the modified high-frequency local base-level curve, the stacking pattern of facies tracts (Fig. 5.3) in the location of repeated canyon/gully activity across the shelf-edge delta-front can be explained as follows (Figs. 5.8C, 5.9A-B). With basinward advancing delta-front, a shelf margin is increasingly subjected to erosional invagination (Sánchez *et al.*, 2012). Examples of such passively filled large inlets with steep aspect ratio near the shelf-edge are exposed cutting across the late stages of FT-F deposits in the Mayaro Formation (Fig. 5.7C). During the fall of the local base-level (*i.e.*, stick/hold-phase), some of the invaginations and locations of steep slump scars are likely to develop into full-fledged canyons or gullies (as in Outcrops 8B-C in Figs. 5.2B, 5.9A), because the delta-front sediments are subjected to intense erosion and slumping (*e.g.*, 'shelf-edge wedge' development; Gulick *et al.*, 2005; Green *et al.*, 2007) due to the lowered base-level, as well as by direct exposure to large oceanic and storm waves. Depending on the dimension of the invagination, these shelf-edge invaginations can be called a gully or a canyon. No clear threshold value for dimension is defined to differentiate a submarine canyon from a submarine gully. Repeated canyon/gully activity at the same geographic locus (as in Figs. 5.2C-D, 5.9B) is a quite common phenomenon due to the inherent mechanical weaknesses (*e.g.*, differential compaction, faulting resulting from compaction, fluid pressure heterogeneities) within the sediment column. Intensified slope instability due to lowered water column by falling local base-level is another potential cause of shelf-margin collapses. The deltaic sediments of previous 'fourth-order' sequence (*i.e.*, the Gros Morne Formation here) and/or the delta-front sediments of the previous 'fifth-order' cycle (*i.e.*, of the Mayaro Formation here) can both potentially get cannibalized by the intensified erosion at the canyon head and shoulders of the flanks of the incision and are funneled through the canyon/gully by the longshore drift.

Coarser-grained clastic sediments were trapped within the topographic furrow (*i.e.*, the canyon/gully) delivered by both the longshore current and the river mouth system, and are transported onto the deep-water fan system. This is also the time of intensified incision within the canyon/gully by chiefly waxing and bypassing gravity flows until the canyon starts backfilling. The erosional exhumation by the incision must have been sufficient enough to

exhume the previous delta-front cycle as sandy firmground substrate, because experimental observations (*e.g.*, Niemeijer *et al.*, 2009) suggest that, with coarser grain-size, the same volumetric strain (*e.g.*, to acquire firmness of sandy substrate in our case) requires much longer burial history. With progressive stabilization of the canyon/gully-flanks, firmground sands and heterolithic deposits of the previous delta-front cycles were colonized by burrowing crustaceans (*Glossifungites* Ichnofacies; Dasgupta and Buatois, 2012). Sporadic deposition of FT-A contributes to the progressive stabilization of the incision walls.

Thereafter onset of the filling of the canyon/gully marks the growing slip activity and the local base-level inflection. The canyon gets progressively backfilled by FT-B to E, whereby the loci of the sand deposition gradually backsteps along the invagination from the deeper water to the shelf-edge. The firmground burrows were thus filled with mud coming from the deposits immediately above the canyon/gully wall (*i.e.*, from FT-B, FT-C, and FT-D) (Dasgupta and Buatois, 2012). The background sedimentation remained dominated by sustained fine-grained gravity flows originating possibly from the hyperpycnal discharges (Plink-Björklund and Steel, 2004) and/or the baroclinic currents (*i.e.*, internal waves and internal tides) amplified by the topographic heterogeneity provided by the canyon/gully (Shanmugam, 2013).

The delta-front (FT-F) got re-established with an erosional base ensuing further progradation and aggradation above the healed topographic heterogeneity created by the canyon/gully activity. Throughout all the stages of the canyon/gully incision and filling, the FT-A, being related to collapse of any steep slope, kept on getting deposited along the flanks of the invagination (Fig. 5.3). With prograding and aggrading delta-front, superincumbent stress accumulated for the next slip event and shelf-edge invaginations reappeared and got gradually enlarged. Also shelf-edge slump activities became more frequent (Fig. 5.9B). Eventually a new invagination developed at the shelf-edge, preferable at the same geographic location, and the cycle continues.

5.3.5 Application of sequence-stratigraphic order in subsurface analogs of the Mayaro Formation megasequence

A repetitively gullied/canyonized shelf-edge delta system may be viewed as consisting of the high-order sequences (*e.g.,* 'fifth-order' sequences within the 'fourth-order' Mayaro Formation sequence; Fig. 5.9B), where the incision surface, sporadically colonized by the *Glossifungites* Ichnofacies, and its correlative conformity (at least at the scale of seismic data resolution) away from the loci of the recurrent canyon/gully activity would act as the 'sequence boundary'. The sequence boundaries separate the 'fifth-order' sequences and mark the localized base-level fall (Figs. 5.3, 5.9B), in response to the interference pattern between the regional/basinal base-level and growth-faulting related subsidence curves (Fig. 5.8C).

At a location of repeated canyon/gully activity, as exhibited by the immediate offshore subcrop equivalent of the Mayaro Formation outcrops (Figs. 5.2D, 5.9B), the 'sixth-order' cycle is likely repeat itself within successive invaginations, provided the younger incision has not omitted the upper facies tracts of the older cycle. The high-frequency heterogeneity within the deep-water sandy architectural elements or the 'reservoir element heterogeneity', as exemplified within the deep-water hydrocarbon reservoirs in Columbus Basin, is likely the result of such high-frequency switching-on and -off of the sand delivery from the shelf-edge delta-front.

Instead of fitting the facies tracts into the systems-tract model corresponding to the basinal/regional base-level changes, the present model envisages their occurrences within a 'fifth-order' sequence as a cycle, because the 'sixth-order' facies tracts variations within the 'fifth-order' sequence are more gradual quasi-autogenic changes (*i.e.,* gradual back-stepping by filling and healing the canyon/gully at shelf-edge) influenced by the local base-level variations than the more contrasting allocyclic systems-tract level changes. Rather, the model tries to explain them according to the physiographic evolution of the canyon(s)/gully(ies) across a shelf-edge delta-front in relation to the interplay between glacio-eustasy and fault tectonics in both regional/basinal and local contexts. Our model provides a cautionary note on the uncritical application of purely glacio-eustatic mechanisms as the drivers of the high-frequency stratal architecture.

5.4 Conclusions

1. Within a recurrently invaginated/canyonized shelf-edge delta-front megasequence of 'fourth-order' hierarchy, the internal 'sixth-order' facies tracts variations constitute together into 'fifth-order' level cyclicity in response to high-frequency fluctuations of the local base-level.

2. The local base-level fluctuations can be influenced by the interaction between a steadily falling eustatic sea-level within a climatic cycle of Milankovitch frequency and episodic activity of growth-faulting.

3. The sequence-stratigraphic model proposed for canyon/gully-fills in relation to the shelf-edge delta deposits within the Mayaro Formation and equivalent sediments in offshore vicinity can be an analog model for recurrently canyonized delta-front of a shelf-edge delta in a growth-fault dominated basinal setting.

4. With a delivery mechanism from a recurrently canyonized/invaginated shelf-edge delta, the very high-frequency heterogeneities at the reservoir-scale up to the individual architectural element level in deep-water depositional system (*i.e.,* at the middle to lower slope and on the ultra-deep marine basin floor) may be related to the depositional cycles associated with the canyon/gully activity across the delta-front as a switching on-and-off mechanism for the delivery of coarse clastic sediments. The cycles should have higher frequency than Milankovich cycles corresponding to the repeated growth-faulting.

5.5 Acknowledgments

The authors deeply acknowledge the initiatives and ingenuities of Carlos Zavala and the continuous support from Livan Blanco Valiente, Rafael Vela, Yrma Vallez, Anderson Arjoon, Jivanti Ramdular, Jose Luis Huedo Cuesta and the entire subsurface group of Repsol E&P T&T Limited. Vital assistances by Marlon Bruce and Balázs Törő are highly appreciated. We thank Ron Steel, Andrea Fildani and three anonymous reviewers for their valuable comments,

suggestions, and critical observations. Logistic and onsite support and assistance from Dinelle Medina, Ann Marie Singh, Michael, Ragoo and health and safety department of Repsol, are highly appreciated. Additional financial support was provided by an NSERC Discovery Grant to Buatois. The AAPG Foundation Merrill W. Haas Memorial Grant, the Saskatchewan Innovation and Opportunity Award from the Provincial Government of Saskatchewan and University of Saskatchewan, and the Dr. Rui Feng Graduate Studies Award to Dasgupta have proven to be vital of the study. The authors are thankful to M. Gabriela Mángano, Dennis Meloche, Alec Aitken, Juan Jose Ponce, Noelia Carmona, Luis Quiroz, Pablo Alonso, Andreas Wetzel, Renata Netto, and Sidhartha Sinharay for meaningful discussions and encouragement.

CHAPTER 6: ICHNOLOGY OF A LATE PLIOCENE HYPERPYCNAL SYSTEM, MORNE L'ENFER FORMATION, FULLARTON, TRINIDAD: IMPLICATIONS FOR RECOGNITION OF AUTOGENIC EROSIONAL SURFACE AND DELINEATION OF STRESS FACTORS ON IRREGULAR ECHINOIDS

Dasgupta, S., Buatois, L.A., Zavala, C., Mángano, M.G., and Törő, B., in review, Ichnology of a late Pliocene hyperpycnal system, Morne L'Enfer Formation, Fullarton, Trinidad: Implications for recognition of autogenic erosional surface and delineation of stress factors on irregular echinoids: *Palaeogeography, Palaeoclimatology, Palaeoecology*.

Keywords: Autogenic, trace fossil, paleo-Orinoco, hyperpycnal-hypopycnal, irregular sea-urchin, marine erosion.

Abstract

The Morne L'Enfer Formation outcrops near Fullarton, Trinidad, expose an erosional discontinuity between shelf deposits below and prograding clastic wedge of the late Pliocene paleo-Orinoco system above. The surface exhibits the similarities as well as dissimilarities with examples of Regressive Surface of Marine Erosion (RSME) in wave-influenced shelf settings and also with the estuarine valley base incision surfaces. However, detailed ichnological studies reveal that the discontinuity surface is a subaqueous, autogenically controlled, erosional surface on a shelf dominated by the hyperpycnal (and potentially hypopycnal) discharges with transient but gradually increasing wave influence. Integration of ichnological and sedimentological characteristics also suggests a complicated interrelationship among different stress factors affecting the infaunal colonizers, especially the irregular echinoids, in different subenvironments of the setting. The study underscores: (1) the importance of the subaqueous progradation of delta through autogenically establishing its lobe on the open shelf accommodation without stratigraphically significant erosional removal of sediments in contrast to to the common regressive delta-front models, and (2) in a subaqueously prograding clastic wedge, fluvial influence pertains high stress conditions not only for the adult endobethos, but also explicably

for their larvae within the water column, especially in and near the subaqueous distributary channels.

6.1 Introduction

Identification and characterization of erosional discontinuity surfaces is essential for sequence-stratigraphic analysis in evaluating basin evolution (see *Chapter 4* in Catuneanu, 2006; *Chapter 12* in Buatois and Mángano, 2011; MacEachern *et al.*, 2012). Trace fossil are often one of the most important diagnostic information in recognizing an erosional discontinuity surface (MacEachern *et al.*, 1992, 2012; Pemberton *et al.*, 2001; Buatois and Mángano, 2011) and often in distinguishing it from an apparent tectonic contact (*e.g.*, Dasgupta and Buatois, 2012, 2015). Where shallow-marine sediments overlie deeper-water deposits along a sharp/erosional surface, the surface can have two sequence-stratigraphic scenarios unless the change-over is completely autogenic:

The first scenario takes place during a forced regression phenomenon (*i.e.*, relative sea-level fall irrespective of sediment supply). The pre-existing sediments deposited in a relatively deeper marine setting get eroded and occasionally incised and then the shallower-water marine sediments are deposited on top of the erosional surface. Such a surface is called Regressive Surface of Marine Erosion (RSME) or Regressive Wave Ravinement Surface in wave-dominated shelf settings (Plint, 1988, 1991; Plint and Nummedal, 2000; Galloway, 2001, 2004). The erosion is commonly attributed to the zone or locus of wave action along the depositional strike with the locus of erosion moving basinward. In this scenario, the surface is characterized by the abrupt occurrence of proximal trace-fossil assemblages, which contrastingly overlie the more distal assemblage across the surface (Pemberton and MacEachern, 1995). As a result, the extensively bioturbated muddy sediments deposited on the shelf in relatively deeper-water settings (*e.g.*, offshore/offshore-transition and/or distal prodelta and/or open shelf) containing either typical *Cruziana* to *Zoophycos* Ichnofacies, are sharply overlain across the surface by the coarser-grained sediments deposited at the shoreface and/or delta-front and/or proximal prodelta belonging to either the *Skolithos* Ichnofacies or proximal *Cruziana* Ichnofacies. The exhumation of a semi-consolidated firmground substrate results in preservation of the *Glossifungites*

Ichnofacies suite at the surface (MacEachern *et al.*, 1992; Pemberton *et al.*, 1992; Chaplin, 1996; Buatois *et al.*, 2002).

In the second scenario, commonly associated with the incised valleys, a fluvially cut subaerial unconformity is modified during the ensuing transgression and a 'coplanar surface of Lowstand and Transgressive Erosion' is generated (Zaitlin *et al.*, 1994; Pemberton *et al.*, 1992; MacEachern and Pembberton, 1994; Buatois and Mángano, 2011). Initially during a relative sea-level fall, valleys are incised on the shelf, which are then filled with the fluvial sediments during the late falling stage. Through the subsequent transgressive phase, estuaries develop within these valley; the older fluvial deposits are commonly not preserved. Because the incision surfaces exhume semiconsolidated (firm) or consolidated (rocky) older marine sediments, either suites of the *Glossifungites* Ichnofacies or the *Trypanites* Ichnofacies are emplaced during the marine transgression depending upon the substrate rheology at the incision surface (Pemberton *et al.*, 1992; MacEachern *et al.*, 1992; Gibert and Martinell, 1992, 1993, 1996; Martinell and Doménech, 1995; MacEachern and Pemberton, 1994; Uchman *et al.*, 2002; Carmona *et al.*, 2006, 2007).

Morne L'Enfer Formation (MLF) outcrops near Fullarton in SW Trinidad expose an erosional surface that has apparent similarities with both the above scenarios. Here a pervasively bioturbated muddy sedimentary unit, which was deposited in a shelf setting and belonging to the distal *Cruziana* Ichnofacies, has a sharply eroded and intermittently incised top surface. The overlying unit consists of a thick coarsening-up interval of sediments deposited as the wave-modified swaley-hummocky cross-stratified (SCS-HCS) sandstones and also laterally accreting incised channel-fill sandstones and conglomerates and overbank deposits consisting of sandstone and heterolithic lithology. Trace fossil characteristics suggests a much higher energy condition and elevated stress factors arising from the increased influence of fluvial discharge. Therefore, although the succession is a candidate for the two sequence-stratigraphic scenarios described above, there are also differences that distinguish the erosional surface from both an RSME or an incised valley, which are known to be scoured either by wave-action or by fluvial erosion during relative sea-level fall. Therefore, the erosional surface requires scrutiny through integration of depositional and ichnological variations across the contact. The aims of this paper are to: (1) to

determine the depositional settings in which the infaunal colonizers either thrived or struggled to survive, (2) to postulate the causes behind the distribution of trace fossils produced by irregular sea-urchins (Spatangoida), and (3) to evaluate the sequence-stratigraphic signature of the erosional surface. The article also briefly discusses the varying degrees of influence of the stress factors arising from the processes (*e.g.*, spatial and temporal variations of salinity, turbidity, and nutrients caused by hyperpycnal and hypopycnal discharges, wave action and longshore current) on the sea-urchin ethology and trophic behaviour though its life cycle.

6.2 Geologic setting

The Southern Basin in southern Trinidad along with the neighbouring Columbus Basin in the eastern offshore evolved as a large and structurally complex depocenter filled with the Neogene-Pleistocene clastic sediments delivered by the paleo-Orinoco River (Di Croce *et al.*, 1999; Wood, 2000; Garciacaro *et al.*, 2011a). Prograding sand-dominated clastic wedges over the Neogene muddy paleo-shelf are known to host prolific petroleum reservoirs in the Southern Basin. The tectonic-stratigraphic evolution of the Southern Basin, its depositional settings, and the structural geology have extensively been documented in the literature (*e.g.*, Kugler, 1956, 2001; Saunders and Kennedy, 1965; Donovan and Jackson, 1994; Dunham *et al.*, 1996; Algar, 1998; Pindell *et al.*, 1998; Babb and Mann, 1999; DiCroce *et al.*, 1999; Wood, 2000; Bowman, 2003; Osman, 2006; Winter, 2006; Pindell and Kennan, 2009; Garciacaro *et al.*, 2011a, 2011b; Gibson *et al.*, 2012; Bowman and Johnson, 2014; Chen *et al.*, 2014). The Southern Basin initially developed as a transpressional foreland basin since the late Oligocene in response to the oblique convergence between the Caribbean and South American Plates along the Serranía del Interior-Central Range system, thereby creating the NEE-SWW trending anticlines. A thin-skinned pull-apart stage followed during the Pliocene along with the extensional growth faulting phenomena due to the rapid sedimentation from the paleo-Orinoco delta-estuarine system. Because the paleo-shelf-margin defined by the earliest basin-bounding growth faults in the adjacent Columbus Basin was far eastward (*Fig. 12* in Bowman and Johnson, 2014; Fig. 4.2A) during Pliocene, the study area therefore was on the continental shelf.

With the paleo-Orinoco rivermouth prograding eastward towards the shelf-break, four grossly regressive cycles of sedimentation took place, which were preceded and followed by transgressive intervals and shelf-wide flooding (Fig. 6.1). Therefore, there were four phases of sedimentation of the delta-estuarine sand-dominated clastic wedges, which were deposited by paleo-Orinoco River system developed across the shelf with overall transit of the system towards north and east during the late Miocene to late Pliocene (Fig. 6.1A-B) (Kugler, 1956, 2001; Saunders and Kennedy, 1965; Donovan and Jackson, 1994; Wach *et al.*, 2003; Vincent *et al.*, 2007; Vincent, 2008; Wach and Vincent, 2008; Osman, 2006; Winter, 2006; Steel *et al.*, 2007; Chen *et al.*, 2014: Bowman and Johnson, 2014). These phases are separated by the three flooding episodes and corresponding transgressive deposits, namely the Lower Forest Clay, the Upper Forest Clay, and the Lot 7 Silt members. The third and fourth phases of clastic wedge deposition were first described together as the MLF possibly by Macready (1921) from the Pitch Lake-Point Fortin-Morne l'Enfer area. Later, Kugler (1956, 1959) delineated the constituent members within it, viz. from bottom to top: the Upper Forest Clay Member (UFCM), the Morne L'Enfer Silt (MLS), the Lower Morne L'Enfer Member (LMLM), the Lot 7 Silt (L7S), and the Upper Morne L'Enfer Member (UMLM) (Figs. 6.1A-B, 6.2A). Therefore, apart from the basinal flooding related deposits of the UFCM, the L7SM, and the L7S, all the other members of the MLF were deposited during the dominantly regressive or deltaic and the minor retrogradational or estuarine cycles across the shelf (Chen *et al.*, 2014).

6.3 Sedimentological and ichnological observations at the Fullarton section

The Fullarton section is exposed along the ca. 2000 m shoreline of the western end of Cedros Bay (part of the Gulf of Paria) at Fullarton (Fig. 6.2A-B). The section has been poorly studied (except in unpublished proprietary field guidebooks and in the older literature; *e.g.*, Kugler, 1959; Saunders, 1997) and comprises the westernmost outcrops of the MLF in Trinidad. The outcrop exposes deposits of the MLS and the LMLM. In Fig. 6.2B, the outcrop is marked with the several reference points (see Table 6.1). Between the terminal reference points FL01 and FL15, outcrops are disrupted into three fault-blocks by the two steep, westerly dipping, NNE-trending, normal faults. The outcrop is subparallel to the strike of the erosional contact between the lower and upper units (*i.e.*, FT-L and FT-U; see below). Hence, the contact has

repeatedly been exposed along the outcrop traverse (almost continuously between reference points FL04 and FL08, and locally at FL14).

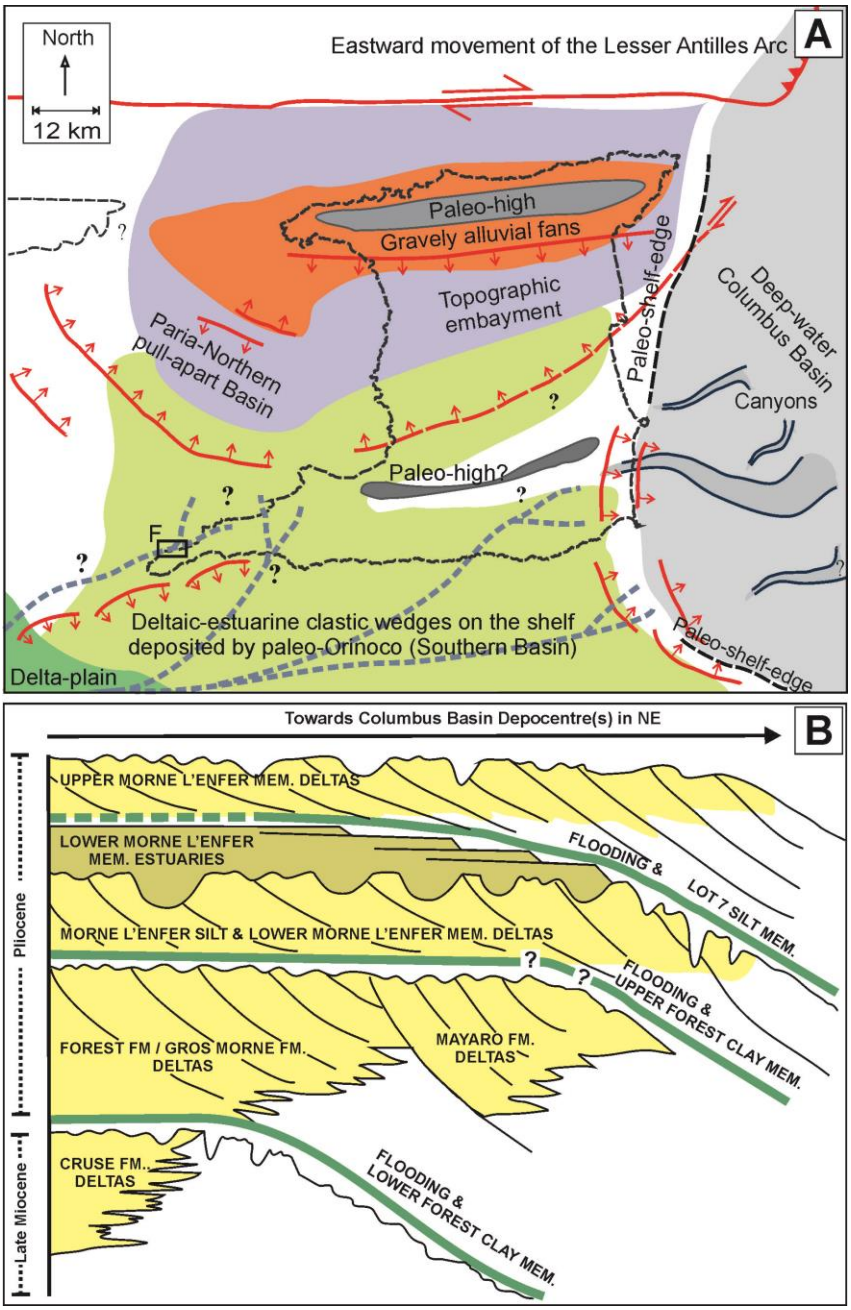

Fig. 6.1. (*N.B.* Figure caption is intentionally moved to the next page due to the large size of the figure and the length of the caption)

Fig. 6.1. Paleogeography and stratigraphy of the late Miocene – Pliocene in the Southern Basin. (A) Pliocene paleogeography of Trinidad and the paleo-Orinoco system (after Bowman and Johnson, 2014; Dasgupta and Buatois, 2015). The rectangle F demarcates the Fullarton area. (B) Schematic diagram displaying stratigraphy of the paleo-Orinoco clastic wedges in Southern Basin, Trinidad (after Steel *et al.*, 2007; Marcano and Pinto, 2009). (*N.B.* The age of Mayaro Formation shown here has never been confirmed by any biostratigraphic data available in public domain. As explained in Chapter 3, the age is assumed to be Gelasian after Bowman (2003), which is relatively younger than late Pliocene Morne L'Enfer Formation.)

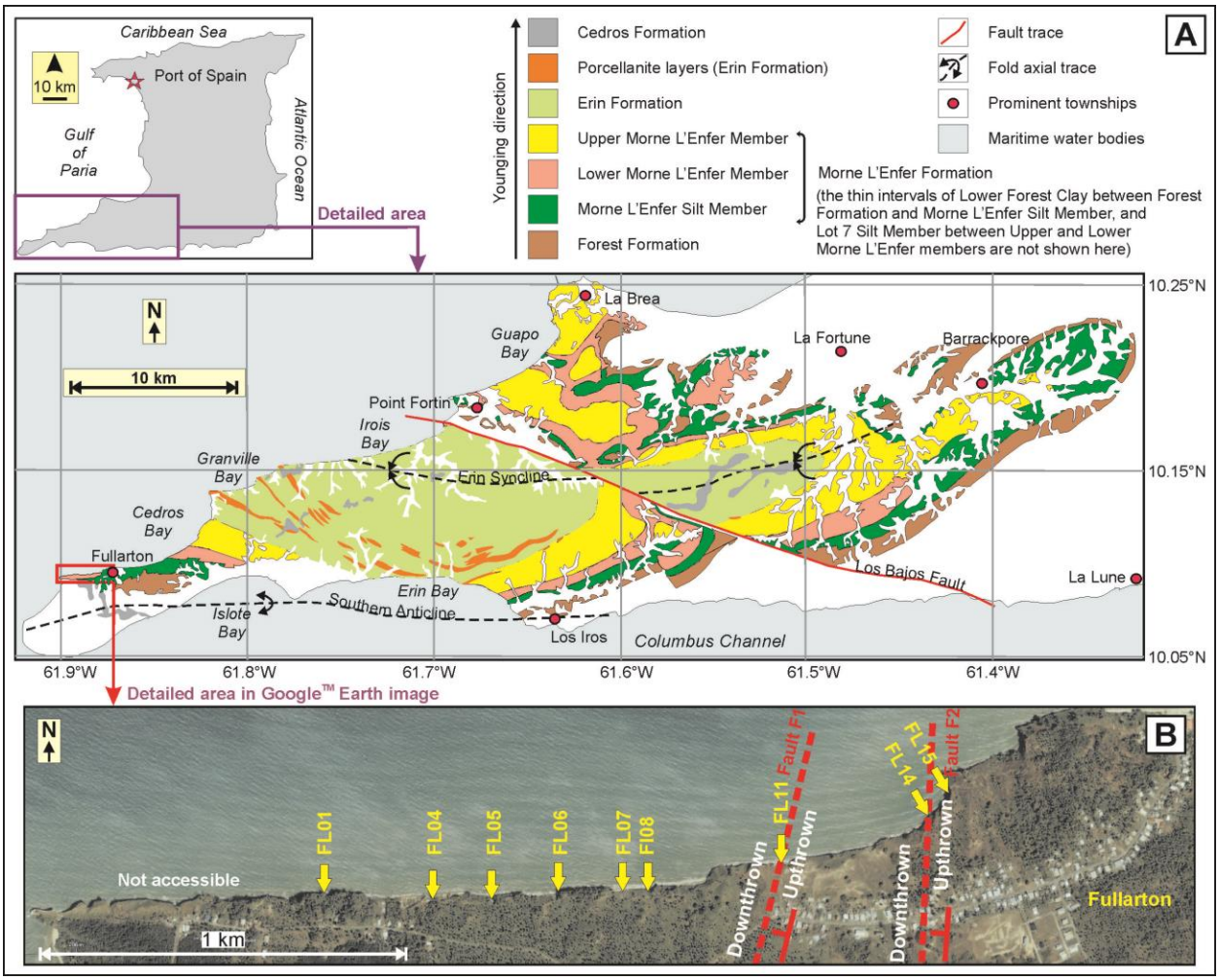

Fig. 6.2. Geological and outcrop maps. (A) Pliocene-Pleistocene geological map of southeast Trinidad (after Kugler, 1959; Saunders, 1997). The inset map of Trinidad shows the areal extent of the geological map. The red rectangle is enlarged in Fig. 6.2B. (B) Google Earth™ image showing reference points (see Table 6.1) on the outcrop section in Fullarton area. The dashed red lines demonstrate the approximate orientation of fault traces.

Table 6.1. Locations of the outcrop reference points in western Cedros Bay section of the Morne L'Enfer Formation, Fullarton, Trinidad.

Ref. Pt.	Latitude	Longitude
FL01	10°05.300′ N	61°54.093′ W
FL04	10°05.290′ N	61°53.935′ W
FL05	10°05.291′ N	61°53.841′ W
FL06	10°05.305′ N	61°53.735′ W
FL07	10°05.311′ N	61°53.636′ W
FL08	10°05.306′ N	61°53.600′ W
FL11	10°05.345′ N	61°53.399′ W
FL14	10°05.415′ N	61°53.164′ W
FL15	10°05.444′ N	61°53.141′ W

While categorizing the MLS and LMLM into a sequence stratigraphic framework, Wach *et al.* (2003), Osman (2006), and Chen *et al.* (2014) have adopted the scheme of categorizing (i) both siltstone-dominated shelfal and prodeltaic deposits and sandy delta-front deposits as the MLS and (ii) the tidally dominated overlying estuarine deposits (not exposed at the Fullarton section) as the LMLM. This establishes the incongruity between (a) lithostratigraphic model with defined boundaries among members as previously delineated by Kugler (1956, 1959) and (b) the more realistic process-sedimentological and sequence-stratigraphic interpretations in the recent studies. Completely circumventing the lithostratigraphic definitions of individual members, we studied the continuous erosional surface between two separate sedimentary units. Fig. 6.3 shows a schematic stratigraphic section of the western fault-block. In Fig. 6.4A-D, the erosional surface is marked by the red dashed curves between the lower (FT-L) and the upper (FT-U) units, which are discussed below.

6.3.1 Unit FT-L (or facies FT-L)

This lower unit (*i.e.*, facies FT-L) comprises thick, monotonous, massive-appearing, and detrital mica- and plant material-bearing siltstone with intermittent thinly laminated sparse very fine-grained sandstone beds. Sheeting or decompaction joints at a regular 2-5 cm intervals are common in the FT-L (Fig. 6.5A). Also the massive appearance is attained by complete bioturbation, thereby mostly obscuring the sedimentary structures and the sharpness of the interfaces of the siltstone with the sparse sandy intervals (Fig. 6.5A-B, D-E, G-I). The surface at

the top of the FT-L is the erosional discontinuity, which is flat, sharp, and intermittently incised by channels (Figs. 6.3, 6.4D). The flat parts of the contact are sparsely wave-rippled (Fig. 6.5C).

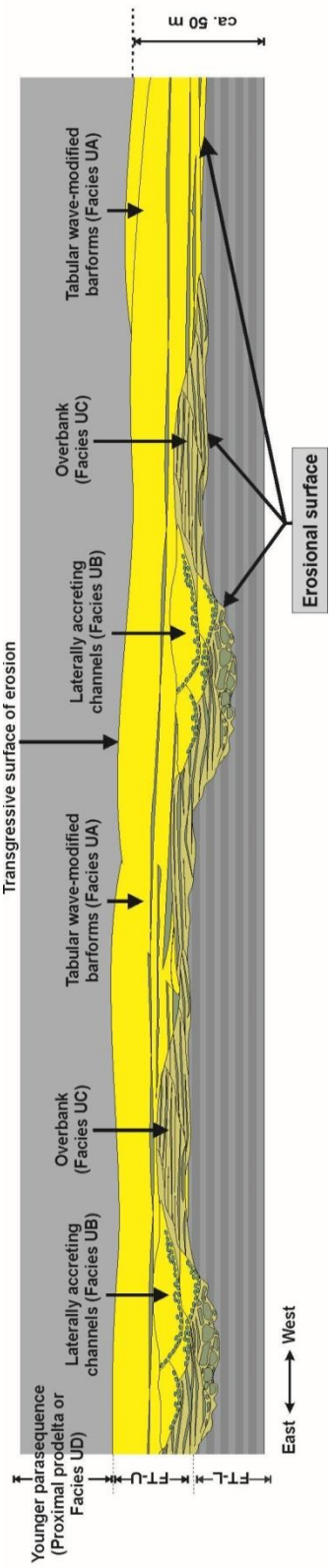

Fig. 6.3. Schematic stratigraphic cross section of the MLF in the westernmost fault block of the Fullarton section (between reference points FL01 and FL08). The FT-L is the lower monotonous siltstone unit deposited on the open shelf condition, whereas the upper FT-U unit consisting of sandstone and sandy heterolithic lithosomes show lateral facies variations (*i.e.,* facies UA, UB, and UC; see text). The scale is approximated and arbitrarily vertically exaggerated for representational purpose of showing all the depositional elements of the FT-U together. The FT-U is eroded on top by a transgressive surface of erosion and is overlain by the younger parasequence.

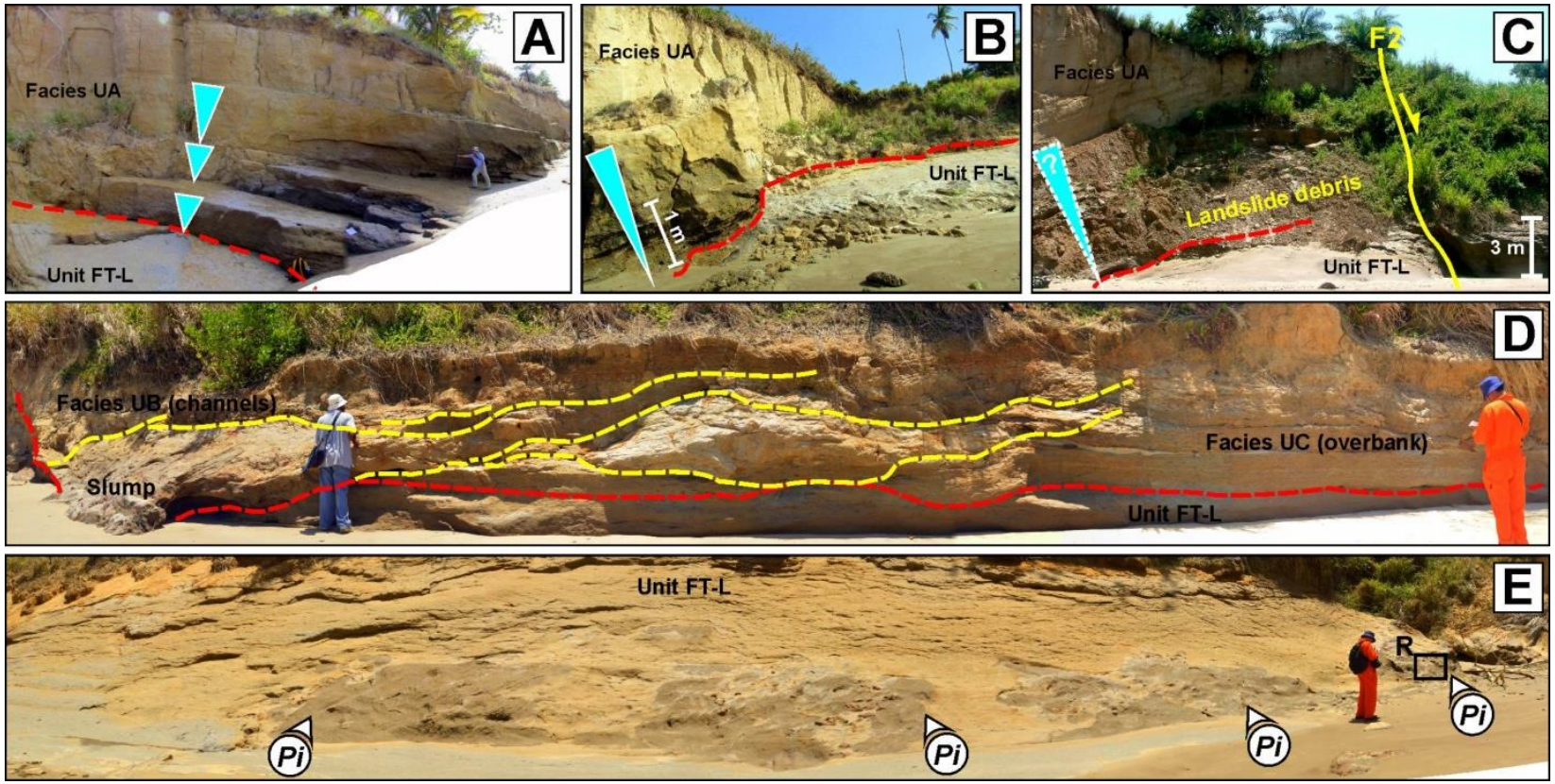

Fig. 6.4. Photographs showing five different locations from the exposures of the FT-L and the contact between the FT-L (underlying) and the FT-U (overlying), which is marked with the dashed red curves. The light blue triangles indicate coarsening- and thickening-upward trend in Fig. 6.4A-C. (A) (B) (C) The FT-L overlain by the facies tract UA in at reference points FL05, FL06, and FL14. (D) East-West section near reference point FT07 showing laterally accreting channel and overbank system above the contact. The channel thalweg shows the slumped materials. The overbank is sand-silt mixed heterolithic deposit. (E) East-West section of the FT-L siltstone with *Piscichnus* isp. blobs between FL05 and FL06. Rectangle R is enlarged in Fig. 6.5F. [*N.B.* Acronym used: *Pi* = *Piscichnus* isp.]

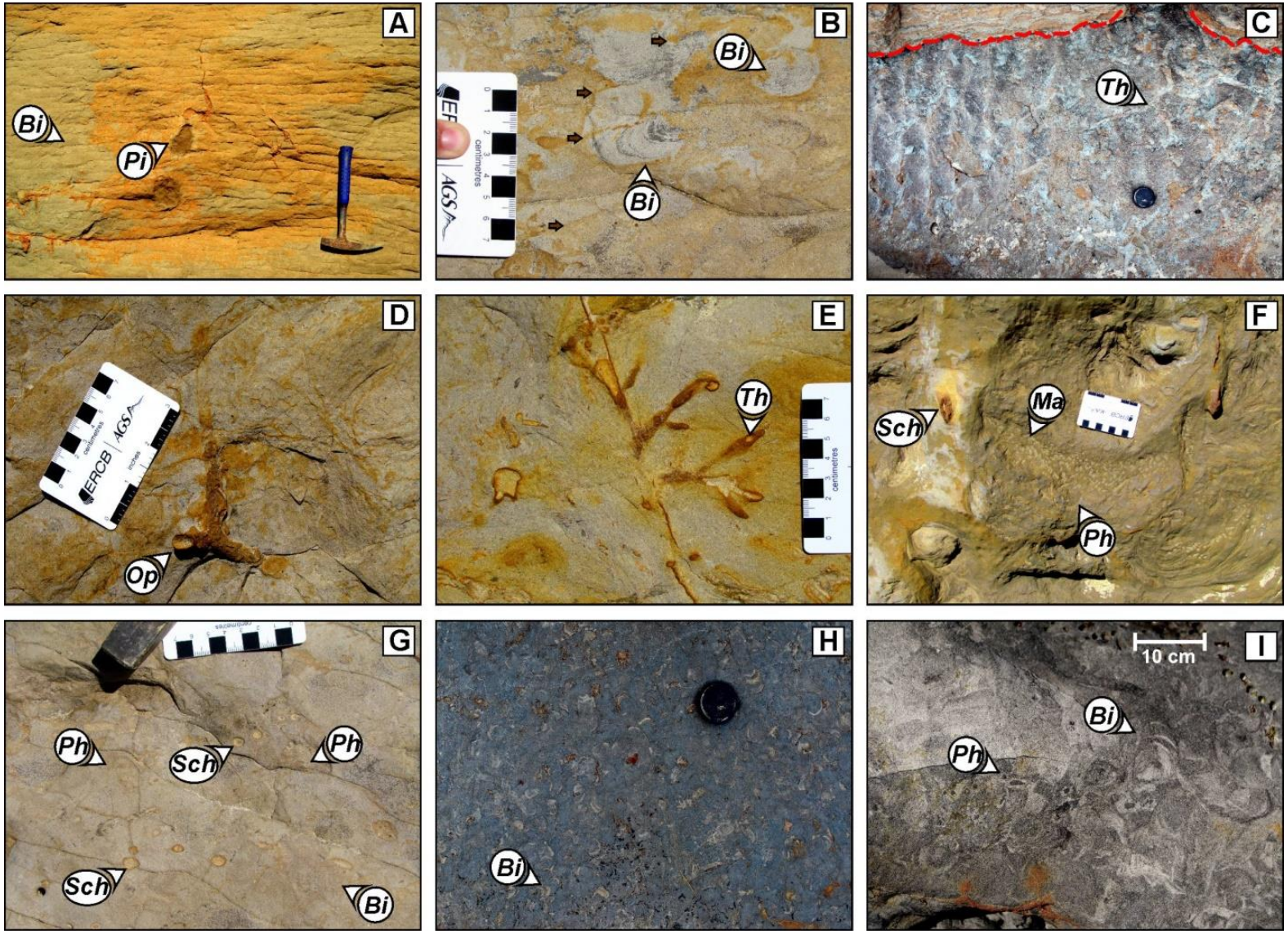

Fig. 6.5. (*N.B.* Figure caption is intentionally moved to the next page due to the large size of the figure and the length of the caption)

Fig. 6.5. Characteristic ichnological features of the unit FT-L. The siltstones are completely bioturbated (BI = 6), with multiple episodes of colonization, especially within organic-rich zones, although the liquefaction blobs are selectively and highly colonized (BI = 4). (A) Sectional view of the siltstone with complete *Bichordites* isp. colonization and small *Piscichnus* isp. blobs. The location is between reference points FL05 and FL06. Decompaction joint surfaces at regular intervals sub-parallel to bedding are conspicuous. Post-depositional mobilization of sediments through fractures following along and cutting across the decompaction joints and propagating away from the blobs are also visible. (B) Complete bioturbation by *Bichordites* isp. in the organic detritus-bearing siltstone pertaining massive appearance. The location is at the reference point FL05. Primary sedimentary features are obscured and only the decompaction joints are visible (shown by small arrows). (C) Wave-rippled top of the FT-L, with softground *Thalassinoides* isp. The location is between reference points FL07 and FL08. The dashed red curve marks the contact between the FT-L and FT-U, the latter being defined by thin-bedded heterolithic sediments belonging to the facies tract UC. (D) (E) Complete, possibly multi-episodes of colonization of the disseminated organic-rich portions of the siltstone, thereby obliterating primary sedimentary features as well as obscuring any identifiable softground trace fossils. The deep-tier *Ophiomorpha nodosa* and *Thalassinoides* isp. are sparse and localized (at reference point FL05). (F) High bioturbation within *Piscichnus* isp. blob (BI = 4). The view is zoomed from rectangle R in Fig. 6.4E. Muddy portions of substrate are colonized primarily by *Phycosiphon incertum* and later by deep-tier *Schaubcylindrichnus* isp. (located near FL07). Patches of intense churning and homogenization are also visible. The rare isolated fine-grained sandy patches are trapped intermittently and are colonized by softground *Macaronichnus* isp. (G) Siltstone completely homogenized by bioturbation and with localized patches of secondary *Phycosiphon incertum* and *Schaubcylindrichnus* isp. (H) (I) Bedding surface view of relatively sandier layers within the siltstone, completely colonized by *Bichordites* isp, with localized patches of *Phycosiphon* incertum colonization (located near FL06). [*N.B.* Acronyms used: *Bi = Bichordites* isp., *Th = Thalassinoides* isp., *Ma = Macaronichnus* isp., *Sch = Schaubcylindrichnus* isp., and *Ph = Phycosiphon incertum.*]

FT-L deposits are completely bioturbated (Bioturbation Index, BI = 6, *sensu* Taylor and Goldring, 1993), mostly by the shallow-tier deposit-feeding spatangoid trace fossils assigned to *Bichordites* isp. (Fig. 6.5A-B, G-I). Disseminated and intermittent patches rich in plant-detrital materials are colonized by the middle tier softground burrows produced by deposit-feeders, *e.g.*, *Schaubcylindrichnus* isp. and *Phycosiphon incertum* (Fig. 6.5F-G, I), and galleries of decapod crustaceans (softground *Thalassinoides* isp. and *Ophiomorpha nodosa*) (Fig. 6.5C-E). The *Thalassinoides* isp. is lined. Both *Thalassinoides* isp. and *O. nodosa* are filled with the siltstone and very fine-grained sandstone, which are similar to the surrounding sediments. No evidence of any firmground suite of trace fossils has been found at the top of the FT-L. This reflects: (1) sedimentation continued before the prograding advancement of the FT-U sediments, (2) the erosional removal of sediments at the top of FT-L was not sufficient enough to exhume silty firmground. Integration of the above sedimentological and ichnological observations suggests

that the sediments were deposited and colonized on an open marine shelf associated with sustained sedimentation of chiefly silt and limited very fine-grained sand, illustrating the distal *Cruziana* Ichnofacies (for subdivisions of the *Cruziana* Ichnofacies, see MacEachern *et al.*, 1999, 2007a).

The FT-L also contains the relatively less bioturbated, sparsely distributed, variably sized (from a decimeter to more than a meter in diameter), and irregular but equant blob-shaped foraging trace fossils, called *Piscichnus* isp. (Gregory, 1991; Schreer *et al.*, 1997; Kotake and Nara, 2002; Kotake, 2007; Gingras *et al.*, 2007; Löwemark, 2015), created by vertebrates (Figs. 6.4E, 6.5A). These predation trace fossils have sharp but irregular boundaries and signature of internal liquefaction. This is possibly due to the repeated mechanical foraging strategy in silty substrate by the large vertebrate predators at the spot of predation (Fig. 6.4E). The liquefied internal materials consist of the less deformed clasts of siltstone and disseminated patches of sandstone in a homogenized sandy-silty mixed matrix. The clasts are partially deformed and preserve original laminations. Although these blob-shaped *Piscichnus* isp. pits are much less bioturbated (BI = 4) than the surrounding sediments, the homogenized mixed matrix in the interstitial spaces among the intraclasts contain the same tiering of trace fossils that characterizes the surrounding substrate (Fig. 6.5F). Furthermore, *Piscichnus* isp. pits in FT-L are also different in their size and shape from the more frequently distributed and smaller *Piscichnus waitemata* foraging pits in the overlying FT-U unit, which have the typical conical, cylindrical, or hemispherical shapes (see section 6.3.2.1). The disseminated rare sandstone patches within the *Piscichnus* blobs contain *Macaronichnus* isp., an ichnotaxon produced by the polychaete worms of Opheliidae family (Clifton and Thompson, 1978; Seike, 2007; Seike *et al.*, 2011; *cf.* Law *et al.*, 2014). Therefore, it is evident that liquefaction due to the foraging strategy occurred at the sediment-water interface during softground colonization of the FT-L. Any possibility of their origin by post-depositional soft-sediment deformation should be completely ruled out. However, there are oriented fractures filled with massive-appearing silt-sand mixture, which can be observed propagating away from the *Piscichnus* blobs following along and across the decompaction joints (Fig. 6.5A). These cracks are quite common suggesting post-depositional pore fluid overpressure within the *Piscichnus* pits with respect to the surrounding sediment. Foraging and predatory behaviour by vertebrates (*e.g.*, elasmobranchs, phocids, cetaceans) on the

open shelf endobenthos is a common phenomenon (Schreer *et al.*, 1997; Gingras *et al.*, 2007; Löwemark, 2015). The preservation of *Macaronichnus* isp. overprinted by foraging and predation trace fossils is also common (Kotake, 2007; Löwemark, 2015). Fig. 6.6 summarises the ichnofabric produced by the upward migration of the shallow and middle tiered community in response to the vertical aggradation of the shelf floor.

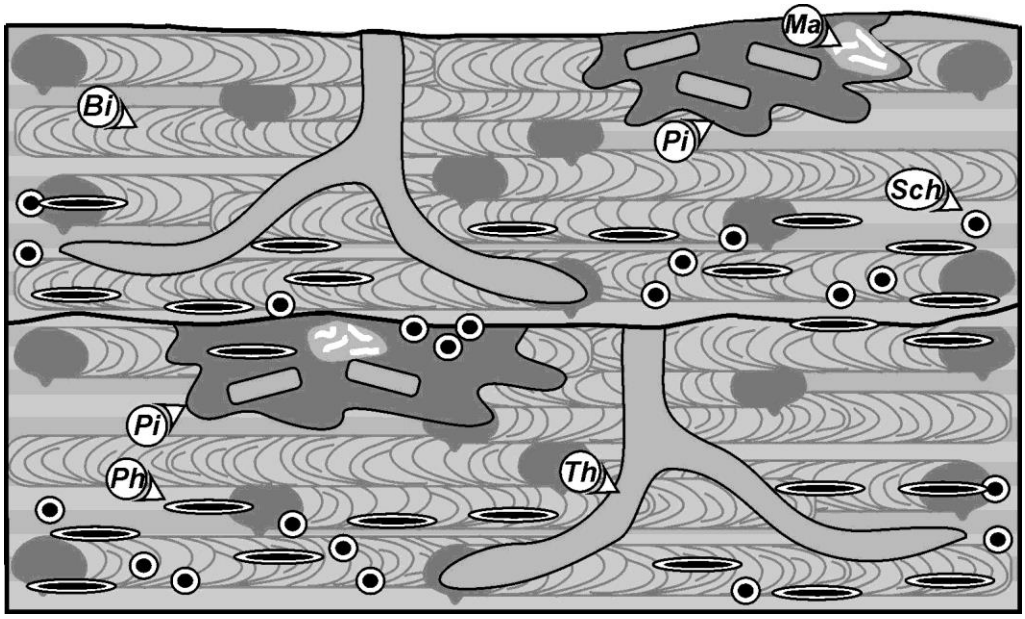

Fig. 6.6. Schematic diagram showing composite ichnofabric of the unit FT-L, produced by the upward migration of the shallow and middle tiered community in response to vertical aggradation of the shelf floor. [*N.B.* Acronyms used: *Bi* = *Bichordites* isp., *Ma* = *Macaronichnus* isp., *Ph* = *Phycosiphon* isp., *Sch* = *Schaubcylindrichnus* isp., *Th* = *Thalassinoides* isp., and *Pi* = *Piscichnus waitemata*.]

6.3.2 Unit FT-U

The upper unit is a 50-70 m thick succession of sandstones and thin-bedded/laminated heterolithic deposits overlying the erosional surface above the FT-L (Fig. 6.3). The depositional architectural elements vary laterally into the following facies:

6.3.2.1 Facies UA

This facies consists of the decimeter–meter thick, intermittently amalgamated, tabular or sheet-like, fine- to medium-grained, SCS-HCS sandstone units, which can be traced laterally for 700-750 m along the section. The sharp erosional contact marks the base, and internal reactivation surfaces separating individual SCS-HCS beds are also sharp. An individual SCS-HCS bed coarsens upward from laminated/ thin-bedded heterolithic sediments near the base to sandstone at the top (Fig. 6.4A-C). The bed thickness also increases upward. The heterolithic parts show HCS, parallel bedding/laminations, combined-flow ripples, and syneresis cracks (Fig. 6.7A).

The heterolithic intervals near base of every SCS-HCS bed are sparse to moderately bioturbated (BI = 1-3; Fig. 6.7A, C, H). High bioturbation (BI = 4) of the sandstone-dominated parts of the heterolithic deposits can also rarely be observed (Fig. 6.7B). The siltstone-dominated parts of the heterolithic sediments close or immediately above the erosional base are intense to completely bioturbated (BI = 5-6), with the same trace fossil assemblage as observed in the FT-L sediments (Fig. 6.7A-H). The ichnofabric of the intense to completely bioturbated zones is also quite similar to that of the FT-L (Fig. 6.6). Therefore, the dissimilarity can be only found in the sandier intervals, which the spatangoids (*i.e.*, the irregular sea-urchins) seem to have relatively avoided colonizing. Fig. 6.6A shows a *Bichordites* isp. (subhorizontal feeding burrows with active meniscate backfill and a single drainage canal at the base; for ichnotaxonomic description and differences from *Scolicia* isp., see *Figs. 7-9* in Uchman and Krenmayr, 1995) recording movement from one thin-bed siltstone to another one avoiding the micro-HCS sandstone thin-beds. This strategy is likely due to (i) the lack of nutrient organic detrital materials in the sand, (ii) avoidance of vertebrate predators that use the hydraulic jetting technique for foraging, which is more effective in sand than in silt, and (iii) possible greater salinity fluctuations in the sands due to much higher permeability than the silt layers. In the zones of intense to complete bioturbation by *Bichordites* isp. and *Cardioichnus* isp. (*i.e.*, heart-shaped resting trace fossil produced by the irregular sea-urchins; for ichnotaxonomic description, see Mayoral and Muñiz, 2001), there are the patches of secondary colonization of *Macaronichnus* isp. and rare *Phycosiphon incertum* (Fig. 6.7D-E; systematic ichnotaxonomic descriptions are available

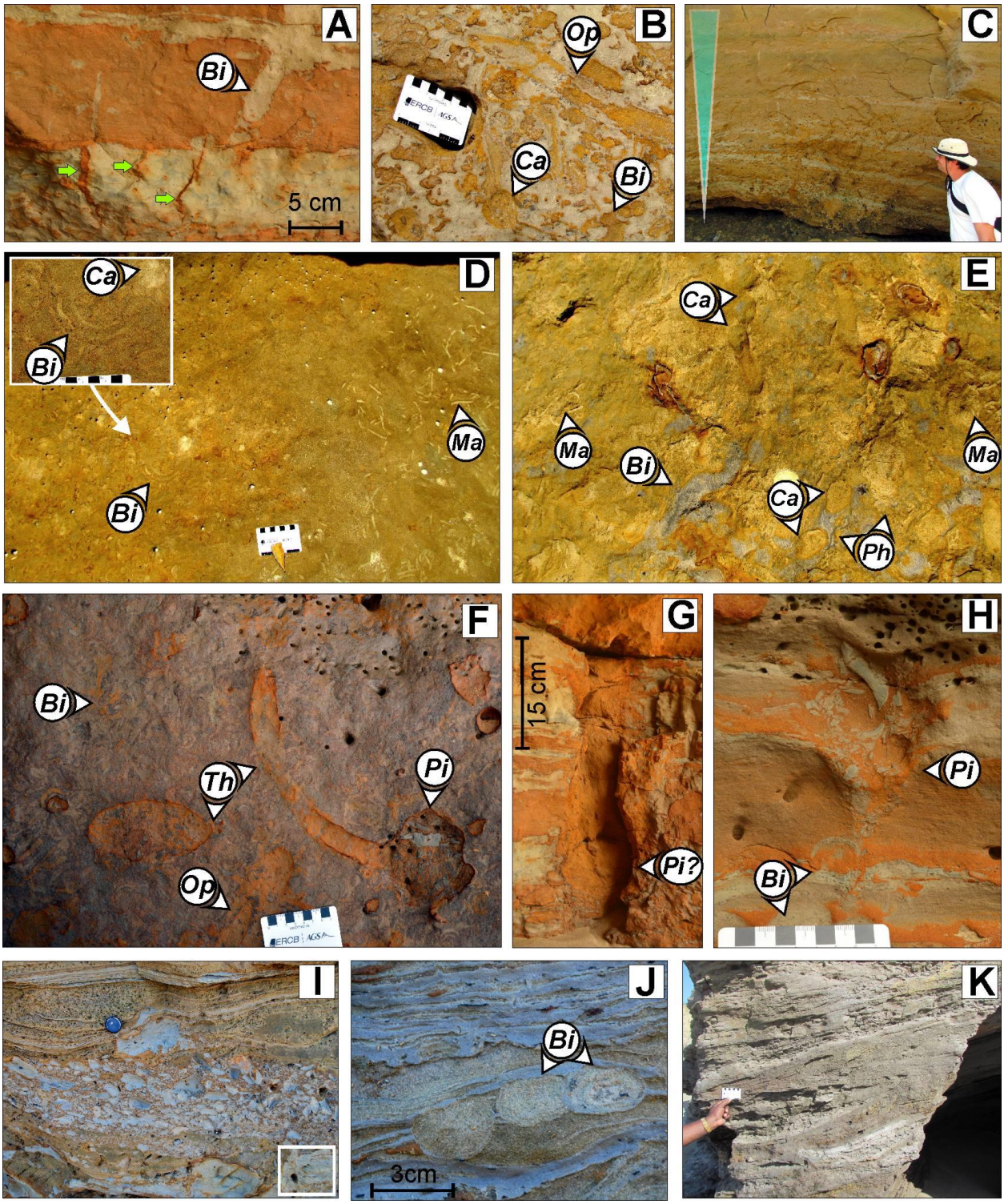

Fig. 6.7. (*N.B.* Figure caption is intentionally moved to the next page due to the large size of the figure and the length of the caption)

Fig. 6.7. Characteristic ichnological features of the unit FT-U within different facies. (A) (B) Respectively vertical and horizontal section views of moderate to high colonization (BI = 3-4) of the heterolithic intervals near the erosional base of the SCS sandstone units (facies UA) located between FL04 and FL05. Shrinkage cracks are marked with green arrows within the silty thin-bed. Escaping *Bichordites* isp. from thin-bedded silt to the upper silty lamination is marked with the annotation in Fig. 6.7A. Resting (*Cardioichnus* isp.) and associated locomotion/grazing behaviour of the sea-urchin trace-maker is documented in Fig. 6.7B, where the *Bichordites* isp. is crosscut by *Ophiomorpha nodosa*. (C) Decreasing BI with coarsening- and thickening-upward within SCS sandstone unit (facies UA; located between reference points FL04 and FL05). (D) Zone of secondary colonization of *Macaronichnus* isp. on the right-side of the photograph taken from facies UA (located between reference points FL05 and FL06). The secondary colonization obscured the previous complete bioturbation by *Bichordites* isp., which is still preserved on the left-side of the view. The inset enlarges the view of *Bichordites* isp. and *Cardioichnus* isp. (E) A view of bedding-parallel surface immediately above the contact between the FT-U and the FT-L, located near reference point FL06, showing high to intense colonization (BI = 4-5) of *Bichordites* isp., *Cardioichnus* isp., *Phycosiphone incertum* within the heterolithic interval. Sand-rich patches are recolonized by *Macaronichnus* isp. (F) (G) (H) Photographs showing vertebrate praedichnial traces, *Piscichnus waitemata*, within the organic detritus-bearing facies UA, predating on invertebrates (crustaceans and spatangoids) by hydraulic jetting as evidenced by targeted liquefaction and brittle fragments of the surrounding siltstone thin-beds (from different locations between FL04 and FL 06). In Fig. 6.7F, *P. waitemata* in phytodetritus-rich sandstone (completely bioturbated by *Bichordites* isp.) terminated the horizontally-bending end of a lined *Thalassinoides* burrow. *Ophiomorpha nodosa* colonization within a *Thalassinoides* burrow can also be noted very close to the spot of predation trace fossil. In Fig. 6.7G-H, the predator trace-makers target plant-debris-bearing siltstone thin-beds completely colonized by *Bichordites* isp. (I) (J) Rarely and sparsely bioturbated (BI = 0-1) channel-fill (facies UB). Isolated *Bichordites* isp. colonizing intraclast-supported conglomerates at the channel-base (located near reference point FL-08) . The rest of the sandy channel-fill is colonized rarely by *Ophiomorpha nodosa* (not in the photograph), and no *Bichordites* isp. is present. The white rectangle in Fig. 6.7I is zoomed and enlarged in Fig. 6.7J. (K) Unbioturbated alternate HCS beds and laminated siltstone beds (facies UD; located between reference points FL08 and FL11). [*N.B.* Acronyms used: *Bi = Bichordites* isp., *Op = Ophiomorpha nodosa*, *Ca = Cardioichnus* isp., *Ma = Macaronichnus* isp., *Th = Thalassinoides* isp., and *Pi = Piscichnus waitemata*.]

elsewhere, *e.g.*, Carmona *et al.*, 2008). The sea-urchins are known to act as an oxygen-infuser into shallow marine substrates (Vopel *et al.*, 2007). Thus, the primary colonization by irregular echinoids might have created enough localized oxygenation for opheliid polychaetes to colonize, thereby partially obscuring the primary fabric of *Bichordites* isp. and *Cardioichnus* isp. (Fig. 6.7D). The deep-tier *Ophiomorpha nodosa* crosscuts the shallow- and middle-tier trace fossils (Fig. 6.7B). There is a steady decrease of abundance of the trace fossils with coarsening- and thickening-upward of the SCS-HCS beds. In the amalgamated SCS beds, trace fossils completely disappear except rare and isolated (BI = 0-1) occurrences of *O. nodosa*.

There is a relative increase in the abundance of predation burrows in the heterolithic intervals compared to the same in FT-L. Their shapes are much more regular (commonly conical to rarely cylindrical or hemispherical), in contrast to those in the FT-L. Also their sizes are much smaller (a few centimeters as in Fig. 6.7F-H). The praedichnial trace fossils in Fig. 6.6F and H are identified to be *Piscichnus waitemata* made possibly by elasmobranchs (rays) preying on the infaunal crustaceans and spatangoids. The large plug-shaped predation trace fossils (Fig. 6.7G) are also quite common in the heterolithic intervals of the facies UA and are possibly produced by phocids (*e.g.*, *Monachus* sp.), which are known to dive quite deep (up to 1 km; Schreer *et al.*, 1997) to forage using the hydraulic jetting technique on the infaunal invertebrates (*Fig.* 5 in Gingras *et al.*, 2007). The tropical seals of the phocid subfamily Monachinae were prevalent in the North Atlantic of late Miocene and Pliocene, especially all over the present-day Caribbean Sea areas (King 1983).

Given the SCS wave lengths (0.5-5 m), the facies UA is interpreted as the bedform deposits produced by storm wave actions and/or longshore current. Having lateral association with the channel-overbank underflow system (*i.e.*, facies UB and UC; see below), the sediments were likely delivered by these feeder system and then got reworked as the splays by wave action (Fig. 6.8A; also see section 6.4.1).

6.3.2.2 Facies UB

Laterally accreting channels (Figs. 6.4D, 6.6I), filled with: (a) siltstone intraclast-supported conglomerate with fine- to medium-grained sandy matrix and intermittent silt-sand mixed matrix at the thalwegs and above the scoured reactivation surfaces; (b) fine- to medium-grained sandstone with planar and sigmoidal cross-stratification and combined-flow ripples; (c) the wave-rippled, combined-flow-rippled, and intermittently wrinkled fine-grained sandstone at the top; and also (d) heterolithic deposits containing thin-bedded/laminated sandstone and siltstone at the top (below reactivation surfaces), showing the reverse overlain by normal grains-size grading trends within beds/laminations.

There is an absence of bioturbation within the channels, except a few, rare, and localized *Bichordites* isp. within intraclast-supported conglomerate filling the channel-base, almost, as if, hiding within the interstitial sandy matrix (Fig. 6.7I-J).

On the FT-L deposits on the shelf, the channels are incised by sediment-gravity flows – mostly of the sustained nature (hyperpycnal flow *sensu lato*), as indicated by the reverse-normal grainsize grading trends within the associated thin-beds and laminations (Mulder *et al.*, 2001, 2003). They are initially filled with the reworked and slumped materials from the FT-L at the base as intraclast-supported conglomerate and debris flow deposits. The channel-fill was later reworked by the background wave action.

6.3.2.3 Facies UC

This facies consists of the sharp-based lens-shaped bodies of sandy heterolithic deposits with SCS-HCS, wave-ripples, combined-flow ripples, and cut and fill structures filled with combined-flow ripples/ micro-HCS, and wedge-shaped bodies of intra-clast conglomerate deposits. The facies UC laterally varies into the facies UA and the UB, having more common reactivation surfaces towards the facies UB (Fig. 6.4D). Also there is increasing abundance of cut and fill structures, guttercasts, and conglomeratic wedges near the channels (*i.e.*, facies UB).

Except a few localized and sparsely distributed (BI = 1-2) *Planolites* isp., *Skolithos* isp., *Teichichnus* isp., and *Phycosiphon* isp., the facies UC is mostly unbioturbated (BI = 0).

Association with facies UB, ichnological similarity with the same, and proximity of the cut and fill structures and the conglomeratic slumped materials more towards the channels indicate that facies UC is in fact the overbank of the channels, though with no discernible levee geometry.

6.3.2.4 Facies UD

This facies comprises alternate beds at almost regular intervals of (a) the HCS very fine- to fine-grained sandstone (Fig. 6.7K) and (b) the parallel-laminated siltstone beds with localized sub-centimeter thick sandy lenticular laminations with combined-flow ripples. The thin-beds/laminations within siltstone often display coarsening- and then fining-upward internal grain-size variations. The facies is intermittently cut by channel/chute shaped furrows, which are filled with breccia containing intraclasts of the parallel-laminated siltstones and mixed silt-sand matrix. The facies UD is unbioturbated, except rare occurrence of *Planolites* isp. (BI = 0, rarely 1).

The facies UD was deposited in a river-dominated and wave-influenced proximal prodelta, receiving sediment input from the tailing fine-grained part of the sustained sediment-gravity flows, whereas the HCS intervals were possibly deposited by storm events or coarse-grained influx of the hyperpycnal discharge seasonally associated with storms. The prodeltaic deposit does not directly overlie the erosional contact above the FT-L. It stratigraphically overlies another erosional contact above the facies UA, UB, and UC (Fig. 6.3), thereby making the second erosional contact (which is beyond the scope of discussion in this article), interpreted as a transgressive surface of erosion separating two parasequences within the FT-U.

6.4 Discussion

The lateral association of the facies UB and UC with UA, and the systematic variation of the ichnological characteristics (*i.e.*, from the highly stressed to the least stressed subenvironments for colonization) together indicate that the facies are likely genetically related and were deposited in hyperpycnal channels, overbanks, and wave-modified splays respectively (Fig. 6.8A). The term ‘hyperpycnal flow’ used here denotes the sustained sediment-gravity flow receiving sediments from river discharge in a broader sense. This implies that the term encompasses the plunge of river discharge strictly both under the elevated sediment-load (‘hyperpycnal’ *sensu stricto*) and also under the additional influence of the convective

instabilities created by waves, storms, and even slope instabilities ('hyperpycnal' *sensu lato*) (Mulder *et al.*, 2003; Pattison, 2005; Milliman and Kao, 2005; Lamb *et al.*, 2008; Bhattacharya and MacEachern, 2009; Kao *et al.*, 2010). Examples of the Neogene-Quaternary Orinoco River system having hyperpycnal phases have been published before (Agard and Gobin, 2000; Wilson, 2008; Gamero Diaz *et al.*, 2011; Zavala *et al.*, 2012; Dasgupta *et al.*, in review). Away from the channel, the background wave action and geostrophic currents produce the SCS-HCS tabular sandstone beds of facies UA as the wave-modified splays. An alternate explanation for the origin of combined-flow dunes developed by the interactions between hyperpycnal flows and ambient standing body of water has also been suggested (Zavala *et al.*, 2011; *cf.* Harms *et al.*, 1975, 1982; Southard, 1991; Mutti *et al.*, 1994). As the Southern Basin evolved along with the tectonic and growth faulting episodes, the paleo-topography of the shelf must have been irregular, as shown in Fig. 6.8A, which should have influenced the distribution of the depositional elements.

6.4.1 Sequence-stratigraphic status of the erosional contact surface – Autogenic erosional surface on shelf setting dominated by hyperpycnal flow

The studied erosional contact exhibits the conspicuous transformation from shelfal paleo-environment into a marginal-marine setting. The latter is dominated by the river discharges with background wave-influence, unlike the case of an RSME, which can develop in a wave-dominated shelf setting. No *Glossifungites* suite as the indicator of forced regression is preserved at the erosion surface in contrast to an RSME scenario, which involves substantial erosion by waves and firmground colonization of the muddy substrate during forced regression (MacEachern *et al.*, 1992; Pemberton *et al.*, 1992; Chaplin, 1996; Buatois *et al.*, 2002). While considering the facies association, especially the sudden occurrence of the channel-overbank-splay deposits resting on the erosion surface above the shelf deposits, invoking an estuarine incised valley may also seem to be a reasonable interpretation. However, there are similar differences with the incised valley scenario as well. At first, the erosional discontinuity surface does not preserve any substrate-controlled ichnofacies unlike the examples of incised valley surfaces (Pemberton *et al.*, 1992; MacEachern *et al.*, 1992; Gibert and Martinell, 1992, 1993, 1996; MacEachern and Pemberton, 1994; Martinell and Doménech, 1995; Buatois *et al.*, 1998; Uchman *et al.*, 2002; Carmona *et al.*, 2006, 2007). The erosion was not deep enough to exhume

the firm or lithified substrates. And the fragile, stenohaline, osmoconformer, and *Bichordites*-producer spatangoids colonizing the facies FT-L seem to have managed to survive even under changed sedimentary condition, though preferably away from the channel axes. In beds of the facies UA immediately above the erosion surface (*i.e.,* just above the red dashed curves in Fig. 6.4A-C), there is hardly any difference in the tiering structure of the trace fossils, except the relative reduction in the BI. As an example to visualize the difference, Fig. 6.5G-I (plan-view parallel to bedding surface from the facies FT-L) and Fig. 6.6B, E-F (plan-view parallel to bedding surface in the facies UA) can be compared. Even under the extremely stressed channel-fill conditions (see discussion below), the *Bichordites*-producers seem to have survived although hiding within the interstitial matrix within intraclast-supported conglomerate (Fig. 6.7I-J). The fragile-tested sea-urchins could not have escaped the mechanical wear and tear of a debris flow. This implies that instead of colonizing the channel-fill sand, the spatangoids from laterally associated depositional settings burrowed into the conglomeratic debris flow deposit after its deposition and colonized the relatively more impervious interstices in order to escape changes in ambient condition (*i.e.,* salinity fluctuations and turbulence) taking place above within the channel. This shows that essentially the same infaunal community persisted during the initial channel deposition, albeit temporarily, indicating that the contact between the FT-L and FT-U neither represents a significant hiatus nor demarcates a drastic departure as a niche away from the laterally associated depositional settings where colonizers survived.

In view of these sedimentological and ichnological similarities especially within the siltstone intervals below and above the contact, the following interpretations can be made:

1) The facies FT-L and UA were in lateral and spatially close association, where the latter was overlain on the former with establishment of the prograding lobe. The progradation did not necessarily involve a relative sea-level fall or forced regression unlike the scenarios involving an RSME or an incised valley, therefore precluding any scope of substantial erosion to exhume firmground substrate. The progradation of the lobe is autogenic and very similar to the establishment of a lobe by avulsive switching, but with only one exception that below the contact the facies FT-L is monotonous and does not show any lateral variation into a lobe.

2) Even after the change-over in the depositional regime, the ecological niche continues to host some endobenthic colonizers, though under stressed condition for a limited duration.

Within the MLF succession at the Fullarton section, the facies FT-L seem to be the last preserved package of sediments deposited in an open shelf, before erosion took place, and until the next flooding event caused deposition of the L7S sediments (see Fig. 6.2B), which are exposed further eastward along the shoreline of Cedros Bay. Having the erosional discontinuity separating the FT-L from the younger underflow-dominated delta-front (the facies of FT-U), the surface can be categorized as an autogenic surface of erosion, which was eroded and scoured dominantly by hyperpycnal flows on a rheologically unconsolidated (softground) sea-bottom. With the dominance of underflows, the waves were also coevally active there in modifying and redistributing the clastic sediments delivered by the un-confining/splaying underflows as in the facies UA.

Also in general, the inner shelf is the area of sediment bypass during forced regression. Therefore, the meter-thick HCS-SCS (*i.e.,* facies UA) beds deposited in lower shoreface can seldom be preserved above the storm wave base, because the locus of lower shoreface moves basinward during a falling relative sea-level, thereby eroding the HCS-SCS beds forming the RSME in wave-dominated shelf-setting (Plint, 1991; Catuneanu, 2006). However, in case of the MLF, preservation of the thick and amalgamated SCS-HCS beds above the erosional contact suggest that the erosion occurred at relatively much greater depth than that of development of an RSME in the wave-dominated inner shelf setting, thereby, pointing towards:

1) Enough accommodation in deeper shelf bathymetric condition was available compared to the wave-dominated inner shelf settings. It is common to find sharp-based SCS beds deposited in upper- to middle-shoreface setting overlying the outer shelf muddy sediments (Plint and Nummedal, 2000; Catuneanu, 2006). But the deep accommodation in our case was still not at the middle or outer shelf, because the contemporaneous shelf-margin was ca. 200 km away from the locality (Chen *et al.*, 2014).

2) The hyperpycnal discharges were the principal cause of subaqueous progradation of the clastic wedge, not necessarily involving forced regression. The underflows caused autogenically controlled erosion of the soft sediments on the inner shelf however at a substantial bathymetric depth, and deposition of the facies UA, UB, and UC. The background wave activity reworked and redistributed sediments with further shallowing of the system.

6.4.2 The role of stress factors

Even after the change-over in the depositional regime across the erosion surface, the ecological niche continued to host some of the same infaunal colonizers. The relative duration, intensities, and pattern of survival of the colonizers, as displayed by the ichnological characteristics, are also variable in the different facies in the overlying FT-U unit. In addition to the increased ecological stresses typical to deltaic influences (*e.g.,* MacEachern *et al.,* 2005, 2007a, 2007b; Hansen and MacEachern, 2007; Buatois *et al.,* 2008, 2011, 2012; Carmona *et al.,* 2008, 2009; Bhattacharya and MacEachern, 2009; Dasgupta *et al.,* in review) in the overlying unit, the surface also marks the selective decrease in the abundance and distribution of trace fossils produced by the spatangoids within the overlying units and their parsimonious extermination within the specific depositional elements.

From ichnological evidence, the primary or dominant stress factors active in the different subenvironments of the overlying FT-U unit are suggested here to be (Table 6.2): (i) the salinity fluctuations due to hyperpycnal and hypopycnal wedging of the water column, (ii) the scarcity and abrupt change of nutrients, (iii) the dispersal by currents both at the sea-bed and at the water column, and (iv) the substrate rheology. These stress factors appear to have influenced the invertebrate colonizers not only at the sea-bed, but also likely affected their planktotrophic larvae in the water-column. This assumption is conjectural but consistent in view of the pattern of estimated stresses in different facies. The salinity fluctuations, food supply, predation in the substrates at the sediment-water interface as well as in the water column are so interrelated that we have to discuss them together.

The noticeably dominant primary tracemakers in the Fullarton outcrops are the shallow-tier deposit-feeding spatangoids (or irregular sea-urchin / heart-urchins), with the minor infaunal middle- and deep-tier colonizers (*e.g.*, decapods, polychaetes) and the predators at the sediment-water interface (vertebrates: possibly elasmobranchs, phocids, or cetaceans). The spatangoids are known to be stenohaline osmoconformers (Böttger *et al.*, 2004). However, like many other endobenthic deposit-feeders, the juvenile and adult spatangoids can escape salinity variations by their infaunal habit (Stickle and Diehl, 1987). This strategy is more effective in the silt than in the sand with much higher permeability.

With the change in sedimentary regime from an open shelf (see section 6.4.1) to the wave-influenced delta-front dominated by subaqueous hyperpycnal channels, the subenvironments with decreasing effects of the salinity changes can explicably be listed as follows: channels, overbank, wave-modified delta-front bars, and river-dominated and wave-influenced proximal prodelta. A sandy substrate, being the most permeable, has the maximum salinity fluctuations affecting the shallow-tier colonizers. This may explain why the spatangoid trace fossils are more abundant in silty intervals (Fig. 6.7A, C, H) or at least in the interstices or matrix of the siltstone intraclast-supported conglomerates (Fig. 6.7J-K).

The grain-size vis-à-vis the rheology of any substrate also seems to have influenced the predatory strategy. In the silty substrate of the FT-L, an individual vertebrate predator apparently excavated a larger diameter for a foraging pit by repeated mechanical churning compared to the much smaller foraging pits in FT-U. This is, perhaps, because the silt grains commonly are more angular than the sand particles. Thefore, a silty substrate is relatively ‘stiffer’ or ‘firmer’ than a sandy substrate. On the other hand, the hydraulic jetting foraging technique seems to be the common feeding strategy of the predators in the FT-U sediments, as evidenced by the more abundant *Piscichnus waitemata* and cylindrical *Piscichnus* isp. Therefore, the ease and intensity of foraging behaviour appears to be more in the sandy substrate above the erosional discontinuity surface. The grainsize (and resultant rheology) of the substrate is therefore a stress factor for the preys.

Also, unlike the endobenthic adults, the echinoid larvae (echinopluteus), as well as the other larvae of infaunal invertebrates, have to live in the water column. An echinopluteus is highly stenohaline and cannot even tolerate a mesohaline brackish condition. It avoids any salinity changes below 21-24 ‰ (Metaxas and Young, 1998). The larvae of the most salinity-resistant taxa of polychaetes can survive only above ca. 20-22 ‰ of salinity (Ushakova and Sarantchova, 2004; Pechenik *et al.*, 2007). Both the embryonic and larval stages of polychaetes are far more sensitive to the temperature and salinity fluctuations than the adults and juveniles (Qiu and Qian, 1997). Therefore, the invertebrate larvae in the water column are highly susceptible to get perished under the hyperpycnal and hypopycnal conditions, under which the endobenthic adults can only survive.

The above situation can get more acute and complexly interrelated with the food supply for the endobenthic mature adults. Irregular sea-urchins are detritivorous deposit-feeders and they feed on diverse marine organic matters mixed within sedimentary particles depending on the local availability of phytodetritus, faunal detritus, microbial mats, and/or a combination of all of them (Barberá *et al.*, 2011). Although they are effecient in digesting complex carbohydrates through microbial fermentation in their gut (Thorsen, 1998), they are not known to feed on land-derived phytodetrital materials. There used to be a general assumption that fluvially delivered terrigenous organic materials are refractory to decomposition (Ittekkot, 1988; Hedges et al., 1997). However, Bourgeois *et al.* (2011) and Fagervold *et al.* (2014) have shown that in a prodeltaic setting and in the adjacent shelf areas, the terrestrial organic matters can be labile enough in flourishing the benthic microbial communities. The benthic microbes also feed on marine organic matter derived from the settling phytoplanktonic biomass, which can bloom with the river plume, not exactly inside it, but in the zone of mixing close to the turbid, high nutrient, brackish fluvial discharge, and more landward and away from the clear, marine salinity, low nutrient marine condition (Turner *et al.*, 1990; Smith and Demaster, 1996; Lohrenz *et al.*, 1999). These benthic microbial communities prefer substrates with finer grainsize (Franco *et al.*, 2007; Böer *et al.*, 2008). And therefore, the terrestrial phytodetritus, especially within fine-grained sediments, serves as the passive source of nutrients for deposit-feeder macrobenthos like the spatangoids, which is also supported by the preferential *Bichordites* bioturbation of the siltstones in facies FT-L and UA, containing detrital organic matters (Figs. 6.5A-I; 6.7F-H). Plant detrital

materials are delivered by hypopycnal plumes, lofting plumes of hyperpycnal flows, and spilling fine-grained hyperpycnal flows into the niches, where finer-grained sediments settle away from the channelized underflows.

A better food supply increases the quality of eggs and decreases the pelagic time of the hatchling larvae before metamorphosis (Fig. 6.8B; McEdward, 1997), thereby reducing the chances of being preyed in the water column. On the other hand, a poor food supply in the areas of sand deposition not only increases the chances of preying on larvae by nektonic predators, but it also reduces the maternal investment in the eggs laid by less nourished adults. A larva from a good quality egg can remain facultative (*i.e.*, with optional feeding strategy) throughout its plantotrophic stage, whereas the less-nourished hatchlings must resort to obligate planktotrophic feeding (*i.e.*, compulsory feeding strategy) during the later advanced larval stage before the metamorphosis (Metaxas and Young, 1998). In the latter scenario, the larvae become further vulnerable to be perished, because:

1) In order to avoid larval mortality, it is beneficial to remain gregarious in habit during the larval stage within the water column above a suitable substrate or site to settle later before the metamorphosis.
2) The obligate feeding strategy causes the larvae to move upward to the photic feeding zones. As a consequence, the larvae are susceptible (a) to be further dispersed, thereby increasing the chances of mortality, (b) to be further predated, and (c) to be extremely influenced by the fatal salinity of the hypopycnal and lofting plumes.

The dispersal of the adults and larvae at or near the sediment-water interface can be caused by all sediment-gravity flows (*e.g.*, the surge-type turbidity currents, seasonal hyperpycnal flows, wave-influenced quasi-sustained underflows, and debris flows), which simply physically remove the juvenile and adult trace-makers (and their larval offspring) away from the locality (Wetzel, 2008). The higher flow velocity causes higher volume of transportation and sedimentation. Elevated sedimentation rate hinders settlement of larvae at their advanced stage before the metamorphosis and endobenthic colonization (Qian, 1999). However, at the same time, the currents in the water column, *e.g.*, seasonal hypopycnal plumes,

geostrophic currents, internal waves and tides, can also disperse planktotrophic larvae causing the vulnerabilities that are discussed above.

The role and complex relationship among all the stress factors – salinity changes, relative scarcity of nutrients, predation, and dispersal by current – in different facies and their depositional subenvironments can be summarized and displayed in a matrix format as in Table 6.2. Fig. 6.8A-B illustrates how the stress factors influenced the colonizers and their planktotrophic offsprings in the different sedimentary subenvironments, by categorizing them into three potential ecological niches A-C, with increasing combinations of intricately interrelated stress factors as discussed above, and with an emphasis on their effects on the maturing echinopluteus as an example. The signatures of the decreased ichnodiversity and ichno-abundance, as well as the disappearance of certain ichnotaxa, not only reveal a hierarchy of the subenvironments (as shown in Table 6.2) in terms of severity of the stress factors affecting the trace-makers in the substrate; but also those factors possess potentially much more severe adverse effects on the phytotrophic larvae of the endobethic colonizers in the water column above. The ichnological signatures should, therefore, be judged as a combined result of both, hence making the interpretation apparently conjectural, but consistent with the ichnology vis-à-vis sedimentary facies and the developing knowledge of irregular sea-urchin ecology.

Table 6.2. Relative influences of ecological stress factors and their cumulative effects on adult invertebrate endobethos (sea-urchin) community and their planktotrophic larvae (echinopluteus) at the sediment-water interface and in the overlying water column in different sedimentary sub-environments on the continental shelf affected by a wave-influenced and fluvial discharge-dominated delta system. Three cases, A, B, and C, of ecological niches listed in Fig. 6.8 are also assigned.

Dominant stress factors	**Facies**				
	UA	**UB**	**UC**	**UD**	**FT-L**
	Tabular wave-modified bars	**Laterally accreting channels**	**Overbank of channels**	**Proximal prodelta**	**Open shelf**
Salinity fluctuations at the substrate level	Episodic, negligible to moderate	Episodic, high	Episodic, moderate	Episodic, low to moderate	Not applicable
Salinity fluctuations in the water column for phytotrophic larvae	Episodic, negligible to high	Episodic, high	Episodic, moderate to high	Episodic, negligible to low	Not applicable
Scarcity of phytodetrital materials in the substrate	Moderate	High	Moderate	Low to moderate	Low
Scarcity of food in the water column for phytotrophic larvae	Moderate	Low	Low	Low to moderate	Low to moderate
Predation at the sediment-water interface	Moderate to high	Low	Moderate to high	High	Low to moderate
Dispersal by current at the sediment-water interface	Moderate	High (extreme)	Moderate	Low	Low
Dispersal by current in the water column above (for phytotrophic larvae)	Moderate	High (extreme)	High (extreme)	Moderate	Low
Cumulative effect	Episodically low and moderate	Hight to extreme	Moderate to High	Moderate	Low to negligible
Type(s) of niche shown in Fig. 6.7	Cases A, B	Case C	Cases B, C	Cases B, C	Case A

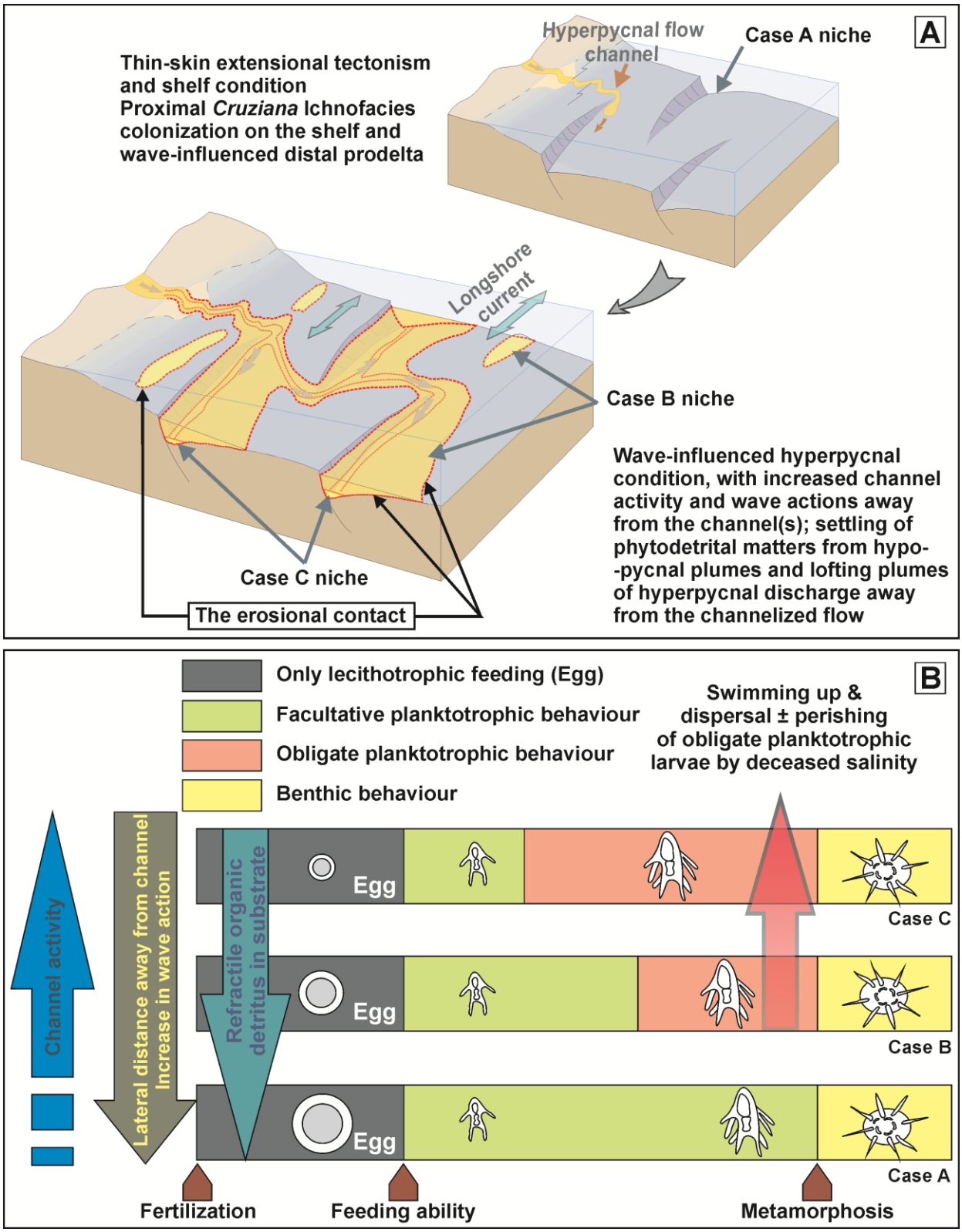

Fig. 6.8. (*N.B.* Figure caption is intentionally moved to the next page due to the large size of the figure and the length of the caption)

Fig. 6.8. Schematic diagram showing different niches of spatangoid colonization on the shelf and in the presence of advancing clastic wedges deposited in settings influenced by hyperpycnal and hypopycnal discharges and wave actions. (A) Ecological niches Cases A, B, and C, where facies tracts FT-L, UA, and UC were respectively deposited (block diagrams adapted from Zavala *et al.,* 2011). (B) Increasing stress factors on maternal investment in terms egg-quality and on echinopluteus (swimming larvae) in varying niches *i.e.,* cases A-C (adapted after McEdward, 1997; Metaxas and Young, 1998; Reitzel *et al.* 2005). With increasing volume and quality of detrital organic matter, maternal investment is higher in eggs. The resulting echinopluteus can stay facultatively planktotrophic lower in the water column until metamorphosis starts as in case A. Limited endobenthic detrital organic food supply in sandy substrate results in poorer egg quality giving rise to echinopluteus population that needs longer obligate feeding stage upper in water column being subjected to dispersal away or perishing under brackish hypopycnal plumes as in case C. The salinity variations due to hyperpycnal flow activity and oxygenation of organic detrital material are also maximum along the channel activity, putting further stress on both endobenthic and plantotrophic stages of sea-urchin life cycle. The case B niche, which possibly can be found in the overbanks of channels, splays, and wave-influenced delta-front barforms, should have intermediate effects of these stress factors in comparison to niches of case A and C.

6.5 Conclusions

1. In the Fullarton section, the discontinuity surface separating the underlying sediments deposited on open shelf (the FT-L) and the overlying coarser clastic wedge (the FT-U) deposited by the prograding paleo-Orinoco River system can be categorized as a subaqueous, autogenically controlled, erosional discontinuity in a hyperpycnal-dominated and transiently wave-influenced shelf setting scoured on the unconsolidated soft sediments. This makes the surface different from the forced regression scenarios like (a) an RSME in wave-dominated inner shelf settings or (b) an incised estuarine valley developed due to subaerial exposure of the shelf.

2. The infaunal colonization of the depositional elements of FT-U is stressed by (i) the salinity changes arising directly from the fluvial influx, (ii) the selective scarcity of nutrients, (iii) the dispersion by current, and (iv) the ease of predation. The stress factors might have impacted differently at the various stages of life cycle of the colonizers, not only within the substrate but presumably in the water-colums affecting their plantotrophic larvae. The cumulative effects of the stress factors as shown by the ichnological characteristics of different facies are demonstrated as high to extreme within the channels, moderate to high in the overbank, moderate in the

proximal prodelta, and from low to moderate in the sandy wave-modified bars to negligible in its fine-grained/heterolithic intervals.

6.6 Acknowledgements

The authors deeply thank Repsol, Trinidad and Tobago, for funding the field studies and making logistic and safety arrangements. We wholeheartedly thank Livan Blanco Valiente, Rafael Vela, Yrma Vallez, Marlon Bruce, Anderson Arjoon, and Andrei Ichaso for their help and discussions. Additional financial support was provided by an NSERC Discovery Grant to Buatois, and the AAPG Foundation Merrill W. Haas Memorial Grant, the Saskatchewan Innovation and Opportunity Award from the Provincial Government of Saskatchewan and University of Saskatchewan, and the Dr. Rui Feng Graduate Studies Award to Dasgupta.

CHAPTER 7: CONCLUSIONS

Traversing along depositional strike, Mayaro Formation outcrops display the associations of laterally and autogenically varying facies, possibly not the allogenic transgressive-regressive cycles as had previously been reported. This is because there is no outcropped stratigraphically important vertical change or any discontinuity surface that can be observed in this area, except the canyon/gully incision surface. The incision surface, previously reported as a fault, has been identified by the unique monospecific *Glossifungites* Ichnofacies suite defined by the firmground *Thalassinoides* isp. colonization of the older delta-front sediments that has been exhumed by the incision process. The high-frequency sequence-stratigraphic model proposed for the canyon/gully-fills in relation to the deltaic deposits can be an analog for the recurrently canyonized/gullied shelf-margins with active fluvial influx and high sediment accumulation rates. The model postulates that, within a recurrently invaginated shelf-edge delta-front megasequence of 'n^{th}-order' hierarchy, the internal '$(n+2)^{th}$-order' facies tracts changes constitute together into '$(n+1)^{th}$-order' level cyclicity in response to the high-frequency fluctuations of local base-level. The cyclicity might be a switching-on-and-off mechanism for the coarse clastic supply (or simply 'sand' supply) into the deep-water system during the late falling stage system tract in an analogous basin constellation.

The Mayaro Formation megasequence was deposited in a river-dominated to wave-influenced deltaic environment at/near the shelf-break with the slope-instability being an additional controlling factor on this delta system. Ichnological evidence suggests that the shelf-edge deltas are one of the most extreme marine environments for benthic infauna. However, the trace fossil content, the combinations and ranking of controlling stress factors, and the preservation potential are also variable and distinct in accordance with the sedimentary and oceanographic processes taking place within individual subenvironments. In the paleo-Orinoco shelf-edge delta system, individual delta-lobes themselves can demonstrate dual ichnological properties of an extremely stressed shelf-edge delta and "regularly" or "normally" stressed "delta on the shelf" (*i.e.*, similar to inner-shelf shoals) characters. The facies model for the Mayaro Formation presented in this study provides a comprehensive combined ichno-sedimentological

analog model for a low-latitude, accommodation-driven, shelf-edge delta of a large river system like the paleo-Orinoco developed on an active continental margin in an oblique foreland setting.

Before reaching the shelf-edge, the same system deposited clastic wedges directly on the open shelf resulting in abrupt sedimentary regime change as displayed by the change from the shelf environment into the highly stressed hyperpycnally and hypopycnally influenced delta-front with the transient wave action. Although the ecologic stress factors increasing towards the hyperpycnal channels is a simplistic observation, the parsimonious preservation of the depauperate suites of burrows produced by the irregular sea-urchins within the different subenvironments of the prograding clastic wedge highlights the complex interrelations among (a) salinity changes, (b) nutrient availability and quality, (c) dispersion of larvae, (d) larval mortality, (e) influences of (a), (b), (c), and (d) at both the sediment-water interface and water column, and (f) physical properties of the substrate. The discontinuity surface marking the sedimentary regime change is a subaqueous autogenically controlled erosional contact, and not a sequence boundary, because there is no substrate-controlled suite of trace fossil marking the surface. Rather the surface marks (a) the end of a niche with a continuous infaunal softground colonization and large foraging burrows throughout the underlying shelf deposit, and (b) the parsimonious crossing of colonizers into the highly stressed newly established niche above. The colonization after the sedimentary regime change is guided by the processes, which are specific to individual subenvironments, and by specific substrate type, before these trace fossils completely disappeared higher-up in the stratigraphic column.

The Ph.D. project characterizes both a shelf-margin delta lobe analog (Outcrops 1A to 9 of Mayaro Formation) and two different types of analogs of the on-shelf delta lobes (Outcrops 10 and 11 of Mayaro Formation as the outer-shelf lobe, and Fullarton outcrops of the Morne L'Enfer Formation as the inner-shelf lobe), thereby serving as a comparative study.

REFERENCES

Agard, J.B., and Gobin, J.F., 2000, The Lesser Antilles, Trinidad and Tobago. *In* Sheppard, C. (Ed.), Seas at the Millennium: An Environmental Evaluation: *Elsevier Science*, Amsterdam, Netherlands, p. 627–641.

Ahmed, S., Bhattacharya, J.P., Garza, D.E., and Li, Y., 2014, Facies architecture and stratigraphic evolution of a river-dominated delta front, Turonian Ferron Sandstone, Utah, USA: *Journal of Sedimentary Research,* v. 84, p. 97–121.

Alfaro, E., and Holz, M., 2014, Seismic geomorphological analysis of deepwater gravity-driven deposits on a slope system of the southern Colombian Caribbean Margin: *Marine and Petroleum Geology*, v. 57, p. 294–311.

Algar, S., 1998, Tectonostratigraphic development of the Trinidad region. *In* Pindell, J.L., and Drake, C.L. (Eds.), Paleogeographic evolution and non-glacial eustasy, northern South America: *SEPM Special Publication*, v. 58, p. 87–109.

Alpert, S.P., 1973, *Bergaueria* Prantl (Cambrian and Ordovician), a probable actinian trace fossil: *Journal of Paleontology*, v. 47, p. 919–924.

Alvarez, T.G., 2008, Tectonic geomorphology of the eastern Trinidad shelf: Implications for influence of structure on reservoir distribution and nature in older basin fill: Master's Thesis, *University of Texas at Austin*, Austin, USA, 237 p.

Andriessen, P.A.M., Helmens, K.F., Hooghiemstra, H., Riezebos, P.A., and Van der Hammen, T., 1993, Absolute chronology of the Pliocene-Quaternary sediment sequence of the Bogotá area, Colombia: *Quaternary Science Reviews*, v. 12, p. 483–501.

Arnott, R.W.C., 2003, The role of fluid-and sediment-gravity flow processes during deposition of deltaic conglomerates (Cardium Formation, Upper Cretaceous), west-central Alberta: *Bulletin of Canadian Petroleum Geology*, v. 51, p. 426-436.

Ashton, A.D., and Giosan, L., 2011, Wave-angle control of delta evolution: Geophysical Research Letters, v. 38, L13405, doi:10.1029/2011GL047630.

Ayranci, K., Dashtgard, S.E., and MacEachern, J.A., 2014, A quantitative assessment of the neoichnology and biology of a delta front and prodelta, and implications for delta ichnology: *Palaeogeography, Palaeoclimatology, Palaeoecology*, v. 409, p. 114–134.

Babb, S., and Mann, P., 1999, Structural and sedimentary development of a Neogene transpressional plate boundary between the Caribbean and South American plates in

Trinidad and the Gulf of Paria. *In* Mann, P. (Ed.), Caribbean Basins: Sedimentary Basins of the World, v. 4: *Elsevier Science B.V.*, Amsterdam, Netherlands, p. 495–557.

Barberá, C., Fernández-Jover, D., Jiménez, J.L., Silvera, D.G., Hinz, H., and Moranta, J., 2011, Trophic ecology of the sea urchin *Spatangus purpureus* elucidated from gonad fatty acids composition analysis: *Marine environmental research*, v. 71, p. 235–246.

Barker, S.P., Haughton, P.D., McCaffrey, W.D., Archer, S.G., and Hakes, B., 2008, Development of rheological heterogeneity in clay-rich high-density turbidity currents: Aptian Britannia Sandstone Member, UK continental shelf: *Journal of Sedimentary Research*, v. 78, p. 45–68.

Bartoli, G., Sarnthein, M., Weinelt, M., Erlenkeuser, H., Garbe-Schönberg, D., and Lea, D.W., 2005, Final closure of Panama and the onset of northern hemisphere glaciation: *Earth and Planetary Science Letters*, v. 237, p. 33–44.

Belaústegui, Z., and de Gibert, J.M., 2013, Bow-shaped, concentrically laminated polychaete burrows: A *Cylindrichnus concentricus* ichnofabric from the Miocene of Tarragona, NE Spain: *Palaeogeography, Palaeoclimatology, Palaeoecology*, v. 381, p. 119–127.

Bhattacharjee, D., Ghosh, S.K., Roychaudhuri, S., and Biswas, N.R., 2006, Quaternary sedimentary environments in Ganga prodeltaic region, northern part of Bay of Bengal: Geological Society of India, v. 67, p. 585–593.

Bhattacharya, J.P., 2006, Deltas: *SEPM Special Publication*, v. 84, 237 p.

Bhattacharya, J.P., and Walker, R.G., 1992, Deltas. *In* Walker, R.G., and James, N.P. (Eds.), Facies Models: Response to Sea-level Change: *Geological Association of Canada*, p. 157–177.

Bhattacharya, J.P., and Giosan, L., 2003, Wave-influenced deltas: geomorphological implications for facies reconstructions: *Sedimentology*, v. 50, p. 187–210.

Bhattacharya, J.P., and MacEachern, J.A., 2009, Hyperpycnal rivers and prodeltaic shelves in the Cretaceous Seaway of North America: *Journal of Sedimentary Research*, v. 79, p. 184–209.

Boettcher, S.S., Jackson, J.L., Quinn, M.J., and Neal, J.E., 2003, Lithospheric structure and supracrustal hydrocarbon systems, offshore eastern Trinidad. *In* Bartolini, C., Buffler, R.T., and Blickwede, J. (Eds.), The Circum-Gulf of Mexico and the Caribbean: Hydrocarbon habitats, basin formation, and plate tectonics: *AAPG Memoir*, v. 79, p. 529–544.

Böer, S.I., Al-Raei, A.M., Böttcher, M.E., Volkenborn, N., and Ramette, A., 2008, Spatial and temporal variations in bacterial activities and community structure associated with faunal

exclusion experiments in intertidal sands of the North Sea (Sylt): *Investigation of the distribution and activity of benthic microorganisms in coastal habitats*, Bremen, Germany, p. 133–168.

Böttger, S.A., Walker, C.W., and Unuma, T., 2004, Care and maintenance of adult echinoderms: *Methods in cell biology*, v. 74, p. 17–38.

Bouma, A.H., 1962, Sedimentology of some flysch deposits: A graphic approach to facies interpretation: *Elsevier*, Amsterdam, Netherlands, 168 p.

Bourgeois, S., Pruski, A.M., Sun, M.Y., Buscail, R., Lantoine, F., Kerhervé, P., Vétion, G., Rivière, B. and Charles, F., 2011, Distribution and lability of land-derived organic matter in the surface sediments of the Rhône prodelta and the adjacent shelf (Mediterranean Sea, France): a multi proxy study: *Biogeosciences*, v. 8, p.3107–3125.

Bourget, J., Ainsworth, R.B., and Thompson, S., 2014, Seismic stratigraphy and geomorphology of a tide or wave dominated shelf-edge delta (NW Australia): process-based classification from 3D seismic attributes and implications for the prediction of deep-water sands: *Marine and Petroleum Geology*, v. 57, p. 359–384.

Bowman, A.P., 2003, Sequence Stratigraphy and Reservoir Characterisation in the Columbus Basin, Trinidad: Ph.D. Thesis, *Imperial College London*, UK, 530 p.

Bowman, A.P., and Johnson, H.D., 2006, Storm dominated shelf edge deltas in a high accommodation setting; an outcrop example from the Columbus Basin, Trinidad, West Indies: *AAPG Search and Discovery Article* # 90057.

Bowman, A.P., and Johnson, H.D., 2014, Storm-dominated shelf-edge delta successions in a high accommodation setting: The palaeo-Orinoco Delta (Mayaro Formation), Columbus Basin, South-East Trinidad: *Sedimentology*, v. 61, p. 792–835.

Boyd, R., Suter, J., and Penland, S., 1989, Sequence stratigraphy of Mississippi delta evolution: *Gulf Coast Association of Geological Societies Transactions*, v. 39, p. 331–340.

Bromley, R., and Ekdale, A., 1984, *Chondrites*: a trace fossil indicator of anoxia in sediments: *Science*, v. 224, p. 872–874.

Bromley, R., and Asgaard, U., 1991, Ichnofacies: a mixture of taphofacies and biofacies: *Lethaia*, v. 24, p. 152–163.

Buatois, L.A., and López Angriman, A., 1992, Trazas fósiles y sistemas deposicionales, Grupo Gustav, Cretácico de la isla James Ross: *Geología de la Isla James Ross. Antártida, Instituto Antártico Argentino*, Buenos Aires, p. 239–262.

Buatois, L.A., and Mángano, M.G., 2011, Ichnology: Organism-substrate interactions in space and time: *Cambridge University Press*, Cambridge, UK, 358 p.

Buatois, L.A., Mángano, M.G., Maples, C.G., and Lanier, W.P., 1998, Allostratigraphic and sedimentologic applications of trace fossils to the study of incised estuarine valleys: an example from the Virgilian Tonganoxie Sandstone Member of Eastern Kansas: *Current Research in Earth Sciences*, v. 241, p. 1–27.

Buatois, L.A., Mángano, M.G., Alissa, A., and Carr, T.R., 2002, Sequence stratigraphic and sedimentologic significance of biogenic structures from a late Paleozoic marginal-to open-marine reservoir, Morrow Sandstone, subsurface of southwest Kansas, USA: *Sedimentary Geology*, v. 152, p. 99–132.

Buatois, L.A., Gingras, M.K., MacEachern, J., Mángano, M.G., Zonneveld, J.P., Pemberton, S.G., Netto, R.G., and Martin, A., 2005, Colonization of brackish-water systems through time: evidence from the trace-fossil record: *Palaios*, v. 20, p. 321–347.

Buatois, L.A., Netto, R.G., and Mángano, M.G., 2007, Ichnology of Permian marginal-marine to shallow-marine coal-bearing successions: Rio Bonito and Palermo Formations, Parana Basin, Brazil. *In* MacEachern, J.A., Bann, K.L., Gingras, M.K., and Pemberton, S.G. (Eds.), Applied Ichnology: *SEPM Short Course Notes*, v. 52, p. 167–177.

Buatois, L.A., Santiago, N., Parra, K., and Steel, R., 2008, Animal-substrate interactions in an early Miocene wave-dominated tropical delta: delineating environmental stresses and depositional dynamics (Tacata Field, eastern Venezuela): *Journal of Sedimentary Research*, v. 78, p. 458–479.

Buatois, L.A., Saccavino, L.L., and Zavala, C., 2011, Ichnologic signatures of hyperpycnal flow deposits in Cretaceous river-dominated deltas, Austral Basin, southern Argentina. *In* Slatt, R.M., and Zavala, C. (Eds.), Sediment transfer from shelf to deep water – Revisiting the delivery system: *AAPG Studies in Geology*, v. 61, p. 153–170.

Buatois, L.A., Santiago, N., Herrera, M., Plink-Björklund, P., Steel, R., Espin, M., and Parra, K., 2012, Sedimentological and ichnological signatures of changes in wave, river and tidal influence along a Neogene tropical deltaic shoreline: *Sedimentology*, v. 59, p. 1568–1612.

Callec, Y., Deville, E., Desaubliaux, G., Griboulard, R., Huyghe, P., Mascle, A., Mascle, G., Noble, M., Padron de Carrillo, C., and Schmitz, J., 2010, The Orinoco turbidite system: Tectonic controls on sea-floor morphology and sedimentation: *AAPG Bulletin*, v 94, p. 869–887.

Carmona, N.B., Ponce, J.J., Mángano, M.G., and Buatois, L.A., 2006, Variabilidad de la icnofacies de *Glossifungites* en el contacto entre las Formaciones Sarmiento (Eoceno

medio-Mioceno temprano) y Chenque (Mioceno temprano) en el Golfo San Jorge, Chubut, Argentina: *Ameghiniana*, v. 43, p. 413–425.

Carmona, N.B., Mángano, M.G., Buatois, L.A., and Ponce, J.J., 2007, Bivalve trace fossils in an early Miocene discontinuity surface in Patagonia, Argentina: burrowing behavior and implications for ichnotaxonomy at the firmground-hardground divide: *Palaeogeography, Palaeoclimatology, Palaeoecology*, v. 255, p. 329–341.

Carmona, N.B., Buatois, L., Mángano, M.G., and Bromley, R.G., 2008, Ichnology of the Lower Miocene Chenque Formation, Patagonia, Argentina: Animal-substrate interactions and the modern evolutionary fauna: *Ameghiniana*, v. 45, p. 93–122.

Carmona, N.B., Buatois, L.A., Ponce, J.J., and Mángano, M.G., 2009, Ichnology and sedimentology of a tide-influenced delta, Lower Miocene Chenque Formation, Patagonia, Argentina: trace-fossil distribution and response to environmental stresses: *Palaeogeography, Palaeoclimatology, Palaeoecology*, v. 273, p. 75–86.

Catuneanu, O., 2006, Principles of sequence stratigraphy: *Elsevier*, Amsterdam, Netherlands, 375 p.

Catuneanu, O., Abreu, V., Bhattacharya, J.P., Blum, M.D., Dalrymple, R.W., Eriksson, P.G., Fielding, C.R., Fisher, W.L., Galloway, W.E., Gibling, M.R., Giles, K.A., Holbrook, J.M., Jordan, R., Kendall, C.G.St.C., Macurda, B., Martinsen, O.J., Miall, A.D., Neal, J.E., Nummedal, D., Pomar, L., Posamentier, H.W., Pratt, B.R., Sarg, J.F., Shanley, K.W., Steel, R.J., Strasser, A., Tucker, M.E., and Winker, C., 2009, Towards the standardization of sequence stratigraphy: *Earth-Science Reviews*, v. 92, p. 1–33.

Catuneanu, O., Bhattacharya, J.P., Blum, M.D., Dalrymple, R.W., Eriksson, P.G., Fielding, C.R., Fisher, W.L., Galloway, W.E., Gianolla, P., Gibling, M.R., Giles, K.A., Holbrook, J.M., Jordan, R., Kendall, C.G.St.C., Macurda, B., Martinsen, O.J., Miall, A.D., Nummedal, D., Posamentier, H.W., Pratt, B.R., Shanley, K.W., Steel, R.J., Strasser, A., and M.E. Tucker, 2010, Sequence stratigraphy: common ground after three decades of development: *First Break*, v. 28, p. 21–34.

Catuneanu, O., and Zecchin, M., 2013, High-resolution sequence stratigraphy of clastic shelves II: Controls on sequence development: *Marine and Petroleum Geology*, v. 39, p. 26–38.

Chakraborty, A., and Bhattacharya, H.N., 2005, Ichnology of a Late Paleozoic (Permo-carboniferous) glaciomarine deltaic environment, Talchir Formation, Saharjuri Basin, India: *Ichnos*, v. 12, p. 31–45.

Chaplin, J.R., 1996, Ichnology of transgressive-regressive surfaces in mixed carbonate-siliciclastic sequences, Early Permian Chase Group, Oklahoma: *Geological Society of America Special Papers*, v. 306, p. 399–418.

Chen, S., Steel, R.J., Dixon, J.F., and Osman, A., 2014, Facies and architecture of a tide-dominated segment of the Late Pliocene Orinoco Delta (Morne L'Enfer Formation) SW Trinidad: *Marine and Petroleum Geology*, v. 57, p. 208–232.

Clifton, H.E., and Thompson, J.K., 1978, *Macaronichnus segregatis*: a feeding structure of shallow marine polychaetes: *Journal of Sedimentary Research*, v. 48, p. 1293–1301.

Coates, L., and MacEachern, J.A., 1999, The ichnological signature of wave-and river-dominated deltas: Dunvegan and Basal Belly River formations, West-Central Alberta: *Digging Deeper, Finding a Better Bottom Line, CSPG and the Petroleum Society of CIM Joint Conference*, 1999, p. 29–46.

Cohen, K.M., Finney, S.C., Gibbard, P.L., and Fan, J.-X., 2013 (updated), The ICS International Chronostratigraphic Chart: *Episodes*, v. 36, p. 199–204.

Corbeanu, R.M., Wizevich, M.C., Bhattacharya, J.P., Zeng, X., and McMechan, G.A., 2004, Three-dimensional architecture of ancient lower delta-plain point bars using ground-penetrating radar, Cretaceous Ferron Sandstone, Utah. *In* Chidsey, J.T.C., Adams, R.D., and Morris, T.H. (Eds.), Regional to wellbore analog for fluvial-deltaic reservoir modeling: the Ferron Sandstone of Utah: *AAPG Studies in Geology*, v. 50, p. 285–309.

Correggiari, A., Cattaneo, A., and Trincardi, F., 2005, The modern Po Delta system: lobe switching and asymmetric prodelta growth: *Marine Geology*, v. 222, p. 49–74.

Covault, J.A., Romans, B.W., and Graham, S.A., 2009, Outcrop expression of a continental-margin-scale shelf-edge delta from the Cretaceous Magallanes Basin, Chile: *Journal of Sedimentary Research*, v. 79, p. 523–539.

Cummings, D.I., Arnott, R.W.C., and Hart, B.S., 2006, Tidal signatures in a shelf-margin delta: *Geology*, v. 34, p. 249–252.

Dalrymple, R.W., 2010, Tidal depositional systems. *In* James, N.P., and Dalrymple, R.W. (Eds.), Facies Models 4: *Geological Association of Canada*, p.201–231.

Dan, S., Walstra, D.J.R., Stive, M.J., and Panin, N., 2011, Processes controlling the development of a river mouth spit: *Marine Geology*, v. 280, p. 116–129.

Dasgupta, S., and Buatois, L.A., 2012, Unusual occurrence and stratigraphic significance of the *Glossifungites* ichnofacies in a submarine paleo-canyon – Example from a Pliocene shelf-edge delta, Southeast Trinidad: *Sedimentary Geology*, v. 269–270, p. 69–77.

Dasgupta, S., and Buatois, L.A., 2015, High-frequency stacking pattern and stages of canyon/gully evolution across a forced regressive shelf-edge delta-front: *Marine and Petroleum Geology*, http://dx.doi.org/10.1016/j.marpetgeo.2015.08.003, in press.

Dasgupta, S., Buatois, L.A., and Mángano, M.G., 2015, Living on the edge: evaluating the impact of stress factors on animal-sediment interactions within subenvironments of a shelf-margin delta, the Neogene Mayaro Formation of Trinidad: *Journal of Sedimentary Research*, in revision.

Dasgupta, S., Buatois, L.A., Zavala, C., Mángano, M.G., and Törő, B., in review, Ichnology of a late Pliocene hyperpycnal system, Morne L'Enfer Formation, Fullarton, Trinidad: Implications for recognition of autogenic erosional surface and delineation of stress factors on irregular echinoids: *Palaeogeography, Palaeoclimatology, Palaeoecology*.

Dashtgard, S.E., 2011, Linking invertebrate burrow distributions (neoichnology) to physicochemical stresses on a sandy tidal flat: implications for the rock record: *Sedimentology*, v. 58, p. 1303–1325.

Dashtgard, S.E., and Gingras, M.K., 2012, Marine invertebrate neoichnology. *In* Knaust, D., and Bromley, R.G. (Eds.), Trace Fossils as Indicators of Sedimentary Environments: *Developments in Sedimentology*, *Elsevier*, Amsterdam, v. 64, p. 273–295.

de Gibert, J.M., and Goldring, R., 2008, Spatangoid-produced ichnofabrics (Bateig Limestone, Miocene, Spain) and the preservation of spatangoid trace fossils: *Palaeogeography, Palaeoclimatology, Palaeoecology*, v. 270, p. 299–310.

de Gibert, J.M., and Martinell, J., 1992, Principales estructuras biogénicas en el Plioceno marino de la Cuenca del Baix Llobregat (Catalunya): *Geogaceta*, v. 12, p. 104–106.

de Gibert, J.M., and Martinell, J., 1993, Controles paleoambientales sobre la distribución de las paleoicnocenosis en el Estuario plioceno del Baix Llobregat: *Revista española de paleontología*, v. 8, p. 140–146.

de Gibert, J.M., and Martinell, J., 1996, Trace fossil assemblages and their palaeoenvironmental significance in the Pliocene marginal marine deposits of the Baix Ebre (Catalonia, NE Spain): *Géologie Méditerranéenne*, v. 23, p. 211–225.

De Mowbray, T., and Visser, M.J., 1984, Reactivation surfaces in subtidal channel deposits, Oosterschelde, Southwest Netherlands: *Journal of Sedimentary Research*, v. 54, p. 811–824.

DiCroce, J., Bally, A.W., and Vail, P., 1999, Sequence stratigraphy of the eastern Venezuelan basin. *In* Mann, P. (Ed.), Caribbean Basins: Sedimentary Basins of the World, v. 4: *Elsevier Science B.V.*, Amsterdam, Netherlands, p. 419–476.

Dixon, J.F., Steel, R.J., and Olariu, C., 2012a, River-dominated, shelf-edge deltas: delivery of sand across the shelf break in the absence of slope incision: *Sedimentology*, v. 59, p. 1133–1157.

Dixon, J.F., Steel, R.J., and Olariu, C. 2012b, Shelf-edge delta regime as a predictor of deep-water deposition: *Journal of Sedimentary Research*, v. 82, p. 681–687.

Dixon, J.F., Steel, R.J., and Olariu, C., 2013, A model for cutting and healing of deltaic mouth bars at the shelf edge: mechanism for basin-margin accretion: *Journal of Sedimentary Research*, v. 83, p. 284–299.

Donovan, S.K., and Jackson, T.A., 1994, Caribbean Geology an Introduction: *The University of the West Indies Publishers' Association*, Mona, Jamaica, p. 209–228.

Draganits, E., and Noffke, N., 2004, Siliciclastic stromatolites and other microbially induced sedimentary structures in an early Devonian barrier-island environment (Muth Formation, NW Himalayas): *Journal of Sedimentary Research*, v. 74, p. 191–202.

Dumas, S., and Arnott, R.W.C, 2006, Origin of hummocky and swaley cross-stratification – the controlling influence of unidirectional current strength and aggradation rate: *Geology*, v. 34, p. 1073–1076.

Dumas, S., Arnott, R.W.C., and Southard, J.B., 2005, Experiments on oscillatory-flow and combined-flow bed forms: implications for interpreting parts of the shallow-marine sedimentary record: *Journal of Sedimentary research*, v. 75, p. 501–513.

Dunham, J., Frankforter, M., Kramer, D., and Weihe, J., 1996, Thin-skinned deformation of the Cretaceous and Tertiary section of eastern offshore Trinidad: *2nd AAPG/SVG International Congress Proceedings*, Caracas, Venezuela, p. A13.

Dykstra, M., 2012, Deep-water tidal sedimentology. *In* Davis, R.A. Jr., and Dalrymple, R.W., Principles of Tidal Sedimentology: *Springer*, Netherlands, p. 371–395.

Edwards, M.B., 1981, Upper Wilcox Rosita delta system of south Texas: growth-faulted shelf-edge deltas: *AAPG Bulletin*, v. 65, p. 54–73.

Ekdale, A., and Mason, T., 1988, Characteristic trace fossil assemblages in oxygen-poor sedimentary environments: *Geology*, v. 16, p. 720–723.

Embry, A.F., 1995, Sequence boundaries and sequence hierarchies: problems and proposals. *In* Steel, R.J., Felt, V.L., Johannessen, E.P., and Mathieu, C. (Eds.), Sequence stratigraphy on the Northwest European Margin: *Norwegian Petroleum Society Special Publication*, v. 5, p. 1–11.

Fagervold, S.K., Bourgeois, S., Pruski, A.M., Charles, F., Kerhervé, P., Vétion, G. and Galand, P.E., 2014, River organic matter shapes microbial communities in the sediment of the Rhône prodelta: *The ISME journal*, v. 8, p.2327–2338.

Fielding, C.R., Bann, K.L., Maceachern, J.A., Tye, S.C., and Jones, B.G., 2006, Cyclicity in the nearshore marine to coastal, Lower Permian, Pebbley Beach Formation, southern Sydney Basin, Australia: a record of relative sea-level fluctuations at the close of the Late Palaeozoic Gondwanan ice age: *Sedimentology*, v. 53, p. 435–463.

Flint, S.S., Hodgson, D.M., Sprague, A.R., Brunt, R.L., Van der Merwe, W.C., Figueiredo, J., Prélat, A., Box, D., Di Celma, C., and Kavanagh, J.P., 2011, Depositional architecture and sequence stratigraphy of the Karoo basin floor to shelf edge succession, Laingsburg depocentre, South Africa: *Marine and Petroleum Geology*, v. 28, p. 658–674.

Flood, R.P., Orford, J.D., McKinley, J.M., and Roberson, S., 2015, Effective grain size distribution analysis for interpretation of tidal–deltaic facies: West Bengal Sundarbans: *Sedimentary Geology*, v. 318, p. 58–74.

Franco, M.A., De Mesel, I., Demba Diallo, M., Van der Gucht, K., Van Gansbeke, D., van Rijswijk, P., Costa, M.J., Vincx, M., and Vanaverbeke, J., 2007, Effect of phytoplankton bloom deposition on benthic bacterial communities in two contrasting sediments in the southern North Sea: *Aquatic Microbial Ecology*, v. 48, p. 241–254.

Galloway, W.E., 1975, Process framework for describing the morphologic and stratigraphic evolution of deltaic depositional systems. *In* Broussard, M. (Ed.), Deltas, Models for Exploration: *Houston Geological Society*, Texas, p. 87–98.

Galloway, W.E., 2001, The many faces of submarine erosion: theory meets reality in selection of sequence boundaries: *AAPG Hedberg Research Conference on "Sequence Stratigraphic and Allostratigraphic Principles and Concepts" Programs and Abstracts Volume*, p. 28–29.

Galloway, W.E., 2004, Accommodation and the sequence stratigraphic paradigm: *Reservoir, CSPG*, v. 31, p. 9–10.

Galloway, W.E., and Hobday, D.K., 1996, Terrigenous Clastic Depositional Systems: *Springer*, Berlin, 489 p.

Gamero Diaz, H., Contreras, C., Lewis, N., Welsh, R., and Zavala, C., 2011, Evidence of Shelfal Hyperpycnal Deposition of Pliocene Sandstones in the Oilbird Field, Southeast Coast, Trinidad: Impact on Reservoir Distribution. *In* Slatt, R.M., and Zavala, C. (Eds.), Sediment transfer from shelf to deep water – Revisiting the delivery system: *AAPG Studies in Geology*, v. 61, p. 193–214.

Gani, M.R., and Bhattacharya, J.P., 2005, Lithostratigraphy versus chronostratigraphy in facies correlations of Quaternary deltas: Application of bedding correlation. *In* Giosan, L., and Bhattacharya, J.P. (Eds.), River delta: concepts, models, and examples: *SEPM special publication*, v. 83, p. 31–48.

Garciacaro, E., Mann, P., and Escalona, A., 2011a, Regional structure and tectonic history of the obliquely colliding Columbus foreland basin, offshore Trinidad and Venezuela: *Marine and Petroleum Geology*, v. 28, p. 126–148.

Garciacaro, E., Escalona, A., Mann, P., Wood, L., Moscardelli, L., and Sullivan, S., 2011b, Structural controls on Quaternary deepwater sedimentation, mud diapirism, and hydrocarbon distribution within the actively evolving Columbus foreland basin, eastern offshore Trinidad: *Marine and Petroleum Geology*, v. 28, p. 149–176.

Gardner, J.V., Dartnell, P., Mayer, L.A., Hughes Clarke, J.E., Calder, B.R., and Duffy, G., 2005, Shelf-edge deltas and drowned barrier–island complexes on the northwest Florida outer continental shelf: *Geomorphology*, v. 64, p. 133–166.

Garrison Jr., J.R., and Van den Bergh, T.C.V., 2004, High-resolution depositional sequence stratigraphy of the upper Ferron Sandstone Last Chance Delta: an application of coal-zone stratigraphy. *In* Chidsey, J.T.C., Adams, R.D., and Morris, T.H. (Eds.), Regional to wellbore analog for fluvial-deltaic reservoir modeling: the Ferron Sandstone of Utah: *AAPG Studies in Geology*, v. 50, p. 285–309.

Gérard, J., and Bromley, R., 2008, Ichnofabrics in clastic sediments: applications to sedimentological core studies: a practical guide: *Gérard, J.*, Madrid, Spain, 100 p.

Gibbard, P.L., Head, M.J., Walker, M.J.C., and the Subcommission on Quaternary Stratigraphy, 2010, Formal ratification of the Quaternary System/Period and the Pleistocene Series/Epoch with a base at 2.58 Ma: *Journal of Quaternary Science*, v. 25, p. 96–102.

Gibson, R.G., Meisling, K.E., and Sydow, J.C., 2012, Columbus Basin, offshore Trinidad: A detached pull apart basin in a transpressional foreland setting. *In* Roberts, D.G., and Bally, A.W. (Eds.), Regional geology and tectonics: Phanerozoic passive margins, cratonic basins and global tectonic maps: *Elsevier*, Amsterdam, Netherlands, v. 1C, p. 635–659.

Gingras, M.K., MacEachern, J.A., and Pemberton, S.G., 1998, A comparative analysis of the ichnology of wave-and river-dominated allomembers of the Upper Cretaceous Dunvegan Formation: *Bulletin of Canadian Petroleum Geology*, v. 46, p. 51–73.

Gingras, M.K., Armitage, I.A., Pemberton, S.G., and Clifton, H.E., 2007, Pleistocene walrus herds in the Olympic Peninsula area: Trace-fossil evidence of predation by hydraulic jetting: *Palaios*, v. 22, p. 539–545.

Gingras, M.K., Dashtgard, S.E., MacEachern, J.A., and Pemberton, S.G., 2008, Biology of shallow marine ichnology: a modern perspective: *Aquatic Biology*, v. 2, p. 255–268.

Giosan, L., 2007, Morphodynamic feedbacks on deltaic coasts: lessons from the wave-dominated Danube delta: *Coastal Sediments*, v. 2007, p. 828–841.

Giosan, L., and Bhattacharya, J.P., 2005, River Deltas: Concepts, Models, Case Studies: *SEPM Special Publication*, v. 83, 502p.

Giosan, L., Donnelly, J.P., Vespremeanu, E., Bhattacharya, J.P., Olariu, C., and Buonaiuto, F.S., 2005, River Delta Morphodynamics: Examples from the Danube Delta: *SEPM Special Publication*, v. 83, p. 393–411.

Green, A.N., Goff, J.A., and Uken, R., 2007, Geomorphological evidence for upslope canyon-forming processes on the northern KwaZulu-Natal shelf, SW Indian Ocean, South Africa: *Geo-Marine Letters*, v. 27, p. 399–409.

Gregory, M.R., 1991, New trace fossils from the Miocene of Northland, New Zealand: *Rorschachichnus amoeba* and *Piscichnus waitemata*: *Ichnos*, v. 1, p. 195–205.

Gulick, S.P., Goff, J.A., Austin, J.A., Alexander, C.R., Nordfjord, S., and Fulthorpe, C.S., 2005, Basal inflection-controlled shelf-edge wedges off New Jersey track sea-level fall: *Geology*, v. 33, p. 429–432.

Hansen, C.D., and MacEachern, J.A., 2007, Application of the asymmetric delta model to along-strike facies variations in a mixed wave- and river-influenced delta lobe, Upper Cretaceous Basal Belly River Formation, Central Alberta. *In* MacEachern, J.A., Bann, K.L., Gingras, M.K., and Pemberton, S.G. (Eds.), Applied ichnology: *SEPM short course notes*, v. 52, p. 1–16.

Harms, J.C., Southard, J.B. , Spearing, D.R., and Walker, R.G., 1975, Depositional environments as interpreted from primary sedimentary structures and stratification sequences: *SEPM Short Course Notes*, no. 2, 161 p.

Harms, J.C., Southard, J.B., and Walker, R.G., 1982, Structures and sequences in clastic rocks: *SEPM Short Course Notes*, no. 9, 249 p.

Harrison, T., Krigbaum, J., and Manser, J., 2006, Primate biogeography and ecology on the Sunda Shelf islands: a paleontological and zooarchaeological perspective. *In* Lehman, S.M., and Fleagle, J.G. (Eds.), Primate biogeography: *Springer*, USA, p. 331–372.

Haughton, P.D.W., Barker, S.P., and McCaffrey, W.M., 2003, Linked Debrites in sand-rich turbidite systems – origin and significance: *Sedimentology*, v. 50, p. 459–482.

Haughton, P., Davis, C., McCaffrey, W., and Barker, S., 2009, Hybrid sediment gravity flow deposits – Classification, origin and significance: *Marine and Petroleum Geology*, v. 26, p. 1900–1918.

Hayward, B.W., 1976, Lower Miocene bathyal and submarine canyon ichnocoenoses from Northland, New Zealand: *Lethaia*, v. 9, p. 149–162.

Hedges, J.I., Keil, R.G., and Benner, R., 1997, What happens to terrestrial organic matter in the ocean?: *Organic geochemistry*, v. 27, p. 195–212.

Hickson, T.A., and Lowe, D.R., 2002, Facies architecture of a submarine fan channel–levee complex: the Juniper Ridge Conglomerate, Coalinga, California: *Sedimentology*, v. 49, p. 335-362.

Hobday, D.K., and Tavener-Smith, R., 1975, Trace fossils in the Ecca of northern Natal and their palaeoenvironmental significance: *Palaeontologia Africana*, v. 18, p. 47–52.

Hooghiemstra, H., and Ran, E.T.H., 1994, Late Pliocene-Pleistocene high resolution pollen sequence of Colombia: An overview of climatic change: *Quaternary International*, v. 21, p. 63–80.

Howard, J.D., 1978, Sedimentology and trace fossils. *In* Basan, P.B. (Ed.), Trace fossil concepts: *SEPM Short Course Notes*, v. 5, p. 11–42.

Hubbard, S.M., and Shultz, M.R., 2008, Deep burrows in submarine fan-channel deposits of the Cerro Toro Formation (Cretaceous), Chilean Patagonia: Implications for firmground development and colonization in the deep sea: *Palaios*, v. 23, p. 223–232.

Hubbard, S.M., Romans, B.W., and Graham, S.A., 2008, Deep-water foreland basin deposits of the Cerro Toro Formation, Magallanes basin, Chile: Architectural elements of a sinuous basin axial channel belt: *Sedimentology*, v. 55, p. 1333-1359.

Ingersoll, R.V. and Graham, S.A., 1983, Recognition of the shelf-and-slope break along ancient, tectonically active continental margins. *In* Stanley, D.J., and Moore, G.T. (Eds.), The Shelfbreak: Critical Interface on Continental Margins: *SEPM Special Publication*, v. 33, p. 107–120.

Ittekkot, V., 1988, Global trends in the nature of organic matter in river suspensions: *Nature*, v. 332, p. 436–438.

Jones, B.M., 2013, Integrated Ichnology and Sedimentology of Mixed River- and Wave-Influenced Delta Complexes, Upper Cretaceous Basal Belly River Formation, Central Alberta, Canada: M.Sc. Thesis, Simon Fraser University, Canada, 204 p.

Kao, S.J., Dai, M., Selvaraj, K., Zhai, W., Cai, P., Chen, S.N., Yang, J.Y.T., Liu, J.T., Liu, C.C., and Syvitski, J.P., 2010, Cyclone-driven deep sea injection of freshwater and heat by hyperpycnal flow in the subtropics: *Geophysical Research Letters*, v. 37, http://dx.doi.org/10.1029/2010GL044893.

King, J.E., 1983, Seals of the world (2nd Edition): *British Museum of Natural History*, 240 p.

Kolla, V., Biondi, P., Long, B., and Fillon, R., 2000, Sequence stratigraphy and architecture of the Late Pleistocene Lagniappe delta complex, northeast Gulf of Mexico: *Geological Society of London*, Special Publications, v. 172, p. 291–327.

Kolla, V., Fillon, R.H., Roberts, H.H., Kohl, B., and Long, B., 2003, Late Pleistocene sequence stratigraphy of the shelf-edge and upper slope in the Viosca Knoll Area of the northeast Gulf of Mexico. *In* Roberts, H.H., Rosen, N.C., Fillon, R.H., and Anderso, J.B. (Eds.), Shelf Margin Deltas and Linked Downslope Petroleum Systems: *23rd Annual GCSSEPM Foundation Bob F. Perkins Research Conference*, p. 79–90.

Kolla, V., Posamentier, H.W., and Wood, L.J., 2007, Deep-water and fluvial sinuous channels – Characteristics, similarities and dissimilarities, and modes of formation: *Marine and Petroleum Geology*, v. 24, p. 388–405.

Korus, J.T., and Fielding, C.R., 2015, Asymmetry in Holocene river deltas: Patterns, controls, and stratigraphic effects: *Earth-Science Reviews*, v. 150, p. 219–242.

Kotake, N., 2007, *Macaronichnus* isp. associated with *Piscichnus waitemata* in the Miocene of Yonaguni-jima Island, southwest Japan. *In* Miller, W. III (Ed.), Trace Fossils: Concepts, Problems, Prospects: *Elsevier*, Amsterdam, p. 492–501.

Kotake, N., and Nara, M., 2002, The Ichnofossil Piscichnus waitemata: Biogenic Sedimentary Structure Produced by the Foraging Behavior Using Water Jet: *Journal of the Geological Society of Japan*, v. 108, p. I–II.

Krapez, B., 1997, Sequence-stratigraphic concepts applied to the identification of depositional basins and global tectonic cycles: *Australian Journal of Earth Sciences*, v. 44, p. 1–36.

Kuehl, S.A., Levy, B.M., Moore, W.S., and Allison, M.A., 1997, Subaqueous delta of the Ganges-Brahmaputra river system: *Marine Geology*, v. 144, p. 81–96.

Kugler, H.G., 1956, Treatise on the geology of Trinidad. *In* Bolli, H.M., and Knappertsbusch, M. (Eds.), Treatise on the Geology of Trinidad: *Switerzland Museum of Natural History*, 309 p.

Kugler, H.G., 1959, Geological Map of Trinidad and Geological Sections through Trinidad: *Orell Fussli SA, Zurich and E. Stanford Limited*, London, not paginated.

Kugler, H.G., 1996, Part 3: 32 Detailed geological maps and sections with explanatory notes. *In* Bolli, H.M., and Knappertsbusch, M. (Eds.), Treatise on the Geology of Trinidad: *Museum of Natural History*, Basel, Switzerland, not paginated.

Kugler, H.G., 2001, Part 4: Paleocene to Holocene formations. *In* Bolli, H.M. and Knappertsbusch, M. (Eds.), Treatise on the geology of Trinidad: Museum of Natural History Basel, Basel, Switzerland, not paginated.

Lamb, M.P., Myrow, P.M., Lukens, C., Houck, K., and Strauss, J., 2008, Deposits from wave-influenced turbidity currents: Pennsylvanian Minturn Formation, Colorado, USA: *Journal of Sedimentary Research*, v. 78, p. 480–498.

Larsen, M., and Surlyk, F., 2003, Shelf-edge delta and slope deposition in the Upper Callovian – Middle Oxfordian Olympen Formation, East Greenland. The Jurassic of Denmark and Greenland: *Geological Survey of Denmark and Greenland Bulletin*, v. 1, p. 931–948.

Law, C.J., Dorgan, K.M., and Rouse, G.W., 2014, Relating divergence in polychaete musculature to different burrowing behaviors: a study using Opheliidae (Annelida): *Journal of Morphology*, v. 275, p. 548–571.

Leonard, R., 1983, Geology and hydrocarbon accumulations, Columbus basin, offshore Trinidad: *AAPG Bulletin*, v. 67, p. 1081–1093.

Lewis, D.W., and Ekdale, A.A., 1991, Lithofacies relationships in a Late Quaternary gravel and loess fan delta complex, New Zealand: *Palaeogeography, Palaeoclimatology, Palaeoecology*, v. 81, p. 229–251.

Li, W., Bhattacharya, J.P., Zhu, Y., Garza, D., and Blankenship, E., 2011, Evaluating delta asymmetry using three-dimensional facies architecture and ichnological analysis, Ferron 'Notom Delta', Capital Reef, Utah, USA: *Sedimentology*, v. 58, p. 478–507.

Liu, J.T., and Lin, H.L., 2004, Sediment dynamics in a submarine canyon: a case of river-sea interaction: *Marine Geology*, v. 207, p. 55–81.

Lobza, V., and Schieber, J., 1999, Biogenic sedimentary structures produced by worms in soupy, soft muds: observations from the Chattanooga Shale (Upper Devonian) and experiments: *Journal of Sedimentary Research*, v. 69, p. 1041–1049.

Lohrenz, S.E., Fahnenstiel, G.L., Redalje, D.G., Lang, G.A., Dagg, M.J., Whitledge, T.E., and Dortch, Q., 1999, Nutrients, irradiance, and mixing as factors regulating primary production in coastal waters impacted by the Mississippi River plume: *Continental Shelf Research*, v. 19, p. 1113–1141.

Lowe, D.R., 1982, Sediment gravity flows: II. Depositional models with special reference to the deposits of high-density turbidity currents: *Journal of Sedimentary Petrology*, v. 52, p. 279–297.

Lowe, D.R., and Guy, M., 2000, Slurry-flow deposits in the Britannia Formation (Lower Cretaceous), North Sea: a new perspective on the turbidity current and debris flow problem: *Sedimentology*, v. 47, p. 31–70.

Lowe, D.R., Guy, M., and Palfrey, A., 2003, Facies of slurry-flow deposits, Britannia Formation (lower Cretaceous), North Sea: implications for flow evolution and deposit geometry: *Sedimentology*, v. 50, p. 45–80.

Löwemark, L., 2015, Evidence for targeted elasmobranch predation on thalassinidean shrimp in the Miocene Taliao Formation, NE Taiwan: *Lethaia*, v. 48, p. 227–234.

MacEachern, J.A., and Pemberton, S.G., 1992, Ichnological aspects of Cretaceous shoreface successions and shoreface variability in the Western Interior Seaway of North America. *In* Pemberton, S.G. (Ed.), Applications of ichnology to petroleum exploration: A core workshop: *SEPM Core Workshop*, v. 17, p. 57–84.

MacEachern, J.A., and Pemberton, S.G., 1994, Ichnological aspects of incised valley fill systems from the Viking Formation of the Western Canada Sedimentary Basin, Alberta, Canada. *In* Boyd, R., Zaitlin, B.A., and Dalrymple, R. (Eds.), Incised Valley Systems: Origin and Sedimentary Sequence: *SEPM Special Publication*, v. 51, p. 129–157.

MacEachern, J.A., Raychaudhuri, I., and Pemberton, S.G., 1992, Stratigraphic applications of the *Glossifungites* ichnofacies: delineating discontinuities in the rock record. *In* Pemberton, S.G. (Ed.), Applications of Ichnology to Petroleum Exploration: *A Core Workshop. SEPM Core Workshop*, No. 17, Tulsa, USA, p. 169–198.

MacEachern, J.A., Zaitlin, B.A., and Pemberton, S.G., 1999, A sharp-based sandstone of the Viking Formation, Joffre Field, Alberta, Canada: criteria for recognition of transgressively incised shoreface complexes: *Journal of Sedimentary Research*, v. 69, p. 876–892.

MacEachern, J.A., Bann, K.L., Bhattacharya, J.P., and Howell, Jr., C.D., 2005, Ichnology of deltas: organism responses to the dynamic interplay of rivers, waves, storms, and tides. *In* Giosan, L., and Bhattacharya, J.P. (Eds.), River delta: concepts, models, and examples: *SEPM special publication*, v. 83, p. 49–85.

MacEachern, J.A., Bann, K.L., Pemberton, S.G., and Gingras, M.K., 2007a, The ichnofacies paradigm: high resolution paleo-environmental interpretation of the rock record. *In* MacEachern, J.A., Bann, K.L., Gingras, M.K., and Pemberton, S.G. (Eds.), Applied ichnology: *SEPM short courses*, v. 52, p. 27–64.

MacEachern, J.A., Pemberton, S.G., and Bhattacharya, J.P., 2007b, Ichnological and sedimentological evaluation of the Ferron Sandstone Cycles in Ivie Creek Cores # 3 and # 11. *In* MacEachern, J.A., Gingras, M.K., Bann, K.L., and Pemberton, S.G. (Eds.),

Ichnological applications to sedimentological and sequence stratigraphic problems: *SEPM research conference abstract volume*, p. 144–174.

MacEachern, J.A., Dashtgard, S.E., Knaust, D., Cataneanu, O., Bann, K.L., and Pemberton, S.G., 2012, Sequence stratigraphy. *In* Knaust, D., and Bromley, R.G. (Eds.), Trace fossils as indicators of sedimentary environments: *Developments in Sedimentology*, v. 64, *Elsevier*, Amsterdam, p. 157–194.

Macready, G.A., 1921, Petroleum Industry of Trinidad: *Transactions of the AIME*, v. 65, p. 58–68.

Mángano, M.G., Buatois, L.A., and Muñiz Guinea, F., 2005, Ichnology of the Alfarcito Member (Santa Rosita Formation) of northwestern Argentina: Animal-substrate interactions in a lower Paleozoic wave-dominated shallow sea: *Ameghiniana*, v. 42, p. 641–668.

Manning, P., 2003, Parliamentary discussions on Finance Committee Report (Friday, September 12, 2003): *Proceedings of House of Representatives of the Republic of Trinidad and Tobago*, http://www.ttparliament.org/hansards/hh20030912.pdf.

Marcano, J., and Pinto, D., 2009, Resumen de Asistencia al "Riomar Paleo Orinoco Field Seminar": proprietary report, unpublished.

Martin, K.D., 2004, A re-evaluation of the relationship between trace fossils and dysoxia. *In* McIlroy, D. (Ed.), The application of ichnology to palaeoenvironmental and stratigraphic analysis: *Geological Society of London*, Special Publications, v. 228, p. 141–156.

Martinell, J., and Domènech, R., 1995, Bioerosion structures on the Pliocene rocky shores of Catalonia (Spain). *Revista española de paleontología*, v. 10, p. 37–44.

Martinius, A.W., Kaas, I., Helgesen, G., and Leith, D.A., 2001, Sedimentology of the heterolithic and tide-dominated Tilje Formation (Early Jurassic, Halten Terrace, offshore mid-Norway): *Norwegian Petroleum Society Special Publications*, v. 10, p.103–144.

Mayall, M.J., Yeilding, C.A., Oldroyd, J.D., Pulham, A.J., and Sakurai, S., 1992, Facies in a shelf-edge delta – an example from the subsurface of the Gulf of Mexico, Middle Pliocene, Mississippi Canyon, Block 109 (1): *AAPG Bulletin*, v. 76, p. 435–448.

Mayoral, E., and Muñiz, F., 2001, New ichnospecies of *Cardioichnus* from the Miocene of the Guadalquivir Basin, Huelva, Spain: *Ichnos*, v. 8, p. 69–76.

McEdward, L.R., 1997, Reproductive strategies of marine benthic invertebrates revisited: facultative feeding by planktotrophic larvae: *The American Naturalist*, v. 150, p. 48–72.

McIlroy, D., 2004, Some ichnological concepts, methodologies, applications and frontiers: *Geological Society of London*, Special Publications, v. 228, p. 3–27.

McIlroy, D., 2007, Lateral variability in shallow marine ichnofabrics: implications for the ichnofabric analysis method: *Journal of the Geological Society*, v. 164, p. 359–369.

Mellere, D., Plink-Björklund, P., and Steel, R., 2002, Anatomy of shelf deltas at the edge of a prograding Eocene shelf margin, Spitsbergen: *Sedimentology*, v. 49, p. 1181–1206.

Metaxas, A., and Young, C.M., 1998, Behaviour of echinoid larvae around sharp haloclines: effects of the salinity gradient and dietary conditioning: *Marine Biology*, v. 131, p. 443–459.

Miall, A.D., 2010, The geology of stratigraphic sequences: 2nd Edition. *Springer*, New York, 520 p.

Michelson, J.E., 1976, Miocene deltaic oil habit, Trinidad: *AAPG Bulletin*, v. 60, p. 1502–1519.

Middleton, G.V., 1973, Johannes Walther's Law of the Correlation of Facies: *Geological Society of America Bulletin*, v. 84, p. 979–988.

Milliman, J.D., and Kao, S.J., 2005, Hyperpycnal discharge of fluvial sediment to the ocean: Impact of Super-Typhoon Herb (1996) on Taiwanese rivers: *The Journal of geology*, v. 113, p. 503–516.

Monaco, P., 1995, Relationships between trace-fossil communities and substrate characteristics in some Jurassic pelagic deposits in the Umbria-Marche basin, central Italy: *Geobios*, v. 28, p. 299–311.

Monaco, P., Caracuel, J.E., Giannetti, A., Soria, J.M., and Yébenes, A., 2007, *Thalassinoides* and *Ophiomorpha* as cross-facies trace fossils of crustaceans from shallow-to-deep-water environments, Mesozoic and Tertiary examples from Italy and Spain. *In* Garassino, A., Feldmann, R.M., and Teruzzi, G. (Eds.), 3rd Symposium on Mesozoic and Cenozoic Decapod Crustaceans: *Memorie della Società Italiana di Scienze Naturali e del Museo Civico di Storia Naturale di Milano*, v. 35, p. 79–82.

Moscardelli, L., and Wood, L., 2008, New classification system for mass transport complexes in offshore Trinidad: *Basin Research*, v. 20, p. 73–98.

Moscardelli, L., Hornbach, M., and Wood, L., 2010, Tsunamigenic risks associated with mass transport complexes in offshore Trinidad and Venezuela. *In* Mosher, D.C., Shipp, R.C., Moscardelli, L., Chaytor, J.D., Baxter, C.D.P., Lee, H.J., and Urgeles, R. (Eds.), Submarine mass movements and their consequences: *4th International Symposium*, *Springer*, Netherlands, p. 733–744.

Moscardelli, L., Wood, L.J., and Dunlap, D.B., 2012, Shelf-edge deltas along structurally complex margins: A case study from eastern offshore Trinidad: *AAPG Bulletin*, v. 96, p. 1483–1522.

Moslow, T.F., and Pemberton, S.G., 1988, An integrated approach to the sedimentological analysis of some lower Cretaceous shoreface and delta front sandstone sequences. *In* James, D.P., and Leckie, D.A. (Eds.), Sequences, Stratigraphy, Sedimentology; Surface and Subsurface: *CSPG Memoir*, v. 15, p. 373–386.

Moss-Russell, A., 2009, The stratigraphic architecture of a prograding shelf-margin delta in outcrop, the Sobrarbe Formation, Ainsa Basin, Spain: Masters Thesis, *Colorado School of Mines*, 192 p.

Mulder, T., Migeon, S., Savoye, B., and Faugères, J.C., 2001, Inversely graded turbidite sequences in the deep Mediterranean: a record of deposits from flood-generated turbidity currents?: *Geo-Marine Letters*, v. 21, p. 86–93.

Mulder, T., Syvitski, J.P., Migeon, S., Faugères, J.C., and Savoye, B., 2003, Marine hyperpycnal flows: initiation, behavior and related deposits. A review: *Marine and Petroleum Geology*, v. 20, p. 861–882.

Muto, T., Steel, R.J., and Swenson, J.B., 2007, Autostratigraphy: a framework norm for genetic stratigraphy: *Journal of Sedimentary Research*, v. 77, p. 2–12.

Mutti, E., Davoli, G., and Tinterri, R., 1994, Flood-related gravity-flow deposits in fluvial and fluvio-deltaic depositional systems and their sequence-stratigraphic implications. *In* Posamentier, H.W., and Mutti, E. (Eds.), Second high-resolution sequence stratigraphy conference, Tremp, Abstract Book: Italy: *Istituto di Geologia, Universita di Parma*, p. 137–143.

Nageswara Rao, K., Subraelu, P., Naga Kumar, K.C.V., Demudu, G., Hema Malini, B., and Rajawat, A.S., 2010, Impacts of sediment retention by dams on delta shoreline recession: evidences from the Krishna and Godavari deltas, India: *Earth Surface Processes and Landforms*, v. 35, p. 817–827.

Nelson, C.H., Maldonado, A., Coumes, F., Got, H., and Manaco, A., 1983, The Ebro deep-sea fan system: *Geo-marine letters*, v. 3, p. 125–131.

Neuberger, D.J., 1987, Swastika (Upper Pennsylvanian) shelf-margin deltas and delta-fed turbidites, Flowers" Canyon Sand" Field area, Stonewall County, Texas: M.A. Thesis, *University of Texas at Austin*, 171 p.

Nie, J., 2011, Coupled 100-kyr cycles between 3 and 1 Ma in terrestrial and marine paleoclimatic records: *Geochemistry Geophysics Geosystems*, v. 12, p. Q10Z32, http://dx.doi.org/10.1029/2011GC003772.

Niemeijer, A., Elsworth, D., and Marone, C., 2009, Significant effect of grain size distribution on compaction rates in granular aggregates: *Earth and Planetary Science Letters*, v. 284, p. 386–391.

Nienhuis, J.H., Ashton, A.D., and Giosan, L., 2015, What makes a delta wave-dominated?: *Geology*, v. 43, p. 511–514.

Nixon, M.F., and Grozic, J.L., 2007, Submarine slope failure due to gas hydrate dissociation: a preliminary quantification: *Canadian Geotechnical Journal*, v. 44, p. 314–325.

Olariu, C., and Bhattacharya, J.P., 2006, Terminal distributary channels and delta front architecture of river-dominated delta systems: *Journal of Sedimentary Research*, v. 76, 212–233.

Olariu, C., Steel, R.J., and Petter, A.L., 2010, Delta-front hyperpycnal bed geometry and implications for reservoir modeling: Cretaceous Panther Tongue delta, Book Cliffs, Utah: *AAPG bulletin*, v. 94, p. 819–845.

Olariu, M.I., Carvajal, C.R., Olariu, C., and Steel, R.J., 2012, Deltaic process and architectural evolution during cross-shelf transits, Maastrichtian Fox Hills Formation, Washakie Basin, Wyoming: *AAPG bulletin*, v. 96, p. 1931–1956.

Olariu, M.I., Hammes, U., and Ambrose, W.A., 2013, Depositional architecture of growth-fault related wave-dominated shelf edge deltas of the Oligocene Frio Formation in Corpus Christi Bay, Texas: *Marine and Petroleum Geology*, v. 48, p. 423–440.

Orton, G.J., and Reading, H.G., 1993, Variability of deltaic processes in terms of sediment supply, with particular emphasis on grain size: *Sedimentology*, v. 40, p. 475–512.

Osman, A., 2006, Deltaic to Estuarine Regime Change on the Proximal Paleo-Orinoco Shelf, Morne L'Enfer Formation, Trinidad: Masters Thesis, *University of Texas at Austin*, 105 p.

Patacci, M., Haughton, P.D., and McCaffrey, W.D., 2014, Rheological complexity in sediment gravity flows forced to decelerate against a confining slope, Braux, SE France: *Journal of Sedimentary Research*, v. 84, p. 270–277.

Patruno, S., Hampson, G.J., Jackson, C.A.L., and Dreyer, T., 2015, Clinoform geometry, geomorphology, facies character and stratigraphic architecture of a sand-rich subaqueous delta: Jurassic Sognefjord Formation, offshore Norway: *Sedimentology*, v. 62, p. 350–388.

Pattison, S.A., 2005, Storm-influenced prodelta turbidite complex in the Lower Kenilworth Member at Hatch Mesa, Book Cliffs, Utah, USA: implications for shallow marine facies models: *Journal of Sedimentary Research*, v. 75, p. 420–439.

Pechenik, J.A., Pearse, J.S., and Qian, P.Y., 2007, Effects of salinity on spawning and early development of the tube-building polychaete *Hydroides elegans* in Hong Kong: not just the sperm's fault?: *The Biological Bulletin*, v. 212, p. 151–160.

Pemberton, E.A., Hubbard, S.M., Fildani, A., Romans, B., and Kostic, S., 2015, The Stratigraphic Expression of Submarine Channel-Lobe Transitions: An Outcrop Example from Southern Chile: Geophysical Research Abstracts - EGU General Assembly, v. 17.

Pemberton, S.G., and Frey, R.W., 1985, The *Glossifungites* ichnofacies: modern examples from the Georgia coast, USA. *In* Curran, H.A. (Ed.), Biogenic Structures: Their use in interpreting depositional environments: *SEPM Special Publication*, v. 35, p. 237–259.

Pemberton, S.G., and MacEachern, J.A., 1995, The sequence stratigraphic significance of trace fossils: examples from the Cretaceous foreland basin of Alberta, Canada. *In* Van Wagoner, J.C., and Bertram, G. (Eds.), Sequence stratigraphy of foreland basin deposits – outcrop and subsurface examples from the Cretaceous of North America: *AAPG Memoir*, v. 64, p. 429–475.

Pemberton, S.G., and MacEachern, J.A., 1997, The ichnological signature of storm deposits: the use of trace fossils in event stratigraphy. *In* Brett, C.E., and Baird, G.C. (Eds.), Peleontological Events. Stratigraphic, Ecological, and Evolutionary Implications: *Columbia University Press*, New York, USA, p. 73–109.

Pemberton, S.G., MacEachern, J.A., and Frey, R.W., 1992, Trace fossils facies models: environmental and allostratigraphic significance. *In* Walker, R.G., and James, N.P. (Eds.), Facies Models and Sea Level Changes: *Geological Association of Canada*, St. Johns, Newfoundland, Canada, p. 47–72.

Pemberton, S.G., Spila, M., Pulham, A.J., Saunders,T., MacEachern, J.A., Robbins, D., and Sinclair, I.K., 2001, Ichnology and sedimentology of shallow to marginal marine systems: Ben Nevis and Avalon Reservoirs, Jeanne d'Arc Basin: *Geological Association of Canada*, Short course notes, St. Johns, Newfoundland, Canada, v. 15, 343 p.

Pemberton, S.G., MacEachern, J.A., and Saunders, T., 2004, Stratigraphic applications of substrate-specific ichnofacies: delineating discontinuities in the fossil record. *In* McIlroy, D. (Ed.), The Application of Ichnology to Palaeoenvironmental and Stratigraphic Analysis: *Geological Society of London*, Special Publications, v. 228, p. 29–62.

Petruncio, E.T., Rosenfeld, L.K., and Paduan, J.D., 1998, Observations of the internal tide in Monterey Canyon: *Journal of Physical Oceanography*, v. 28, p. 1873–1903.

Pindell, J. L., and Kennan, L., 2009, Tectonic evolution of the Gulf of Mexico, Caribbean and northern South America in the mantle reference frame: an update: *Geological Society of London*, Special Publications, v. 328, p. 1–55.

Pindell, J.L., Higgs, R., and Dewey, J.F. 1998, Cenozoic palinspastic reconstruction, paleogeographic evolution,and hydrocarbon setting of the northern margin of South America. *In* Pindell, J.L., and Drake, C.L. (Eds.), Paleogeographic evolution and non-glacial eustasy, northern South America: *SEPM Special Publication*, v. 58, p. 45–85.

Plinius *Secundus*, C., ca. 77-79, Naturalis Historia.

Plink-Björklund, P., and Steel, R.J., 2004, Initiation of turbidity currents: outcrop evidence for Eocene hyperpycnal flow turbidites: *Sedimentary Geology*, v. 165, p. 29–52.

Plint, A.G., 1988, Sharp-based shoreface sequences and "offshore bars" in the Cardium Formation of Alberta: their relationship to relative changes in sea level. Sea-Level Changes: An Integrated Approach. *In* Wilgus, C.K., Hastings, B.S., Kendall, C.G.St.C., Posamentier, H.W., Ross, C.A., and Van Wagoner, J.C. (Eds.), Sea Level Changes – An Integrated Approach: *SEPM Special Publication*, v. 42, p. 357–370.

Plint, A.G., 1991, High-frequency relative sea-level oscillations in Upper Cretaceous shelf clastics of the Alberta foreland basin: possible evidence for a glacio-eustatic control? *In* Macdonald, D.I.M. (Ed.), Sedimentation, Tectonics and Eustasy: Sea-level Changes at Active Margins: *International Association of Sedimentologists Special Publication*, v. 12, p. 409–428.

Plint, A.G., and Nummedal, D., 2000, The falling stage systems tract: recognition and importance in sequence stratigraphic analysis. *In* Hunt, D., and Gawthorpe, R.L. (Eds.), Sedimentary Response to Forced Regression: *Geological Society of London*, Special Publications, v. 172, p. 1–17.

Pollard, J.E., Steel, R.J., and Undersrud, E., 1982, Facies sequences and trace fossils in lacustrine/fan delta deposits, Hornelen Basin (M. Devonian), western Norway: *Sedimentary Geology*, v. 32, p. 63–87.

Pomar, L., Morsilli, M., Hallock, P., and Bádenas, B., 2012, Internal waves, an under-explored source of turbulence events in the sedimentary record: *Earth-Science Reviews*, v. 111, p. 56–81.

Porębski, S.J., and Steel, R.J., 2003, Shelf-margin deltas: their stratigraphic significance and relation to deepwater sands: *Earth-Science Reviews*, v. 62, p. 283–326.

Porębski, S.J., and Steel, R.J. 2006, Deltas and sea-level change: *Journal of Sedimentary Research*, v. 76, p. 390–403.

Posamentier, H.W., Allen, G.P., James, D.P., and Tesson, M., 1992, Forced Regressions in a Sequence stratigraphic framework: concepts, examples and exploration significance. *AAPG Bulletin*, v. 76, p. 1687–1709.

Potter, P.E, Maynard, J.B., and Depetris, P.J., 2005, Mud and mudstone: Introduction and overview: *Springer*, Berlin, Germany, 297 p.

Pratt, B.R., 2001, Septarian concretions: internal cracking caused by synsedimentary earthquakes: *Sedimentology*, v. 48, p. 189–213.

Puig, P., Ogston, A.S., Mullenbach, B.L., Nittrouer, C.A., and Sternberg, R.W., 2003, Shelf-to-canyon sediment-transport processes on the Eel continental margin (northern California): *Marine Geology*, v. 193, p. 129–149.

Purkait, B., and Majumdar, D.D., 2014, Distinguishing different sedimentary facies in a deltaic system: *Sedimentary Geology*, v. 308, p. 53–62.

Qian, P.Y., 1999, Larval settlement of polychaetes. *In* Dorresteijn, A.W.C., and Westheide, W. (Eds.), Reproductive Strategies and Developmental Patterns in Annelids: *Springer*, Netherlands, p. 239–253.

Qiu, J.W., and Qian, P.Y., 1997, Combined effects of salinity, temperature and food concentration on the early development of the polychaete *Hydroides elegans* (Haswell, 1883): *Marine Ecology Progress Series*, v. 152, p. 79–88.

Quiroz, L.I., Buatois, L.A., Mángano, M.G., Jaramillo, C.A., and Santiago, N., 2010, Is the trace fossil *Macaronichnus* an indicator of temperate to cold waters? Exploring the paradox of its occurrence in tropical coasts: *Geology*, v. 38, p. 651–654.

Răbăgia, T., Matenco, L., and Cloetingh, S., 2011, The interplay between eustacy, tectonics and surface processes during the growth of a fault-related structure as derived from sequence stratigraphy: the Govora–Ocnele Mari antiform, South Carpathians: *Tectonophysics*, v. 502, p. 196–220.

Ramsay, J.G., and Huber, M.I., 1987, The techniques of modern structural geology: Folds and fractures, v. 1: *Academic press*, London, 381 p.

Reitzel, A.M., Miles, C.M., Heyland, A., Cowart, J.D., and McEdward, L.R., 2005, The contribution of the facultative feeding period to echinoid larval development and size at metamorphosis: a comparative approach: *Journal of Experimental Marine Biology and Ecology*, v. 317, p. 189–201.

Rio, D., Sprovieri, R., Castradori, D., and Di Stefano, E., 1998, The Gelasian Stage (Upper Pliocene): A new unit of the global standard chronostratigraphic scale, *Episodes*, v. 21, p. 82–87.

Romero-Otero, G.A., Slatt, R.M., and Pirmez, C., 2010, Detached and shelf-attached mass transport complexes on the Magdalena deepwater fan. *In* Mosher, D.C., Shipp, R.C., Moscardelli, L., Chaytor, J.D., Baxter, C.D.P., Lee, H.J., and Urgeles, R. (Eds.), *Submarine mass movements and their consequences: 4th International Symposium*, Springer, Netherlands, p. 593–606.

Rouby, D., Nalpas, T., Jermannaud, P., Robin, C., Guillocheau, F., and Raillard, S., 2011, Gravity driven deformation controlled by the migration of the delta front: The Plio-Pleistocene of the Eastern Niger Delta: *Tectonophysics*, v. 513, p. 54–67.

Saller, A., and Blake, G., 2003, Sequence stratigraphy and syndepositional tectonics of Upper Miocene and Pliocene deltaic sediments, offshore Brunei Darussalam. *In* Sidi, F.H., Nummedal, D., Imbert, P., Darman, H., and Posamentier H.W. (Eds.), Tropical Deltas of Southeast Asia: Sedimentology, Stratigraphy, and Petroleum Geology: *SEPM Special Publication*, v. 76, p. 219–234.

Sánchez, C.M., Fulthorpe, C.S., and Steel, R.J., 2012, Miocene shelf-edge deltas and their impact on deepwater slope progradation and morphology, Northwest Shelf of Australia: *Basin Research*, v. 24, p. 683–698.

Saunders, J.B., 1997a, Trinidad Stratigraphic Chart and Geological Map: *Trinidad and Tobago Ministry of Energy*, 1(100), 000, not paginated.

Saunders, J.B., 1997b, SBC Seismic Basemap on Surface Geology (modified after H.G. Kugler, 1959): *Geological Survey of Trinidad and Tobago*, not paginated.

Saunders, J., and Kennedy, J., 1965, Sedimentology of a section in the upper Morne L'Enfer Formation, Guapo Bay, Trinidad: *Transactions of the IV Caribbean Geological Conference*, Port of Spain, Trinidad, p. 121–140.

Savrda, C.E., Browning, J.V., Krawinkel, H., and Hesselbo, S.P., 2001, Firmground ichnofabrics in deep-water sequence stratigraphy, Tertiary Clinoform-toe Deposits, New Jersey Slope: *Palaios*, v. 16, p. 294–305.

Schieber, J., Bose, P.K., Eriksson, P.G., Banerjee, S., Sarkar, S., Altermann, W., and Catuneanu, O., 2007, Atlas of microbial mat features preserved within the siliciclastic rock record (Vol. 2): *Elsevier*, 324 p.

Schneider, B., and Schmittner, A., 2006, Simulating the impact of the Panamanian seaway closure on ocean circulation, marine productivity and nutrient cycling: *Earth and Planetary Science Letters*, v. 246, p. 367–380.

Schreer, J.F., and Kovacs, K. M., 1997, Allometry of diving capacity in air-breathing vertebrates: *Canadian Journal of Zoology*, v. 75, p. 339–358.

Schwartz, T.M., and Graham, S.A., 2015, Stratigraphic architecture of a tide-influenced shelf-edge delta, Upper Cretaceous Dorotea Formation, Magallanes-Austral Basin, Patagonia: *Sedimentology*, v. 62, p. 1039–1077.

Seike, K., 2007, Palaeoenvironmental and palaeogeographical implications of modern *Macaronichnus segregatis*-like traces in foreshore sediments on the Pacific coast of central Japan: *Palaeogeography, Palaeoclimatology, Palaeoecology*, v. 252, p. 497–502.

Seike, K., Yanagishima, S.I., Nara, M., and Sasaki, T., 2011, Large *Macaronichnus* in modern shoreface sediments: Identification of the producer, the mode of formation, and paleoenvironmental implications: *Palaeogeography, Palaeoclimatology, Palaeoecology*, v. 311, p. 224-229.

Seilacher, A., 1967, Fossil behaviour: *Scientific American*, v. 217, p. 72–80.

Seilacher, A., 1990, Aberrations in bivalve evolution related to photo-and chemosymbiosis: *Historical Biology*, v. 3, p. 289–311.

Seilacher, A., 2007, Trace fossil analysis: *Springer Science & Business Media*, 226 p.

Shanmugam, G., 2013, Modern internal waves and internal tides along oceanic pycnoclines: Challenges and implications for ancient deep-marine baroclinic sands: *AAPG Bulletin*, v. 97, p. 799–843.

Shanmugam, G., and Moiola, R.J., 1988, Submarine fans: characteristics, models, classification, and reservoir potential: *Earth-Science Reviews*, v. 24, p. 383–428.

Shanmugam, G., Lehtonen, L.R., Straume, T., Syvertsen, S.E., Hodgkinson, R.J., and Skibeli, M., 1994, Slump and debris-flow dominated upper slope facies in the Cretaceous of the Norwegian and northern North seas (61-67 N): implications for sand distribution: *AAPG Bulletin*, v. 78, p. 910–937.

Shi, Z., 1998, Acoustic observations of fluid mud and interfacial waves, Hangzhou Bay, China: *Journal of Coastal Research*, v. 14, p. 1348–1353.

Sidi, F.H., Nummedal, D., Imbert, P., Darman, H., and Posamentier H.W., 2003, Tropical deltas of Southeast Asia: Sedimentology, stratigraphy and petroleum geology: *SEPM Special Publication*, v. 76, 269p.

Siggerud, E.I.H., and Steel, R.J., 1999, Architecture and Trace-Fossil Characteristics of A 10,000-20,000 Year, Fluvial-to-Marine Sequence, Seebro Basin, Spain: *Journal of Sedimentary Research*, v. 69, p. 365–383.

Silva, C.G., Araújo, E., Reis, A.T., Perovano, R., Gorini, C., Vendeville, B.C., and Albuquerque, N., 2010, Megaslides in the Foz do Amazonas Basin, Brazilian Equatorial Margin. *In*

Mosher, D.C., Shipp, R.C., Moscardelli, L., Chaytor, J.D., Baxter, C.D.P., Lee, H.J., and Urgeles, R. (Eds.), *Submarine mass movements and their consequences: 4th International Symposium*, Springer Netherlands, p. 581–591.

Smith, A.B., and Crimes, T.P., 1983, Trace fossils formed by heart urchins-a study of *Scolicia* and related traces: *Lethaia*, v. 16, p. 79–92.

Smith, W.O., and Demaster, D.J., 1996, Phytoplankton biomass and productivity in the Amazon River plume: correlation with seasonal river discharge: *Continental Shelf Research*, v. 16, p. 291–319.

Sneider, J.S., 2003, Shelf Margin Deltas and Associated Deep-Water Deposits: Implications on Reservoir Distribution and Hydrocarbon Entrapment, Block VI-1, Ulleung Basin, East Sea, South Korea. *In* Roberts, H.H., Rosen, N.C., Fillon, R.H., and Anderson, J.B. (Eds.), Shelf margin deltas and linked down slope petroleum systems: *Gulf Coast Section SEPM (GCSSEPM), 23rd Annual Research Conference*, Houston, not paginated.

Sonibare, W.A., Mikeš, D., and Cole, D.I., 2011, Facies architecture of Kookfontein shelf edge delta, Tanqua-Karoo Basin (South Africa): Implications for facies analysis and modelling: *South African Journal of Geology*, v. 114, p. 299–324.

Southard, J.B., 1991, Experimental determination of bedform stability: *Annual Review of Earth and Planetary Sciences*, v. 19, p. 423–455.

Steel, R.J., Porębski, S.J., Plink-Björklund, P., Mellere, D., and Schellpeper, M., 2003, Shelf-edge delta types and their sequence-stratigraphic relationships. *In* Roberts, H.H., Rosen, N.C., Fillon, R.H., and Anderson, J.B. (Eds.), Shelf margin deltas and linked down slope petroleum systems: *Gulf Coast Section SEPM (GCSSEPM), 23rd Annual Research Conference*, Houston, p. 205–230.

Steel, R.J., Uroza, C., Huggins, G., Osman, A., and Winter, R., 2007, The growth of the Orinoco shelf prism on Trinidad: interaction of sediment supply, tectonics, sea level and basinal processes: *Geological Society of Trinidad and Tobago Annual Meeting Extended abstract volume*, p. 1–12.

Stickle, W.B., and Diehl, W.J., 1987, Effects of salinity on echinoderms. *In* Jangoux M, and Lawrence J.M. (Eds.), Echinoderm studies. Vol. 2. *A.A. Balkema*, Rotterdam, p. 235–285.

Suter, H.H., 1960, The general and economic geology of Trinidad, B.W.I., 2d ed. *with* Higgins, G.E., Revisionary Appendix: *H.M. Stationery Office*, London, 145 p.

Suter, J.R., and Berryhill, Jr., H.L., 1985, Late Quaternary shelf-margin deltas, northwest Gulf of Mexico: *AAPG Bulletin*, v. 69, p. 77–91.

Sydow, J., and Roberts, H.H., 1994, Stratigraphic framework of a late Pleistocene shelf-edge delta, northeast Gulf of Mexico: *AAPG bulletin*, v. 78, p. 1276–1312.

Sydow, J.C., Finneran, J., and Bowman, A.P., 2003, Stacked shelf-edge delta reservoirs of the Columbus Basin, Trinidad, West Indies. *In* Roberts, H.H., Rosen, N.C., Fillon, R.H., and Anderson, J.B. (Eds.), Shelf margin deltas and linked down slope petroleum systems: *Gulf Coast Section SEPM (GCSSEPM), 23rd Annual Research Conference*, Houston, p. 441–465.

Sylvester, Z., and Lowe, D.R., 2004, Textural trends in turbidites and slurry beds from the Oligocene flysch of the East Carpathians, Romania: *Sedimentology*, v. 51, p. 945–972.

Talling, P.J., 2013, Hybrid submarine flows comprising turbidity current and cohesive debris flow: Deposits, theoretical and experimental analyses, and generalized models: *Geosphere*, v. 9, p. 460–488.

Taylor, A. M., and Goldring, R., 1993, Description and analysis of bioturbation and ichnofabric: *Journal of the Geological Society*, v. 150, p. 141–148.

Thorsen, M.S., 1998, Microbial activity, oxygen status and fermentation in the gut of the irregular sea urchin *Echinocardium cordatum* (Spatangoida: Echinodermata): *Marine Biology*, v. 132, p. 423–433.

Turner, B.R., Stanistreet, I.G., and Whateley, M.K.G., 1981, Trace fossils and palaeoenvironments in the Ecca Group of the Nongoma Graben, northern Zululand, South Africa: *Palaeogeography, Palaeoclimatology, Palaeoecology*, v. 36, p. 113–123.

Turner, R.E., Rabalais, N.N., and Nan, Z.Z., 1990, Phytoplankton biomass, production and growth limitations on the Huanghe (Yellow River) continental shelf: *Continental Shelf Research*, v. 10, p. 545–571.

Uchman, A., and Krenmayr, H.G., 1995, Trace fossils from lower Miocene (Ottnangian) molasse deposits of Upper Austria: *Paläontologische Zeitschrift*, v. 69, p. 503–524.

Uchman, A., Demircan, H., Toker, V., Derman, S., Sevim, S., and Szulc, J., 2002, Relative sea level changes recorded in borings from a Miocene rocky shore of the Mut Basin, southern Turkey: *Annales Societatis Geologorum Poloniae*, v. 72, p. 263–270.

Uroza, C.A., 2008, Processes and architectures of deltas in shelf-break and ramp platforms: examples from the Eocene of West Spitsbergen (Norway), the Pliocene Paleo-Orinoco Delta (SE Trinidad), and the Cretaceous Western Interior Seaway (S Wyoming & NE Utah): Ph.D. Thesis, *University of Texas at Austin*, 243 p.

Uroza, C.A., and Steel, R.J., 2008, A highstand shelf-margin delta system from the Eocene of West Spitsbergen, Norway: *Sedimentary Geology*, v. 203, p. 229–245.

Ushakova, O.O., and Sarantchova, O.L., 2004, The influence of salinity on fertilization and larval development of *Nereis virens* (Polychaeta, Nereidae) from the White Sea: *Journal of Experimental Marine Biology and Ecology*, v. 301, 129–139.

Vail, P.R., Mitchum, R.M. Jr., and Thompson, S., III, 1977, Seismic stratigraphy and global changes of sea level, part four. *In* Payton, C.E. (Ed.), Seismic stratigraphy: applications to hydrocarbon exploration: *AAPG Memoir*, v. 26, p. 83–98.

Vail. P.R., Audermard, F., Bowman, S.A., Eisner, P.N., and Perez-Cruz, C., 1991, The stratigraphic signatures of tectonics, eustasy and sedimentology – an overview. *In* Einsele, G., Ricken, W., and Seilacher, A. (Eds.), Cycles and events in stratigraphy: *Springer-Verlag*, p. 617–659.

Vakarelov, B.K., Ainsworth, R.B., and MacEachern, J.A., 2012, Recognition of wave-dominated, tide-influenced shoreline systems in the rock record: Variations from a microtidal shoreline model: *Sedimentary Geology*, v. 279, p. 23–41.

Vincent, H., 2008, Cenozoic Sediment Dispersal Patterns Across Trinidad, West Indies: Ph.D. Thesis, *Dalhousie University*, 540 p.

Vincent, H., Wach, G.D., and Johnson, N., 2007, Lithofacies Assemblages and depositional processes in the Morne L'Enfer Formation: outcrop insights into Pliocene Southern Basin sedimentary fill: *Abstracts – The 4th Geological Conference of the Geological Society of Trinidad and Tobago*, http://archives.datapages.com/data/gstt/GSTT4_89.pdf.

Visser, M.J., 1980, Neap-spring cycles reflected in Holocene subtidal large-scale bedform deposits: A preliminary note: *Geology*, v. 8, p. 543–546.

Vopel, K., Vopel, A., Thistle, D., and Hancock, N., 2007, Effects of spatangoid heart urchins on O-2 supply into coastal sediment: *Marine Ecology Progress Series*, v. 333, p. 161–171.

Wach, G.D., and Vincent, H., 2008, Reservoir Heterogeneity and Characterization in Deltaic Depositional Systems- Outcrop Analogs for Heavy Oil and Oil Sand Developments: *AAPG Search and Discovery Article* # 50064.

Wach, G.D., Frampton, J., Sydow, J., Wood, L.J., and Johnson, S., 2003a, Plio-Pleistocene shelf margin deltas from Trinidad; outcrop and subsurface examples. *In* Roberts, H.H., Rosen, N.C., Fillon, R.H., and Anderson, J.B. (Eds.), Shelf-Margin Deltas and Linked Downslope Petroleum Systems: Global Significance and Future Exploration Potential: *23rd Annual GCSSEPM Foundation Bob F. Perkins Research Conference*, Houston, USA, p. 38.

Wach, G.D., Lolley, C.S., Mims, D.S., and Cellars, C.A., 2003b, Well placement, cost reduction and increased production using reservoir models based on outcrop, core, well logs,

seismic data and modern analogs, onshore and offshore western Trinidad. *In* Grammer, G.M., Harris, P.M., and Eberli, G.P. (Eds.), Integration of Outcrop and Modern Analogs in Reservoir Modeling: *AAPG Memoir*, v. 80, p. 279–307.

Weaver, P.P., Wynn, R.B., Kenyon, N.H., and Evans, J., 2000, Continental margin sedimentation, with special reference to the north-east Atlantic margin: *Sedimentology*, v. 47, p. 239–256.

Webb, S.D., 2006, The Great American Biotic Interchange: patterns and processes: *Annals of the Missouri Botanical Garden*, v. 93, p. 245–257.

Weimer, P., and Slatt, R.M., 2007, Introduction to the petroleum geology of deepwater settings: *AAPG Studies*, v. 57, 816 p.

Wilson, B., 2008, Distributions of ostracod (Crustacea) biofacies on the continental shelf off south-east Trinidad, western central Atlantic Ocean, suggest the location of an offshore river-induced front within the Orinoco Plume: *Senckenbergiana Lethaea*, v. 88, p. 199–211.

Winter, R., 2006, The Cruse Formation of Southern Trinidad: Analog for Offshore Columbus Basin Reservoirs: MS Dissertation, *University of Texas at Austin*, 85 p.

Wood, L.J., 2000, Chronostratigraphy and tectonostratigraphy of the Columbus Basin, eastern offshore Trinidad: *AAPG Bulletin*, v. 84, p. 1905–1928.

Xie, X., and Mann, P., 2014, U-Pb detrital zircon age patterns of Cenozoic clastic sedimentary rocks in Trinidad and its implications: *Sedimentary Geology*, v. 307, p. 7–16.

Young, M.J., Gawthorpe, R., and Sharp, I.R., 2003, Normal fault growth and early syn-rift sedimentology and sequence stratigraphy: Thal Fault, Suez Rift, Egypt: *Basin Research*, v. 15, p. 479–502.

Zaitlin, B.A., Dalrymple, R.W., and Boyd, R., 1994, The stratigraphic organization of incised-valley systems associated with relative sea-level changes. *In* Boyd, R., Zaitlin, B.A., and Dalrymple, R. (Eds.), Incised Valley Systems: Origin and Sedimentary Sequence: *SEPM Special Publication*, v. 51, p. 45–60.

Zavala, C., Arcuri, M., Di Meglio, M., Gamero Diaz, H., and Contreras, C., 2011, A genetic facies tract for the analysis of sustained hyperpycnal flow deposits. *In* Slatt, R.M., and Zavala, C. (Eds.), Sediment transfer from shelf to deep water – Revisiting the delivery system: *AAPG Studies in Geology*, v. 61, p. 31–51.

Zavala, C., Arcuri, M., and Blanco Valiente, L., 2012a, The importance of plant remains as diagnostic criteria for the recognition of ancient hyperpycnites: *Revue de Paléobiologie, Genève*, v. 31, p. 457–469.

Zavala, C., Arcuri, M., and Blanco Valiente, L., 2012b, Plant remains in recent deposits of the Orinoco fan: a direct evidence of hyperpycnal discharges of the Orinoco river: *GSTT 5th Geological Conference 2012*, Trinidad & Tobago.

Zecchin, M., Mellere, D., and Roda, C., 2006, Sequence stratigraphy and architectural variability in growth fault-bounded basin fills: a review of Plio-Pleistocene stratal units of the Crotone Basin, southern Italy: *Journal of the Geological Society*, v. 163, p. 471–486.

Zhang, Y.G., Ji, J., Balsam, W., Liu, L., and Chen, J., 2009, Mid-Pliocene Asian monsoon intensification and the onset of Northern Hemisphere glaciation: *Geology*, v. 37, p. 599–602.

End

---- ○ ----